THE

LONDON, EDINBURGH, AND DUBLIN

PHILOSOPHICAL MAGAZINE

AND

JOURNAL OF SCIENCE.

[SEVENTH SERIES.]

JULY 1928.

I. *The Complete Photo-electric Emission from Potassium.*

By Miss JESSIE BUTTERWORTH, *B.Sc.**

THIS paper is concerned mainly with the negative emission from potassium, but some account of experiments designed to investigate the possibility of a positive photo-electric emission from the metal will be given at the outset. Since Dember (*Ann. d. Phys.* xxx. p. 142, 1910) found that a cylinder surrounding a metal plate acquired a positive charge, when the plate was illuminated with ultra-violet light, a suitable field being applied, many experimenters have endeavoured to justify Dember's assumption that the phenomenon is due to the emission of positive photo-electric particles. Most of the later work seems to show that the effect is the result of the emission of electrons by metal parts of the apparatus which are not adequately screened from stray ultra-violet light. Du Bridge (Phys. Rev. p. 201, Feb. 1925) and E. J. Lorentz (Phil. Mag. vol. i. p. 499, 1926) in particular were unable to obtain a positive charging up when precautions against defective screening were taken. No observer, however, appears to have worked with the alkali metals, though, if the positive photo-electric effect does exist, it seems, *a priori*, probable that these metals would exhibit the effect to a greater degree than other metals known to be much less active as regards the normal effect.

* Communicated by Prof. William Wilson, F.R.S.

Experiments on the Positive Photo-electric Effect.

A glass bulb (fig. 1) 10 cm. in diameter, with two inlet tubes which terminated in a bottle-neck, was used. Sealed through the inverted end of the neck, as shown, was a filament of platinum wire, so that the loop of the wire was at the centre of the spherical bulb. Round the filament, but not touching it, was a spiral of platinum wire. Thus the filament was surrounded at the sides and bottom by a grid, and both grid and filament could be electrically heated. A fine

Fig. 1.

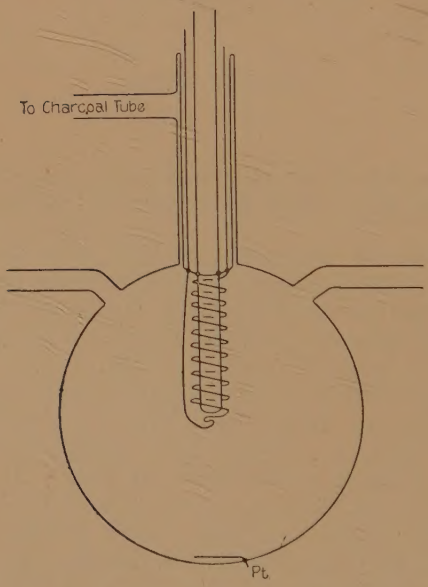

platinum wire was sealed through the bottom of the bulb to make contact with the potassium, which was to act as the third electrode.

A glass bottle containing clean potassium was allowed to slide down one of the side-tubes until stopped by a constriction. By means of the other side-tube the bulb was connected to liquid-air traps and a mercury-diffusion pump, backed by a "Hyvac" pump. After baking and pumping out, with the grid and filament glowing and the charcoal tube heated, the potassium was run over the constriction, which was then sealed off. This was done while the pumps were

working and the liquid-air traps were being cooled. After further pumping, the tube was sealed off and left overnight. Then the potassium was heated slightly once more, and run down to the bottom of the bulb to make contact with the platinum wire.

The glowing filament acted as a source of light, and in so doing gave off thermions, both negative and positive. The latter emission would, of course, almost disappear with constant glowing and a field helping the emission. If a positive photo-electric effect did exist, there would be positive and negative photo-electric currents from both the platinum grid and the potassium. When the connexions are made, as shown in fig. 2, the negative current from the grid and the positive one from the potassium alone can affect the quadrant electrometer.

Fig. 2.

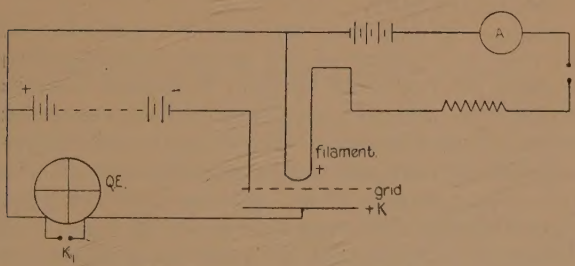

The grid is negative with respect to the potassium, so that any electrons from the potassium are turned back, while any positive particles are attracted across to the grid, leaving a negative charge on the potassium, which, when the key K_1 is open, causes a deflexion of the needle of the electrometer. The field between the filament and grid will turn back any electrons emitted by the filament, while any positive particles from the same source will be turned back once they have passed through the grid. Hence the emission from the filament cannot affect the electrometer. There may be a negative photo-electric current from the grid, however, which will reach the potassium and charge it in the same manner as the positive current leaving it would do. Any positive photo-electric current from the grid will be turned back. The highest threshold frequency of potassium is known to be well in the infra-red portion of the spectrum, while that of platinum is in the ultra-violet. Consequently,

if no effect is produced upon the electrometer, using light whose wave-length is between the two threshold frequencies, it will mean that no positive photo-electric current is emitted from the potassium—at any rate, when those particular wave-lengths are employed.

The sensitivity of the electrometer was such that with 120 volts on the needle and a potential difference of one volt between the quadrants the deflexion produced would be 140 cm. on the lamp scale. The capacity of the system, the electrometer, and the bulb in series was very nearly 100 cm.

Owing to a slight charging up of the sealing-wax key and also to a small leak across the inside of the glass bulb, even when the filament was unheated, the image moved in the direction indicating a positive charging up of the potassium. Fortunately it was not too fast to be timed, and was constant over a short range of time—long enough for measurements to be taken. The effect looked for would mean a still slower rate of charging.

No change in the rate was noticed until the filament current rose to a value of 1·8 amps., corresponding to a temperature of over 800° C., and it seemed reasonable to suppose that the negative platinum current was causing the change at this temperature. However, at this temperature the negative current was quite large (nearly 10^{-6} amp.). A stop-clock reading to ·2 sec. was used, and it would have been easy to detect a change in the rate of 1 cm. in 10 secs. The difference of potential between the potassium and the grid was 96 volts: sufficient to saturate the negative currents at the temperatures employed.

TABLE I.

Filament current.	Time for image to travel 22 cm.
0	10·2 secs.
1·5 amps.	10·2 „
0	10·4 „
1·6 „	10·2 „
0	10·2 „
1·7 „	10·4 „
0	10·2 „
1·8 „	11·2 „

A change in the rate of charging up of 1 cm. in 10 secs. would mean a photo-electric current of 10^{-13} amp. For the potential difference

$$= \frac{\text{current} \times \text{time}}{\text{capacity}}$$

$$= \frac{1}{140 \times 300} \text{E.S.U.}$$

$$\therefore \quad \text{current} = \frac{1}{1{\cdot}26} \times 10^{-13} \text{ amp.}$$

Hence a current of little over 1×10^{-14} amp. could have been detected.

Dember found the ratio of his negative to positive photo-electric currents to be $\frac{10^{-9}}{10^{-13}}$, *i.e.* 10^4, whereas these experiments give the ratio as more than $\frac{10^{-6}}{10^{-13}}$, *i.e.* 10^7. Hence, if the positive photo-electric effect does occur, it is at least a thousand times smaller than the current which Dember attributed to the emission of positive ions by photo-electric action.

The Threshold Frequencies of Potassium.

Richardson and Young (Proc. Roy. Soc. ser. A, vol. cvii. p. 377, 1925) found for a normal potassium surface a threshold frequency corresponding to a wave-length of 7000 A.U. After sensitizing the potassium surface by passing a glow-discharge through an atmosphere of hydrogen, the critical wave-length appeared to be somewhere between 9000 A.U. and 10,000 A.U. A usual thermionic threshold at a temperature of 200° C. is 10,000 A.U., and another occurs at about 30,000 A.U. No trace of a photo-electric threshold of this magnitude, however, was to be found, even for the sensitized surface. The following account gives details of the production, by vaporizing the metal, of a sensitized surface, for which two threshold frequencies were found.

Experiments on the Threshold Frequencies of Potassium.

The apparatus used to investigate the existence of the positive photo-electric effect was also used to measure the threshold frequency or frequencies of potassium, by measuring the complete photo-electric effect when in equilibrium with black-body radiation of known temperature. By heating the potassium at the bottom of the bulb with a small electric heater, it was vaporized and deposited in a thin film over the cool part of the spherical surface. To prevent the vapour condensing on or near the filament and grid, both

were heated throughout the operation, and also another electric heater was wound round the outside of the bottle-neck. By repeated heating and cooling of the potassium it was possible to obtain a comparatively thick and quite opaque mirror over the whole spherical surface. The gap on the glass in contact with the heater was covered by tipping the tube while the metal was still in the liquid state. At the first attempt the mirror of potassium evidently was not of sufficient thickness to make good electrical contact over the whole surface, for inconsistent readings of the photo-electric currents were obtained, doubtless due to certain portions of the surface becoming charged up after subjection to radiation for a few minutes. At the second attempt the film of potassium was made thicker, and this difficulty disappeared. Owing to repeated reflexions of the light emitted by the filament at the bright potassium surface, the system should give approximately black-body radiation, and at the same time a fresh metal surface could easily be obtained by heating and vaporizing the potassium. Also each heating would improve the conditions until all the substances, which had been left in the bulb and were capable of reacting with potassium, had been used up,

The law governing the relation between the saturated current and the temperature in the case of the complete photo-electric effect is expressed by $C = AT^{\lambda}e^{-\frac{b}{T}}$ (see Richardson, Phil. Mag. vol. i. 1912), where C is the saturated photo-electric current, T is the temperature of the radiator, λ a constant which can take the values 2 or $\frac{1}{2}$, and b is the work function (ϕ) divided by the gas constant for one molecule (k). A is a constant depending on the area of the surface. Therefore plotting values of $\log_{10}\frac{C}{T^{\lambda}}$ against $\frac{1}{T}$ should give a straight line, the slope giving the value of b.

The saturated currents C were comparatively large, and a sensitive galvanometer G_1 was used to measure them. The connexions were as shown in fig. 3. The two grid connexions and one side of the filament were connected to the positive side of a lamp-board in which the ten lamps were arranged in series and connected to the 240 volt-mains. The galvanometer G_1 was connected between two of the lamps, the other galvanometer terminal being connected straight to the potassium mirror. The resistance of the filament was measured at the various temperatures by means of a Wheatstone bridge arrangement. R_1 and R_2 were two

arms of a Post Office box, and Y was a coil of eureka wire 2 metres long, immersed in a flask filled with paraffin-oil, which in turn was surrounded by a water-bath. The resistance of the coil was 2·056 ohms. Its resistance was previously measured at 20° C. and at 100° C., no difference being detectable, and when surrounded by a water-bath the

Fig. 3.

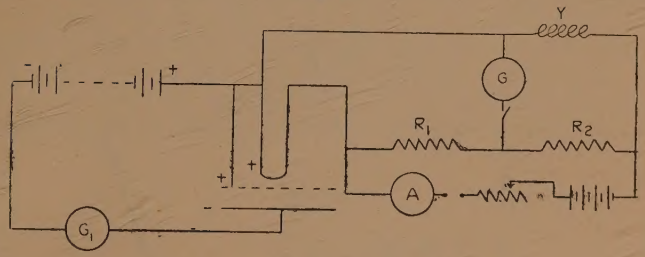

Fig. 4.

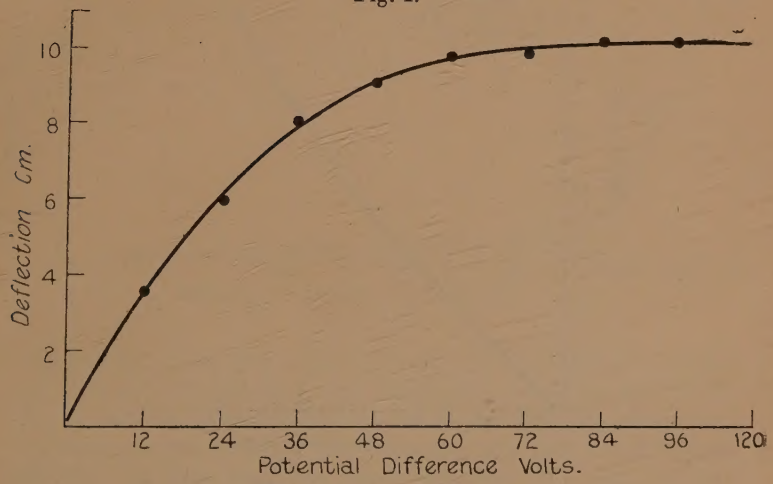

Filament current 2·5 amps.

Potential Difference. Volts.	Deflexion. cm.	Potential Difference. Volts.	Deflexion. cm.
12	3·6	60	9·8
24	6·0	72	9·9
36	8·0	84	10·2
48	9·1	96	10·2

temperature varied over a range of less than 10° C., when the largest filament currents were used. Consequently under the conditions of experiment it was an invariable

resistance. The filament was heated by a battery of accumulators and the steady balance in the bridge found, using a dead-beat Onwood galvanometer G, which gave a deflexion of about 10 cm. on the scale for a change of resistance of 1 ohm in the variable arm of the box.

The photo-electric currents were well saturated, as is shown by fig. 4, the current-potential difference curve corresponding to a filament current of 2·5 amps. With the

Fig. 5.

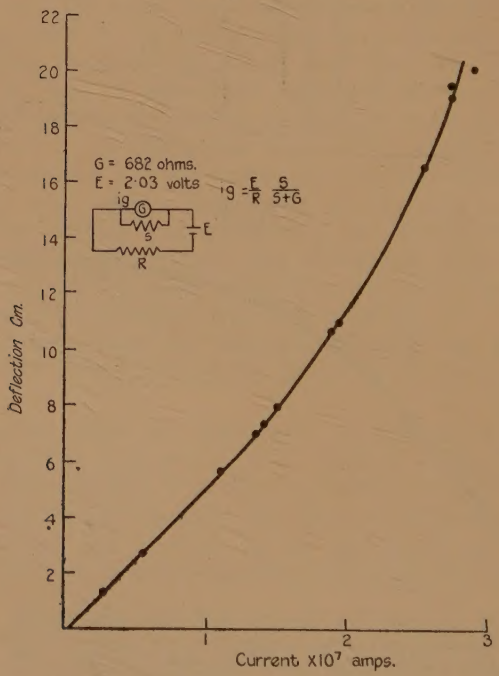

R ohms.	S ohms.	Current $\times 10^7$ amps.	Deflexion cm.
10^6	10	·29	1·3
10^6	20	·57	2·7
5×10^5	20	1·14	5·6
10^6	50	1·39	6·9
4×10^5	20	1·45	7·3
9×10^5	50	1·54	7 9
3×10^5	20	1·93	10·6
7×10^5	50	1·98	10·9
10^6	100	2·59	16·5
5×10^5	50	2·78	19·0
5×10^5	50	2·78	19·4
10^5	10	2·93	20·0

largest filament current used (3·5 amps.), saturation was secured by having 108 volts potential difference between the potassium and the filament, so this value was used throughout.

The graph plotted between current and resistance in the variable arm of the box, *i. e.* between current and filament temperature in arbitrary units, was of the form shown in figs. 6 *a* and 6 *b*. The initial rise and following flat portion was assumed to be due to a second and lower threshold frequency, for at this stage the filament was not glowing.

In order to ensure the best possible conditions, the potassium was then melted off the walls of the bulb and a completely fresh film deposited. As soon as this film was

Fig. 6 *a*.

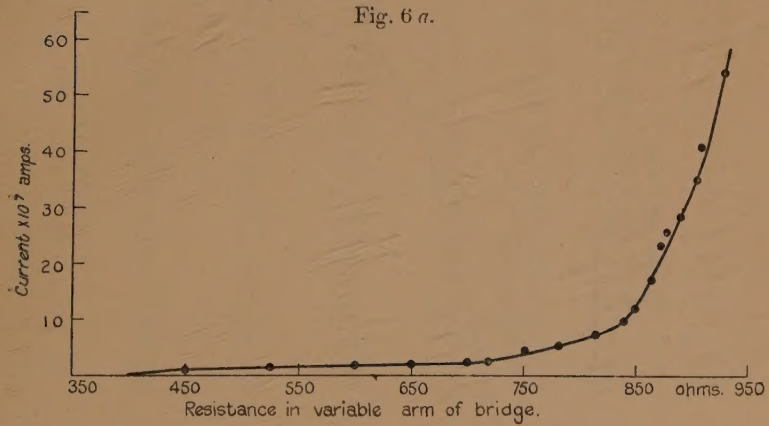

sufficiently thick the charcoal tube was immersed in liquid air. A set of deflexion and resistance readings was taken about half an hour after the mirror had been deposited, and another set taken after the lapse of two and a half hours. Neither at this time nor next morning was any fatigue noticed ; in fact, as will be mentioned later, the current over a certain range increased with time. The curves obtained with this fresh film agreed with those previously obtained.

Hysteresis effects were considerable. Readings were taken when the filament current was gradually increased, but if taken in the reverse order the difference between corresponding current readings was so great that for the lowest temperatures used the descending reading would be as much as twice the ascending reading. The effect disappeared quite rapidly with time ; in the case of the high

temperatures so rapidly that the effect was not noticeable. Though the decay at lower temperatures was slower, the original ascending reading would be reached by leaving the apparatus for 10 to 15 minutes. The descending readings are inconsistent, for they depend on the time that lapses between altering the filament current and taking the reading of the deflexion and the corresponding filament resistance.

Fig. 6*b*.

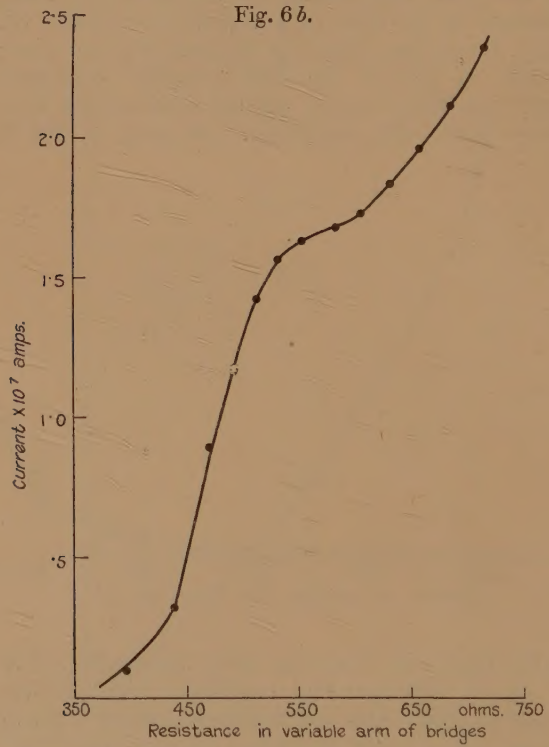

Resistance. ohms.	Deflexion. cm.	Current $\times 10^7$. amps.	Resistance. ohms.	Deflexion. cm.	Current $\times 10^7$. amps.
395	·45	·10	584	8·8	1·68
440	1·45	·32	607	9·1	1·73
472	4·3	·89	632	9·9	1·84
513	7·2	1·42	659	11·0	1·97
534	8·0	1·56	688	1·8 *	2·12
555	8·5	1·63	717	2·0 *	2·33

* Shunt 150 ohms.

The effect appeared to be in no way altered in the second case, when a presumably higher vacuum was contained in the bulb.

TABLE II.

Shunt ohms.	Resistance in variable arm of box. ohms.	Deflexion. cm.	Temperature. ° C.	$\frac{1}{T} \times 10^4$.	Current $\times 10^7$ amps.	$\log_{10} \frac{C}{T^2}$ +13.	$\log_{10} \frac{C}{T}$ +10.
∞	400	·50	340	29·4	·12	·016	·813
	425	1·05	380	26·3	·23	·202	1·072
	437	1·60	405	24·7	·35	·323	1·240
	450	2·35	425	23·5	·49	·433	1·376
	462	3·35	445	22·5	·70	·547	1·507
	475	4·40	470	21·3	·90	·610	1·618
	487	5·30	485	20·5	1·08	·662	1·691
	500	6·75	505	19·8	1·35	·724	1·779
	525	7·60	553	18·1	1·50	·691	1·805
	550	8·25	605	16·5	1·60	·641	1·813
	575	8·60	657	15·2	1·65	·582	1·809
	600	9·25	712	14·0	1·75	·538	1·817
	625	9·65	777	12·9	1·80	·475	1·810
	650	10·40	830	12·1	1·90	·441	1·819
150	675	1·75	890	11·2	2·05	·413	1·837
	700	1·95	920	10·9	2·25	·470	1·916
	717	2·00	945	10·6	2·33	·417	1·877
	753	3·6	1005	9·95	4·16	·615	2·118
	782	4·6	1070	9·35	5·21	·658	2·202
	815	6·6	1135	8·80	7·32	·760	2·337
	839	9·4	1180	8·48	9·82	·848	2·456
50	850	5·2	1200	8·33	12·00	·921	2·540
	867	5·8	1230	8·13	17·13	1·054	2·689
	876	8·2	1248	8·00	23·28	1·176	2·819
	882	10·4	1260	7·94	25·72	1·209	2·860
	890	10·8	1275	7·85	28·65	1·245	2·904
	905	16·6	1302	7·69	35·33	1·319	2·991
20	911	5·8	1338	7·60	41·10	1·381	3·056
	935	8·85	1360	7·35	59·30	1·506	3·206
			After lapse of three days.				
∞	542	9·3	600	16·7	1·75	·687	1·854
150	579	1·9	675	14·8	2·22	·688	1·932
	607	2·1	725	13·8	2·44	·667	1·957
	649	2·4	810	12·4	2·79	·639	1·991
	654	2·5	820	12·2	2·88	·632	2·003
	706	2·8	915	10·9	3·33	·540	2·042
	715	3·1	935	10·7	3·60	·615	2·071
	751	3·9	1000	10·0	4·44	·647	2·147

The relation between filament temperature and resistance was found by opening the bulb and withdrawing the filament and grid, and then finding the resistances of the filament at the melting-points of certain crystals. The bridge arrangement was exactly the same as when taking readings of the photo-electric current, and minute crystals of substances

having well-defined melting-points were placed on the filament at its hottest part. The current passing through the filament was gradually increased, the Wheatstone balance being readjusted continually until the crystal, which was viewed through a microscope, melted. The graph obtained by plotting the melting-point temperature against the resistance in the variable arm of the box was a straight line (fig. 7).

Fig. 7.

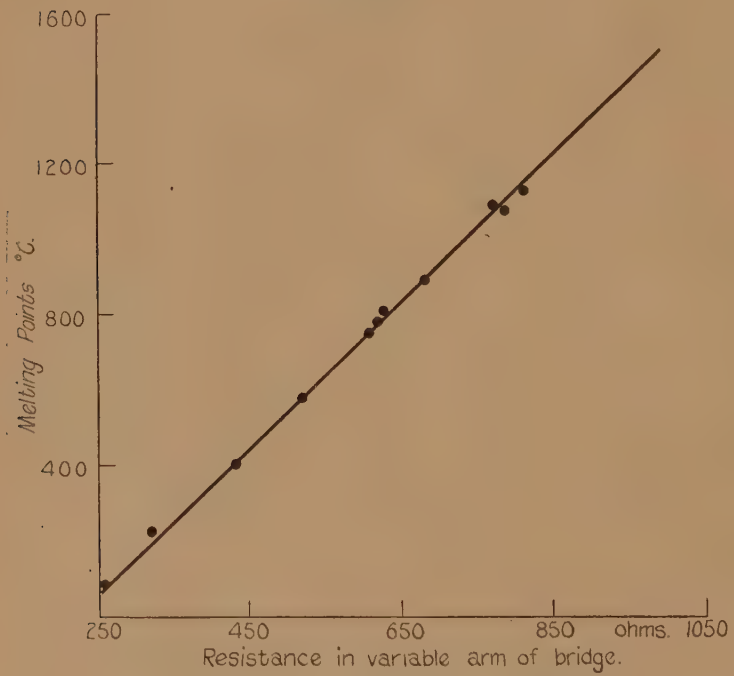

Crystal.	Melting-Point C.	Resistance. ohms.
Naphthalene.....	79	256
Silver nitrate	218	325
Potassium bichromate	400	435
Barium nitrate.....	575	525
Potassium bromide...	750	625
Sodium chloride	801	635
Sodium sulphate	884	683
Potassium sulphate...	1070	780
Stannic oxide	1130	815

Having determined the temperatures and the corresponding currents, graphs were plotted between $\log_{10}\frac{C}{T^2}$ and $\frac{1}{T}$, and

also between $\log_{10}\frac{C}{T^{\frac{1}{2}}}$ and $\frac{1}{T}$ (figs. 8 and 9). In both cases

Fig. 8.

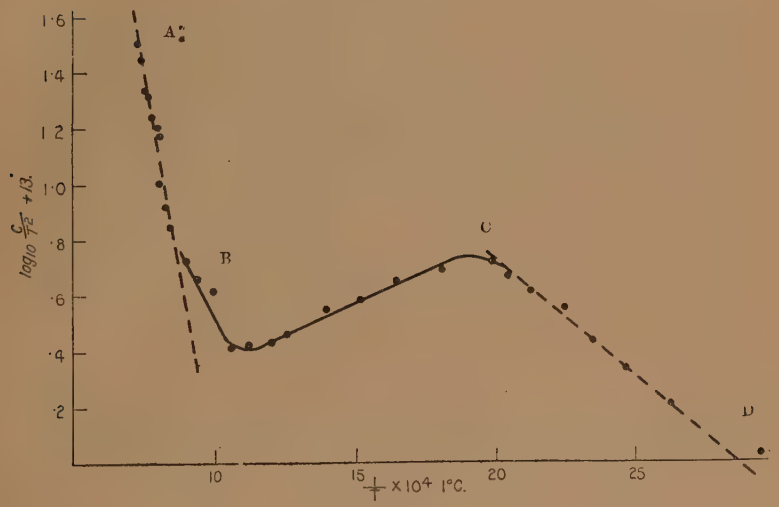

Fig. 9.

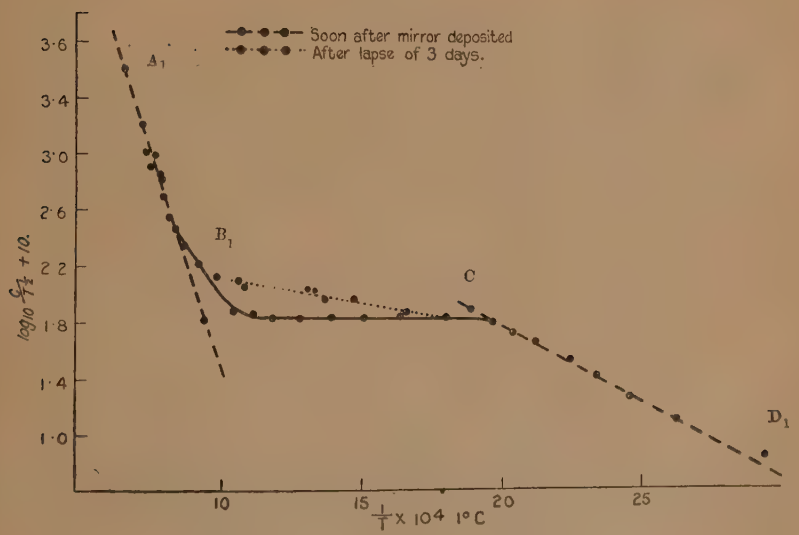

nearly all the points lie on three straight lines, and the slopes of the portions AB and CD are nearly the same in

both graphs. The intermediate portion BC, however, is quite different. When taking $\log_{10}\frac{C}{T^2}$ we have a line sloping in the positive direction, apparently indicating a value for b that is negative. In the other case the central line B_1C_1 is very nearly horizontal, but has a slight slope in the negative direction. This central portion corresponds to the almost horizontal part of the current-temperature curve in fig. 5, and this part does not appear to be very stable. The currents in this region gradually increased with time, not becoming absolutely constant until about three days after the potassium mirror had been deposited. Using readings obtained after this lapse of time, the general characteristics of this part of the two curves are unaltered, but the slope is different. The slope in the negative direction when plotting $\log_{10}\frac{C}{T^{\frac{1}{2}}}$ is increased and equal to ·026. This is smaller than the others, namely ·64 and ·11. Apparently this would mean that for potassium there are three threshold frequencies for the sensitized surface. On the other hand, the intermediate portion may be represented by the sum of terms such as

$$C = A_1 T^{\lambda} e^{-\frac{b}{T}} + A_2 T^{\lambda} e^{-\frac{b_1}{T}},$$

where both terms are of about the same magnitude. The instability would then be due to some small portions, taking some time to decide which work-function to assume.

The results obtained show that potassium has at least two work-functions, corresponding to two critical wave-lengths, one at 9700 A.U. and the other at 57,000 A.U.

Since

$$C = A_1 T^{\lambda} e^{-\frac{b_1}{T}},$$

$$\log_e \frac{C}{T^2} = \log_e A_1 - \frac{b_1}{T},$$

so $$b_1 = \frac{\text{slope} \times 10^4}{\log_{10} e}\,^{\circ}\text{C.};$$

and since $k = 1{\cdot}37 \times 10^{-16}$ ergs/° C.,

$$\phi = \frac{\text{slope} \times 10^4}{\log_{10} e} \times 1{\cdot}37 \times 10^{-16} \text{ ergs};$$

and since $h = 6{\cdot}547 \times 10^{-27}$ ergs/sec.,

it follows that

$$\lambda_c = \frac{3\times10^{10}\times 6{\cdot}547\times10^{-27}\times\log_{10}e}{\text{slope}\times10^{4}\times1{\cdot}37\times10^{-16}}.$$

Also $\log_{10}A_1=\log_{10}\frac{C}{T^{\frac{1}{2}}}+\frac{b_1}{T}\log_{10}e.$

To determine the multiplying constants A_1 and A_2, points are selected on the portions AB and CD respectively, where only one term is of importance in determining the value of the photo-electric current.

To determine A_1 :

$$T=1248^\circ\text{ C.}$$

$$C=23{\cdot}28\times10^{-7}\text{ amp.}$$

To determine A_2 :

$$T=405^\circ\text{ C.}$$

$$C={\cdot}35\times10^{-7}\text{ amp.}$$

TABLE III.

	AB.	A_1B_1.	CD.	C_1D_1.
Slope	·64	·64	·086	·11
b ° C.	$1{\cdot}46\times10^{4}$	$1{\cdot}46\times10^{4}$	$1{\cdot}98\times10^{3}$	$2{\cdot}53\times10^{3}$
ϕ ergs	$2{\cdot}02\times10^{-12}$	$2{\cdot}02\times10^{-12}$	$2{\cdot}71\times10^{-13}$	$3{\cdot}47\times10^{-13}$
λ_c A.U.	9700	9700	70,000	57,000
Constant ...	·0089	·0089	$2{\cdot}3\times10^{-7}$	$5{\cdot}11\times10^{-7}$

Thus the relation governing the photo-electric current can be represented by

$$C={\cdot}0089\,T^{\frac{1}{2}}e^{-\frac{1{\cdot}46\times10^{4}}{T}}+5{\cdot}11\times10^{-7}\,T^{\frac{1}{2}}e^{-\frac{2{\cdot}53\times10^{3}}{T}}.$$

The constant A_2 multiplying the larger work-function is $1{\cdot}8\times10^{4}$ times as great as the second. This supports the theory of "patches" put forward by Richardson and Young (Proc. Roy. Soc. Ser. A, 1925), indicating, as it does, that only a small portion of the surface responds to the lower frequency, while a much larger part, if not the whole surface, is excited by the higher frequency. If the whole of

the surface could respond to any of two or more threshold frequencies depending on the condition of the surface and illumination, the hysteresis effects could be explained. After being subjected for a few minutes to the illumination from the filament when at a high temperature, the "patch" of lower value ϕ might gradually acquire the larger value of the work-function, and so the current would increase, since at high temperatures, at any rate, the term containing the greater b predominates. When the filament temperature is reduced, this part of the surface does not revert to its former state directly, and while so reverting the current is larger than the corresponding one when ascending the scale of temperature. If this change does occur, it would also account for a creeping up of current noticed at high temperatures, the galvanometer mirror taking some time to come to a steady position. Consequently it seems probable that the whole of a sensitized potassium surface has one characteristic work-function, while certain small portions, distributed over the whole surface or collected together in patches, can possess one or more lower work-functions. When illuminated with light of long wave-length, only the smaller portion will contribute to the photo-electric current, and at shorter wave-lengths the rest of the surface plays its part, the smaller portion gradually changing until all the surface has acquired the greater work-function. This implies that the second constant A_2 is itself a function of the temperature. However, if the function is a low power of the temperature, it will have a negligible effect on the $\log_{10}\frac{C}{T^{\frac{1}{2}}}$ against $\frac{1}{T}$ graph and on the value of ϕ determined.

Summary.

No evidence has been found for the existence of a positive photo-electric emission, and it has been shown that, if such an effect does exist, it is less than 10^{-7} times the negative emission, from the same surface, measured in these experiments.

It is shown that potassium has at least two work-functions corresponding to the wave-length 9700 A.U. and 60,000 A.U. The results indicate that the "patches" of lower work-function form a very small part of the whole surface, and can acquire the greater work-function under the influence of prolonged illumination.

II. *A New Method of Determination of the Volume of* 1 *Curie Radon.* *By* L. Wertenstein, *Professor of the Free University, Warsaw* *.

I. *Principle of the Method.*

THE first determinations of the volume of 1 curie of radon were made by Rutherford †, Debierne ‡, and Ramsay§. Their results were concordant; the volume of 1 curie of radon at 0° and normal pressure (called in this paper V_0) was found equal to ·6 c.c. This value was in an excellent agreement with expectations from the theory of radioactive transformations based on the values of the fundamental radioactive and atomic constants as known at that period. The agreement is, however, not so good if one uses for calculations the values of those constants which are generally accepted at the present time. Adopting for Z the number of α-particles emitted in 1 sec. by 1 gm. Ra, $3{\cdot}72 \cdot 10^{10}$, for N, the number of molecules of a perfect gas in 1 c.c. at N.T.P. $2{\cdot}705 \cdot 10^{10}$, and for λ_r, the radioactive constant of radon, $2{\cdot}1 \cdot 10^{-5}$, we get for V_0 ·652 c.c. a value about 10 per cent. higher than the values obtained by Rutherford, Debierne, and Ramsay.

The methods used by those physicists were similar in principle; they consisted essentially in compressing carefully purified radon into a calibrated fine capillary.

The disadvantage of this method is that it is very difficult to prove that the final product is pure. Moreover, concentrated radon undergoes considerable changes of volume during the first hours after its preparation, and it is generally assumed that it is the final volume which is the right one.

It seemed to me interesting to attack this problem by a method which would permit the analysis of the purified radon. Owing to the extremely small quantities of gas involved, the only methods suitable for a quantitative analysis seemed to be methods based on the properties of highly rarefied gases. If we consider that the pressure of ·1 curie of radon in a volume of 100 c.c. is equal to about ·65 bar, we arrive at the conclusion that we are dealing in this problem with the range of pressure to which the laws of highly rarefied gases are fully applicable.

* Communicated by Sir E. Rutherford, O.M., P.R.S.

† E. Rutherford, Phil. Mag. p. 300 (1908).

‡ A. Debierne, *C. R.* p. 1264 (1909).

§ Gray and W. Ramsay, Trans. Chem. Soc. vol. iv. pp. 95, 1073 (1900).

The method described in this paper consists in measuring simultaneously the pressure and the coefficient of (external) friction of the gas. This coefficient is proportional in a highly rarefied chemically pure gas to its pressure and to the square root of its molecular weight, in a mixture of gases to the sum of the products of the pressure and the square root of the molecular weight of each constituent. The pressure was determined by means of a calibrated Knudsen gauge and the coefficient of friction by means of a quartz-fibre gauge. The "damping," indicated by this gauge as the inverse of the time during which the amplitude of the oscillations of the quartz fibre diminishes in a given ratio, is proportional to the coefficient of friction. Let p be the total pressure, p_r, p_x, p_y . . . partial pressures of radon and other gases mixed with it, M_r, M_x, M_y . . . molecular weights of these gases, d the damping. We shall have

$$p = p_r + p_x + p_y - \ldots .$$
$$d = a_r p_r + a_x p_x + a_y p_y + , \ldots \quad (1)$$

where $a_r = c\sqrt{M_r}$, $a_x = c\sqrt{M_x}$ . . . .

The constant c can be determined experimentally, and so we see that equations (1) enable us to calculate the partial pressure of radon if there is only *one* gas of known molecular weight mixed with the radon.

In a previous paper * I have shown that purified radon contains always, apart from water and mercury vapour, traces of all gases initially present with the radon. Of these gases, however, CO_2 is by far the most important, and it is the only one which condenses with radon at the temperature of liquid air.

It is obvious that we can apply the above method for determining the pressure of radon if we can analyse the mixture of radon and CO_2. This analysis can be made under good conditions if (1) it is possible to get rid of H_2O and Hg vapours, (2) the total pressure of the mixture is of the order of 1 bar, (3) the partial pressure of all impurities is small compared with that of radon.

Condition (1) is easily fulfilled. The only precaution is that the radon must be introduced into the apparatus through a trap cooled to $-120°$, at which temperature the saturated vapour pressure of water and mercury is smaller than 10^{-3} bar, while radon and CO_2 remain in the gaseous state. A suitable thermostat for this temperature consists in a

* L. Wertenstein, "On the Purification of Radon," Phil. Mag. vol. v. p. 1017 (1928).

pentane bath heated electrically, and contained in a moderately exhausted non-silvered Dewar tube, surrounded by liquid air.

If conditions (2) and (3) are satisfied, which we shall see to be the case in the present work, we determine (*a*) the total pressure, p_1, and damping, d_1, of the mixture, (*b*) the pressure, p_a, and damping, d_a, found when a small part of the apparatus is cooled to the temperature of liquid air. The differences $p_1 - p_a = \Delta p$ and $d_1 - d_a = \Delta d$ are the pressure and damping due to radon and carbon dioxide. In order to calculate the partial pressure p_r of the radon and the degree

Fig. 1.

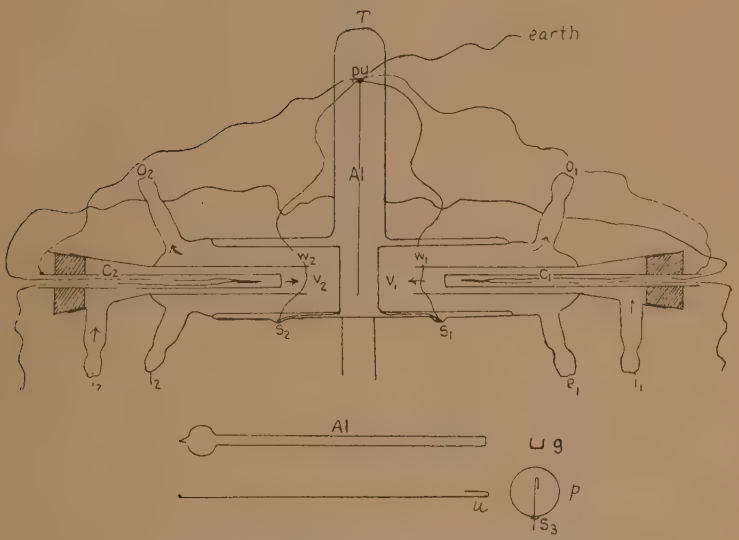

of its purity we have only to substitute in equations (1) Δp and Δd for p and d.

Knowing p_r we deduce V_0, the volume of 1 curie of radon at N.T.P., from the equation

$$V_0 = \frac{p_r \,.\, V \,.\, 273}{(273+t)\gamma 1{\cdot}013 \,.\, 10^6},$$

where V is the volume of the apparatus, t the temperature, and γ the quantity of radon expressed in curies.

II. *Gauges and their Calibration.*

The Knudsen gauge used in this work is shown in fig. 1. An aluminium leaf, about ·6μ thick, cut off in the form

shown in Al (fig. 1), hangs between flat and parallel faces the temperature of which can be changed by circulating water in vessels V_1 and V_2. l_1, l_2, i_1, i_2 o_1, o_2 is the system of inlet and outlet tubes used for this circulation. The difference of temperature of the vessels is measured by means of thermocouples b_1, b_2, and the deflexion of the leaf by means of a microscope provided with an eyepiece scale. We shall call "indication" π of the gauge the ratio of the deflexion

Fig. 2.

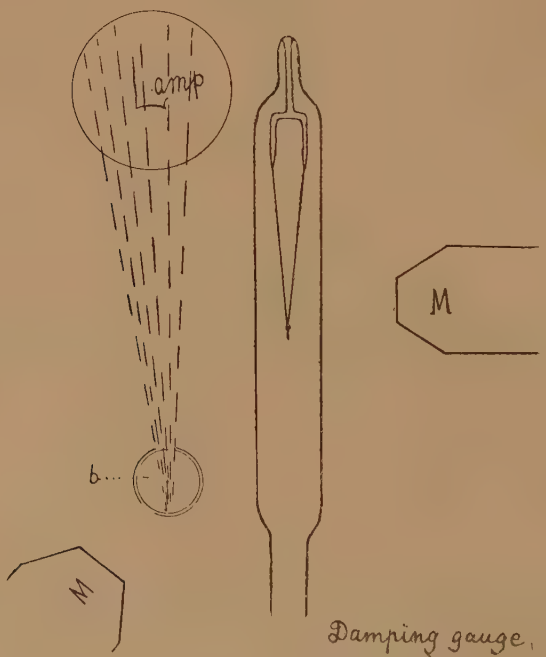

expressed in divisions of the microscope scale to the difference of temperatures expressed in divisions of the galvanometer scale.

The quartz-fibre gauge is represented in fig. 2. Its essential part is a system of two quartz fibres, about ·03 mm. thick, sealed at the lower end at a sharp angle, while the upper ends are sealed into a lead glass fork fixed in the top of an ordinary glass tube. The lower end bears a short piece of a ·1 mm. thick iron wire, by means of which the vibrations of the quartz system can be excited magnetically.

A microscope with an eyepiece scale is used for measuring the amplitude; if the illumination (shown on the left side of fig. 2) is convenient, the vibrating systems appear as a bright band with sharp ends. The band is seen to diminish slowly in width. The damping d is inversely proportional to the time during which the amplitude decreases in a given ratio.

For calculation purposes it was found convenient in this paper to use for this ratio the value 1·2 and to express the time in 10^5 sec.

For calibration, the gauges were joined to a McLeod gauge through a trap cooled to $-120°$ in order to freeze out vapours. By means of a mercury fork the apparatus could be put into communication with a diffusion pump or with auxiliary arrangements for preparing and transferring small quantities of chemically pure gases. Hydrogen, oxygen, carbon dioxide, and xenon were used for calibration.

The whole apparatus must be thoroughly evacuated, after which we read the pressure p_0 at the McLeod gauge and the indications π_0 and d_0 of the Knudsen and damping gauges. p_0 is generally negligibly small. π_0 and d_0 correspond, under good experimental conditions, to a residual pressure of the order of ·01 bar. This pressure is due to traces of water and mercury vapours, to which the McLeod gauge is insensitive.

We introduce into the apparatus one of the above-mentioned gases under a pressure of 2–3 bars, and we read the indications p_1, π_1, d_1, of all instruments. We pump some gas off and obtain a new set of values p_2, π_2, d_2.

These operations are repeated until the pressure drops to about ·5 bar.

For each of the gases (k) used in this calibration we draw curves $\pi_k = f(p)$ and $d_k = \phi(p)$.

The functions are linear, and we have $\pi_k = b_k p + \pi_0$, and $d_k = a_k p + d_0$.

It is generally assumed that the Knudsen gauge is an absolute manometer, *i.e.*, that its indications are independent of the nature of the gas. If this were true b_k ought to have for all gases the same value.

If, however, we examine this question more closely, we find that the force exerted on the leaf must depend on the kinetic energies of the molecules falling on it and reflected from it. If the temperatures of the faces between which the leaf hangs are given, these energies are functions of the accommodation coefficient of the gas filling the gauge. The accommodation coefficient increases in general with the

molecular weight ; it has for hydrogen the value ·28, for oxygen ·8, for carbon dioxide ·87. The highest value, ·93, has been found for mercury vapour. Its upper theoretical limit is unity.

General considerations show that the indications of a Knudsen gauge, *i. e.*, the constant b_k, must increase with the accommodation coefficient. In accordance with these considerations I have found for the four mentioned gases

$$b_{H_2} : b_{O_2} : b_{CO_2} : b_{Xe} = 79 : 100 : 104 : 105.$$

For our problem it is necessary to know the radon constant b_r. We cannot determine it directly. We see, however, that the values of b for the last three gases show only small variations. Assuming for b a value 1 per cent. higher than that of Xe, we are probably very close to the true value, for it must be expected that radon and xenon will behave in a very similar way.

During the course of the experiments the leaf had once to be changed and recalibrated. Before the change the sensitivity b_r of the gauge for radon was ·0707 division of microscope per 1 bar and 1 division of the galvanometer scale. After the change b_r was ·096 division of microscope per 1 bar and 1 division of the galvanometer scale. The deflexion of the galvanometer in actual experiments corresponded generally to 50 to 100 divisions and the deflexion of the leaf could be determined within 1/10 of a division, so that for pressures of the order of 1 bar the accuracy of measurement was about 1 per cent.

In the case of the damping gauge the problem of finding the constant a_r for radon is much easier as we have only to apply the formula

$$a_r/a_k = \sqrt{\frac{\overline{M}_r}{\overline{M}_k}}.$$

being the expression of Knudsen's law.

We can get a check of this formula by comparing the values a_r calculated from experimental values a_k for each of the gases used in the calibration. The comparison is represented on Table I.

The agreement is very good. I have used for calculations the value $a_r = 1164$, being the arithmetic average of values extrapolated from the oxygen and xenon data, which were obtained under the best conditions.

For CO_2 I have assumed the value $a_c = 517$ calculated from the same data. It seemed to me more reliable than the measured value 506, because the adsorption properties

of this gas described in a previous paper* obviously introduce some uncertainty in determinations of its pressure.

In equation (1) it was assumed implicitly that the indications of a Knudsen gauge do not depend on the nature of

TABLE I.

Gas.	Mol. weight.	a_k.	a_r.
Hydrogen	2·015	111·5	1175
Oxygen	32	442	1168
Carbon dioxide	44	506	1137
Xenon	130	890	1160

the gas. In reality, however, the experiment does not give us Δp, but

$$\Delta\pi = b_c p_c + b_r p_r.$$

Putting $b_c = \cdot 98 b_r$ we can write these equations:

$$\left.\begin{aligned} \Delta p' = \frac{\Delta\pi}{b_r} &= p_r + \cdot 98 p_c \\ \Delta d &= 1164 p_r + 517 p_c \end{aligned}\right\} \quad . \quad . \quad . \quad . \quad (1a)$$

$\Delta p'$ is an apparent change of pressure, *i.e.*, a change of pressure to which a change $\Delta\pi$ of indications of the gauge would correspond if the gas was pure radon.

From equations (1*a*) we get, writing for simplicity Δp instead of $\Delta p'$,

$$p_r = \frac{\cdot 98\Delta d - 517\Delta p}{623} \qquad p_c = \frac{1164\Delta p - \Delta d}{623}.$$

III. *Experimental arrangement.*

The apparatus has been constructed in such a way that purified radon could be introduced without having to open the apparatus to the atmosphere.

This precaution is essential, for since the pressure of the admitted gases is of the order of 1 bar, the apparatus must be exhausted beforehand to a "high vacuum." As is well known, such a state is destroyed if atmospheric air is admitted even for a short time.

* L. Wertenstein, *l. c.*

The general arrangement can be seen from fig. 3. It comprises three parts: (1) the manometric part with the Knudsen gauge K and damping gauge D and the trap T; (2) the purification apparatus A containing KOH and P_2O_5 in glass boats, CuO and Cu in a pyrex tube, and the tube *l* used for condensing radon in liquid air; and (3) the volumetric part, the use of which will be explained later. All parts can be evacuated by way of the mercury fork *f*. Part A can be put into communication with remaining parts by means of the mercury "tap" M operated electromagnetically.

Fig. 3.

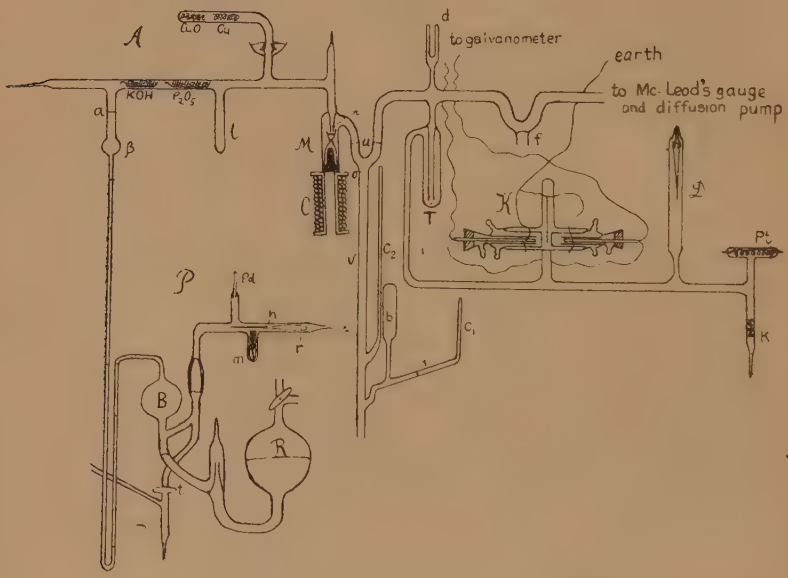

Before the experiment the whole apparatus has to be very carefully exhausted. The first operation consists in introducing partially purified radon into Part A by means of the transfer pump P, which has the advantage of avoiding the use of greased taps. The left branch of the capillary U-shaped tube has more than the barometric length, and, owing to this fact, it is possible to introduce air into the bulb B, while vacuum remains in A and other parts.

While the transfer pump is open to air we place in the horizontal tube *p* a thin-walled tube *r* containing partly purified radon (about ·2 c.c. of gas), after which the tube *p* is sealed.

The bulb B is evacuated by means of a separate pump through the tap *t*, which is afterwards closed and covered with a column of mercury. The tube *r* is then broken by means of a simple magnetic device *m* and the radon is transferred to the purification part by operating the transfer pump, in which the movements of mercury are controlled by varying the pressure over the reservoir R. The radon is then left for 15–18 hours in contact with the KOH and P_2O_5.

At the beginning and at the end of that period the pyrex tube containing CuO is heated for 30 minutes to about 600°.

After that time the radon contains only a small quantity of CO_2, but an appreciable amount of gases which do not condense at the temperature of the liquid air. In order to pump out these gases, we surround the tube *l* with liquid air and open several times for 10 seconds the "tap" M, the mercury fork establishing the communication with the diffusion pump. When the evacuation is finished, the communication with the diffusion pump is cut off, the tube *l* allowed to warm up, and radon is distilled into the manometric apparatus by introducing a few drops of liquid air in the small Dewar tube *d*. After that we raise the mercury in the tube V, enclosing radon in the manometric part.

We can now proceed to determinations of pressure and damping. While the radon and CO_2 are still condensed in the small Dewar tube *d* we measure the residual pressure p_a and damping d_a of uncondensable gases. The liquid air is then evaporated quickly by introducing a copper wire into the small Dewar tube, and when this tube is at room temperature we determine the total pressure p_1 and damping d_1.

We get in this way the values Δp and Δd defined on page 23. Liquid air can be used again in the same way as described above in order to obtain another set of values of Δp and Δd.

IV. *Results.*

I have executed in all four series of experiments. The first two series were of a preliminary character ; they enabled me to work out the technique of the measurements, and also revealed some unforeseen experimental difficulties.

It was found that after introduction of radon the pressure and damping increased steadily, so that after some 30 minutes the pressure was twice as great as in the beginning. This increase is due to the evolution of gases from glass bombarded by α-rays. The increase of damping was, however, very small, and by measuring simultaneously the rate of increase of

pressure and damping, I found that the evolving gas was nearly pure hydrogen, so that the relative amount of CO_2 remains unchanged. This observation enabled me to calculate Δp and Δd in the following way :—

Curves $p_1 = f(t)$, $d_1 = p(t)$ were drawn for the total gas and similar curves for uncondensable gases. By taking the difference of ordinates of curves interpolated for the same time t, we get the values of Δp and Δd. Owing to the small number of experimental points [each determination takes a long time] the interpolations were a little uncertain. The results were, however, better than could be expected.

In the first experiments ·0718 curie of radon was introduced into the apparatus. Its volume V was 157 c.c., the temperature of the room was 19°.

Three sets of measurements were taken. After the first set the radon was distilled back into the purification part, the evolved gases were pumped out and redistilled into the manometric part. During these operations ·0018 curie radon was lost.

The results are represented in Table II. The first column of this table contains the value of Δp ; the second and third give the partial pressures p_r and p_c of radon and CO_2, in the fourth we find the relative amount (or degree of purity) of the radon, in the fifth the quantity of radon in curies, in the sixth the value V_0 of the volume of 1 curie of radon deduced from the experimental data.

Table II.

Δp bar.	p_r bar.	p_c bar.	$\frac{p_r}{\Delta p}$.	γ curie.	10^{-4} c.c.
·55	·289	·261	·528	·0718	5·83
·537	·323	·114	·749	·070	6·68
·465	·285	·180	·63	·070	5·9

The average value of V_0 is $6{\cdot}14 \cdot 10^{-4}$ c.c., showing that the method gives results very near to the truth even under unfavourable conditions.

In order to improve these conditions it was necessary to eliminate the effect of the gases evolved from the glass walls by the bombardment of the α-particles.

The measurements of damping indicating that the evolving gases consisted chiefly of hydrogen, I added to the apparatus

a device for oxidizing the hydrogen. The water-vapour formed on oxidation ought to be condensed in the trap cooled to $-120°$.

For this purpose I used a small tube, Pt (fig. 3), containing a thin platinum wire through which a current could be sent. The platinum wire was covered by electrolysis with copper oxidized afterwards by glowing the wire.

It was found that this simple device enabled me to realise the steady conditions necessary for taking reliable measurements. The next experiment performed with this arrangement was, however, not quite satisfactory owing to some imperfections of the technique. The temperature of the glowing wire was not adjusted to the right value ; during the experiment the temperature of the trap went up to $-105°$. The result was that the evolution of gas was still half as much as in the first experiment, and the water-vapour formed was not completely removed by the trap, as was shown by the fact that the pressure of *condensable* gases increased steadily, while in the previous experiment it remained constant.

It was, however, found possible to deduce from the measurement the partial pressure of radon. Δp and Δd being in this case due to three gases, radon, CO_2, and H_2O, it was necessary to calculate the amount of water-vapour. This was done in the following way. By measuring simultaneously the increase of total pressure and damping, we can analyse the evolving gas consisting of hydrogen and water-vapour and determine the partial pressure of water-vapour. The additional damping due to that vapour can be calculated from its molecular weight. Subtracting from Δp and Δd the partial pressure and damping due to water-vapour, we have again the case of two constituents only, to which equations (1*a*) are applicable.

In this experiment ·1386 curie radon was used.

The volume of the apparatus was 180 c.c. The results of two sets of measurements are shown on Table III.

TABLE III.

Δp bar.	p_r bar.	p_c bar.	$\frac{p_r}{\Delta p}$.	γ curies.	$\frac{V_0}{10^{-4}}$ c.c.
·817	·519	·298	·635	·1386	6·2
·961	·527	·434	·55	·1386	6·29

The larger amount of CO_2 in the second set is probably to be explained by the fact that in the interval between the two sets radon was kept condensed during about 15 minutes in order to pump off evolved gases. As was shown in my previous paper, glass contains always traces of absorbed CO_2 which distil on to the radon during its condensation in liquid air.

The agreement of values of V_0 obtained in the two sets is satisfactory. The method of calculating the results is, however, complicated, so that these experiments cannot be considered as conclusive.

Fig. 4.

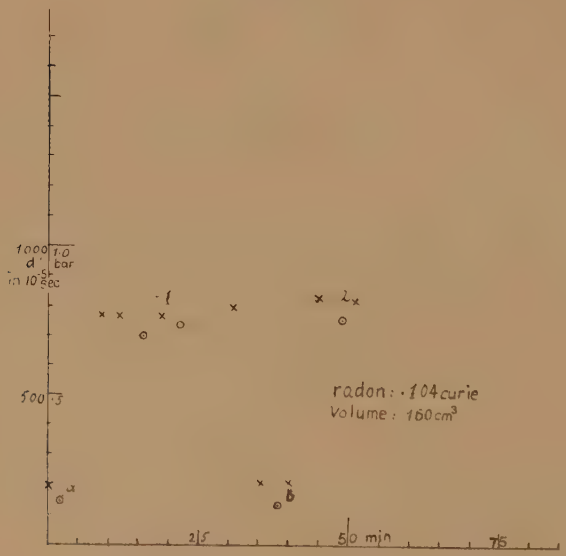

In the third and fourth experiments, which will be described now, I succeeded in surmounting the experimental difficulties of the problem. In these experiments (1) the whole apparatus was baked out to 350° before the introduction of radon, (2) a tube containing a few pieces of KOH was added in order to reduce the amount of CO_2, (3) the temperatures of the glowing wire and of the trap were carefully adjusted. The volume of the apparatus was 160 c.c., ·104 curie radon was used in the third, and ·176 curie in the fourth experiment.

The results are represented graphically in figs. 4 and 5. In these figures the values of pressures are represented by

crosses, the values of damping by circles. Groups of points and circles marked by figures 1, 2, etc., were obtained with total gas, those marked by letters *a*, *b*, etc., with uncondensable gas only. The group marked 4 on fig. 5 was obtained after the current through the Pt wire was cut off. This group shows that hydrogen is still evolved but disappears nearly completely when the CuO is heated, as may be seen from the approximate constancy of the pressure of the total

Fig. 5.

gas during the first period of the experiment. The oscillation of individual values of total pressure and damping are relatively small, those corresponding to uncondensed gases are more important, which is probably due to the smallness of effects observed. There was still a slow general increase of pressure, about 8 per cent. during a whole experiment. In order to eliminate the error due to this residual evolution of gas, the results have been calculated in the following way

For each group an arithmetic average p_1, d_1, p_a, d_a, etc., was calculated. From these values Δp, Δd were calculated as

$$\frac{p_1+p_2}{2}-p_a \ldots\ldots, \quad d_2-\frac{d_a+d_b}{2}, \text{ etc.}$$

The final results are collected in Table IV.

TABLE IV.

Experiment.	Δp bar.	p_r bar.	p_c bar.	$\frac{p_r}{\Delta p}$.	γ curie.	$\frac{V_0}{10^{-4}}$ c.c.
3	·586 ·597	·433 ·454	·143 ·143	·75 ·77	·104	6·15 6·41
4	·896	·743	·153	·825	...	6·26
	·909	·753	·153	·825	·176	6·33
	·908	·808	·1	·89	...	6·8

It will be noticed that the degree of purity of radon was in these experiments higher than in the first experiments.

The average value of V_0 is $6{\cdot}39 \cdot 10^{-4}$ c.c., and is probably correct within 5 per cent.

The average of the values obtained in the first two experiments is $6{\cdot}19 \cdot 10^{-4}$ c.c., differing by about 3 per cent. from the final value. This small disagreement shows that with this method even in very imperfect conditions relatively good results can be obtained.

The constant V_0 is connected directly with the number of α-particles emitted in one second by 1 g. Ra. From $V_0 = 6{\cdot}39 \cdot 10^{-4}$ c.c., we get $Z = 3{\cdot}62 \cdot 10^{10}$.

The method described in this paper could be further improved by constructing more sensitive gauges. The main difficulties arise from the violent effects taking place in presence of radon. It would therefore seem desirable to find a material which does not give off gases when bombarded by α-rays *. On the other hand, it seems that the method could be applied successfully to another similar problem, viz., the determination of the volume of He produced in one second by 1 g. Ra.

* Since this paper was written I have found that glass baked out to a temperature of 450° does not give out any appreciable amount of gas under the action of α-rays.

V. *Determination of* V_0 *by use of Capillary Tubes.*

The results of this work show that I was unable to obtain pure radon ; the relative amount of CO_2 varied in different experiments from 15 per cent. to 45 per cent. of the total quantity of gas. It will be remembered that in the method of compressing the purified radon into a capillary tube the initial volume undergoes generally a marked diminution ranging from 30 per cent. to 50 per cent. of its final value. It seems clear that in this method also pure radon was not obtained by use of chemical processes only. It is highly probable that the final purification takes place in the capillary, the impurities being absorbed by glass under the action of α-rays.

In order to throw some light on this question, I have executed some experiments by the method of the capillary tube using an apparatus described in a previous paper*, and also the arrangement shown on fig 3. To the vertical tube V a sloped tube S, ending in a calibrated capillary C_1, was sealed. Another capillary C_2 of the same bore as C_1 sealed to V, allowed the pressure of compressed gas to be determined by means of a cathetometer. The use of the bulb b will be explained later.

The first experiment was performed with the apparatus described in my previous paper. The results were very similar to those obtained by Rutherford. 40·5 millicuries radon were introduced into a capillary. The contraction amounted to 30 per cent. of the final value, which corresponded to $V_0 = 6{\cdot}4 \,.\, 10^{-4}$ c.c.

It would seem surprising that in presence of rarefied radon gas is evolved, while the concentrated radon acts as a "clean-up" agent. This apparent contradiction is easily explained if we consider that the first effect is due to collisions between α-particles and the walls of the apparatus, while the second one is a consequence of collisions between molecules and α-particles. It is probable that, in analogy with the clean-up effects observed in a triode valve, ionized or excited molecules are readily absorbed by the material of walls. If the pressure is very low the number of collisions with free molecules is negligibly small, and therefore under these conditions the evolution of gas is more important than its absorption.

In a concentrated state radon atoms as well as molecules of impurities are struck by α-particles, and it seemed there-

* L. Wertenstein, *loc. cit.*

fore probable that radon itself may be partly absorbed in the capillary tubes.

In order to verify this hypothesis I have tried to repeat the experiment with radon as pure as possible ; if radon was absorbed, the final volume ought to be smaller than its theoretical value.

I have used for this experiment radon the degree of purity of which has been tested by the "damping" method. This radon was distilled into the tube S (wrapped for this purpose, as usual, with cotton wool, soaked in liquid air). This tube contained some fused KOH in order to diminish further the amount of CO_2. Before compressing the radon into the capillary, it was submitted to another kind of purification based on laws of flow of highly rarefied gases. For that purpose the bulb *b*, connected to S through a ·5 mm. wide capillary, was used. After the radon had been condensed, mercury was brought into such a position that the communication with *b* was shut off. When the radon was set free after removal of liquid air, the mercury was lowered for a few seconds below the opening of the capillary.

During that short time a part of the radon passed into the bulb *b*, but, according to the laws of flow of gases, the relative amount of CO_2 which went to this bulb must have been much larger. The remaining gas was introduced into the capillary C_1.

The results of the experiment confirmed my hypothesis. The initial volume of the radon corresponded to $V_0 = 5{\cdot}9 \,.\, 10^{-4}$ c.c., the final volume (determined on the next day and corrected for radioactive decay) to $V_0 = 4{\cdot}34 \,.\, 10^{-4}$ c.c.

We see that nearly 30 per cent. of the radon was absorbed.

In order to ascertain the nature of this absorption the radon was pumped out and the tube heated during exhaustion to 200°. Subsequent measurements of the γ-ray activity showed that the tube retained about 20 per cent. of the initial quantity of radon (taking account of the radioactive decay).

The amount of concentrated radon absorbed on glass seems to increase with the time during which the radon is kept in the capillary. In another experiment performed with less pure radon the initial volume corresponded to $V_0 = 7{\cdot}91 \,.\, 10^{-4}$ c.c., the final value, measured on the next day, to $6{\cdot}2 \,.\, 10^{-4}$ c.c. After four days the radon was pumped off as in the previous experiments. It was found that the glass retained strongly 40 per cent. of the initial quantity of radon absorbed.

It is probable that the "clean-up" effect of α-rays is selective. It is obviously much smaller for radon than for other gases, and this explains probably why the method of the capillary tube gives in general results very close to truth.

The work described in this paper was performed during the years 1925/1926 and 1926/1927 in the Cavendish Laboratory.

It is a great pleasure for me to express my best thanks to Sir Ernest Rutherford for his kindness in receiving me in the Cavendish Laboratory, in placing at my disposal the large quantities of radon and other experimental resources, and in showing a permanent interest in the progress of my work.

I am grateful to Dr. J. Chadwick for his help and interest.

My stay in England was made possible by a fellowship granted by the International Education Board.

I wish to express my thanks to this Board.

III. *The Classical Reasonableness of the Quantum Theory and Simple Operative Solutions of Schrödinger's Equation.* *By* Prof. A. Press*.

Part I.

The Differential Equation of an Excitation Field.

In a paper appearing in the Philosophical Magazine for Dec. 1927, the writer likened the action of a radiating harmonic oscillator to that of a reed or organ-pipe fed by a source of air under pressure. As the pressure was increased the organ-pipe responded but slightly to an increase in intensity of the note emitted, for a point was soon reached when the dominant note suddenly changed to a higher harmonic. It was later shown by strictly classical analysis that the amplitude of the radiation wave always bore a definite ratio to the amplitude of the normal non-radiating component. In the following, therefore, reference to the normal non-radiating component will be sufficient.

For the pipe above referred to, the excitation field contemplated would be that due to the blowing stream causing it to emit a note. It will be on the basis of the above analogy with the radiating harmonic oscillator that the following analysis will be developed. In general there will be a

* Communicated by the Author.

variable velocity potential P in such an exciting stream because of the action of the organ-pipe wall of the slit or the reed, which, due to the vibrations, affects the distribution of pressure head in the stream contiguous thereto. As the slit wall or reed vibrates outwardly and inwardly the stream becomes blocked and more open alternately. The wave-front of pressure intensity (and therefore of velocity potential) will travel backwards along the stream toward the source as long as the slit wall in its alternations gives freer egress to the excitation stream. With the return of the slit wall or reed and the blocking of the stream, the wave-front of pressure intensity (and therefore of velocity potential) returns in the direction of the stream-flow. There is thus an alternation of the wave-front position along the stream depending on the frequency of the note emitted. The equation of the velocity potential therefore becomes

$$\frac{\partial^2 P}{\partial x^2} = \frac{1}{u^2}\frac{d^2 P}{dt^2}, \quad \ldots\ldots\ldots \quad (1)$$

with u as the velocity with which a disturbance can travel along the stream for a given mean velocity w of the stream itself.

Relationship between the various Velocities concerned.

As the momentary velocity w of the stream is increased relative to x, the momentary velocity u at x, with which any disturbance in the velocity potential can proceed, will diminish in value, but correspondingly the momentum at any moment of the slit wall or reed (mv), and therefore the velocity v, will increase. That is to say, although there is phase correspondence between the v of the alternating slit wall or reed and u with which the phase of the potential disturbance travels with respect to the excitation stream velocity w at x, the one velocity v increases, whereas the u at any x diminishes inversely with increasing w. The above complies with one of Schrödinger's * conditions, in which u represents the velocity of his ψ-function, and v the momentary velocity occurring in the kinetic energy expression of Hamilton's function E_0.

Postulates of the Mechanical Constraints

If, now, in the hypothetical case of a "Radiating Harmonic Oscillator" the maximum kinetic energy of the alternating member due to its extreme position (analogous to that of

* See Schrödinger, "Undulatory Mechanics," Phys. Rev., Dec. 1926.

the slit wall or reed above) is so limited that we have a connecting equation of the type

$$\nu = \frac{E_0}{\frac{3}{4}h_0'} = \frac{E_0}{h_0'} = \frac{1}{\frac{3}{4}h_0'}\left(\tfrac{1}{2}mv^2_{\max.}\right)^*, \quad . \quad . \quad . \quad (2)$$

then the function solving equation (1) must be of the form

$$P = P(x) \,.\, \sin\left(\frac{2\pi E_0}{h_0}t\right). \quad . \quad . \quad . \quad . \quad (3)$$

This will enable a considerable simplification to be performed in solving symbolically equation (1).

It has already been stated that u, at any moment pertaining to the instantaneous velocity of the P wave-front, is inversely proportional to the mean stream velocity w. Similarly the v of the kinetic energy term, having reference to the radiator (the wall of the slit or reed, as it were), is for the same moment directly proportional to the mean stream velocity w. It would be therefore reasonable to write that

$$u = h_1\frac{E_0}{mv} = h_1\frac{\left(\frac{1}{2}mv^2_{\max.}\right)}{mv}, \quad . \quad . \quad . \quad . \quad (4)$$

and the Fourier law of dimensions will be satisfied.

Schrödinger's Differential Equation. Split Form of Planck's Constant.

By virtue of equation (2), the solution of equation (1) being of the form

$$P = P(x) \,.\, \sin\frac{2\pi E_0}{h_0}t, \quad . \quad . \quad . \quad . \quad . \quad (5)$$

this enables us to write symbolically that

$$\frac{d^2}{dt^2} = -\frac{4\pi^2 E_0^{\,2}}{h_0^{\,2}} = -\frac{4\pi^2}{h_0^{\,2}}\left(\tfrac{1}{2}mv^2_{\max.}\right)^2. \quad . \quad . \quad (6)$$

Making use of the latter, (1) transforms to

$$\frac{\partial^2 P}{\partial x^2} + \frac{4\pi^2 E_0^{\,2}}{u^2 h_0^{\,2}}P = 0. \quad . \quad . \quad . \quad . \quad . \quad (7)$$

There then remains to express u in terms of E_0 by virtue of (4). Introducing the latter, we have that

$$\Delta P + \frac{8\pi^2 m}{\left(\frac{3}{4}h_0' h_1\right)^2}\left(\tfrac{1}{2}mv^2\right)P = 0, \quad . \quad . \quad . \quad . \quad (8)$$

* The justification of this type of Quantum Formula will be gone into later. See end Part I.

indicating that what Schrödinger calls Planck's constant h is in the above analogy really given by the following split form, namely

$h = \frac{3}{4}h_0'h_1 =$ Planck's constant

= (proportionality factor for the frequency with respect to the normal energy content) × (proportionality factor of the phase velocity in the stream with respect to the inverse of the velocity of the radiator *. . . . . (9)

To throw equation (8) into the form used by Schrödinger with such telling effect, we note that the kinetic energy $\frac{1}{2}mv^2$ is really given by

$$E_0 - V = \tfrac{1}{2}mv^2, \quad . \quad . \quad . \quad . \quad . \quad (10)$$

where V is the potential (elastic energy content analogously of the flexed slit wall or reed), and E_0 is the maximum energy content, kinetic plus potential, which for any given frequency is conservatively a constant. Thus we have that

$$\Delta P + \frac{8\pi^2 m(E_0 - V)}{h^2}P = 0, \quad . \quad . \quad . \quad (11)$$

where the P above corresponds to Schrödinger's ψ-function.

If, now, the excitation stream is considered expressible by means of the radius coordinate r instead of the x, then V can also be expressed in the form

$$V = \frac{-e^2}{r}, \quad . \quad . \quad . \quad . \quad , \quad (12)$$

where e is the electronic charge. Then, as Schrödinger has shown, E_0 must conform to the requirement

$$E_0 = \frac{-2\pi^2 me^4}{h^2 n^2}; \quad n = 1, 2, 3, 4, \quad . \quad . \quad (13)$$

in order that finite single-valued solutions shall follow. The whole quantum theory therefore hinges on the above apparently classical type of development. A simple derivation of (13) by Operator Methods will be given herewith.

The Hamiltonian Mechanics of the Radiating Harmonic Oscillator.

It is well to bear in mind that, if $\dot{e}$ in electrical theory is the applied force and q is the displacement, the work equation is

$$\partial H = \dot{e}\,\partial q, \quad . \quad . \quad . \quad . \quad . \quad . \quad (14)$$

* See footnote with reference to (2).

and for hysteresis as well as radiation the $\dot{e}$ is not in time-phase with the displacement $\dot{q}$. Thus, if

$$\left.\begin{aligned} \dot{q} &= q_1 \sin \nu t + q_2 \cos \nu t = (q_1 + q_2 j) \sin \nu t, \\ \dot{e} &= e_1 \sin \nu t + e_2 \cos \nu t = (e_1 + e_2 j) \sin \nu t, \end{aligned}\right\}^{*} \quad (15)$$

then with

$$\dot{q} = \dot{k}\dot{e}$$

the $\dot{k}$ is complex, time operationally, and is of the form

$$\left.\begin{aligned} \dot{k} &= k_1 - k_2 j, \\ \text{with} \quad \nu j &= \frac{d}{dt}. \end{aligned}\right\} \quad \ldots\ldots \quad (15\,a)$$

Adopting, now, Maxwell's definition of momentum $\dot{p}$, we can write

$$\frac{\partial \dot{p}}{\partial t} = \dot{e}, \quad \ldots\ldots \quad (15\,b)$$

which leads to the equation

$$\dot{q} = -\nu^2 (k_1 - k_2 j) p_0 \dagger \quad \ldots\ldots \quad (16)$$

That is to say, whenever radiation occurs the momentum p is not to be taken in time-phase with the velocity $\dot{q}$ of the displacement. The out-of-phase component corresponds to the radiation requirement.

The Modified Hamiltonian Equations of motion for radiation can now be written as

$$d\dot{\mathrm{H}} = \frac{\partial \dot{\mathrm{H}}}{\partial \dot{q}} d\dot{q} + \frac{\partial \dot{\mathrm{H}}}{\partial \dot{p}} d\dot{p},$$

where it would follow, if $\dot{\mathrm{H}}$ diminishes with $\dot{q}$, that then, by virtue of (14) and (15), we should adopt the minus sign and write

$$\frac{\partial \dot{\mathrm{H}}}{\partial \dot{q}} = -\dot{p}\,; \quad \frac{\partial \dot{\mathrm{H}}}{\partial \dot{p}} = \dot{q}. \quad \ldots\ldots \quad (17)$$

Note that the first of (17) is of potential type and the second of (17) kinetic or motional. Now, solving equations (17) in the light of (16), and adopting the form provisionally that

$$\dot{p} = p_0 \sin \nu t, \quad \ldots\ldots \quad (18)$$

* See paper by writer in Phil. Mag. (Dec. 1927) for this type of analysis in radiation theory.

† For the interpretation of this formula in terms of mechanical momentum and the reaction equivalence for radiation, see further.

it follows, after integration, that

$$\ddot{H} = -\frac{\nu^2 k_1}{2} p^2 + k_2 \nu p \dot{p} - \dot{p} q. \quad . \quad . \quad . \quad (19)$$

The latter leads to the equations :

$$\left.\begin{aligned} \ddot{H} &= \ddot{E}_0 + \ddot{H}_v, \\ \text{where} \quad \ddot{H}_v &= \tfrac{1}{4}\nu^2 p_0^2 k_1 \cos 2\nu t, \\ \dot{E}_0 &= \tfrac{3}{4}\nu^2 p_0^2 k_1. \end{aligned}\right\} \quad . \quad . \quad . \quad . \quad (20)$$

The last of (20), since it is independent of time, applies to the conservative part of the system, whereas the second or H_v represents the radiation term of energy. The conclusion is then forced upon us, that whenever *simply sinoidal* radiation takes place from an harmonic oscillator, then the condition is *ipso facto* imposed, with regard to amplitudes, that

$$\frac{E_0}{H_v} = 3. \quad . \quad . \quad . \quad . \quad . \quad . \quad (21)$$

In other words, a pure radiative harmonic action of an oscillator cannot exist classically save under the condition that the radiation system regularly absorbs and radiates energy equal to one-third of its normal non-radiating content. The above therefore explains why E_0 alone can be used in the Schrödinger equation.

Relationship of Momentum to Velocity.

Turning to the justification of equation (2), which is fundamental in Quantum Theory, by the aid of (15) and (15 *a*) we have for the velocity the expression

$$\dot{q} = \frac{d}{dt} q = q_1 \frac{d}{dt} \sin \nu t + \frac{1}{\nu} q_2 \frac{d^2}{dt^2} \sin \nu t$$

$$= -q_2 \nu \,.\, \sin \nu t + q_1 \,.\, \frac{d}{dt} \sin \nu t. \quad . \quad (23)$$

With respect to a true mechanical momentum p (of non-radiative character therefore), it follows, postulating as before

$$p = p_0 \sin \nu t, \quad . \quad . \quad . \quad . \quad . \quad . \quad (18)$$

that by virtue of (16) we have

$$\dot{q} = -\nu^2 k_1 p_0 \sin \nu t + \nu k_2 p_0 \frac{d}{dt} \sin \nu t. \quad . \quad . \quad (24)$$

It is the first term that corresponds to the mechanical momentum component sought, since (18) itself involves the

sine function of the time. The second term of (24), which is radiatively necessary, then complies with the second of (23). That is to say, with regard to the "velocity complex" $\dot{q}$, the first or real part gives the true velocity component growing out of an actual bodily displacement of the slit wall or reed. *The second or imaginary component of* $\dot{q}$ *in* (16), *which really depends on the rate with which the bodily displacement takes place, has reference to the radiation reaction.*

Equating coefficients for the first terms of (23) and (24), we have

$$\nu^2 k_1 p_0 = -q_2 \nu$$

$$\text{or} \qquad \nu k_1 p_0 = q_2. \quad . \quad . \quad . \quad . \quad . \quad . \quad (25)$$

Yet for a reed flexing merely to produce a fundamental the bodily velocity will be relatively small, but the maximum displacement q_2 will be large. On the other hand, for an overtone the displacement q_2 will be relatively small (whether due to a note produced because of the progressive flattening of the reed or not *), but the momentum p_0, and therefore the velocity v, will be large. We are therefore justified in assuming the possible proportionality

$$q_2 = \frac{h_0'}{p_0}. \quad . \quad . \quad . \quad . \quad . \quad . \quad (26)$$

If, then, this is equated to (25), to find the value of k_1 we have that

$$h_0' = \nu k_1 p_0^2. \quad . \quad . \quad . \quad . \quad . \quad . \quad (27)$$

Substituting in the classical requirement of (20), we have that

$$E_0 = \tfrac{3}{4} h_0' \nu = h_0 \nu \quad . \quad . \quad . \quad . \quad . \quad (28)$$

which clearly suggests Planck's Quantum formula.

Part II.

The Differential Equation for the Balmer Series.

Given the equation (1), namely

$$\frac{d^2 P}{dt^2} = u^2 \Delta P, \quad . \quad . \quad . \quad . \quad . \quad . \quad (1)$$

* In the case of the Harmonica or "mouth-organ" a visible flattening of the reed takes place. In fact, with too much air-pressure the slot becomes closed and no note is emitted.

the symbolical solution leading to (5) above would be of the form

$$P = A(r, \theta, \phi) \cdot \epsilon^{(u \cdot \Delta^{1/2})t} *. \quad . \quad . \quad . \quad (27')$$

The latter will lead to a sinoidal time function such as (5), provided it can be shown that $u\Delta^{1/2}$ as an operator really can be made equal in succession to a series of constants (Eigenwerthe) which are imaginary and not real.

Consider, then, preferably the argument P of the type

$$\left.\begin{array}{ll} & P = RYT, \\ \text{where} & T = f(t), \\ & Y = F(\theta, \phi), \\ & R = F(r). \end{array}\right\} \quad . \quad . \quad . \quad . \quad . \quad (27\,a)$$

Introducing the latter into ΔP and noting that

$$\Delta = \frac{\partial^2}{\partial r^2} + \frac{2}{r}\frac{\partial}{\partial r} + \frac{1}{r^2}\left\{\frac{1}{\sin^2\theta}\cdot\frac{\partial^2}{\partial\phi^2} + \frac{\partial^2}{\partial\theta^2} + \cot\theta\cdot\frac{\partial}{\partial\theta}\right\}, \quad . \quad . \quad . \quad (28\,a)$$

it is quickly seen that

$$\Delta P = TY(\Delta R) + TR(\Delta Y),$$

and Y can preferably be taken as a surface zonal harmonic. Since on substituting $r^l Y_l$ in (28 *a*), we find

$$\Delta Y = -\frac{l(l+1)}{r^2}\cdot Y. \quad . \quad . \quad . \quad . \quad . \quad (29)$$

Therefore

$$\Delta P = YT\left\{\Delta R - R\frac{l(l+1)}{r^2}\right\} P$$

$$= \left\{\frac{\Delta R}{R} - \frac{l(l+1)}{r^2}\right\} P, \quad . \quad . \quad . \quad . \quad (30)$$

and symbolically as a multiplying operator coefficient,

$$\Delta = \frac{\Delta R}{R} - \frac{l(l+1)}{r^2}. \quad . \quad . \quad . \quad . \quad . \quad (31)$$

If, then, in (1) we can set (with n instead of l)

$$u^2\Delta = u^2\left\{\frac{\Delta R}{R} - \frac{n(n+1)}{r^2}\right\} = -c^2, \quad . \quad . \quad (32)$$

* This sort of value practically applies where the A-function is given arbitrarily for some moment ($t=0$). Subsequent values of P follow from developing the exponential and applying it to A.

where c is one of a possible set of whole numbers, equation (27′) will give the needed sinoidal time function.

Cross multiplying (32) and reducing, we have

$$\Delta R = \left\{ \frac{c^2}{u^2} - \frac{n(n+1)}{r^2} \right\} R = 0.$$

Substituting now the value of u^2 from (4), it follows that

$$\frac{c^2}{u^2} = c^2 \cdot \frac{m^2 v^2}{h_1^2 (\frac{1}{2} m v_{\max.}^2)^2} = \frac{2c^2 m (E_0 + e^2/r)}{h_1^2 E_0^2}.$$

The equation then becomes

$$\Delta R + \left\{ \frac{2c^2 m}{h_1^2 E_0^2} \left(E_0 + \frac{e^2}{r^2} \right) - \frac{n(n+1)}{r^2} \right\} R = 0. \quad . \quad (33)$$

On the other hand, starting with equation (11), in which we set $V = -e^2/r$ and $K = h/2\pi$, we have that

$$\Delta P + \frac{2m}{K^2} \left\{ E_0 + \frac{e^2}{r} \right\} P = 0.$$

Making use of (30) and (27 a), it then follows that

$$TY \left\{ \Delta R - R \frac{n(n+1)}{r^2} \right\} + \frac{2m}{K^2} \left\{ E_0 + \frac{e^2}{r} \right\} TYR = 0,$$

which, on reduction and rearrangement, gives

$$\Delta R + \left\{ \frac{2m}{K^2} \left(E_0 + \frac{e^2}{r} \right) - \frac{n(n+1)}{r^2} \right\} R = 0. \quad . \quad (34)$$

On comparison with (33) it is at once seen that we need to equate

$$\frac{2c^2}{h_1^2 E_0^2} = \frac{8\pi^2}{h^2}; \quad \text{with} \quad c^2 = \left(\frac{2\pi h_1}{h} E_0 \right)^2 = \left(\frac{2\pi}{\frac{3}{4} h_0'} \right)^2 E_0^2 = (2\pi\nu)^2.$$

. . . (35)

It is from (34) that the possible values of n are to be obtained to produce the Balmer series of energy levels.

The Schrödinger Equation and the Bohr's Levels.

Equation (34) can also be written symbolically in the form $\left(\frac{d}{dr} = r_1 \right)$,

$$\left\{ r_1^2 + \frac{2}{r} r_1 + \left(A + \frac{B}{r} - \frac{C}{r^2} \right) \right\} y = 0. \quad . \quad . \quad (37)$$

The writer has already shown (see Trans. Roy. Soc. Canada, 1927) that the above can be factored operationally into the form

$$\{(r_1+\rho)r_1\mathrm{M}\}\,y$$
$$= \mathrm{M}\left[r_1^2+\left(\rho+\frac{2}{\mathrm{M}}\frac{d\mathrm{M}}{dr}\right)r_1+\frac{1}{\mathrm{M}}\left\{\rho\frac{d\mathrm{M}}{dr}+\frac{d^2\mathrm{M}}{dr^2}\right\}\right]y$$
$$= (r_1^2+\mathrm{P}_0r_1+\mathrm{Q}_0)y = 0^*, \quad . \quad . \quad . \quad . \quad . \quad . \quad . \quad . \quad (38)$$

provided we set

$$\mathrm{P}_0 = \rho+\frac{2}{\mathrm{M}}\frac{d\mathrm{M}}{dr},$$

$$\mathrm{Q}_0 = \frac{1}{\mathrm{M}}\left\{\rho\frac{d\mathrm{M}}{dr}+\frac{d^2\mathrm{M}}{dr^2}\right\}.$$

On eliminating M from the two equations, it follows that we need to satisfy the relation

$$\mathrm{P}_0^2+2\frac{d\mathrm{P}_0}{dr}-4\mathrm{Q}_0 = \rho^2+2\frac{d\rho}{dr}. \quad . \quad . \quad . \quad (39)$$

Clearly, from (37) and (38), we have

$$\mathrm{P}_0^2 = \frac{4}{r^2}; \qquad 2\frac{d\mathrm{P}_0}{dr} = -\frac{4}{r^2},$$

so that (39) reduces to

$$\rho^2+2\frac{d\rho}{dr}+4\left(\mathrm{A}+\frac{\mathrm{B}}{r}-\frac{\mathrm{C}}{r^2}\right) = 0. \quad . \quad . \quad (39')$$

Now, a solution of (39′) is obviously of the form

$$\rho = a-\frac{b}{r}, \quad . \quad . \quad . \quad . \quad . \quad . \quad . \quad (40)$$

for we then have that

$$a^2-2\frac{ab}{r}+\frac{b^2}{r^2}+\frac{2b}{r^2}+4\left(\mathrm{A}+\frac{\mathrm{B}}{r}-\frac{\mathrm{C}}{r^2}\right) = 0. \quad . \quad (41)$$

This can be satisfied by equating coefficients separately to zero, as we have

$$\left.\begin{aligned} a^2+4\mathrm{A} &= 0,\\ -2ba+4\mathrm{B} &= 0,\\ b^2+2b-4\mathrm{C} &= 0, \end{aligned}\right\} \quad . \quad . \quad . \quad . \quad . \quad (42)$$

* The algebra of these operators is non-commutative because of the variable coefficients.

with

$$A = \frac{2mE}{K^2}; \quad B = \frac{2me}{K^2}; \quad C = n(n+1). \quad . \quad (43)$$

Evaluating the unknown parameters in terms of the known, the first of (42) gives

$$a = 2\sqrt{-A} = 2\sqrt{\frac{-2mE}{K^2}}. \quad . \quad . \quad . \quad (44)$$

On the other hand, introducing (44) into the second of (42) results in

$$4B = 4\sqrt{-A}\,.\,b; \quad b = B/\sqrt{-A}. \quad . \quad . \quad (45)$$

Again, the last of (42) gives

$$\left(\frac{b}{2}\right)^2 + \frac{b}{2} = n^2 + n,$$

and the solution of (46) is clearly of the form

$$n = \frac{b}{2} = \frac{B}{2\sqrt{-A}} = \frac{me^2}{K^2}\Big/\sqrt{-2mE/K^2}\,*, \quad . \quad (47)$$

which agrees with Schrödinger's formula (15[1]), p. 368 of his 'Wellenmechanik.'

If, then, n is to be taken as a whole number to ensure single-valued solutions, it follows that E_0 must be taken negatively to avoid imaginaries in (47). It thus follows, on squaring, that we have the condition from (47) that

$$-E = \frac{me^4}{2K^2} \cdot \frac{1}{n^2}.$$

Substituting, therefore, the value of K in terms of the Planck constant $h/2\pi$, we have, finally, that

$$-E = \frac{2\pi^2 me^4}{h^2 n^2}\Big|_{n=1,2,3,4,\ldots}, \quad . \quad . \quad . \quad (48)$$

which is identical with Bohr's requirement for the energy levels as referred to by Schrödinger, p. 371, *l. c.*

* $n = b/2$ is not the only type of solution. Solving for n in terms of b, we can take $b/2 = n+1$ because of the square-root sign in (45).

Part III.

The Linear Oscillator Problem.

Taking the case of a single coordinate q, we have for the kinetic energy the expression

$$T = \tfrac{1}{2}\dot{q}^2,$$

wherein the mass m is properly included in q. Then for the potential energy we have

$$V = 2\pi^2\nu_0^2 q^2.$$

Schrödinger's equation then becomes, as he has shown ('Wellenmechanik'), p. 514,

$$\frac{d^2P}{dq^2} + \frac{8\pi^2}{h^2}(E_0 - 2\pi^2\nu_0^2 q^2)P = 0. \quad . \quad . \quad . \quad (49)$$

If, then, we set

$$a = \frac{8\pi^2 E_0}{h^2}; \qquad b = \frac{16\pi^4\nu_0^2}{h^2},$$

the equation becomes

$$\frac{d^2P}{dq^2} + (a - bq^2)P = 0 = \frac{d^2y}{dq^2} + (a - bq^2)y. \quad . \quad (50)$$

To solve the latter, again the method just indicated can be employed.

In this case operationally the differential equation becomes

$$\{q_1^2 + (a - bq^2)\}\, y = 0 = \{q_1^2 + P_1 q_1 + Q_1\}\, y$$
$$= \{(q_1 + \rho)q_1 M\}\, y,$$

wherein the new P_1 is really zero and Q_1 stands for

$$Q_1 = (a - bq^2).$$

The subsidiary equation takes the form, therefore,

$$P_1^2 + 2\frac{dP_1}{dq} - 4Q_1 = \rho^2 + 2\frac{d\rho}{dq},$$

$$\rho^2 + 2\frac{d\rho}{dq} + 4(a - bq^2) = 0. \quad . \quad . \quad . \quad . \quad . \quad (51)$$

Now, the solution of this type of equation is either

$$\left.\begin{aligned} &\rho = Aq \\ \text{or} \quad &\rho = Aq + \frac{B}{q} \end{aligned}\right\}. \quad . \quad . \quad . \quad . \quad . \quad (52)$$

Taking the first solution, it follows, on introduction, that

$$A^2q^2+2A+4(a-bq^2)=0. \quad . \quad . \quad . \quad (53)$$

This will be satisfied if we set

$$\left.\begin{aligned} 2A+4a=0 \quad ; \quad A^2=4b, \\ A=-2a\ ; \quad 4a^2=4b, \\ \frac{a}{\sqrt{b}}=-1, \end{aligned}\right\} \quad . \quad . \quad . \quad (54)$$

which corresponds to one of the "Eigenwerthe" or better parametral values, or "parametrals," quoted by Schrödinger (see *l. c.* Eq. (25), p. 515).

Turning now to the second type of solution, viz.

$$\rho=Aq+\frac{B}{q},$$

we have to satisfy the relation

$$A^2q^2+B^2/q^2+2AB+2A-\frac{2B}{q^2}+4(a-bq^2)=0. \quad (55)$$

This will be met if we equate

$$\left.\begin{aligned} 2AB+2A+4a=0, \\ A^2-4b=0, \\ B^2-2B=0. \end{aligned}\right\} \quad . \quad . \quad . \quad . \quad (56)$$

The last gives

$$B=2\ ;$$

so that, introduced into the first of the set, we have

$$6A+4a=0,$$

$$A=-\tfrac{2}{3}a.$$

Thus, on substitution into the second, it results that

$$\tfrac{4}{9}q^2=4b$$

or

$$\frac{a}{\sqrt{b}}=3, \quad . \quad . \quad . \quad . \quad . \quad . \quad . \quad (57)$$

which is the second of the Eigenwerthe enumerated by Schrödinger.

To obtain further values the solution of (51) needs to be generalized. This will permit the introduction of a general parametral expression N similar to the $n(n+1)$ term

occurring in the solution for the Bohr energy levels. Thus for the term Aq in (52) we can set

$$\chi = f(q),$$

whereas for the B/q term we can preferably take

$$\frac{1}{Y} \cdot \frac{dY}{dq} = F(q).$$

In this way we have

$$\rho = A\chi + \frac{B}{Y} \cdot \frac{dq}{dY} \quad . \quad . \quad . \quad . \quad . \quad . \quad (57')$$

Introducing the latter into (51) gives

$$\rho^2 = A^2\chi^2 + \left(\frac{B}{Y} \cdot \frac{dY}{dq}\right)^2 + 2AB\frac{\chi}{Y} \cdot \frac{dY}{dy},$$

$$2\frac{d\rho}{dq} = 2A\frac{d\chi}{dq} + 2\frac{B}{Y}\left\{\frac{d^2Y}{dq^2} - \frac{1}{Y} \cdot \left(\frac{dY}{dq}\right)^2\right\},$$

and we have, instead of (51),

$$A^2\chi^2 + 2A\frac{d\chi}{dq} + 4(a - bq^2)$$

$$= \frac{1}{Y^2}\left(\frac{dY}{dq}\right)^2 (2B - B^2) + \frac{2B}{Y}\left\{\frac{d^2Y}{dq^2} + A\chi\frac{dY}{dq}\right\}. \quad (58)$$

The first term on the right-hand side can easily be avoided by setting

$$B = 2.$$

On the other hand, no harm will be done by placing

$$A = 1.$$

If, then, in addition, we set

$$\frac{4}{Y}\left\{\frac{d^2Y}{dq^2} + \chi\frac{dY}{dq}\right\} = -4N,$$

or, what is the same thing,

$$\frac{d^2Y}{dq^2} + \chi\frac{dY}{dq} + NY = 0, \quad . \quad . \quad . \quad . \quad (59)$$

the resulting equation will be of the form

$$\chi^2 + 2\frac{d\chi}{dq} + 4\{(a - N) - bq^2\} = 0 \quad . \quad . \quad (60)$$

Whether N can be introduced into (60) will depend on what values are possible for N in the equation (59) *.

The new solution ρ of (51) thus becomes

$$\rho = \chi + \frac{d}{dq}(\log Y).$$

Dealing, then, with (60) instead of (51), we know that

$$\chi = Aq \quad . \quad . \quad . \quad . \quad . \quad . \quad (62)$$

is a solution. This should at least lead to the result (54) as well as (57). Introducing (62) in (60) gives

$$A^2q^2 + 2A + 4\{(a-N) - bq^2\} = 0. \quad . \quad . \quad (63)$$

Equating coefficients separately to zero gives

$$A^2 = 4b\,; \quad A = -2\sqrt{b}\,; \quad A = 2(N-a) = -2\sqrt{b},$$

whence

$$\frac{a-N}{\sqrt{b}} = 1. \quad . \quad . \quad . \quad . \quad . \quad . \quad (64)$$

If, now, we make

$$N = 0, \quad . \quad . \quad . \quad . \quad . \quad . \quad (65)$$

$$\frac{a}{\sqrt{b}} = 1\,; \quad . \quad . \quad . \quad . \quad . \quad . \quad (54)$$

but with

$$\frac{N}{\sqrt{b}} = 2 \quad . \quad . \quad . \quad . \quad . \quad . \quad . \quad (66)$$

we shall have

$$\frac{a}{\sqrt{b}} = 1 + \frac{N}{\sqrt{b}} = 3, \quad . \quad . \quad . \quad . \quad . \quad (57)$$

which is the second Eigenwerthe magnitude required.

* In reality equation (59) can be written as

$$\frac{d^2Y}{dq^2} + P_1\frac{dY}{dq} + Q_1 y = 0,$$

where

$$P_1 = \chi\,; \quad Q_1 = N.$$

Under these conditions a solution can then be made to depend, as already shown, on the subsidiary equation of the type

$$\chi^2 + 2\frac{d\chi}{dq} + 4N = \rho^2 + 2\frac{d}{dq},$$

which, of course, is identical with (60). Whatever N's are solutionally possible in (51) are equally possible in (59). Thus it remains to determine what discrete values N needs to have in order to be able to build up a set of parametral values and functions.

However, if we take the more general type of solution, viz.

$$\chi = Aq + \frac{B}{q},$$

then we have, by the steps leading to (54), on substituting there $a-N$ for a, that

$$\left.\begin{aligned} \frac{a-N}{\sqrt{b}} &= 3, \\ \frac{a}{\sqrt{b}} &= 3 + \frac{N}{\sqrt{b}}. \end{aligned}\right\} \quad . \quad . \quad . \quad . \quad (67)$$

This will surely give (57) by taking condition (65), namely

$$N = 0. \quad . \quad . \quad . \quad . \quad . \quad . \quad . \quad (65)$$

On the other hand, introducing condition (66) would give

$$\frac{a}{\sqrt{b}} = 3 + \frac{N}{\sqrt{b}} = 5 \quad . \quad . \quad . \quad . \quad . \quad (68)$$

or

$$\frac{a-N}{\sqrt{b}} = 5. \quad . \quad . \quad . \quad . \quad . \quad . \quad (69)$$

For the further parametral values of the series an additional parametral expression M′ can be introduced into (57) in exactly the same way as N was introduced into (51), and then we have to consider an equation of the type

$$Z^2 + 2\frac{dZ}{dq} + 4\{(a-N-M') - bq^2\} = 0, \quad . \quad . \quad (70)$$

with an equation of condition to suit, namely

$$\frac{d^2Y}{dq^2} + Z\frac{dY}{dq} + M'y = 0, \quad . \quad . \quad . \quad . \quad (71)$$

etc.

The parametral values (Eigenwerthe) are evidently now of the form

$$\frac{a}{\sqrt{b}} = 2n+1 \Big|_{n=0,\,1,\,2,\,3\ \text{etc.}} \quad . \quad . \quad . \quad . \quad (72)$$

Substituting values of a and b as indicated above, we finally have for the energy-level values

$$E_0 = \frac{2n+1}{2} h\nu_0 \Big|_{n=1,\,2,\,3\ \text{etc.}}, \quad . \quad . \quad . \quad (73)$$

showing that half quanta are needed for their designation.

Summary.

On the bases of a mechanical analogy Schrödinger's Wave Equation is obtained by employing the idea of an excitation stream of air to a reed or organ-pipe. The above equation of wave-motion then applies to the varying velocity potential of the stream. It is found that the reed or organ-pipe when excited gives a relationship between the velocity of the vibrating reed or slit wall and the mean velocity of the stream. In this way, also, a relationship is found between the speed of the pulsating wave-front of the velocity potential and the mean stream velocity. By combining the two a proportionality factor h_1 results, which latter needs to be combined with the constant h_0 derived from assuming a proportionality law between the normal energy content of the oscillator wall and the frequency set up. It is shown that the latter really follows because, as the pressure goes up, the maximum displacement of the reed or slit wall actually diminishes with the increase in momentum. This is in conformity with the fact that in the harmonica or "mouth-organ" the reed-opening becomes more and more closed as one blows harder and harder. That is, the Planck constant h is split up according to the formula $h=h_0h_1$.

Introducing the above factors into the differential equation of wave-motion results in the final form of Schrödinger without the use of the Hamilton Varying Action principle or the Hamilton-Jacobi equation.

It had already been shown by the writer that on purely classical grounds there must always be a fixed relationship between the amplitude of the pure harmonic radiated energy and the normal non-radiated content of the oscillator. This explains why, in solving Schrödinger's Equation for the Balmer series, we need only consider the conservative system of the radiator.

By means of a general operational method analogous to the factoring method employed by Heaviside, the writer has shown that equations of the type used by Schrödinger can be solved in an effectively simple way. The "Eigenwerthe" are first deduced, and later only are the Eigenfunktionen developed automatically, without having to resort to a previous study of Laguerre polynomials or Hermitian functions.

1314 18th St., N.W.,
Washington, D.C., U.S.A.,
Jan. 1, 1928.

IV. *The Electronic Theory of Valency.*—Part VI. *The Molecular Structure of Strong and Weak Electrolytes.* (b) *Reversible Ionization.* *By* T. Martin Lowry *.

THE theory of complete ionization has met with such marked success that it might easily be supposed that it could be applied to all electrolytes. The present paper therefore contains a review of some cases in which the ionization of an electrolyte is reversible instead of complete.

True Electrolytes and Pseudo-electrolytes.

The most obvious examples of reversible ionization are provided by those compounds in which neutralization of the opposite charges of the ions is rendered possible by a change of molecular structure. Thus, according to the electronic theory of valency, a quaternary ammonium chloride must remain permanently ionized, since both the ammonium ions and the chloride ions carry complete shells of electrons and cannot share electrons without creating a surplus. There are, however, a number of cases in which this surplus can be disposed of by a rearrangement of bonds within the molecule, giving rise to a wholly covalent compound. This change takes place with greater readiness when the chlorine is replaced by an anion of a less strongly negative character, *i. e.*, by a radicle which is less hungry for electrons, and therefore more ready to share them with another atom. Thus methylphenylacridinium chloride is a true electrolyte, which remains permanently ionized in aqueous solutions: but, when sodium cyanide is added, a progressive fixation of cyanogen ions takes place, until after about a day at 25°, the conductivity is found to have fallen almost to the value for sodium chloride, as a result of the complete conversion of the ionized "true salt" into an insoluble "pseudo-salt" †.

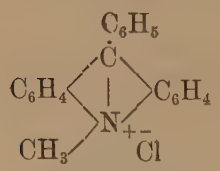

Methylphenyl-acridinium chloride.

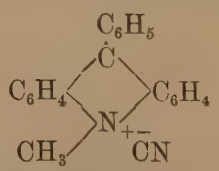

Methylphenylacridinium cyanide.

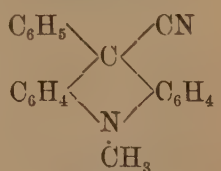

Methylphenylcyano-acridine.

* Communicated by the Faraday Society.

† Hantzsch and Kalb, *Ber.* xxxii. p. 3109 (1899).

A similar change of structure can be effected in the diazocyanides by separating the "salt" from aqueous solutions and dissolving it in a non-ionizing solvent, when it behaves as a typical non-electrolyte, whereas in water it behaves just like the chloride

$$C_6H_5.\overset{+}{N}\overset{\|}{C}\overset{-}{N} \rightleftharpoons C_6H_5.N:N.CN$$

Diazonium cyanide. Diazo-cyanide.

Precisely similar considerations apply to the fixation of a hydroxyl-ion. Thus a solution of methylphenylacridinium chloride, when mixed with an equivalent quantity of sodium hydroxide, shows at first the normal conductivity of such a mixture ; but this conductivity diminishes progressively to that of sodium chloride as the hydroxyl is "fixed" by the anion.

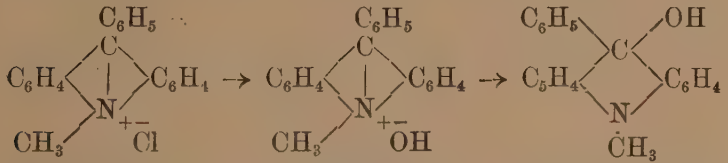

Methylphenyl-acridinium chloride. Methylphenyl-acridinium hydroxide. Methylphenylacridol.

The acridol, which is formed as a product, is a tertiary amine-alcohol, compare $(C_6H_5)_2NMe$ and $(C_6H_5)_3C.OH$. It is therefore just as true a base as trimethylamine, but differs from other tertiary bases in that one of the alkyl radicles carries a hydroxyl-group, which is eliminated in the form of water as soon as the base has performed its characteristic function of accepting a proton from an acid. Although, therefore, it is commonly referred to as a "pseudo-base," it would perhaps be described more accurately as a "pseudo-alkali," *i. e.*, as a non-electrolytic isomer of a quaternary ammonium hydroxide.

Strong and Weak Acids.

Whilst the conception of a "strong electrolyte" is a very modern one, the existence of strong and weak acids has been familiar for 1000 years or more, and had already been interpreted in many other ways before the strength of an acid was finally correlated with its electrical conductivity in

dilute solutions. The theory of complete ionization therefore receives its most serious challenge from the existence of weak acids, which obey Ostwald's dilution law ($\alpha \propto c^{-\frac{1}{2}}$, where α is small), and cannot therefore also obey the dilution formula for strong electrolytes ($1-\alpha \propto c^{\frac{1}{3}}$, where α is large).

In order to account for the existence of these weak acids, Hantzsch has suggested * that carboxylic acids can exist in two interconvertible isomeric forms, thus :

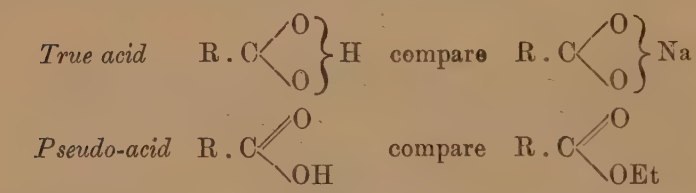

A dynamic isomerism of this type is actually observed in the nitro-paraffins,

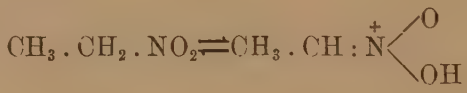

or

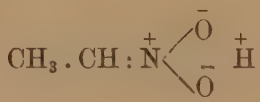

and is an obvious factor in reducing the acidity of the compound, which must be diminished in direct proportion to the extent to which the true acid is converted into the isomeric pseudo-acid. It is, however, by no means certain that the contrast between strong and weak acids depends in other cases on so definite a phenomenon. For instance, we need not suppose that phenol owes its weak acidity to conversion into an isomeric pseudo-phenol,

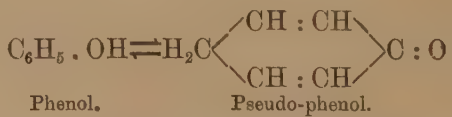

since it is sufficient to postulate that, whilst the $-\overset{-}{O}\overset{+}{N}a$ radicle of sodium phenate is permanently ionized, the $-OH$ radicle of phenol is held together by a real bond, just

* *Ber.* l. p. 1438 (1917).

as in the case of the alcohols. Dissolution of the sodium compound in water would then give rise to a direct dissociation of ready-made ions as indicated by the equation,

$$C_6H_5 . \overset{-}{O}\overset{+}{Na} \rightleftharpoons C_6H_4\overset{-}{O} + \overset{+}{Na},$$

whereas, in the case of phenol itself, ions could only be produced as the result of a destruction of neutral molecules, by the rupture of the hydrogen-oxygen bond, as in the equation:

$$C_6H_5 . O . H \rightleftharpoons C_6H_5\overset{-}{O} + \overset{+}{H}.$$

Some care is needed in order to formulate these views in accordance with modern theories of atomic structure, since, as I pointed out in an article on "The Uniqueness of Hydrogen" *, exceptional difficulty is experienced in deciding whether an atom of hydrogen is linked to the rest of the molecule by a real bond or by a mere electrovalence. This difficulty arises from the fact that, since the hydrogen "shell" contains 0 or 2 instead of 8 electrons, the ordinary static symbolism makes no distinction between these two forms of union. Thus, in the case of $H:\overset{\cdot\cdot}{\underset{\cdot\cdot}{Cl}}:$, the same electronic formula serves equally well to represent a pair of ions, $\overset{+}{H}\overset{-}{Cl}$, with 0 and $2+8+8$ electrons, or a covalent compound, $H-Cl$, in which 2 of the 18 electrons are shared by the two atoms. When, however, a dynamic model is used, and shared electrons are regarded as moving in binuclear orbits, a clear distinction between the two types of union again becomes possible, according as the orbits of the electrons in question surround two nuclei or only one. If this distinction is admitted, it appears probable that hydrogen is covalent in all its compounds, and that the free hydrogen ion or naked proton represented by the symbol $\overset{+}{H}$ does not exist except as a transient product in a vacuum-tube or the like. This conclusion follows, on the one hand, from the fact that there are no electrostatic forces to prevent such a nucleus from falling inside the electronic orbits of any other atom with which it may collide, and, on the other hand, from numerical data which show that the union of a proton with water to form a hydrated hydrogen ion would liberate not less than 260,000 calories †. The ionization of an acid

* Lowry, 'Chemistry and Industry,' xlii. p. 43 (1923).
† Fajans, *Ber. deut. physik. Ges.* xxi. p. 709 (1919).

(which does not take place when the pure compound is merely melted) must then be formulated as depending on an interaction of the acidic hydride with water, or the like, giving rise to an oxonium ion, as in the equation,

$$C_6H_5 . O . H + OH_2 \rightleftharpoons C_6H_5\bar{O} + \overset{+}{O}H_3.$$

It will be seen, however, that this scheme still possesses the characteristic which is now put forward as a typical property of "weak" electrolytes, that the opposite electric charges of the ions can be neutralized without any violation of the "octet" rule, giving rise to products in which the electrovalence of the ions is replaced by a real bond.

Strong and Weak Bases.

Bases resemble acids in exhibiting a very wide range of strengths. Thus the soluble metallic hydroxides (which include the alkalis) are all strong bases, and their strength is shared by the quaternary ammonium hydroxides, where the formation of a covalent bond between nitrogen and oxygen is prevented by the fact that the nitrogen is unable to attach itself by real bonds to five atoms simultaneously. Weak bases appear to be of two main types, since covalent compounds can be formed, either by fixing the hydroxyl-group by a real bond to an isomeric form of the kation, as in the acridinium compounds cited above, or by eliminating it in the form of a covalent molecule of water. The latter case is extremely common. Thus the amines generally behave as weak bases, since the concentration of hydroxyl-ions in their solutions depends on an interaction with water : *e. g.*,

$$NH_3 + H_2O \rightleftharpoons [NH_4]^+OH^-$$

compare $$CO_2 + H_2O \rightleftharpoons [CO_3]^{--}H_2^{++}$$

the ready reversibility of which is shown by the complete removal of ammonia from its aqueous solutions by boiling, or of aniline by steam-distillation. Since, however, this dehydration has the effect of eliminating the unbalanced electric charges from the system, giving rise exclusively to covalent compounds, this explanation is in close agreement with the general proposition set out above as regards the essential characteristics of a weak electrolyte.

The problem of weak bases has, however, been carried one stage further by Moore and Winmill *, who have shown by

* Journ. Chem. Soc. ci. p. 1675 (1912).

distribution experiments that the weakness of the primary, secondary, and tertiary amines can only be partially attributed to dehydration of the hydroxide, and by Latimer and Rodebush *, who have suggested that the hydrate NH_3, H_2O may be formulated as

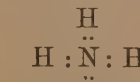

This formula represents the monohydrate as a covalent isomer of ammonium hydroxide,

$$\overset{+}{N}H_4\overset{-}{O}H \rightleftharpoons H_3N \,.\, H \,.\, O \,.\, H,$$

in which the hydroxyl radicle is united to the ammonium radicle by a real bond, as required by our definition of a weak electrolyte. The fulfilment of this condition is not vitiated by the fact that, since quadrivalent nitrogen is positively-charged, and bivalent hydrogen is negatively charged, the resulting molecule would exhibit the phenomenon which J. J. Thomson has described as "intramolecular ionization" †.

The bivalency of hydrogen is also of value in accounting for the fact that the polymerization of liquid water is not accompanied by ionization. Thus, if hydrogen were always univalent, the formation of a double-molecule would be represented by the scheme,

$$H_2O + H_2O \rightleftharpoons [\overset{+}{O}H_3]\overset{-}{O}H$$

compare $$H_2O + HCl \rightleftharpoons [\overset{+}{O}H_3]\overset{-}{Cl},$$

and the product would be an oxonium hydroxide, just like ammonium hydroxide ; but, if the hydrogen is bivalent, the formation of double and triple molecules can be represented, *without any formation of free ions*, by the schemes,

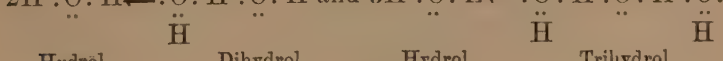

Hydrol. Dihydrol. Hydrol. Trihydrol.

* Journ. Amer. Chem. Soc. xlii. p. 1431 (1920); *cf.* G. N. Lewis, 'Valence,' p. 110 (1923).

† Phil. Mag. (6) xxvii. p. 757 (1914); *cf.* Lowry, Trans. Faraday Soc. xviii. p. 285 (1923), and Phil. Mag. (6) xlv. p. 1105 (1923).

Here again the polymerized molecules must exhibit "intramolecular ionization," since the tervalent oxonium oxygen is positively-charged, and the bivalent hydrogen negatively-charged, as in the formula,

$$H_2\overset{+}{O}.\overset{-}{H}.O.\overset{-}{H}.\overset{+}{O}H_2 \quad \text{compare} \quad H_3\overset{+}{N}.\overset{-}{H}.O.\overset{-}{H}.\overset{+}{N}H_3.$$

Alternatively the trihydrol can be represented by a ring structure dissected from the crystal-lattice of ice, thus

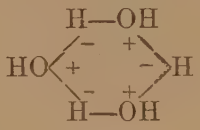

Strong and Weak Salts.

The number of metallic salts which are obviously "strong electrolytes" is so large that it is not always easy to realize that a salt, like an acid or base, may be a "weak electrolyte." In the following paragraphs, therefore, a number of examples have been brought together of salts which behave as weak electrolytes; and evidence is again cited to show that these compounds owe their peculiar inertness to the possibility of forming covalent bonds between the ions.

(a) *Stannic Chloride.*—An ionic aggregate, in which each ion is surrounded by a number of ions of opposite sign (*e. g.*, 6 in the NaCl lattice or 8 in the CsCl lattice), provides ideal conditions for utilizing the residual affinity of the ions to produce a rigid crystal structure. When therefore a substance, which has the formula of a salt, exhibits the fusibility and volatility of an organic compound, the view at once suggests itself that we are probably dealing with integral molecules, rather than with a continuous network of ions. We are therefore not surprised when stannic chloride (b.p. 114°, f.p. −33°) fails to show the electrolytic properties of a typical fused salt, since its obvious properties are those of a collection of individual molecules and not of an aggregate of ions. This general conclusion has received specific confirmation from the X-ray analysis of crystals of stannic iodide, where it has been shown that each atom of tin is surrounded tetrahedrally by four atoms of iodine, just as in the case of a covalent carbon-compound.

No data are given in the tables for the conductivity of pure stannic chloride, which appears to behave as an

insulator, like pure hydrogen chloride or pure water. In aqueous solution it is hydrolyzed to colloidal stannic acid, $SnCl_4 + 4H_2O \rightleftharpoons Sn(OH)_4 + 4HCl$, which appears to contribute nothing to the conductivity of the acid solution*. In liquid sulphur dioxide, however, it behaves as a weak electrolyte, giving $\Lambda_6 = 0{\cdot}068$, $\Lambda_{14} = 0{\cdot}04$, $\Lambda_{262} = 0{\cdot}262$. Although, therefore, the metal and the halogen in stannic chloride carry complete octets of electrons, it is still possible to ionize one of the bonds; but, as the tin is then left with an outer shell of only 6 electrons, this condition is too unstable to persist except as a minor feature of the final equilibrium.

Stannic chloride can, however, be converted in a strong electrolyte by combination with potassium chloride to form potassium stannic chloride,

$$2\overset{+}{K}\overset{-}{Cl} + SnCl_4 \rightleftharpoons \overset{++}{K_2}[SnCl_6]^{--}.$$

The crystals of this compound have been shown by X-ray analysis to be an ionic aggregate of the same type as fluorspar; but, in forming this aggregate, the tin has not been separated from the chlorine, since (if we accept Langmuir's theory of coordination †) it now forms part of a complex anion in which *six* atoms of chlorine, instead of only *four*, are united by real bonds to the central atom of metal. This change is obviously accompanied by conversion of a tetrahedral into an octahedral configuration. The view that an octahedral 6-coordination compound gives rise to a square configuration when converted into a 4-coordination compound, cannot therefore be maintained in this case, although it appears to have been established in the case of platinum.

(b) *Mercury Salts.*—Special interest attaches to the behaviour of the salts of mercury, since this element resembles hydrogen in the readiness with which it gives rise to "weak electrolytes," both in the molten state and in solution. This peculiar behaviour can, however, be attributed to the fact that this element, in complete defiance of the simple octet rule of the electronic theory, is equally ready to form covalent and electrovalent compounds. Evidence in support of this statement is set out in Tables I. and II. and in the paragraphs which follow.

* Foster, Phys. Rev. ix. p. 41 (1899).
† Journ. Amer. Chem. Soc. xli. p. 868 (1919).

TABLE I.

Specific Conductivity of Fused Salts.

(a) *Strong Electrolytes.*

NaCl	3·34 at 800°	AgCl	4·98 at 800°	4·48 at 600°	
NaBr	3·06 „	AgBr	3·50 „	3·18 „	
NaI	2·70 „	AgI	2·52 „	2·52 „	
KCl	2·19 at 800°	TlCl	1·700 at 800°	1·082 at 427°	(m.p.)
KBr	1·75 „	TlBr	1·127 „	0·803 „ 457°	
KI	1·64 „	TlI	0·840 „	0·523 „ 436°	

(b) *Weak Electrolytes.*

HgI_2 0·0066 at 320°	$HgCl_2$ 0·0078 at 276° (m.p.)
0·0071 „ 288°	
0·0085 „ 260°	
0·0118 „ 253° (m.p.)	

Data for aqueous solutions of mercury-salts are as follows :—

TABLE II.

Equivalent Conductivities of Mercury Salts.

Mercurous Salts.	*Mercuric Salts.*
$HgClO_4$ $\Lambda_{10}^{25}=110$ $\alpha=0·76$	$\frac{1}{2}Hg(ClO_4)_2$ $\Lambda_{10}^{25}=105$ $\alpha=0·77$
$HgNO_3$ $\Lambda_{32}^{18}=59$ $\alpha=0·56$	$\frac{1}{2}Hg(NO_3)_2$ $\Lambda_{32}^{25}=6·3$ $\alpha=0·04$
(in $N/10$ HNO_3)	$\frac{1}{2}HgCl_2$ $\Lambda_{32}^{25}=1·77$ $\alpha=0·013$
	$\frac{1}{2}Hg(CN)_2$ $\Lambda_{16}^{25}=0·10$ $\alpha=0·0007$

The weak and variable electrolytic conductivities of the mercury salts are just what one might expect if the positively-charged mercury ions were able to unite with the negatively-charged anions to form covalent compounds, *e.g.*,

$$Hg^{++}+2Cl^{-}\rightleftharpoons Cl-Hg-Cl,$$

but it would be merely arguing in a circle to use these low conductivities as evidence of the formation of covalent compounds. It should be noted, however, that the conductivity of mercuric chloride is much lower than that of the nitrate, and that, whilst the coefficient of ionization of mercuric chloride is only about 1 per cent. at $N/32$, the two perchlorates, in which the halogen is completely enveloped by four tetrahedrally disposed atoms of oxygen, have actually passed over into the group of strong electrolytes (compare barium perchlorate) with coefficients of 76 per cent. and 77 per cent. respectively at a concentration of $N/10$.

On the other hand, mercuric cyanide, which was described by Prussia in 1898 * as a non-conductor, behaves exactly like an organic compound in which ionization is just beginning to be possible (compare CMe_3I in liquid SO_2).

Fortunately, however, direct evidence is available to prove that mercury does actually form covalent compounds of the type that has been postulated as characteristic of "weak electrolytes." Thus, as long ago as 1898, Ogg showed † that the ratio between the two nitrates of mercury, when in equilibrium with metallic mercury and a given concentration of nitric acid, is constant. This result cannot be reconciled with the equation,

$$Hg + Hg(NO_3)_2 \rightleftharpoons 2HgNO_3 \quad \text{or} \quad Hg + Hg^{++} \rightleftharpoons 2Hg^{+}$$

but is in close agreement with the requirements of the equation,

$$Hg + Hg(NO_2)_2 \rightleftharpoons \begin{matrix} HgNO_3 \\ | \\ HgNO_3 \end{matrix} \quad \text{or} \quad Hg + Hg^{++} \rightleftharpoons Hg_2^{++}$$

The mercurous ion is, therefore, not a simple charged atom $\overset{+}{H}g$ but a covalent complex $\overset{+}{H}g-\overset{+}{H}g$. This conclusion was confirmed by determinations of the electromotive force of concentration-cells, as well as by other methods of investigation. The later measurements by Schilow ‡ of the transport-number and conductivity of mercurous nitrate, in aqueous solutions and in presence of dilute nitric acid, also support Ogg's conclusion that mercurous nitrate is a *ternary* electrolyte, the ionization of which must be represented by the scheme,

$$Hg_2(NO_3)_2 \rightleftharpoons Hg_2^{++} + 2NO_3^{-}$$

and not by the simple scheme for a *binary* electrolyte,

$$\overset{+}{H}g\overset{-}{N}O_2 \rightleftharpoons \overset{+}{H}g + \overset{-}{N}O_3 \quad \text{compare} \quad \overset{+}{A}g\overset{-}{N}O_3 \rightleftharpoons \overset{+}{A}g + \overset{-}{N}O_3.$$

Even more conclusive are the recent observations of Mauguin § and of Havighurst ‖ on the X-ray analysis of crystals of mercurous chloride, bromide, and iodide. Nearly

* *Gazz.* xxviii. p. 117.
† *Zeit. phys. Chem.* xxvii. pp. 285–311 (1898).
‡ *Zeit. anorg. Chem.* cxxxiii. p. 55 (1924).
§ *Compt. Rend.* clxxviii. p. 1913 (1924).
‖ Am. Journ. Sci. x. p. 15 (1925).

all of the binary haloid salts crystallize in the cubic lattice, *e. g.*,

NaCl, KCl, AgCl, AgBr, on a face-centred cubic lattice,
CsCl, CsI, TlCl, TlBr, on a body-centred cubic lattice,
CuCl, CuBr, CuI, AgI, on the diamond or zinc sulphide type of cubic lattice.

The mercurous haloids, however, all crystallize in the tetragonal system ; and X-ray analysis has shown that the arrangement of the atoms of metal and halogen is not a simple alternation, as in rock-salt or cæsium chloride,

$$\overset{+}{\mathrm{Na}}\ \overset{-}{\mathrm{Cl}}\ \overset{+}{\mathrm{Na}}\ \overset{-}{\mathrm{Cl}} \qquad \overset{+}{\mathrm{Cs}}\ \overset{-}{\mathrm{Cl}}\ \overset{+}{\mathrm{Cs}}\ \overset{-}{\mathrm{Cl}}$$

$$\text{or} \quad \overset{-}{\mathrm{Cl}}\ \overset{+}{\mathrm{Na}}\ \overset{-}{\mathrm{Cl}}\ \overset{+}{\mathrm{Na}} \qquad \overset{-}{\mathrm{Cl}}\ \overset{+}{\mathrm{Cs}}\ \overset{-}{\mathrm{Cl}}\ \overset{+}{\mathrm{Cs}}$$

but an alternation of *pairs* of atoms as in the scheme,

$$\mathrm{Cl-Hg-Hg-Cl} \qquad \mathrm{Cl-Hg-Hg-Cl}$$
$$\mathrm{-Hg-Cl} \qquad \mathrm{Cl-Hg-Hg-Cl} \qquad \mathrm{Cl-Hg-}$$

Since the scheme,

$$- + + - - + + -$$
$$+ - - + + - - +$$

is impossible as a stable arrangement of positive and negative ions, Havighurst concludes that "The structure of these crystals indicates the existence of the chain-molecule Cl—Hg—Hg—Cl. The strong double refraction which has been observed is to be expected from a crystal having this structure" *. The unusual cleavage of the compound is also in agreement with this structure.

From this evidence it is clear that mercury can exhibit either a covalence of 2 as in calomel,

$$\mathrm{Cl-Hg-Hg-Cl},$$

or a covalence of 1 and a positive electrovalence of 1 as in mercurous nitrate,

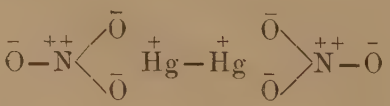

* Am. Journ. Sci. x. p. 15 (1925).

or a positive electrovalence of 2 as in mercuric perchlorate,

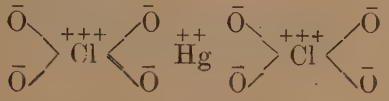

The way is therefore open for a reversible equilibrium between free ions and real molecules, of precisely the same type as has been postulated in the case of other weak electrolytes, *e.g.*,

$$Cl-Hg-Cl \rightleftharpoons \overset{++}{Hg} + 2\,\overset{+}{Cl}.$$

(c) *Coordinated Salts.*—In the category of weak electrolytes we must also include a large number of coordination compounds, since it is clear that, as the firmness with which a metal is coordinated to the negative radicle is increased, its coefficient of ionization must be diminished, or, in other words, that its efficiency as an electrolyte must decay *pari passu* with the increase of the efficiency of the coordination. Since, however, Sidgwick considers that the act of coordination consists in the formation of a bond by the transfer of an electron from one atom to another, these cases can obviously be included within the limits of our specification of the principal condition for the production of weak electrolytes.

Unfortunately, data in reference to the ionization of compounds of this type are scanty, since most of them, in losing their character as strong electrolytes, become insoluble in water, and therefore pass right over to the category of non-electrolytes. Intermediate cases are, however, provided by the salts of organic hydroxy-acids. Thus Calame has shown by determinations of freezing-point that, whilst calcium *lactate* is ionized to the extent of 40 per cent. at a concentration of 0·257 *N*, the copper salt is ionized only to the extent of 17 per cent. at 0·271 *N* *. In the same way, Tower has reported † that, whilst the molecular conductivities of the *succinates* of Ni, Co, and Mg are very similar at all concentrations, the molecular conductivities of the *tartrate* and *malate* of cobalt and nickel are very much smaller than those either of the magnesium salts or of the corresponding succinates. Again, Calame has shown that the coefficient of ionization of copper *malate* is only 4 per cent. in *N*/4·628 solution, 10 per cent. in *N*/74 solution, and 19 per cent. in *N*/592 solution, whereas zinc *maleate* (where coordination is

* *Zeit. phys. Chem.* xxvii. p. 401 (1898).

† Journ. Amer. Chem. Soc. xxii. p. 501 (1900); xxiv. p. 1012 (1902).

prevented by the elimination of the hydroxyl group) is dissociated to the extent of 22 per cent., 44 per cent., and 69 per cent. in solutions of similar concentrations. All these results are in accord with the view that the coordination of the ions of a metallic salt tends to convert it into a "weak electrolyte."

Other examples of weak electrolytes are afforded by the so-called "non-valent" coordination-complexes. Thus the following values are recorded for the conductivities of the ammines of platinous nitrite * :—

$Pt(NO_2)_2.4NH_3$ or $[Pt.4NH_3]^{++}(NO_2)_2^{--}$ $\Lambda_{1000}^{25}=276{\cdot}5$
$Pt(NO_2)_2.3NH_3$ or $[Pt.3NH_3.NO_2]^{+}NO_2^{-}$ $\Lambda_{1000}^{25}=96{\cdot}5$
$Pt(NO_2)_2.2NH_3$ or $[Pt.2NH_3.2NO_2]^{\pm}$ $\Lambda_{1000}^{25}=0{\cdot}95$ (cis.)
$=2{\cdot}42$ (trans.).

It is commonly stated that substances such as $[Pt.2NH_3.2NO_2^{\pm}]$, $[Pt.2NH_3.4Cl]^{\pm}$ and $[Co.3NH_3.3NO_2]^{\pm}$ are "non-electrolytes," but this statement is not in harmony with a summary of the experimental data in which it is said that "the compound *is a very poor conductor* of the electric current in aqueous solutions." If this description is correct, *i. e.*, if the feeble conductivity which is observed even in freshly-prepared solutions of these compounds cannot be explained away by the hydrolysis of the complex, these "non-valent" ammines must be classed with the "weak electrolytes," which exhibit a small electrolytic conductivity as a result of the reversible ionization of a covalent complex, compare

$$Cl-Hg-Cl \rightleftharpoons \overset{++}{Hg} + 2\overset{-}{Cl}.$$

(d) *Carbonium Salts.*—These salts are characterized by very wide range of conductivities. Thus Walden † found the following values for the equivalent conductivities of a series of halogen salts dissolved in liquid sulphur dioxide at 0° :—

KI	$\Lambda_{98}=59{\cdot}5$	$\Lambda_{2000}=142{\cdot}3$
$(C_6H_5)_3CBr$	$\Lambda_{26}=108{\cdot}5$	$\Lambda_{2001}=152$
$(C_6H_5)_3COCl$	$\Lambda_{105}=15{\cdot}0$	
$(CH_3)_3CI$	$\Lambda_{17}=0{\cdot}7$	

The tertiary halides therefore cover the whole of the available range of conductivities, some of them being better conductors than a typical "strong electrolyte" like potassium iodide, whilst others have no conductivity at all. The same

* Tschugaeff and Wladimiroff, *Journ. Russ. phys. Chem. Ges.* lii. p. 135 (1920).

† *Ber.* xxxv. p. 2023 (1902).

conclusion follows from the observations of Gomberg *, who gives the following values for the degree of dissociation of some carbonium salts at $-8°$ and $v = 100$, in comparison with the value for tetramethylammonium bromide,

$(C_6H_5)_3CCl$ 12 per cent.	$(C_6H_5 . C_6H_4)_3CCl$ 45 per cent.
$(C_6H_5)_3CBr$ 61 per cent.	$(CH_3)_4NBr$ 56 per cent.

In all these carbonium salts the rules of valency permit the formation of a covalent bond between the carbon of the kation and the halogen of the anion, giving rise to a true molecule instead of an ionic doublet. Since the carbon-halogen bond is usually too strong to be ionized by mere dissolution in a solvent, most of the compounds of the type

are non-conductors; but when the bond is weakened †, *e. g.*, by substitution and by replacing chlorine or bromine by iodine, so that ionization according to the scheme

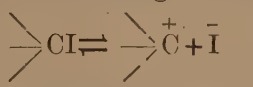

becomes possible, the compounds pass into the group of "weak electrolytes," although they do not usually exhibit this property in aqueous solutions; and, finally, when the formation of a bond is rendered even more difficult † by the introduction of bulky aromatic substituents the salts are actually better conductors than many "strong electrolytes."

Summary.

(*a*) Although most electrolytes are ionized completely, even in the solid state, there are many compounds in which ionization is incomplete and reversible.

(*c*) Compounds of this type, in which neutralization of the ionic charges is not prevented by the laws of valency, behave as "weak electrolytes," unless the bond between the radicles is too weak to hinder the ionization of the molecule.

(*d*) "Weak electrolytes" of this class are found amongst acids and bases, pseudo-electrolytes, coordinated salts, and a few simple metallic salts such as mercuric chloride, where covalent molecules can be formed from the ions.

University Chemical Laboratory,
Cambridge.

* Journ. Amer. Chem. Soc. xliv. p. 1818 (1922); xlv. p. 206 (1923).
† Flürscheim, *loc. cit.* and Journ. Chem. Soc. xcv. p. 718 (1909).

V. *Multiple Ionization and the Absorption of X-Rays.* By F. K. Richtmyer, *Professor of Physics, Cornell University**.

1. A VERY large majority of the lines in the X-ray spectra of the elements are produced by transitions between ionized states in which one electron is missing from one or the other of the several levels—K, L, M. . . . These lines, frequently called "diagram lines," belong to the so-called "X-ray spectra of the first kind."

As is well known, there are, in addition to these "diagram" lines, numerous faint lines which cannot be explained by transitions between the levels which give rise to the spectra of the first kind. These faint lines are variously known as: (1) "satellites," since they accompany a prominent line of the first kind, usually on the short wave-length side of the latter, although satellites on the long wave-length side are also known; (2) "non-diagram" lines, since they cannot be represented on the energy-level diagram usually adopted for lines of the first kind; (3) "spark" lines, since Wentzel proposed a theory of the origin of these lines which involved multiple ionization in the inner electron shells in the same way that the optical spark lines originate in multiple ionization, or excitation, in optical levels; or (4) "X-ray spectra of the second, third . . . . kind," according as the excited states giving rise to the lines are due, according to Wentzel's theory, to double, triple . . . . ionization of the respective electron shells.

The intimate relation which is known to exist between the X-ray spectra of the first kind and the directly-observed absorption discontinuities (K, L . . .), suggest the query: Are there in X-ray absorption spectra discontinuities or other peculiarities corresponding to these spectra of the second, third . . . . kind? Before discussing this question it is pertinent to review briefly the evidence pro and con regarding Wentzel's theory of the origin of these lines.

2. In Table I. are given some typical examples of non-diagram lines, together with the initial and final states corresponding to each line according to Wentzel's† scheme

* Communicated by the Author. The Author acknowledges with many thanks assistance from the Heckscher Research Fund of Cornell University.

† *Ann. der Phys.* lvi. p. 437 (1921). *Zeits. f. Phys.* xxxi. p. 445 (1925).

of multiple ionization. In Wentzel's terminology K^2 stands for an atom which has lost both K-electrons; KL^2 for an atom which has lost one K- and two L-electrons; etc. The lines $K\alpha_3$ and $K\alpha_4$ form a close doublet, which has been measured over the range of elements Na(11) to Zn(30), but

TABLE I.

Some typical Non-diagram Lines and their origin.

Line.	Origin.		Kind.	Reference.
	Initial state.	Final state.		
Satellites of the $K\alpha$ doublet. ($K \longrightarrow L$.)				
$K\alpha_3$	KL	L^2	Second	1
$K\alpha_4$	K^2	KL	Second	1
$K\alpha'$	KM	LM	Second	1
$K\alpha_5$	KL^2	L^3	Third	1
$K\alpha_6$	K^2L	KL^2	Third	1
Satellite of $K\beta$. ($K \longrightarrow M$.)				
$K\beta''$	KL	LM	Second	2
Satellites of $L\beta_2$. ($L_{III} \longrightarrow N_{IV, V}$.)				
$L\beta_2'$	$L_{III}M_V$	$M_VN_{IV, V}$	Second	2
$L\beta_2''$	$L_{III}M_{IV}$	$M_{III}N_{IV, V}$	Second	2

[1] Quoted in Siegbahn's 'The Spectroscopy of X-Rays,' p. 106, from the measurements of Hjalmer, Dolejšek, and Dolejšek & Siegbahn. Wetterblad (*Zeits. f. Phys.* xlii. p. 611, 1927) gives the results of some careful measurements of the wave-lengths of these lines for Na, Mg, and Al.

[2] Druyvesteyn, *Zeits. f. Phys.* xliii. p. 707 (1927). Druyvesteyn gives also measurements of satellites of $L\gamma_1$ and $L\gamma_{2,3}$. Some of the data used by Druyvesteyn are from the previous measurements of Coster (Phil. Mag. xliii. p. 1070, 1922), who also reports satellites of $L\alpha_1$.

the components of the doublet have not been separated for elements of higher atomic number than Ca(20). The pair $K\alpha_5$ and $K\alpha_6$ has been measured for only four elements Na(11) to Si(14). Druyvesteyn's measurements of $K\beta''$

extend from K(19) to Fe(26); and of $L\beta_2'$ and $L\beta_2''$ from Nd(41) to Sb(51). For elements heavier than Sb(51) these latter lines are not resolved, and are listed by Siegbahn and by Coster as β_{11} and β_{12}.

The evidence in favour of Wentzel's scheme of multiple ionization as an explanation of the origin of satellites falls under several heads :—

(*a*) According to the theory, the difference in frequency $(K\alpha_5 - K\alpha_3)$ for a given element should equal the difference $(K\alpha_3 - K\alpha_1)$ for the same element. Data are available for only four elements, Na(11) to Si(14), to check this predicted equality.

According to the recent measurements of Wetterblad *, the frequency difference $(K\alpha_3 - K\alpha_1)$ is some 8 per cent. higher than the difference $(K\alpha_5 - K\alpha_3)$—which is, perhaps, as good a check as could be expected, considering the difficulties of the measurements.

(*b*) The frequency difference $(K\alpha_6 - K\alpha_4)$ for one element should equal the difference $(K\alpha_3 - K\alpha_1)$ for the element of next higher atomic number. Wetterblad's measurements confirm this within 1 or 2 per cent. This is, perhaps, the strongest support for Wentzel's theory.

(*c*) Druyvesteyn † shows that the difference in frequency between a satellite and its "parent" line is for a given element computable from certain of the energy levels of that element and of the element of next higher atomic number. For example, the frequency difference $(K\beta'' - K\beta)_Z$ for an element of atomic number Z should, subject to certain very close approximations, be given by

$$(K\beta'' - K\beta)_Z = (L - M)_{(Z+1)} - (L - M)_Z,$$

where L and M are the *frequencies* of the L and M levels. Druyvesteyn applies this general principle to the satellites of $K\beta_2$, $L\beta_2$, $L\gamma_1$, and $L\gamma_{2,3}$, and obtains experimental verification of the predicted equality, which, again considering the difficulties of the wave-length measurements and the small wave-length differences involved, is perhaps within the limits of error of measurement for the satellite $K\beta'''$ (parent line : $K\beta_1$). The agreement is much less satisfactory for the L satellites.

(*d*) Wentzel originally assumed that double ionization of an atom might be brought about by *successive* collisions with two cathode-ray electrons. For example, an atom which

* *Zeits. f. Phys.* xlii. p. 611 (1927).
† *Loc. cit.* xliii. p. 707 (1927).

had already lost an electron in a collision might, before making a capture to fill the vacant place, collide with a second cathode-ray electron and become doubly ionized. But it was later shown that the life of the atoms in the excited states is so short that the probability of double ionization by this method is far too small to account for the observed intensities of the satellites. Accordingly, doubly-ionized atoms, if present in the target of an X-ray tube in sufficient numbers to produce spark lines as observed, must be produced as a result of a *single* collision with a cathode-ray electron which, then, must have sufficient energy to remove *both* electrons from the atom. Thus, to remove both K-electrons from an atom should require a cathode-ray electron *the energy of which is a little more than twice as great as the energy required to remove only one* K-*electron.* In other words, the critical exciting voltage for $K\alpha_4$ should be a little more than twice as great as that for $K\alpha_{1,2}$. Coster* showed that only one of the satellites of the $L\alpha$ line of silver, namely $L\alpha_3$, was produced at an excitation voltage of 4700, the other satellites appearing only at a voltage in excess of *twice* the excitation voltage (3350) of $L\alpha$—as was to be expected from the theory.

3. However, the above experimental evidence in favour of the double ionization theory is neither so extensive nor so exact as to be altogether convincing. Further, there is some evidence, both direct and indirect, against the theory :—

(*a*) Of the direct evidence, the most significant is the observation of Bäcklin †, who studied the critical excitation voltage for the satellites of $K\alpha_{1,2}$ of aluminium, and showed that the lines $K\alpha_3$ and $K\alpha_4$ could be produced at an exciting voltage somewhat *less* than twice the exciting voltage of the $K\alpha_{1,2}$ lines. Bäcklin concluded that, on the theory of double ionization, the lines $K_{3,4}$ should be produced only at voltages *above* 3100; whereas actually Bäcklin found that these lines were produced at 2900 ± 50 volts. Taken at face value, this result is at variance with the observations of Coster, mentioned in the preceding paragraph, regarding the critical excitation voltage of the satellites of $L\alpha$. But in comparing these two observations account must be taken of two circumstances: (1) Bäcklin was working very close to the critical voltage, and it is quite possible that his maximum

* Phil. Mag. xliv. p. 569 (1922).
† *Zeits. f. Phys.* xxvii. p. 30 (1924).

voltages may have been sufficiently above the estimated values to exceed the critical value, 3100 volts. Coster's voltages were not adjusted to as narrow limits as were Bäcklin's. (2) Bäcklin found the lines $K\alpha_3$ and $K\alpha_4$ were produced by an exciting voltage some 5 per cent. *below* the estimated maximum; while Coster showed that the $L\alpha$ satellites were *not* produced by an exciting voltage 30 per cent. below the estimated minimum. Perhaps if these limits had been narrower the two experiments would have been in agreement.

(*b*) Siegbahn and Larson* report that a number of the satellites of the $L\alpha$ lines of Mo(42) are found at an exciting voltage only 30 per cent. above the critical excitation for $L\alpha$; and that *no new satellites appear when the voltage passes twice the exciting voltage for* $L\alpha$, indicating that, even when the energy of a cathode-ray electron is sufficient to remove two L-electrons by "a single act," such doubly-ionized atoms, if present in the target, do not contribute to the production of the *observed* satellites.

(*c*) The satellites appear to have certain physical characteristics which differentiate them from the "diagram" lines, and which indicate that the method of production must be somewhat more complex than that suggested by Wentzel's original scheme. Many writers report that some, at least, of the satellites are much broader than the corresponding diagram lines, and probably have a complex structure. Thus Coster† reports that the lines $L\beta_2'$ and $L\beta_2''$ for Ag(47), satellites of $L\beta_2$, are "very broad and diffuse; that they are symmetrical at low exciting voltages, but that at higher voltages they become "much more intense on their long wave-length side," suggesting that the lines are made up of (unresolved) components which behave differently with increasing voltage.

4. The well-known relation which exists between the absorption of X-rays and the *fluorescent* spectra of the first kind suggests that, if it can be shown that the *spark* lines can be produced by fluorescence, then one might, *perhaps*, expect that the evidence concerning the spark lines should be found in X-ray absorption spectra: for example, absorption discontinuities, very small, of course, since the spark lines are weak, might appear at the wave-lengths corresponding to the critical excitation frequencies of the several groups of

* 'Spectroscopy of X-Rays,' p. 194.

† Phil. Mag. xliv. p. 569 (1922). Coster calls these lines $L\beta_{11}$ and $L\beta_{12}$.

spark lines, just as similar discontinuities are observed in connexion with the spectra of the first kind. Early attempts to produce spark lines by fluorescence were either negative or inconclusive. But recently Coster and Druyvesteyn * have shown that it is possible to produce satellites in the X-ray spectrum of Fe(26) by using the radiation from a copper target excited by 30,000 volts. However (and, from the standpoint of the absorption of X-rays, this is a matter of greatest importance), according to the estimates of Coster and Druyvesteyn, the intensity of the satellites was certainly not over 2 per cent., and probably less than 1 per cent., of the intensity of the fluorescent lines of the first kind. Therefore, absorption discontinuities, corresponding to these spark lines, *if present at all* in absorption spectra, are probably less than 1 per cent. as large as the discontinuities corresponding to lines of the first kind. It is quite obvious that to detect such small discontinuities with certainty would require that the measurements of absorption coefficients be made with the highest precision—indeed, with a precision higher than any which, in the writer's opinion, have been reported up to the present.

However, it does not necessarily follow that the hypothesis of multiple ionization, as an explanation of the origin of spark lines, requires that there should be corresponding absorption discontinuities in X-ray absorption spectra. In order that there should be such discontinuities it would be necessary that the energy, $h\nu$, of an incident quantum should, by a "primary act," cause the expulsion of *two* electrons either from the same or from different levels. The preponderance of evidence, however, seems to be opposed to this possibility, and Coster and Druyvesteyn are of opinion that double ionization comes about as a *secondary* process: an absorbed quantum causes the expulsion of a *single* electron (call it the primary photoelectron) from a given level; if this primary electron possesses sufficient energy, it may, on its way out of the atom, collide with an electron of the same or of another level, and cause the expulsion of the latter electron, the process resulting in a doubly-ionized atom. It should be pointed out, however, that if this latter be the correct sequence of events which produces multiply ionized states. *no increase in absorption of the primary X-ray beam should be observed as, with increasing frequency, the frequency of the primary beam passes the frequency ν_m corresponding to the energy $h\nu_m$ necessary for multiple ionization.* Rather, on

* *Zeits. f. Phys.* xl. p. 265 (1927).

this view, the *energy* for producing the spark lines comes from the kinetic energy initially given to the *primary* photoelectron, which, as it leaves the atom after having knocked out another electron, must therefore possess less energy than it would have had if no secondary process had occurred, by at *least* the energy necessary to remove the second electron. There is no reason to expect that these *secondary* events *in any way* modify the absorption probability of the primary quantum. No discontinuity in the absorption spectrum should be observed at a frequency corresponding to the energy required for double ionization. Rather, as Robinson* points out, evidence concerning spark lines is to be expected in the magnetic spectrum of the photoelectrons ejected by a monochromatic beam of incident X-rays.

5. In this connexion mention may be made of a recent important paper by Alexander † which touches on the subject of multiple ionization. Alexander concludes, from a careful study of certain data on the variation of (X-ray) mass absorption coefficients $\frac{\mu}{\rho}$ as a function of wave-length, that at a wave-length λ_K', approximately $\frac{\lambda_K}{2}$, where λ_K is the wave-length of the K absorption discontinuity, the coefficient k in the well-known empirical equation

$$\frac{\mu}{\rho} = k\lambda^3 + \frac{\sigma}{\rho}$$

undergoes a sudden change, the value of k for $\lambda < \lambda_K'$ being some 30 per cent. greater than the value of k for $\lambda > \lambda_K'$. Alexander interprets this "break" in the absorption curve, shown diagramatically by the full line in fig. 1, as marking the frequency ν_K' at which the energy of the quantum $h\nu$ becomes just sufficient "to remove both K-electrons as a single act. At this point twice as many electrons should be produced, although their speed at the periphery of the atom is .... zero." ‡

This *empirical* description of the relation between $\frac{\mu}{\rho}$ and λ^3, as shown graphically in fig. 1, is perhaps justified by the experimental data. It has been long known that the λ^3

* Phil. Mag. iv. p. 763 (1927).
† *Loc. cit.* iv. p. 670 (1927).
‡ Alexander, *loc. cit.* p. 679.

law of absorption gives only a close approximation to the experimental facts, and that if the equation

$$\frac{\mu}{\rho} = k\lambda^3 + \frac{\sigma}{\rho}$$

be established empirically for frequencies considerably in excess of the K limit, the values of $\frac{\mu}{\rho}$ determined by extrapolation toward the K limit are higher than the observed values. The present writer pointed this out some years ago *, and indeed, in the graph of the data on the absorption

Fig. 1.

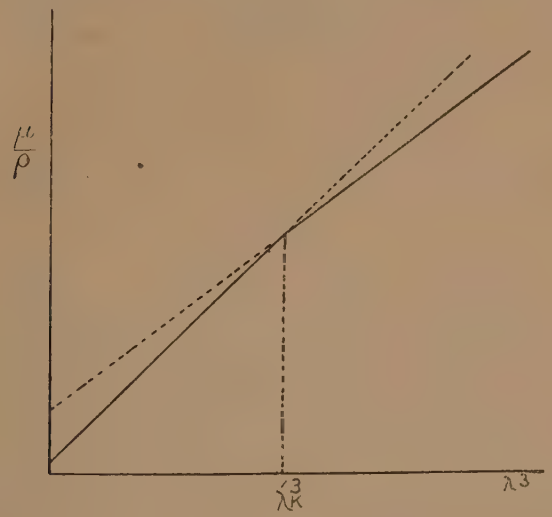

of molybdenum as a function of λ^3 (see fig. 6 of article cited), two straight lines, slightly inclined to each other, were drawn †. Further, in connexion with a precision study of the λ^3 law in the neighbourhood of the K limit ‡, the writer has observed that, although the graph of $\frac{\mu}{\rho}$ as a function of λ^3 on the short wave-length side of, but near to, the K limit is *rigorously* a straight line with no suggestion of deviation therefrom as the limit is approached, the slope

* Phys. Rev. xviii. p. 13 (1921). See p. 26 of article cited.

† These data on molybdenum are included by Alexander in his discussion above cited.

‡ Phys. Rev. xxvii. p. 794 (1926).

of this line is somewhat less than that of the *similar* straight line observed at much shorter wave-lengths. This point is brought out by the writer's data on Sn(50) *, from which two slopes k' and k (in the above terminology) are respectively 755 and 592, in substantial agreement with Alexander's values (data by Allen) of 750 and 583.

In any event the observational data do not seem to *preclude the possibility* that there may be a "break" in the $\frac{\mu}{\rho}-\lambda^3$ curve as suggested by Alexander, although the deviations from the λ^3 law may be represented empirically in different ways. For example, Allen † concludes, from a study of observed data on absorption coefficients of several substances over a wide range of wave-lengths, that absorption-coefficients as a function of λ can be given by a formula (derived on theoretical grounds by Wentzel) of the type

$$\frac{\mu}{\rho}=k_1\lambda^3+k_2\lambda^{3\cdot5}+k_3\lambda^{2\cdot5}+\frac{\sigma}{\rho}.$$

Previously Allen was of the opinion that the empirical relation was

$$\frac{\mu}{\rho}=k\lambda^{2\cdot92}+\frac{\sigma}{\rho}.$$

These various empirical formulæ illustrate the fact that more precise experimental data on absorption-coefficients are needed to establish, unambiguously, the exact *empirical* law of X-ray absorption. (See, for example, section 7, p. 84.)

However, granted for the moment that the data on X-ray absorption are such as to warrant the conclusion that a "break" in the $\frac{\mu}{\rho}-\lambda^3$ curve occurs at λ_K' as suggested by Alexander, the interpretation of this break as indicating the beginning of double ionization of the K shell seems by no means justified by the present experimental facts. There are several very weighty arguments against such an interpretation :—

(*a*) If the wave-length λ_K' of the "break," corresponding to frequency ν_K', represents the beginning of double ionization of the K shell as a result of the photoelectric expulsion of both K-electrons by the absorption of the *single* quantum $h\nu_K'$ or greater, then the energy $h\nu_K'$ must be at least a little greater than *twice* the energy $h\nu_K$ required to remove a *single*

* National Academy of Sciences, Washington Meeting, April 1927. Phys. Rev. Dec. 1927.

† Phys. Rev. xxix. p. 918 (1927).

K-electron, since, because of the effective increase in nuclear charge, the energy required to remove the *second* electron should be a little greater than the energy required for the removal of the first. However, of the thirteen values of ν_K' determined by Alexander, *only four occur at frequencies more than twice the frequency of the* K *limit*, as is shown in Table II., in which columns 1 and 2 are taken from Alexander's paper, column 3 from Siegbahn's 'Spectroscopy of X-Rays,' and column 4 is the ratio of column 2 to column 3. Alexander's interpretation would require, in the case of Ag(47) for example, that the energy required to remove the *second* K-electron should be only 75 per cent. as great as that required to remove the

TABLE II.

Element.	$\left(\frac{\nu}{R}\right)_{K'}$ =A.	$\left(\frac{\nu}{R}\right)_{K}$ =B.	Ratio A/B.
Fe 26.....	1235	524	2·36
Ni 28.....	1311	612	2·14
Cu 29.....	1451	661	2·20
„	1235	„	1·87
„	1078	„	1·63
Zn 30.....	1715	703	2·44
Mo 42.....	2745	1474	1·86
Ag 47.....	3350	1879	1·78
„	3290	„	1·75
Sn 50.....	3781	2148	1·76
W 74.....	8064	5117	1·57
Pt 78..	9027	5764	1·56
Au 79.....	9214	5941	1·56

first K-electron—a conclusion quite at variance with our fundamental concepts of multiple ionization.

On the basis of Wentzel's theory of the origin of spark lines, it is possible to compute the energy required for double ionization of the K shell, by the method used by Turner*, for the elements Na(11) to Zn(30), and by an extrapolation (of course only approximately justifiable) as far as Sn(50). Turner showed that the energy K_Z^2 (in $\frac{\nu}{R}$ units) necessary to remove *both* K-electrons from an atom of atomic number Z is given, to a very close approximation, by the expression

$$K_Z^2 = K_Z + L_{(Z+1)} + (\alpha_4)_Z, \quad . \quad . \quad . \quad . \quad (1)$$

* Phys. Rev. xxvi. p. 143 (1925). Turner's computations, based on the only data then available, are for the elements Na(11) to S(16).

where K_Z is the value of $\frac{\nu}{R}$ for the K limit of the atom in question, $(\alpha_4)_Z$ is the value of $\frac{\nu}{R}$ of the satellite $K\alpha_4$, and $L_{(Z+1)}$ is the value of $\frac{\nu}{R}$ for the L limit of an atom of atomic number $(Z+1)$. Siegbahn* gives the measurements of Hjalmer, of Dolejšek, and of Dolejšek and Siegbahn for the wave-lengths of the spark lines $K\alpha_3$ and $K\alpha_4$ from Na(11) to Zn(30). (These lines are not separated for elements of higher atomic number than Ca(20).) The wave-lengths of these are given in columns 2 and 3 of Table III. For purposes of computation and extrapolation we may write equation (1) in the form (by adding and subtracting $K\alpha_2$)

$$K_Z^2 = 2K_Z + (L_{II,(Z+1)} - L_{II,Z}) + (K\alpha_4 - K\alpha_2)_Z, \quad . \quad (2)$$

in which, for reasons which will appear presently, we identify the L limit of equation (1) with L_{II}. The sum of the two brackets on the right represents the amount by which the energy required for the double ionization of the K shell is in excess of that required for single ionization. Both brackets are always positive. A very interesting, and perhaps suggestive, relation may be shown to exist between the satellites $K\alpha_{3,4}$ and the diagram line $K\alpha_2$. If the *square root* of the *difference* in frequency between $K\alpha_4$ and $K\alpha_2$ be plotted as a function of atomic number, the upper *straight line* shown in fig. 2 results. A similar plot for the difference $(K\alpha_3 - K\alpha_2)$ gives the *lower* straight line. Since the satellites $K\alpha_3$ and $K\alpha_4$ are not separated for elements above Ca(20), the observed wave-lengths for elements of atomic number greater than 20 are therefore the centre of gravity of the two lines, and are seen to fall between the two straight lines extended. These two differences, $(K\alpha_4 - K\alpha_2)$ and $(K\alpha_3 - K\alpha_2)$, have the characteristic of a screening doublet, with a *difference* in screening constant of (almost) unity. From this graph one finds that over the range Na(11) to Cu(29) the difference in $\frac{\nu}{R}$ between $K\alpha_4$ and $K\alpha_2$ is given empirically by

$$\left(\frac{\Delta\nu}{R}\right)_{(K\alpha_4 - K\alpha_2)} = 49 \times 10^{-4}(Z+0{\cdot}4)^2 \ldots \quad . \quad . \quad (3)$$

An extension of equation (3) as far as Sn(50) is approximately justified. The values of $\frac{\Delta\nu}{R}$ computed from this equation are given under "B" in column 10 of Table III.

* 'Spectroscopy of X-Rays,' p. 106.

TABLE III.—Computation of the Energy required for Double Ionization of the K-level.
Data from Siegbahn's 'Spectroscopy of X-Rays,' except where indicated.

Element.	Wave-length (ångströms).		$(\Delta\nu/R)$.		$\sqrt{\Delta\nu/R}$.		$\left(\frac{\nu}{R}\right)_{L_{II}}$.	$\left(\frac{\nu}{R}\right)_{K}=K$.	B.	K^2.	K^2/K.
	$K\alpha_3$.	$K\alpha_4$.	$\alpha_4-\alpha_2$.	$\alpha_3-\alpha_2$.	$\alpha_4-\alpha_2$.	$\alpha_3-\alpha_2$.					
Na 11	11·8039[1]	11·7869[1]	0·63	0·52	0·79	0·72	2·16	78·84[3]	0·64	159·63	2·0248
Mg 12	9·8000[1]	9·7842[1]	0·79	0·64	0·89	0·80	3·47	95·81	0·75	194·04	2·0·46
Al 13	8·2658[1]	8·2501[1]	0·92	0·71	0·96	0·84	5·14	114·67	0·88	232·09	2·0240
Si 14	7·0638	7·0537	1·01	0·83	1·01	0·91	7·01	135·19[3]	1·02	274·28	2·0289
P 15	6·1022	6·0950	1·16	0·96	1·08	0·98	9·89	158·26	1·16	319·71	2·0202
S 16	5·3294	5·3233	1·29	1·10	1·14	1·05	11·92	181·81	1·32	367·85	2·0232
K 19	3·7110	3·7088	1·86	1·72	1·36	1·31	21·49	265·33	1·85	536·89	2·0235
Ca 20	3·3323	3·3300	2·04	1·84	1·42	1·36	25·87	297·48	2·04	601·40	2·0216
Sc 21	—	—	—	—	1·50		30·27	331·17	2·25	668·00	2·0171
Ti 22	2·7269		2·42		1·56		33·68	365·43	2·45	737·71	2·0188
Va 23	2·4846		2·56		1·60		38·08	402·27	2·69	812·27	2·0192
Cr 24	2·2733		2·75		1·66		43·12[2]	441·23[2]	2·92	890·44	2·0181
Mn 25	—		—		—		48·18[2]	481·83[2]	3·16	972·08	2·0175
Fe 26	1·9233		3·22		1·79		53·44[2]	524·00[2]	3·42	1057 02	2·0172
Co 27	1·7774		3·49		1·89		59 04[2]	568·24[2]	3·68	1145·82	2·0165
Ni 28	1·6476		3·63		1·91		64·70[2]	614·12[2]	3·95	1237·81	2·0156
Cu 29	1·5307		4·05		2·02		70·32[2]	661·59[2]	4·25	1334·21	2·0167
Zn 30	—		—		—		77·10[2]	—	—	—	—
Zr 40	—		—		—		169·6	1325·8	8·0	2671·4	2·0149
Nb 41	—		—		—		181·4	—	—	—	—
Sb 51	—		—		—		323·6	2241·7	12·9	4517·9	2·0132
Te 52	—		—		—		340·3	—	—	—	—

[1] Wetterblad, *Zeits. f. Phys.* xlii. p. 611 (1927). [2] Thoræus, Phil. Mag. ii. p. 1107 (1926). [3] Estimated by Turner (*loc. cit.*).

The value of K^2 is then readily computed by use of equation (2). Column 12 of Table III. shows the ratio $\frac{K^2}{K}$, which is seen to decrease very slowly with increasing atomic number, but of course remains in excess of 2·000. In fig. 3 is shown

Fig. 2.

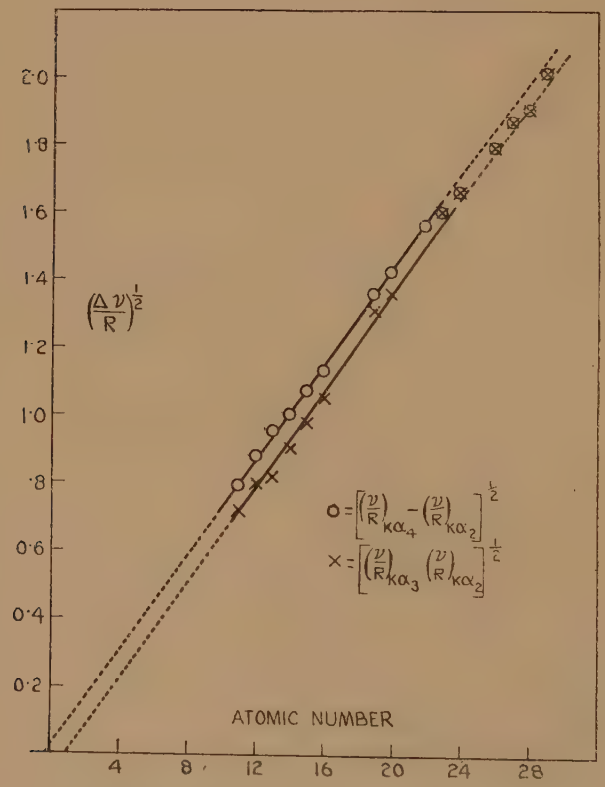

the ratio $\frac{K^2}{K}$ for double K-ionization as computed from equation (2) and, for comparison, the ratio $\frac{\nu_K'}{\nu_K}$ from Table I., as determined by Alexander. It is quite apparent that, *so far as existing data go*, one is not justified in concluding that there is any obvious relation between Alexander's ν_K' break and the double ionization of the K level.

(*b*) As pointed out above, the intensity of the spark lines is so weak that, granted Wentzel's theory, one would not

expect to find a change of shape in the $\frac{\mu}{\rho} - \lambda^3$ curve as great as that reported by Alexander. Further, if λ_K' marks the beginning of double ionization, one should find a "jump" or discontinuity in the curve similar to the K, L_I, L_{II}, ... discontinuities, instead of simply a bend *. But Alexander's curves show no such "jump."

Fig. 3.

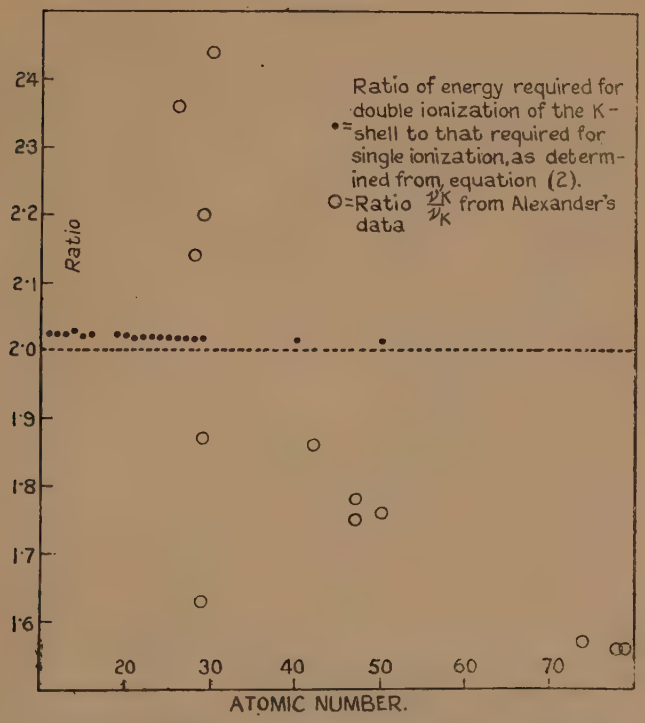

* Alexander's suggestion that, beginning with the wave-length λ_K', "both K-electrons are removed by a single act" and that "twice as many electrons are produced" implies that, beyond this critical wave-length, all K absorption results in double ionization of the K shell and that no single ionization occurs. Were this the case, and were the values of λ_K' those given by Alexander, the fluorescent K series lines produced by absorption of radiation of wave-length $\lambda < \lambda_K'$ should be quite different from those wave-lengths when produced by radiation $\lambda > \lambda_K'$. In other words, the fluorescent spectra of the first kind, when produced by absorption of radiation extending on both sides of λ_K', as, for example, in the experiments of Coster and Druyvesteyn (*loc. cit.*) should be double. No such duplicity in fluorescent spectra has been reported.

(*c*) Wentzel's theory attributes the line $K\alpha_3$ to the transition $KL \rightarrow L^2$. One should expect, therefore, a break in the $\frac{\mu}{\rho} - \lambda^3$ curve at the frequency corresponding to simultaneous ionization of the K and the L shells. This "break" should occur for an element of atomic number Z at a frequency ν_{KL}, given to a close approximation, by

$$h\nu_{KL} = h\nu_K + h\nu_{L(Z+1)}.$$

The writer's data on Sn(50) * show that no such break is observed in the predicted region.

(*d*) As pointed out above (Sect. 4), the existing data seem to indicate that double ionization occurs as a *secondary* process, rather than as a *primary* act in which two electrons are simultaneously expelled by the absorption of a single quantum. We should not therefore expect to find in the X-ray absorption spectra evidence concerning the processes which give rise to the (fluorescent) spark spectra.

In short, the conclusion seems justified that the "break" represented in fig. 1, *if real*, must be explained on some other grounds than multiple ionization.

6. The two straight lines in fig. 2 resemble a Moseley diagram, and perhaps warrant a few brief suggestions, admittedly highly speculative, concerning a possible alternative theory of the origin of X-ray satellites. The lines $K\alpha_4$ and $K\alpha_3$ are usually considered satellites of $K\alpha_1$. But if the square root of the difference in frequency between either of these lines and $K\alpha_1$ be plotted against atomic number, one does not obtain a straight line. The straight lines of fig. 2 suggest the possibility that $K\alpha_4$ and $K\alpha_3$ are satellites of $K\alpha_2$ instead of $K\alpha_1$. One inquires whether satellites of other lines, when plotted as in fig. 2, yield similar straight lines. Unfortunately, data bearing on this question are exceedingly limited, partly because measurements of many of the satellites have been made for only a few elements, and partly because the diffuse nature of some of the satellites and their closeness to the parent line make it difficult to obtain wave-length measurements with high precision—a matter of considerable importance in consideration of the fact that the differences in frequency between satellites and the "parent" lines are, in general, only a fraction of 1 per cent. In Table IV. are given the square roots of the frequency differences between some of the more prominent satellites and the respective parent lines. A Moseley plot of these data is shown in figs. 2

* *Loc. cit.* Phys. Rev., Dec. 1927.

and 4. Fig. 4 contains data on *eight* satellites: three of $L\alpha_1$, two of $L\beta_1$, two of $L\beta_2$, and one of $L\gamma_1$. The points seem to fall into *five* groups, through which *parallel* * straight lines, A, B, C, D, and E, have been drawn. Although there is considerable scattering, the points seem to fit these straight lines reasonably well. Further, in several cases, points from different satellites fall upon, or near, the same line. For example, from atomic number 45

Fig. 4.

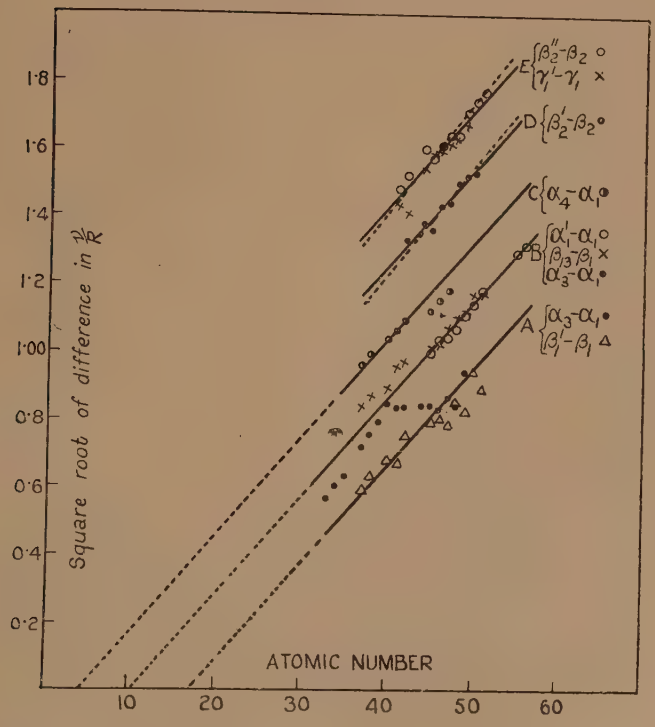

to 51, the difference $(L\alpha_1' - L\alpha_1)$ coincides very nearly with $(L\beta_{13} - L\beta_1)$. The difference $(L\beta_2'' - L\beta_2)$ is almost the same as $(L\gamma_1' - L\gamma_1)$.

One is now tempted to suggest the hypothesis that these satellites are produced by *two-electron* transfers, similar to the primed lines (terms) in optical spectra. Or, for example, that the line $K\alpha_4$ is the result of the *simultaneous* jump of

* Perhaps the dotted lines at D and E are better

Table IV.

Square Root of Frequency Difference between Satellites and the respective "Parent" Lines, in $\frac{\nu}{R}$ units.

Element.	K Satellites.			L Satellites.							
	$\alpha_4-\alpha_2$*. 1	$\alpha_3-\alpha_2$†. 1	$\beta'''-\beta_1$‡. 2	$\alpha_1'-\alpha_1$‡. 3	$\alpha_3-\alpha_1$‡. 3	$\alpha_4-\alpha_1$‡. 3	$\beta_1'-\beta_1$‡. 3	$\beta_{13}-\beta_1$‡. 3	$\beta_2'-\beta_2$†. 2	$\beta_2''-\beta_2$†. 2	$\gamma_1'-\gamma_1$†. 2
11 Na	0·63	0·52									
12 Mg	0·79	0·64									
13 Al	0·92	0·71									
14 Si	1·01	0·83									
15 P	1·16	0·96									
16 S	1·29	1·10									
19 K	1·86	1·72	1·88								
20 Ca	2·04	1·84	1·94								
21 Sc	—		1·93								
22 Ti	2·42		1·92								
23 Va	2·56		1·98								
24 Cr	2·75		1·98								
25 Mn	—		2·07								
26 Fe	3·22		2·16								
27 Co	3·49										

28 Ni	3·63										
29 Cu	4·05										
33 As	—										
34 Se	—	—	—	0·568							
35 Br	—	—	—	0·602							
	—	—	—	0·630							
37 Rb											
38 Sr	—	—	—	0·716	0·960	0·59	0·84				
39 Y	—	—	—	0·757	0·992	0·63	0·87				
40 Zr	—	—	—	0·791	—	—	—				
41 Nb	—	—	—	0·846	1·033	0·68	0·89				
	—	—	—	0·832	1·062	0·67	0·95	—	1·48	1·43	
42 Mo	—										
44 Ru	—	—	—	0·836	1·091	0·75	0·97	1·33	1·52	1·41	
45 Rh	—	—	—	0·84	—	—	—	1 38	1·60	1·54	
46 Pd	—	—	0·996	0·84	1·120	0·79	1·02	1·36	1·57	1·57	
47 Ag	—	—	1·037	0·83	1·153	0 80	1·04	1·43	1·61	1·59	
		—	1·040	0·863	1·180	0·78	1·07	1·44	1·64	1·61	
48 Cd	—										
49 In	—	—	1·056	0·84	—	0·85	1·10	1·50	1·64	1·63	
50 Sn	—	—	1·108	0·942	—	0·82	1·12	1·52	1·71	1·67	
51 Sb	—	—	1·137	—	—	0·94	1·17	1·53	1·74	1·65	
55 Cs	—	—	1·183	—	—	0·89	1·18				
56 Ba	—	—	1·293					1·77			
		—	1·315								

* Siegbahn, 'Spectroscopy of X-Rays.'

† Druyvesteyn, *Zeits. f. Phys.* xliii. p. 707 (1927).

‡ Coster, Phil. Mag. xliii. p. 1070 (1922).

one electron from the L_{II} level to a vacancy in the K shell, and of another electron from an optical level into a vacancy in the M shell, *both transfers cooperating to emit a single quantum*. The fact that the graphs of figs. 2 and 4 are, at least approximately, similar to the Moseley diagram for X-ray lines is itself strongly suggestive of the possibility that the graphs represent X-ray *lines* (perhaps semi-optical lines) such as might be produced by *single*-electron transfers.

If so, we might picture the production of $K\alpha_4$ as follows :— An atom becomes, by one of several possible processes, doubly ionized; *i. e.*, it lacks one K-electron and one M-electron. First, let us say, the vacant M shell is filled by an electron dropping from an optical orbit for which transfer the atom behaves (since it lacks a K-electron) very nearly like an atom of the next higher atomic number; and an amount of energy, call it $(M-O)_{(Z+1)}$, is released. The transfer L_{II} to K then occurs and energy $(K-L_{II})_Z$ is released, which gives the first-order line $K\alpha_2$. If these two events occur simultaneously, a single quantum, corresponding to $K\alpha_4$, might be emitted, and we should have

$$K\alpha_4=(K-L_{II})_Z+(M-O)_{(Z+1)}$$

or $$K\alpha_4-K\alpha_2=(M-O)_{(Z+1)}.$$

It might, perhaps, be expected that a Moseley plot of the "line" $(M-O)_{(Z+1)}$ would yield (approximately) a Moseley graph.

In support of this hypothesis one may introduce the following evidence :—

(*a*) The lines of figs. 2 and 4, particularly of fig. 2, *are* Moseley graphs.

(*b*) The order of magnitude of the quantity $(K\alpha_4-K\alpha_2)_Z$ is what one might expect for the quantity $(M-O)_{(Z+1)}$. Unfortunately, only a qualitative check of this predicted equality is possible. Taking Na(11), for example, we do not know what *optical* frequencies would be emitted by an atom which has lost a K-electron. But the work required to remove the valence electron from such a K-ionized Na atom should be of the order of magnitude of, or a little greater than, the work to remove the *second* valence electron from a Mg(12) atom. The latter is *, in terms of $\frac{\nu}{R}$, 1·105. The term $(M-O)_{(Z+1)}$ should be somewhat smaller than this. Actually $(K\alpha_4-K\alpha_2)$ for Na is

* Paschen and Götze, 'Serien Gesetze der Linien Spektren.' Berlin, 1922.

0·64. Going to the other end of the series of elements for which we have data on $K\alpha_4$, namely Cu(29), we should expect that $(K\alpha_4 - K\alpha_2)$ should be somewhat smaller than the energy of the M levels of Cu. Siegbahn gives for $M_{III,IV}$ for Cu, $5{\cdot}2\frac{\nu}{R}$. From Table II. one observes that $(K\alpha_4 - K\alpha_2)$ for Cu is $4{\cdot}05\frac{\nu}{R}$. Further, the order of magnitude of the corresponding differences for the L satellites is the same as that of the energy of the outermost electron levels of the respective atoms.

(*c*) On this hypothesis we should expect that there might be several different semi-optical transfers of the "(M—O)" type which could co-operate with a given parent line in producing the observed satellite, which, then, should have a "fine structure." As previously mentioned, many of the satellites are broader and more diffuse than the diagram lines.

Opposed to this hypothesis of two-electron transfers as an explanation of satellites are the following arguments :—

(1) Wetterblad's * recent measurements confirm with reasonable precision the equality of the differences $(K\alpha_6 - K\alpha_4)_Z$ and $(K\alpha_3 - K\alpha_1)_{(Z+1)}$, predicted by Wentzel's theory of multiple ionization. This confirmation, however, has been made only for the four elements Na(11) to Si(14), and only for the satellites of $K\alpha_{1,2}$.

(2) Druyvesteyn's † computation of the frequency of the satellite $K\beta'''$ from that of the parent line $K\beta_1$, for the elements K(19) and Fe(26) on the basis of Wentzel's theory agrees within experimental error with observations.

(3) Coster's measurements seem to indicate that the critical excitation potentials for satellites are considerably higher than would be expected if they were produced by the two-electron transfers herein suggested. On the contrary, Bäcklin's measurements ‡ appear to invalidate the measurements of Wetterblad referred to in (1) above, since the latter, on the one hand, confirm Wentzel's postulate that the line $K\alpha_4$ arises from double ionization of the K shell, while the former, on the other hand, show that $K\alpha_4$ is produced under conditions where double ionization seems impossible.

In short, the only categorical statement concerning X-ray satellites which at present seems entirely justified is that the theory of their origin is as yet an unsolved problem !

* *Loc. cit.*
† *Loc. cit.*
‡ *Loc. cit.*

7. In making measurements of X-ray absorption-coefficients with a precision sufficient to detect such small discontinuities as might correspond to the spectra of the second kind as discussed above, it is necessary to be meticulous in the elimination of, or correction for, the various experimental errors. Among these is the error introduced by the fact that the slit system used in the X-ray spectrometer is of finite width. With sufficiently narrow slits the error is negligible. But with slit-widths as great as have been used in some of the measurements of absorption-coefficients reported in the literature of the subject, the error may amount to several per cent. The magnitude of the error depends on the slit-width, the material under investigation, the wave-length at which the measurement is made, and the voltage applied to the X-ray tube. By making certain justifiable simplifications, one can compute the order of magnitude of the error in any particular case.

Fig. 5.

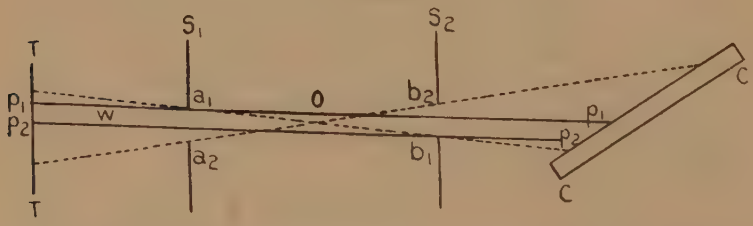

In fig. 5, let S_1 and S_2 be the two slits of the X-ray spectrometer; TT the target of the X-ray tube; and CC the crystal. Let the slit-widths be equal and be represented by a_1a_2 and b_1b_2*. Let the X-ray "brightness" of the target be uniform, and assume that we have a perfect crystal. Then X-rays will be incident onto the crystal at all angles from that corresponding to the incident direction a_1b_1, reflected wave-length λ_1, to that corresponding to a_2b_2, reflected wave-length λ_2. Let the angle† $a_1oa_2=\Delta\theta$. Then the wave-length range, $\lambda_1-\lambda_2=\triangle\lambda$, included in the bundle of X-rays reflected from the crystal, is, from Bragg's equation,

$$\triangle\lambda=2d\cos\theta_0\triangle\theta,$$

where d is the grating space of the crystal and θ_0 is the

* The slit-widths are grossly exaggerated in the figure in comparison with the distance between slits.

† In any actual case very small.

angle which the axis of the slit system makes with the crystal. The X-ray energy corresponding to a wave-length λ within this range $\triangle\lambda$ and entering the ionization chamber after reflexion from the crystal, is limited by the edges of the slit system and varies from zero at λ_1 to a maximum at angle θ_0, and back to zero at λ_2. For example, the intensity of radiation of wave-length λ_p corresponding to the incident direction p_1p_1 is determined, as is readily seen from the figure, by the distance W between the parallel lines p_1p_1 and p_2p_2.

Fig. 6.

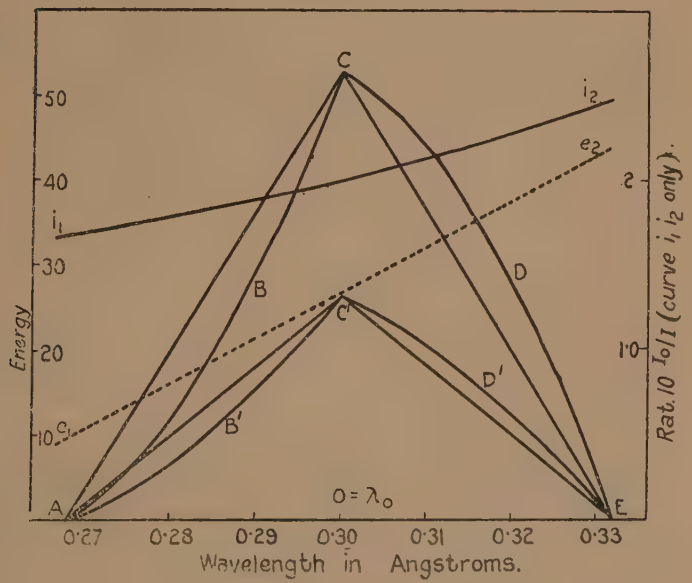

If we assume that the X-ray *spectral* energy distribution *from the target* is constant over the range $\lambda_1 - \lambda_2$, then it follows, since in any actual case the angle a_1oa_2 is very small, that the energy distribution reflected from the crystal into the ionization chamber is given, in this ideal case, by the triangle ACE of fig. 6. If, now, there be inserted in the path of the beam an absorber which transmits, at each wave-length between λ_1 and λ_2, exactly 50 per cent. of this incident radiation, the energy distribution of the reflected radiation will be given by the triangle AC'E, each ordinate of which is exactly half of the corresponding ordinate of

ACE. The ratio I/I_0 (ratio of transmitted to incident radiation in the equation $I=I_0e^{-\mu x}$) will be given by

$$\frac{I}{I_0}=\frac{\text{area AC'B}}{\text{area ACB}}=\frac{OC'}{OC}=\frac{1}{2}.$$

It is obvious that the finite width of the slit has in this case introduced no error in the observed ratio I/I_0. If, however, (1) the spectral energy distribution in the incident radiation is not uniform, and (2) the absorber, because of variation of absorption-coefficient with wave-length, transmits different amounts at each wave-length, the result is somewhat different.

To take a concrete case:—Certain measurements of absorption-coefficients have been reported in which the slit-widths were such that the angle a_1oa_2 of fig. 5 was about 30 minutes of arc. Let us consider the error introduced in measuring the absorption-coefficient of copper at a wave-length 0·3 Å., when the spectral energy distribution in this region is that corresponding to the continuous spectrum excited by some 50,000 volts. In this case the spectral range λ_1 to λ_2 of fig. 5 corresponds to, roughly, 0·06 Å. (calcite crystal). The spectral energy distribution over this range is represented by the line * e_1e_2 of fig. 6, the ordinate at λ_0 being arbitrarily taken as unity. Let the copper absorber be chosen of such thickness that at $\lambda=0{\cdot}3$ Å. it transmits 0·50 of the incident energy. Then, assuming the approximate linear relation between λ^3 and the mass absorption-coefficient in this region, the ratio I_0/I of the incident to the transmitted radiation at each wave-length λ in the region $0{\cdot}27<\lambda<0{\cdot}33$ is given by the line i_1i_2 of fig. 6. Multiplying each ordinate of the triangle ACE by the corresponding ordinate of the spectral energy distribution curve of the incident radiation (e_1e_2) gives ABCDE, which is the spectral energy distribution of the radiation I_0 as reflected into the ionization chamber. Dividing the ordinates of this latter curve by the ratio I_0/I at each wave-length gives AB'C'D'E, which is the energy distribution in the radiation I (*i. e.*, the radiation entering the ionization chamber after passing through the absorber). The *observed* ratio I/I_0 is given by

$$\frac{I}{I_0}=\frac{\text{area AB'C'D'E}}{\text{area ABCDE}}.$$

* A linear relation is assumed for the energy distribution between λ_1 and λ_2 for simplicity in computation. The final result is not materially changed by this assumption.

This ratio is not quite equal to the ratio $OC'/OC = 0{\cdot}500$, which is the ratio to be expected if an infinitely narrow slit system were used. By measuring the two areas, and observing how much the observed ratio I/I_0 differs from 0·500, one can obtain the error in the resulting value of the mass absorption-coefficient.

As an illustration of order of magnitude, there are given in Table V. the errors, computed as above, for copper of three thicknesses such as to transmit, respectively, 1/10, 1/2, and 4/5 of the incident beam, and for spectral energy distributions corresponding roughly to 50,000 and to 60,000 volts.

TABLE V.

Errors, in per cent., in measuring mass absorption-coefficients of copper at $\lambda = 0{\cdot}3$ Å. with a slit system 0·06 Å. wide, at two voltages. A positive error means that the observed value is too large.

Transmission at $\lambda = 0{\cdot}3$ Å.	Error in per cent.	
	V=60,000.	V=50,000.
0·100	−0·8	+1·7
0·500	0·0	+1·8
0·800	+0·4	+3·8

Of course, the values are only approximate because of the simplifying assumptions which have been made. For elements of higher atomic number than copper the error becomes greater (so long as $\lambda = 0{\cdot}3$ is in the K-absorption region). The error becomes greater at shorter wave-lengths and *vice versa*. The error becomes rapidly smaller the smaller the slit-width (rather, the smaller the ratio $\triangle\lambda/\lambda$).

While these errors are not large, they must be taken into account when attempting to measure absorption-coefficients with a precision of the order of 1/10 per cent. Either a correction for the finite width of the slit must be made, or one must use a slit system sufficiently narrow so that the error is less than the desired precision. This latter is made somewhat difficult by the fact that the energy transmitted by a slit system of the type shown in fig. 5 decreases as the *square* of the slit-width.

Summary.

1. The question has been raised: Are there in X-ray absorption spectra discontinuities corresponding to the so-called "spark" lines analogous to the K, L, K .... discontinuities corresponding to the diagram lines? The present evidence seems to indicate that the processes which give rise to the spark lines are secondary processes, and we should not therefore expect to find evidence concerning their origin in absorption spectra. But in any event the spark lines are so weak compared with the diagram lines that existing data on X-ray absorption-coefficients are not sufficiently precise to detect such discontinuities as might occur.

2. It is shown that a straight line (Moseley graph) results when one plots the square root of the difference in frequency between a spark line and its "parent" line as a function of atomic number. This suggests the possibility that spark lines may originate in two-electron transfers.

3. In making precise measurements of X-ray absorption-coefficients, it is necessary to use slits sufficiently narrow to eliminate the "slit-width" error. The magnitude of this error is computed for one special case, and it is shown that with slit-widths as wide as some which have been used, errors as large as several per cent. may occur in the neighbourhood of 0·3 Å.

Göttingen,
January 14, 1928.

VI. *Polarization of Infra-red Radiation by Calcite.* *By* A. M. Taylor, *M.A., Ph.D., Ramsay Memorial Research Fellow* *.

Introduction.

In a recent communication [1] it was shown by examination between wave-lengths 8 μ and 14 μ that interference effects are to be observed in the absorption spectrum of a thin slice of calcite, and it was further suggested that a great many absorption bands which were found by Schaefer, Bormuth, and Matossi [2] in their work on various carbonates, and which they attributed to "combination tones" formed from the several fundamental frequencies of vibration, were spurious and in reality owed their origin to

* Communicated by Dr. E. K. Rideal.

interference within the crystal film. That these bands are not, however, all due to such a cause is shown by the fact that, while the wave-lengths of successive maxima or minima when substituted in an interference formula $(1/\lambda_1 - 1/\lambda_2) = 1/2nz$, where z is the thickness of the crystal film, give a series of values for n, the refractive index of the material, which indicate the general course of the λ, n curve, the experimental points lie very raggedly about the mean, having divergencies considerably greater than would be expected solely from error in observation. This must imply that the bands found are due to the superposition of interference fringes upon a real variation in intensity caused by selective absorption at particular wave-lengths. It may be remarked that the greatest raggedness occurs about $\lambda = 11{\cdot}3\,\mu$, where there is known to be an intense absorption band for waves having any component of their electric vector along the axis of the crystal, and it is reasonable to suppose that other gross divergencies from the mean line are similarly due to the presence of real absorption.

Accordingly some method was sought by which the true absorption could be differentiated from interference effects. The immediately obvious one of using thicker slices of the absorbing material, thereby causing the interference bands to become finer and less pronounced and the absorption bands to be intensified, did not appear practicable owing to the fact that general absorption usually masked the whole when thicker slices were employed, the more particularly because in the most debatable region from $8\,\mu$ to $14\,\mu$ the spectral energy is very weak. In the following pages is described a method, based on polarization of the infra-red radiation by the absorbing crystal itself, by which the desired analysis has been effected.

Method.

The three fundamental frequencies of vibration in carbonates, which are active in absorbing radiation [3] (*i. e.* which involve a periodic variation of the electric moment of the CO_3 group), lie at wave-lengths of about $7\,\mu$, $11\,\mu$, and $14\,\mu$ [4], and are polarized with the electric vector of the first and last perpendicular to, that of the other parallel to, the the optic axis. If, therefore, a thin slice of crystal be cut parallel to the optic axis, radiation of wave-length approximating to any of these fundamentals will, on transmission normally to the slice, suffer partial absorption, and the transmitted beam will be more or less polarized with the electric vector at right angles to that of the particular

vibration concerned in the absorption. Clearly, if such radiation be now allowed to fall upon a second crystal similarly cut, the final intensity of the transmitted beam will depend upon the angle θ at which the optic axis of the second crystal is disposed relatively to that of the first, being a maximum when the axes are parallel and a minimum when they are perpendicular. In short, the two crystals will behave in the infra-red region at the appropriate wave-

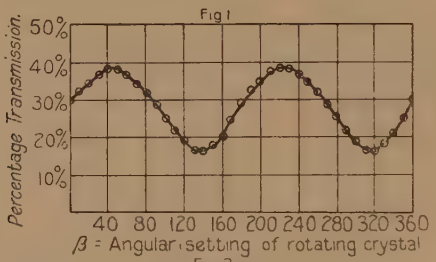

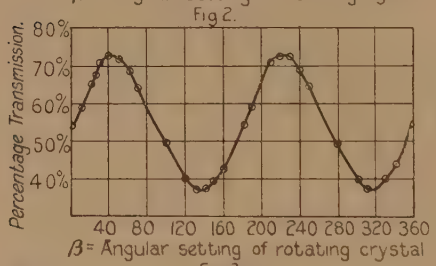

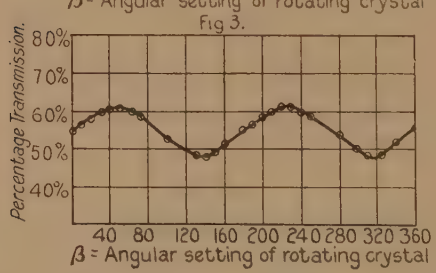

lengths, just as two crystals of tourmaline do in the visible, the first acting as a polarizer, the second as an analyser.

To test this the author examined the behaviour of two pieces of calcite 0·1 mm. and 0·05 mm. thick respectively, which were cut parallel to the optic axis. Observed under crossed nicols in sodium light the orientation of the crystals appeared to be perfectly accurate, so far as could be judged by eye from the character of the interference brushes.

The crystals were mounted in brass holders, and one was arranged so as to rotate * with great precision some 1 mm. or so in front of the second crystal, of which the setting was fixed. Both crystals were then mounted in the sliding crystal holder of a spectrometric apparatus already described in previous papers [5], and the ratio of the intensity I_t of the transmitted beam to I_0, that of the incident beam, was measured for different values of θ, using only radiation of one particular wave-length. It should be mentioned that each crystal was provided with a circular stop to limit the width of the beam, and the stop of the fixed crystal was smaller than that of the rotating crystal, both stops, however, being carefully centred about the axis of rotation. This axis was normal to both crystal slices, and coincided with

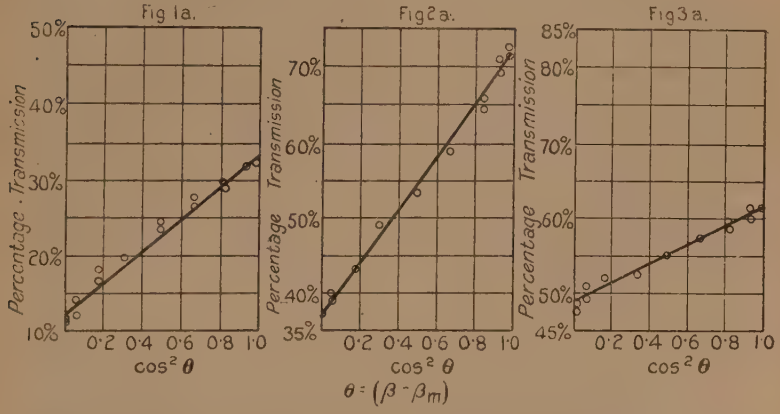

the central ray of the cone of radiation passing through them. The slices were ground accurately plane-parallel, and therefore, with the above precautions, any observed variation with θ of the intensity of the transmitted beam must of necessity be ascribed to polarization effects.

The experimental values of the ratio I_t/I_0 for three different values of λ, each in the neighbourhood of an absorption band, are plotted in figs. 1 to 3, against β, the reading of the pointer on the divided circle bearing the rotating crystal. The angle β_m, at which I_t/I_0 becomes a maximum, is the same in each case, and I_t/I_0 goes through a complete cycle in 180° of arc. If I_t/I_0 be plotted against $\cos^2(\beta-\beta_m)$ a straight line is obtained (figs. 1 *a* to 3 *a*),

* For the loan of a suitably divided circle I am indebted to Dr. W. A. Wooster of the Mineralogical Department here.

indicating the character of the relation which exists between I_t and θ, where $\theta = (\beta - \beta_m)$. As will be shown, this relationship is demanded by theory, and is a proof that the effect is due to polarization of the radiation by the crystals, and, moreover, it will be seen that the effect may be used for obtaining a solution of the problem in hand.

Consider the passage of a beam of monochromatic radiation of incident intensity $2I_0$ through the crystals along the axis of rotation of the movable specimen. The beam is supposed to be unpolarized, and the direction of the electric vector is therefore a random one. There must then be an even distribution of the components of the electric vectors resolved parallel and perpendicular to the optic axis of the first crystal, so that the intensities of the radiation polarized in these two directions must be equal, and given by I_0. The absorption and reflexion coefficients of the crystal for these two portions of the incident beam are not, however, the same; they may be written as α_1 and R_1 parallel to, and α_2 and R_2 perpendicular to, the optic axis. Treating each part separately, and taking into account only the first two terms of the series of multiply reflected beams which are produced, and which can reinforce or interfere with each other, the intensity I of each part after transmission is, following the method of a previous paper [1], given by an expression

$$I = I_1 + I_2 + 2\cos\phi\sqrt{I_1 I_2},$$

where I_1 is the direct and I_2 the intensity of the twice reflected beam, and ϕ is the angle of the phase difference between them. As before [1]

$$I_1 = I_0(1-R)^2 e^{-\alpha z},$$

$$I_2 = I_0(1-R)^2 R^2 e^{-3\alpha z},$$

where z is the thickness of the crystal slice, whence

$$I = I_0(1-R)^2(e^{-\alpha z} + R^2 e^{-3\alpha z} + 2R\cos\phi e^{-2\alpha z}),$$

which, as R is dependent upon α and upon n the refractive index, which is itself an implicit function of α, may for brevity be written (ϕ also being a function of n),

$$I = I_0 . F(\alpha_1, z) \quad \text{parallel to the optic axis,}$$

and

$$I = I_0 . F(\alpha_2, z) \quad \text{perpendicular to the optic axis.}$$

Now consider these two portions of the transmitted beam, when incident upon the second crystal, of which the optic axis is inclined at an angle θ to that of the first. As there is a random distribution of phase between the two portions of the beam transmitted through the first crystal, the equivalent intensities of the components obtained by resolving the electric vectors parallel to and perpendicular to the optic axis of the second, may be expressed by squaring and adding the amplitudes resolved in the appropriate directions, so that

$$I = I_0 . F(\alpha_1, z_1) \cos^2\theta + I_0 . F(\alpha_2, z_1) \sin^2\theta$$

parallel to the optic axis,

and

$$I_y = I_0 . F(\alpha_1, z_1) \sin^2\theta + I_0 . F(\alpha_2, z_1) \cos^2\theta$$

perpendicular to the axis.

After transmission through the second crystal these parts have intensities given by $I_x . F(\alpha_1, z_2)$ and $I_y . F(\alpha_2, z_2)$ respectively, and since the random distribution of phase is still preserved the total intensity of the transmitted beam of radiation is given by

$$I_t = I_0[\{(\alpha_1, z_1) . F(\alpha_1, z_2) + F(\alpha_2, z_1) . F(\alpha_2, z_2)\} \cos^2\theta + \{F(\alpha_2, z_1) . F(\alpha_1, z_2) + F(\alpha_1, z_1) . F(\alpha_2, z_2)\} \sin^2\theta].$$

If $\alpha_1 = \alpha_2$ this reduces to

$$I_t = 2I_0 . F(\alpha, z_1) . F(\alpha, z_2),$$

so that the intensity is therefore independent of θ.

If, however, $\alpha_1 \neq \alpha_2$, this becomes, on making the substitution $\sin^2\theta = 1 - \cos^2\theta$,

$$I_t = 2I_0(A + B \cos^2\theta),$$

where A and B are functions of the α's and z's. That is to say, the intensity varies as $\cos^2\theta$, which is, in fact, the relation that was found experimentally (*cf.* figs. 1 *a*–3 *a*), and this is a definite proof that the effect observed is indeed due to partial polarization of the radiation on transmission through a plate of calcite cut parallel to the optic axis. Having verified this, the expression for I_t may be used to discover the presence of true absorption as distinct from decrease in intensity due to interference fringes. The importance of the expression is that it gives a value for I_t, which is independent of θ so long as $\alpha_1 = \alpha_2$, but if

this condition be not fulfilled, I_t passes through maximum and minimum values as θ varies from 0 to 2. The expression is cumbrous, and must be simplified by neglecting the terms due to multiply reflected beams. $F(\alpha, z)$ is then replaced by the approximation $e^{-\alpha z}$, and if the further simplification be made that the two crystals are of equal thickness, so that $z_1 = z_2$,

$$I_t = I_0\{(e^{-2\alpha_1 z} + e^{-2\alpha_2 z})\cos^2\theta + 2e^{-(\alpha_1+\alpha_2)z}\sin^2\theta\}.$$

The maximum value of I_t occurs when $\theta = 0$, the minimum when $\theta = \pi/2$, so that

$$I_t(\text{max.})/I_t(\text{min.}) = (e^{-2\alpha_1 z} + e^{-2\alpha_2 z})/2e^{-(\alpha_1+\alpha_2)z}$$

or

$$I_t(\text{max.})/I_t(\text{min.}) = \tfrac{1}{2}\{e^{-(\alpha_1-\alpha_2)z} + e^{(\alpha_1-\alpha_2)z}\}. \ldots$$

Fig. 4.

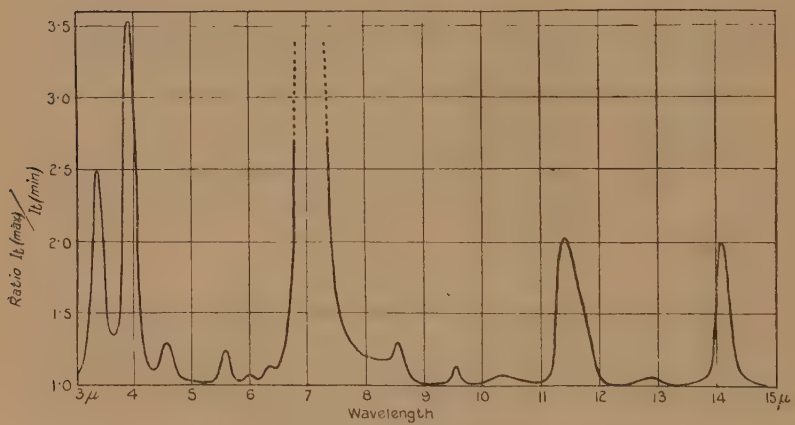

This ratio is a maximum when $(\alpha_1 - \alpha_2)$ is either a maximum or a minimum, and is unity so long as $\alpha_1 = \alpha_2$. If experimental curves be constructed to show the variation of this ratio for different wave-lengths throughout the spectrum, they will indicate clearly the absorption bands by maxima of I_t(max.)/I_t(min.), and by this means true absorption may be differentiated from the spurious variation in the intensity of the transmitted beam produced by interference within each crystal slice.

Using the two pieces of calcite already examined, such a curve was obtained experimentally, and it shows the three

fundamentals at 7 μ, 11 μ, and 14 μ, together with some other bands (fig. 4). In order to try to amplify the effect at the less pronounced maxima, two thicker pieces of calcite 0·65 mm. thick were ground and polished * and the curve re-determined by their aid. At wave-lengths greater than 6 μ this was not possible, however, as the opacity of the material became too great to allow of making accurate measurements of the transmitted intensity.

On comparison of fig. 4, with the results given by Schaefer, Bormuth, and Matossi [2] for the bands found in the absorption spectrum of calcite, it will be seen that a number of lines which they attributed to combination tones, but which Taylor and Rideal [1] showed were really due to interference, are eliminated, and the number of bands which remain to be explained in terms of combination tones is much smaller than before. Previously, Schaefer assumed that the inactive frequency predicted from mathematical analysis [3], *i. e.* the frequency of symmetrical expansion and contraction of the CO_3 group, which involves no alteration in electric moment, is, nevertheless, active when combined with other frequencies ; in other words, though itself it is not connected with any variation of electric moment, merely referring to a mechanical vibration of frequency ν_0, yet it develops an effective variation of electric moment of the same frequency when combined with other active vibrations. Schaefer states that without this assumption it is impossible to account for the whole of the observed spectrum. Even so, his observed and calculated wave-lengths do not agree to any very high order of accuracy, and, as the following table shows, equally good correspondence may be obtained without making use of the inactive frequency ν_0. Only those frequencies are shown in this table which are verified by the method described (*cf.* fig. 4).

Table of Frequencies.

Nature of band.	Observed λ.	Observed $1/\lambda$.	Origin.	Calculated $1/\lambda$.
Fundamental	94 μ	0·0106	ν'''	—
Fundamental	55 μ	0·0182	ν''	—
Fundamental	30 μ	0·0333	ν'	—

* For which I am indebted to the Department of Mineralogy in Cambridge.

Table of Frequencies (*continued*).

Nature of band.	Observed λ.	Observed 1/λ.	Origin.	Calculated 1/λ.
Fundamental	14·16 μ	0·0706	ν_1	—
	12·9 μ	0·077	$\nu_1-\nu_2$	0·078
Fundamental	11·38 μ	0·088	ν_3	—
	10·4 μ	0·096	$\nu_3+\nu'''$	0·098
	9·5 μ	0·105	$\nu_3+\nu''$	0·106
	8·47 μ	0·118	$\nu_2+\nu'+\nu''$	0·122
Fundamental	6·7 μ	0·143	ν_1	—
	7·0 μ	0·149		
	6·3 μ	0·159	$\nu_2+\nu_3$	0·159
	6·0 μ	0·167	$\nu_1+\nu''$	0·161 0·167
	5·54 μ	0·181	$\nu_1+\nu'$	0·176 0·182
	4·64 μ	0·216	$\nu_1+\nu_2$	0·213
	4·50 μ	0·222		0·220
	3·93 μ	0·255	$2\nu_1-\nu'$	0·255
	3·87 μ	0·259		0·265
First Harmonic	3·47 μ	0·239	$2\nu_1$	0·286
	3·35 μ	0·298		0·298
	3·10 μ	0·323	$2\nu_1+\nu'$	0·319
	3·04 μ	0·329		0·331
	2·78 μ	0·360	$2\nu_1+\nu_2$	0·357
	2·74 μ	0·365		0·367
	2·53 μ	0·395	$2\nu_1+\nu_2+\nu'$	0·390
	2·50 μ	0·400		0·402
Second Harmonic	2·33 μ	0·430	$3\nu_1$	0·429
	2·30 μ	0·435		0·447

The criticisms which may be made of the table are sufficiently obvious, but it may be noted that a great many possible combinations would fall about the region 6 to 7 μ and are therefore not separately observable; but it may be that their presence contributes to the great depth and breath of the absorption band at this point, which is exceptionally intense for a single "line," even though a fundamental lies within the limits of the band. One other point of interest is concerned with the band at 3·9 μ, which Schaefer explains as being due to the combination $\nu_1+\nu_0$, and which should therefore have the same structure as $2\nu_1$ which falls at 3·4 μ. In the above table it is suggested that it is formed by $2\nu_1-\nu'$, but it is also possible that $\nu_1+\nu_2+\nu'$ contributes to the production of the band. Such a superposition would

mask the sharpness of the doublet structure associated with ν_1, and this is in agreement with observation, for throughout the series of carbonates the band at $3{\cdot}9\,\mu$ is unresolved, only the merest suggestion of a doublet being given by Schaefer's curves [2], in contrast to that at $3{\cdot}4\,\mu$, which is a very clearly defined doublet.

At the same time a very awkward detail is that of the relative intensities of the bands at $3{\cdot}9\,\mu$ and $3{\cdot}1\,\mu$, that which in the above table is supposed to be due to $2\nu_1-\nu'$ being very strong, whereas that due to $2\nu_1+\nu'$ is comparatively weak. It is not claimed that the suggestions embodied in the above table are in any sense final, because it is impossible to expect exact numerical agreement between calculated and observed values, so long as a correction analogous to that found by Kratzer [6] in the overtones of gaseous molecules is neglected, as has perforce been the case in this paper.

Summary.

The experiments have shown that infra-red rays are partially polarized by transmission through thin plates of calcite cut parallel to the optic axis, and such polarization effects have been used to determine which of the bands observed in the absorption spectrum of calcite really correspond to maxima of absorption, and which are merely spurious and due to interference effects. It is also suggested that the spectrum can be explained without assuming the inactive frequency to be active in combination.

The apparatus used was that described in previous papers [5]. My thanks are specially due to Dr. E. K. Rideal for his continued interest and encouragement.

The Laboratory of Physical Chemistry,
The University of Cambridge.
March 1928.

References.

(1) Taylor & Rideal, Phil. Mag. iv. p. 682 (1927).
(2) Schaefer, Bormuth, & Matossi, *Zeit. für Phys.* xxxix. p. 648 (1927).
(3) Kornfeld, *Zeit. für Phys.* xxvi. p. 205 (1924).
(4) Schaefer & Schubert, *Ann. der Phys.* l. p. 283 (1916).
(5) Taylor & Rideal, Proc. Roy. Soc. A, cxv. p. 589 (1925); Rawlins, Taylor, & Rideal, *Zeit. für Phys.* xxxix. p. 660 (1926).
(6) Kratzer, *Zeit. für Phys.* iii. p. 289 (1920).

VII. *A Method of Calculation suitable in certain Physical Problems.* *By* T. J. I'A. Bromwich *.

IN certain physical problems, there are many examples of pairs of quantities (say x, y) which are connected by a relation of the type

$$y = Ax^n, \quad . \quad . \quad . \quad . \quad . \quad . \quad . \quad (1)$$

A and n being constants (independent of x, y).

Naturally one would usually reduce such a formula as (1) to the logarithmic form

$$\log y = \log A + n \log x \quad . \quad . \quad . \quad . \quad . \quad (2)$$

for the purposes of numerical work.

But, during 1918, I was placed in the position of having to make many calculations of this kind; and the conditions were such that x and y could not differ greatly from certain standard values x_0 and y_0. After some experience in the actual work of the calculations, I convinced myself that a more accurate (as well as a more rapid) method was to calculate the value of the difference $(y - y_0)$ in terms of $(x - x_0)$.

Having recently learned that this transformation could be used with great advantage (in a totally different problem), it has seemed worth while to write out a short account of my method, with the hope that it may prove as useful to other calculators as it has been to myself.

Write, for brevity,

$$(x - x_0)/x_0 = t, \quad (y - y_0)/y_0 = v. \quad . \quad . \quad . \quad (3)$$

Then the equation (1) leads to

$$y/y_0 = (x/x_0)^n \quad . \quad . \quad . \quad . \quad . \quad . \quad . \quad (4)$$

or $$1 + v = (1 + t)^n. \quad . \quad . \quad . \quad . \quad . \quad . \quad . \quad (5)$$

Thus, using the binominal theorem, we have, from (5),

$$v = nt + \tfrac{1}{2}n(n-1)t^2 + \ldots. \quad . \quad . \quad . \quad . \quad (6)$$

For such problems as can be handled conveniently by this method, t is so small that t^3 may safely be neglected (and in many cases t^2 is also negligible).

* Communicated by the Author.

Thus we can write

$$v=nt\{1+\tfrac{1}{2}(n-1)t\} \quad . \quad . \quad . \quad . \quad . \quad (7)$$

or

$$y-y_0=k(x-x_0)\{1-(x-x_0)/x_1\} \quad . \quad . \quad . \quad (8)$$

where we have written

$$k=ny_0/x_0, \qquad x_1=2x_0/(1-n), \quad . \quad . \quad . \quad (9)$$

these values being independent of x, y.

To illustrate the actual working of the method, let us take an idealised example of the actual problem with which I was concerned in 1918: that is, the "adjustment" of cordite charges. Without giving exact values, the naval 15-inch guns (in 1914–1918) may be represented by taking y_0 to be a charge of 420 lb. and x_0 to be a velocity of 2400 f./s. For M.D. cordite the index n may be taken to be $-10/7$ (with four-figure accuracy).

Thus from (9) we find that

$$k=-\tfrac{1}{4}\frac{\text{lb.}}{\text{f./s.}}, \qquad x_1=2000 \text{ f./s. (roughly)} \quad . \quad . \quad (10)$$

To complete the illustration, let us consider the adjustments necessary for differences of velocity $x-x_0=\pm 50$ f./s.

Then (8) gives on substitution from (10)

$$x-x_0=+50 \text{ f./s.}, \qquad y-y_0=-12{\cdot}2 \text{ lb.}$$

and $$x-x_0=-50 \text{ f./s.}, \qquad y-y_0=+12{\cdot}8 \text{ lb.}$$

That is, in the practical forms,

$$x=2450 \text{ f./s.}, \qquad y=407 \text{ lb. } 12\text{oz.}$$

$$x=2350 \text{ f./s.}, \qquad y=432 \text{ lb. } 12\text{oz.}^*$$

Again, if $x-x_0=\pm 20$ f./s., the second-order terms are negligible and the adjustment is simply ∓ 5 lb.

* With large charges the results are only worked out to the nearest $\frac{1}{4}$ lb (=4 oz.). The meaning of the last line (for example) is that, if a charge of 420 lb. gives a velocity of 2350 f./s., then 432 lb. 12 oz. should give 2400 f./s. But so large a correction as 50 f./s. would not usually be made without further firing-proofs.

VIII. *Some Problems in Electrical Machine Design involving Elliptic Functions.* *By* R. T. Coe, *M.A.*, *M.Sc.Tech.*, *A.M.I.E.E.*, *and* H. W. Taylor, *M.I.E.E.**

Summary.

In this paper the authors investigate four problems, three concerning the air-gap flux-distribution of a machine for various conditions of slotting and grooving on one side of the gap, and the other concerning the temperature distribution in the insulation between two conductors and the sides of a slot. The former have special reference to the subject of pole-face losses, and experimental results available for one of the cases considered are found to be in satisfactory agreement with the theoretical results obtained.

These four problems, which can all be treated as two-dimensional, are dealt with by the method of conformal transformation, and, by considering symmetrical figures, the results are obtained in the form of equations involving elliptic functions.

By a systematic treatment the authors show how numerical results may be calculated from such expressions without the difficulties usually associated with elliptic functions.

The results are collected together in the form of curves ready for immediate application to any particular problem.

Synopsis.

I. Introduction.

II. The Variation of Flux-Density on a smooth Pole-face opposite a Succession of Open Slots.

(*a*) Analysis of Problem.

(*b*) Practical Deductions.

(i.) Maximum, Minimum, and Mean Flux-densities on smooth Pole-face.

(ii.) The Gap Coefficient K_g.

(iii.) Calculation of Flux-density Variation along smooth Pole-face.

* Communicated by Sir Richard T. Glazebrook, K.C.B., F.R.S.

III. The Flux-Distribution associated with a Slot of Finite Depth.

(*a*) Analysis of Problem.

(*b*) Practical Deductions.

(i.) Flux-Density at Centre of Slot Bottom.

(ii.) Effective Width of Slot.

(iii.) Gap Coefficient K_g for Repeated Slots.

IV. The Temperature indicated by an Embedded Temperature Detector placed between the two Layers of Conductors in a large Stator Winding.

V. The Flux-Distribution associated with a Grooved Pole-face.

(*a*) Analysis of Problem.

(*b*) Practical Deductions.

(i.) Flux Density on Grooved Surface.

(ii.) The Additional Gap Length equivalent to the Grooves.

(iii.) Gap Coefficient K_g for Air-gap of finite length.

I. Introduction.

The writing of this paper arose, in the first place, out of a consideration of the flux-distribution in the air-gap between a smooth pole-face and a succession of open slots. The mathematical analysis of this problem has already been given by F. W. Carter in a recent paper *, and he shows that the solution involves elliptic functions having two parameters which depend on the relative dimensions of the slot, tooth, and gap. He also indicates the difficulty that arises in choosing suitable values of these parameters to correspond to any given dimensions.

By a systematic treatment the authors of the present paper show how numerical results can be obtained. Values of two parameters which fix the relative dimensions of the slot, tooth, and gap are determined for a large number of particular cases, and hence the values of quantities required are calculated over the whole practical range.

In addition to the above problem, three other problems in electrical machine design are investigated by the methods developed.

* F. W. Carter, "The Magnetic Field of the Dynamo Electric Machine," Journal I. E. E. lxiv. p. 1117 (1926).

II. The Variation of Flux-Density on a smooth Pole-face opposite a Succession of Open Slots.

(a) *Analysis of Problem.*

A knowledge of the manner in which the flux-density varies on a smooth pole-face opposite a succession of open slots is of interest in connexion with a study of pole-face losses. In some cases large fluctuations are possible in this flux-density, and the resulting eddy currents set up in the surface skin of the pole-face may cause considerable heating. A particular case in point is that of the solid pole-face of turbo-alternator rotors.

It will be shown later that for practical purposes the variation in pole-face flux-density can be taken as sinusoidal between a maximum value B_1 under the centre of a tooth and a minimum value B_2 under the centre of a slot.

To give some useful information as to the way in which the magnitude of this flux ripple depends on the ratio of slot opening to gap length, and also on the ratio of slot opening to tooth width, the authors have made calculations over a range of values of $\frac{s}{g}$ from 0 to 3 and $\frac{s}{t}$ from 0 to 5,

where g = gap length,

s = slot width,

and t = tooth width.

Most practical cases will be within the above range.

The problem can be considered as two-dimensional and is solved by the method of conformal transformation.

The most convenient transformation for the first part of the problem is that used by F. W. Carter, since by making suitable changes in the form of the resulting equations the calculations can be made almost entirely from existing tables of Elliptic Functions. Since this same transformation is modified for use in several other problems dealt with later in the present paper, it is developed briefly below in a form particularly suited for calculation purposes.

The method of conformal transformation as applied to the solution of such a problem in two dimensions may be regarded as a means of relating the field in a simplified figure representing the problem in a plane called the z plane to a portion of a uniform rectangular field in a plane called the χ plane.

If x and y are the coordinates of a point in the z plane, z is taken as the complex quantity $x+jy$, and if ϕ and ψ are the amounts of magnetic potential and flux associated with the given point, then χ is taken either as $\psi+j\phi$ or $\phi+j\psi$ according to whether the flux lines in the uniform field are to be vertical or horizontal.

The flux-density at any point is given by the differential coefficient $\frac{d\chi}{dz}$ at that point.

The transformation between z and χ is made through one or more intermediate variables ζ, ζ_1, etc., each of which represents a flux-distribution in a plane. Points in the various planes are represented by the complex quantities $\zeta=\xi+j\eta$, $\zeta_1=\xi_1+j\eta_1$, etc.

Since the only figures considered have straight line boundaries, the Schwarz transformation theorem can be employed to obtain the relation between successive variables. The Schwarz transformation theorem gives the values of the differential coefficients $\frac{dz}{d\zeta}$, $\frac{d\zeta}{d\zeta_1}$, etc., while the constants of integration that arise are evaluated from the various boundary conditions of the problem. It is generally best to express both z and χ in terms of ζ rather than consider the very complicated direct relation between them.

Since the process of integration is considerably simplified by considering a symmetrical figure in the z plane, the figure considered in the given problem is taken as the smallest repeating section of the air-gap field together with its image relative to the smooth pole-face, as indicated by $OABCDC_1B_1A_1$ in fig. 1.

The point O is taken as the origin of the z plane and made to correspond to the origin of the ζ plane, while the pairs of points A and A_1, B and B_1, C and C_1, D and D_1 are made to correspond to the values of $\zeta=\pm 1, \pm\frac{1}{k}, \pm\frac{1}{k_1}$ and $\pm\infty$ respectively.

By the Schwarz theorem the transformation from the z plane to the ζ plane is given by

$$\frac{dz}{d\zeta}=A\frac{(1-k^2\zeta^2)^{\frac{1}{2}}}{(1-k_1^2\zeta^2)(1-\zeta^2)^{\frac{1}{2}}}, \quad \ldots \quad (1)$$

whence

$$z=A\int_0^{\zeta}\frac{(1-k^2\zeta^2)^{\frac{1}{2}}\,d\zeta}{(1-k_1^2\zeta^2)(1-\zeta^2)^{\frac{1}{2}}} \quad \ldots \quad (2)$$

Putting $\zeta = \operatorname{sn} p$ to modulus k

and $k_1 = k \operatorname{sn} \alpha$ to modulus k,

$$z = A\left\{ p - \frac{\operatorname{cn}\alpha}{\operatorname{sn}\alpha \operatorname{dn}\alpha}\Pi(p.\alpha)\right\}. \quad . \quad . \quad . \quad (3)$$

Using the fact that there is a sudden increase in z of

Fig. 1.

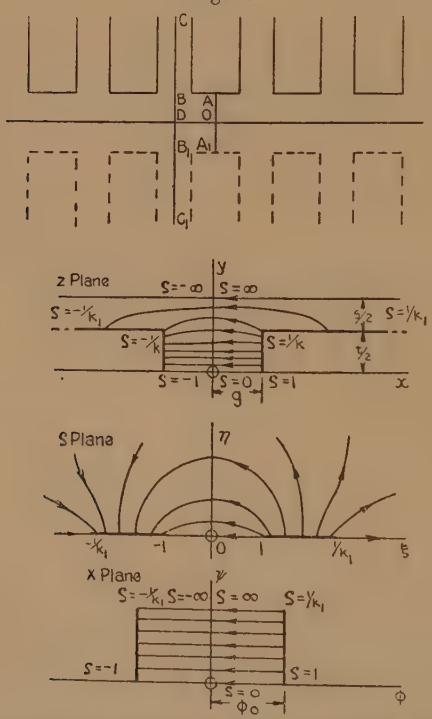

Flux-distribution in an air-gap uniformly slotted on one side.

amount $j\frac{s}{2}$ as ζ increases through the value $\frac{1}{k_1}$ on its real axis we obtain from equation (2)

$$A = \frac{s}{\pi}\frac{\operatorname{sn}\alpha \operatorname{dn}\alpha}{\operatorname{cn}\alpha} \quad . \quad . \quad . \quad . \quad . \quad . \quad . \quad (4)$$

Also using the fact that $z = g + j\frac{t}{2}$ when $\zeta = \frac{1}{k}$,

$$g + j\frac{t}{2} = A\left\{ (K + jK')\left(1 - \frac{\operatorname{cn}\alpha\, Z(\alpha)}{\operatorname{sn}\alpha \operatorname{dn}\alpha}\right) - j\frac{\operatorname{cn}\alpha}{\operatorname{sn}\alpha \operatorname{dn}\alpha}\frac{\pi\alpha}{2K}\right\},$$

whence equating real and imaginary parts and substituting for A from equation (4),

$$\frac{g}{s}=\frac{K}{\pi}\left(\frac{\operatorname{sn}\alpha\operatorname{dn}\alpha}{\operatorname{cn}\alpha}-Z(\alpha)\right), \quad \ldots\ldots \quad (5)$$

and

$$\frac{t}{s}=\frac{2K'}{\pi}\left(\frac{\operatorname{sn}\alpha\operatorname{dn}\alpha}{\operatorname{cn}\alpha}-Z(\alpha)\right)-\frac{\alpha}{K}. \quad \ldots\ldots \quad (6)$$

The elliptic functions in the above expressions are all to modulus k.

Equations (5) and (6) determine the relation between $\frac{g}{s}$ and $\frac{t}{s}$ on the one hand and k and α or their equivalents on the other.

For the purpose of numerical calculation, it is preferable to deal with the modular angle θ and the amplitude angle ϕ of the first elliptic integral involved in the above equations. These are defined by the relations

$$k=\sin\theta$$

and

$$k_1=k\operatorname{sn}\alpha=k\sin\phi,$$

so that equations (5) and (6) become

$$\frac{g}{s}=\frac{K}{\pi}(\tan\phi\cos\theta_1-Z(\alpha)) \quad \ldots\ldots \quad (7)$$

and

$$\frac{t}{s}=\frac{2K'}{\pi}(\tan\phi\cos\theta_1-Z(\alpha))-\frac{r^\circ}{90}, \quad \ldots \quad (8)$$

where

$$\theta_1=\text{arc sin}\,k_1=\text{arc sin}\,(\sin\theta\sin\phi)$$

and

$$\frac{r^\circ}{90}=\frac{\alpha}{K}=\frac{F(\phi.\theta)}{K}.$$

The chief difficulty in using the above results lies in the fact that we usually wish to investigate a problem for which the values of $\frac{s}{g}$ and $\frac{s}{t}$ are specified, and this requires recourse to the method of cross plotting in order to determine corresponding values of θ and ϕ.

By the method outlined below, the authors have found the values of θ and ϕ as given in Table I. for a large number of cases in the range of $\frac{s}{g}$ from 0 to 3 and $\frac{s}{t}$ from 0 to 5.

Values $\frac{s}{g}$ and $\frac{s}{t}$ were calculated from equations (7) and (8) for a number of values θ and $r°$, the intermediate

TABLE I.

Values of θ and ϕ in degrees for Problem of Slots opposite smooth Pole-face.

$\frac{s}{g}$.		0·5.	0·75.	1·0.	1·5.	2·0.	2·5.	3·0.
$\frac{s}{t}=0$	θ	0	0	0	0	0	0	0
	ϕ	76·0	69·5	63·4	53·1	45·0	38·6	33·7
$=0·25$	θ	33·2	13·7	5·65	1·03	0·195	—	—
	ϕ	77·0	69·7	63·6	53·13	45·0	—	—
$\frac{s}{t}=0·5$	θ	65·1	42·1	26·9	10·9	4·50	1·90	0·82
	ϕ	81·1	72·2	64·7	53·3	45·0	38·6	33·7
$\frac{s}{t}=0·75$	θ	77·3	59·5	43·8	23·4	12·8	7·18	4·10
	ϕ	84·0	72·5	67·1	54·3	45·4	38·8	33·7
$\frac{s}{t}=1·0$	θ	82·7	68·7	54·9	34·2	21·4	13·6	8·70
	ϕ	85·8	77·8	69·3	55·6	46·0	39·1	33·9
$\frac{s}{t}=1·25$	θ	85·0	74·3	62·2	42·4	29·1	20·3	14·3
	ϕ	88·6	79·5	71·4	57·1	46·9	39·6	34·1
$\frac{s}{t}=1·5$	θ	86·2	77·8	67·5	49·1	35·3	25·6	20·5
	ϕ	87·3	81·0	72·9	58·6	47·9	40·1	34·7
$\frac{s}{t}=2·0$	θ	87·9	81·9	74·1	57·7	44·9	35·4	29·4
	ϕ	88·1	83·0	75·3	60·9	49·7	41·4	35·5
$\frac{s}{t}=3·0$	θ	—	85·4	79·4	67·2	56·7	48·2	41·7
	ϕ	—	84·8	78·1	64·5	52·7	44·0	37·5
$\frac{s}{t}=5·0$	θ	—	87·5	83·8	75·3	67·4	60·7	55·5
	ϕ	—	86·1	80·7	68·2	56·7	47·6	40·6

quantities ϕ and $Z(\alpha)$, being obtained directly by reference to the "Smithsonian" Tables of Elliptic Functions*. Curves were drawn giving θ, ϕ, and $\frac{s}{g}$ plotted against $\frac{s}{t}$ for a number of values of $r°$ and from values obtained from

* "Smithsonian" Mathematical Formulæ and Tables of Elliptic Functions. Smithsonian Publication 2672.

these curves further curves were drawn giving θ and ϕ against $\frac{s}{g}$ for a number of values of $\frac{s}{t}$.

Having determined the relation between the z and ζ planes we now turn to that between the ζ plane and χ plane, the latter representing a uniform field.

Since both the potential difference and amount of flux associated with the problem figure are finite, the upper half of the ζ plane is transformed into a finite portion of the uniform χ plane as indicated in fig. 1.

To preserve similarity between the figures in the various planes, the flux lines in the χ plane are made horizontal so that

$$\chi=\phi+j\psi.$$

The transformation from the ζ to the χ plane is given by

$$\frac{d\chi}{d\zeta}=\frac{\mathrm{B}}{(1-\zeta^2)^{\frac{1}{2}}(1-k_1{}^2\zeta^2)^{\frac{1}{2}}}. \quad . \quad . \quad . \quad . \quad (9)$$

Making the origins of the two planes correspond

$$\chi=\mathrm{B}\int_0^{\zeta}\frac{d\zeta}{(1-\zeta^2)^{\frac{1}{2}}(1-k_1{}^2\zeta^2)^{\frac{1}{2}}}=\mathrm{BF}(\zeta,k_1). \quad . \quad (10)$$

Using the fact that when $\zeta=1$, $\chi=\phi_0$ the potential difference across the gap, we obtain

$$\mathrm{B}=\frac{\phi_0}{\mathrm{K}_1}. \quad . \quad . \quad . \quad . \quad . \quad . \quad (11)$$

From equations (1), (4), (9), and (11) the flux-density at any point is given by

$$\frac{d\chi}{dz}=\frac{d\chi}{d\zeta}\cdot\frac{d\zeta}{dz}=\frac{\phi_0\pi}{\mathrm{K}_1 s}\frac{\mathrm{cn}\,\alpha}{\mathrm{sn}\,\alpha\,\mathrm{dn}\,\alpha}\frac{(1-k^2\,\mathrm{sn}^2\,\alpha\,.\,\zeta^2)^{\frac{1}{2}}}{(1-k^2\zeta^2)^{\frac{1}{2}}}$$

$$=\frac{\phi_0}{g}\times\frac{\mathrm{K}}{\mathrm{K}_1}\left(1-\frac{\mathrm{cn}\,\alpha\,\mathrm{Z}(\alpha)}{\mathrm{sn}\,\alpha\,\mathrm{dn}\,\alpha}\right)\frac{(1-k^2\,\mathrm{sn}^2\,\alpha\,.\,\zeta^2)}{(1-k^2\zeta^2)^{\frac{1}{2}}}, \quad . \quad . \quad . \quad . \quad (12)$$

where $\frac{\phi_0}{g}$ is the flux-density that would exist in a uniform gap of the given length and with the given potential difference across it.

In the form best suited for calculation

$$\frac{d\chi}{dz}=\frac{\phi_0}{g}\times\frac{\mathrm{K}}{\mathrm{K}_1}\left(1-\frac{\mathrm{Z}(\alpha)}{\tan\phi\cos\theta_1}\right)\frac{(1-\sin^2\theta_1\,.\,\zeta^2)^{\frac{1}{2}}}{(1-\sin^2\theta\,.\,\zeta^2)^{\frac{1}{2}}}. \quad (13)$$

(b) *Practical Deductions.*

(i.) *Maximum, Minimum, and Mean Flux-densities on smooth Pole-face.*

The maximum flux-density B_1 on the smooth pole-face occurs opposite the middle of a tooth where $\zeta=0$. From equation (13)

$$B_1=\frac{\phi_0}{g}\times\frac{K}{K_1}\left(1-\frac{Z(\alpha)}{\tan\phi\cos\theta_1}\right). \quad . \quad . \quad . \quad (14)$$

The minimum flux-density, B_2, occurs opposite the middle of a slot where $\zeta=1$ and is given by

$$\left.\begin{aligned} B_2&=\frac{\phi_0}{g}\times\frac{K}{K_1}\left(1-\frac{Z(\alpha)}{\tan\phi\cos\theta_1}\right)\sin\phi \\ &=B_1\sin\phi \end{aligned}\right\} \quad . \quad . \quad . \quad (15)$$

From equations (10) and (11) the increase in χ as ζ increases from 1 to $\frac{1}{k_1}$ is $j\frac{\phi_0 K_1'}{K_1}$. This gives the flux per half-tooth pitch, so that

$$\text{Mean flux-density } B_m=\frac{\phi_0\frac{K_1'}{K_1}}{\frac{s+t}{2}}=\frac{\phi_0}{g}\times\frac{2\frac{g}{s}}{1+\frac{t}{s}}\frac{K_1'}{K_1}. \quad . \quad (16)$$

The values of B_1, B_2, and B_m are given in Table II., these having been calculated at the same time as the values of θ and ϕ for Table I. The variation of maximum and minimum flux-densities with $\frac{s}{g}$ are shown in fig. 2 for the three cases where $\frac{s}{t}=0$, 1·0, and 2·0 respectively. For the sake of completeness, values have been included in Table II. for the limiting case where $\frac{s}{t}=\infty$, *i. e.*, where the tooth has zero width. In this case

$$B_1=\frac{\phi_0}{g}\times\frac{\frac{g\pi}{s}}{K_1\tanh\frac{g\pi}{s}},$$

$$B_2=\frac{\phi_0}{g}\times\frac{\frac{g\pi}{s}}{K_1},$$

Table II.

Values of maximum flux-density B_1, minimum flux-density B_2, and mean flux-density B_m, on smooth pole-face as percentages of flux-density in uniform gap.

	$\frac{s}{g}$	0·25.	0·5.	0·75.	1·0.	1·5.	2·0.	2·5.	3·0.
$\frac{s}{t}=0$	B_1	100·0	100·0	100·0	100·0	100·0	100·0	100·0	100·0
	B_2	99·2	97·0	93·7	89·5	80·0	70·7	62·5	55·5
	B_m	100·0	100·0	100·0	100·0	100·0	100·0	100·0	100·0
$\frac{s}{t}=0·25$	B_1	99·2	99·5	99·7	99·9	100·0	100·0	100·0	100·0
	B_2	99·1	97·0	93·5	89·5	80·0	70·7	62·5	55·5
	B_m	99·2	98·4	97·7	97·0	95·6	94·4	93·4	92·5
$\frac{s}{t}=0·5$	B_1	98·8	98·1	98·1	98·9	99·5	99·9	100·0	100·0
	B_2	,,	96·8	93·4	89·4	80·0	70·7	62·5	55·5
	B_m	,,	97·6	96·1	94·9	92·6	90·6	89·0	87·8
$\frac{s}{t}=0·75$	B_1	98·4	97·0	96·4	97·1	98·5	99·2	99·7	99·9
	B_2	,,	96·5	93·2	89·3	80·0	70·7	62·5	55·5
	B_m	,,	96·8	95·1	93·5	90·5	87·9	85·7	83·9
$\frac{s}{t}=1·0$	B_1	98·1	96·3	95·0	95·3	96·8	98·3	99·1	99·7
	B_2	,,	96·0	93·0	89·2	79·8	70·7	62·5	55·5
	B_m	,,	96·2	94·3	92·3	89·1	86·0	83·3	81·4
$\frac{s}{t}=1·25$	B_1	97·8	95·7	94·2	93·9	95·2	96·6	98·0	98·9
	B_2	,,	95·5	92·7	89·1	79·8	70·6	62·5	55·5
	B_m	,,	95·6	93·4	91·4	87·7	84·5	81·5	79·1
$\frac{s}{t}=1·5$	B_1	97·5	95·1	93·5	92·6	93·6	95·2	96·9	98·1
	B_2	,,	,,	92·4	88·7	79·8	70·6	62·5	55·5
	B_m	,,	,,	92·7	90·4	86·5	83·1	80·0	77·3
$\frac{s}{t}=2·0$	B_1	97·2	94·5	92·5	91·1	91·1	92·7	94·3	95·7
	B_2	,,	,,	91·7	88·4	79·7	70·5	62·5	55·5
	B_m	,,	,,	91·9	89·5	85·1	81·2	77·8	74·7
$\frac{s}{t}=3·0$	B_1	96·8	93·8	91·2	89·1	87·7	88·4	89·9	91·2
	B_2	,,	,,	90·7	87·2	79·0	70·2	62·4	55·5
	B_m	,,	,,	90·9	88·2	83·3	78·9	75·0	71·8
$\frac{s}{t}=5·0$	B_1	96·4	93·0	89·7	87·1	84·2	83·5	84·1	85·4
	B_2	,,	,,	89·5	85·7	77·5	69·6	62·1	55·4
	B_m	,,	,,	89·6	86·5	81·1	76·3	72·3	69·2
$\frac{s}{t}=\infty$	B_1	94·7	89·9	85·8	82·0	76·3	72·5	70·0	69·1
	B_2	,,	,,	,,	81·7	74·0	66·5	59·6	53·9
	B_m	,,	,,	,,	81·9	75·2	69·3	64·5	60·8

and

$$B_m = \frac{\phi_0}{g} \times \frac{2g}{s} \frac{K_1'}{K_1},$$

where K_1 is the complete first elliptic integral to modulus

$$k_1 = \text{sn}\,\alpha = \tanh \frac{g\pi}{s}.$$

Fig. 2.

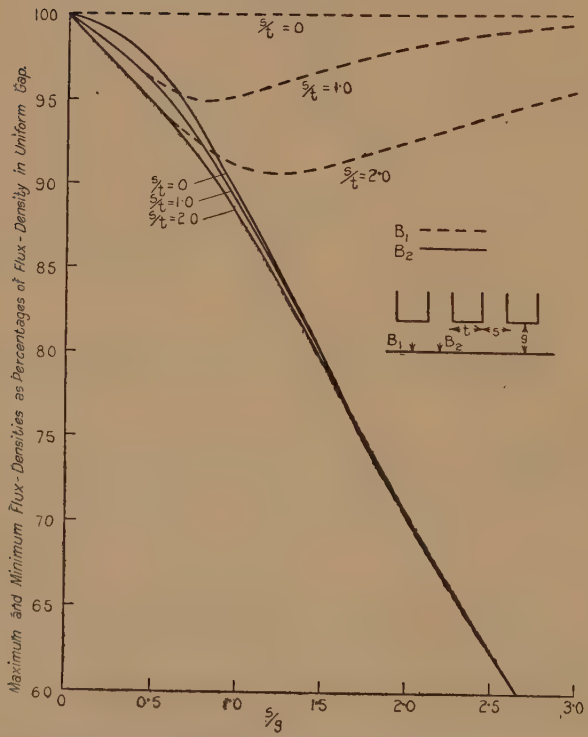

Curves giving maximum and minimum flux-densities on smooth pole-face opposite a succession of open slots.

In practice it is the mean flux-density in the air-gap that is known, and so it is desirable to give the total variation of flux-density on the smooth pole-face due to the opposing slots as a factor or percentage of the mean flux-density. The curves of fig. 3 have therefore been calculated from

Table II. and show the way in which $\frac{B_1 - B_2}{B_m}$ expressed as a percentage varies with the ratio $\frac{s}{g}$ for a number of values of $\frac{s}{t}$.

Assuming the flux variation to be sinusoidal, the pole-face eddy-current loss will be proportional to the square of the total variation between the maximum and minimum values.

Fig. 3.

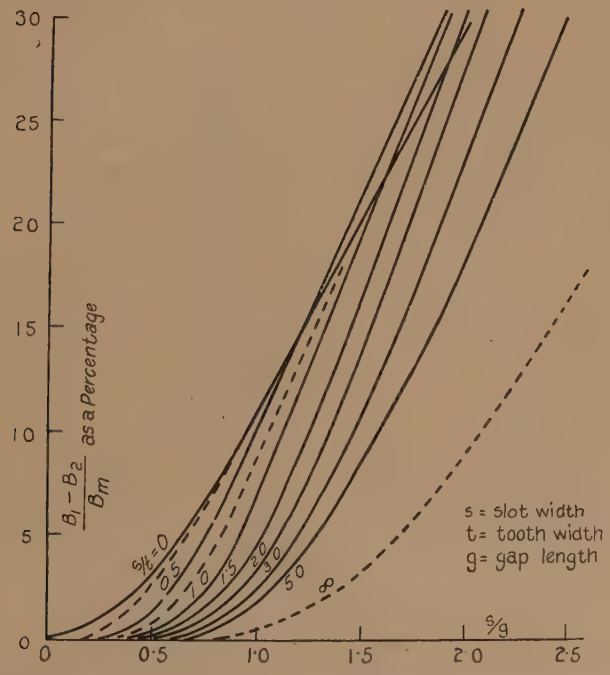

Curves giving total variation of flux-density on smooth pole-face as percentage of mean flux-density.

The curves of fig. 4 show the way in which the pole-face eddy-current loss varies with the ratio $\frac{s}{g}$ for various values of $\frac{s}{t}$, the mean gap flux-density, the slot pitch, and the relative velocity between the slots and pole-face being assumed to be constant. It is seen that for any given value of $\frac{s}{t}$ the pole-face loss is negligible up to a certain value of

$\frac{s}{g}$ and then increases very rapidly. Thus, for instance, if the ratio $\frac{s}{g}$ is increased from 0·8 to 1·2 by shortening the air-gap of a machine the eddy-current pole-face loss will be increased by an average of eight times for values of $\frac{s}{t}$ between 0·5 and 1·0. It is therefore important to keep down the value of the ratio $\frac{s}{g}$ if a small pole-face loss is required.

Fig. 4.

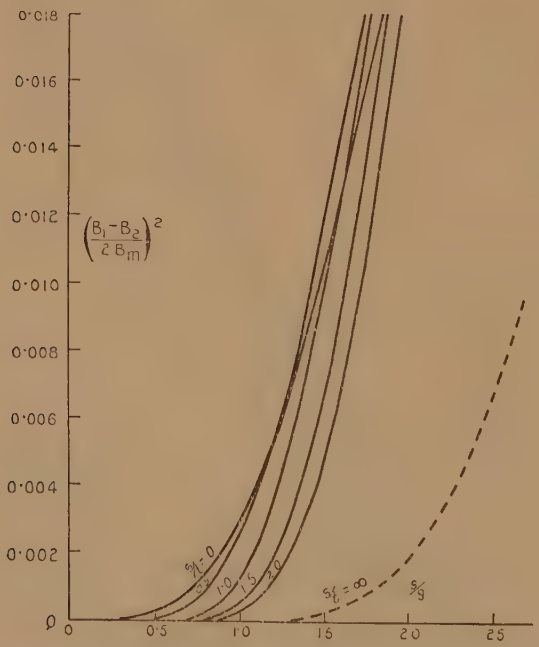

Curves showing variation of pole-face eddy-current loss with $\frac{s}{g}$.

There is usually a limit to the extent by which the ratio $\frac{s}{g}$ can be reduced either by decreasing the slot width or by increasing the length of the gap, and so a knowledge of the critical value of $\frac{s}{g}$ shown by the above results is of some importance to electrical machine designers.

Experimental confirmation of the above theoretical results for a particular ratio of slot to tooth width is obtained from tests carried out by T. F. Wall and S. P. Smith * with the particular object of investigating pole-face losses due to armature teeth. The particular machine on which tests were made had open slots, the ratio of slot width to tooth width being 0·72. The pole-face loss was measured with the machine on no load for various lengths of air-gap, the mean gap flux-density being maintained at the same value in each case. From results obtained over a range of values of $\frac{s}{g}$ from 1·2 to 4·8 it was deduced that the losses were proportional to $\left(\frac{s}{g}\right)^{3\cdot5}$.

This result may be compared with that for the theoretical case considered where $\frac{s}{t}=0\cdot75$. The amplitude of the flux ripple, as given by the appropriate curve of fig. 3, is found to be proportional to $\left(\frac{s}{g}\right)^{1\cdot66}$ over the range of $\frac{s}{g}$ from 1·2 to 3. The eddy-current pole-face loss, which is proportional to the square of this variation in flux-density, is, therefore, proportional to $\left(\frac{s}{g}\right)^{3\cdot3}$. The hysteresis loss will only be a small fraction of the eddy-current loss, and so the agreement must be regarded as very satisfactory.

In an actual machine there is considerable difficulty in the way of separating the pole-face loss from the other losses. General experience, however, supports the above conclusions that, beyond a certain value of $\frac{s}{g}$, the pole-face losses may become excessive.

(ii.) *The Gap Coefficient* K_g.

By the gap coefficient is meant the ratio of the length of the equivalent unslotted gap to the length of the actual gap, the equivalent gap being such that for a flux-density equal to the mean flux-density in the actual gap the same potential difference is required across it.

* T. F. Wall & S. P. Smith, "Experimental Determination of the Losses in Pole Shoes due to Armature Teeth," Journal I. E. E. xl. p. 577 (1908).

If g' is the length of the equivalent unslotted gap

$$\phi_0 = B_m g',$$

therefore

$$K_g = \frac{g'}{g} = \frac{\phi_0}{g} \times \frac{1}{B_m} \quad . \quad . \quad . \quad . \quad . \quad . \quad (17)$$

Curves calculated from the above expression are shown in fig. 5.

Fig. 5.

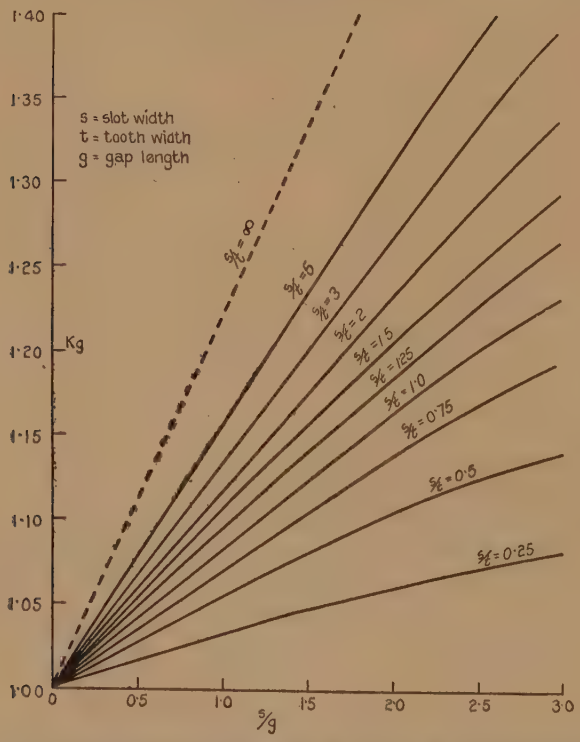

Curves giving the gap coefficient K_g for an air-gap uniformly slotted on one side.

An approximate method of calculating the gap coefficient for the case considered was first worked out by F. W. Carter * on the assumption that the effective width of each slot was the same as that of a single slot with the gap extending to infinity on either side.

* F. W. Carter, "Air-Gap Induction," 'Electrical World and Engineer,' xxxviii. p. 884 (1901).

The formula given reduces to

$$K_g = \frac{1+\frac{t}{s}}{1+\frac{t}{s}-\frac{2}{\pi}\left\{\arctan\frac{s}{2g}-\frac{g}{s}\log\left(1+\frac{s^2}{4g^2}\right)\right\}}. \quad (18)$$

Comparing values given by this formula with those calculated from equation (17) for the more exact case, the agreement is found to be surprisingly good, the error being less than 0·5 per cent. (negative), for values of $\frac{s}{t}$ less than 3, and $\frac{s}{g}$ less than 2·5. The error increases somewhat for larger values of $\frac{s}{t}$ and $\frac{s}{g}$, but the approximation is sufficiently good for practical calculations involving the total air-gap flux.

It must not be concluded from the above that the influence of a slot does not extend beyond the middle of the adjacent teeth, for, as Table II. clearly shows, for most practical cases the flux-density on the smooth pole-face opposite the middle of a tooth has by no means reached the limiting value for the uniform field. The method used in this paper has therefore been essential for the complete study of the flux-density variation on the smooth pole-face.

(iii.) *Calculation of Flux-density Variation along smooth Pole-face.*

Although, as already shown, the values of the maximum and minimum flux-densities on the smooth pole-face can readily be determined, the calculation of the flux-density at intermediate points is much more involved, as it requires a knowledge of the relation between z and ζ in the range where ζ has purely imaginary values between 0 and $j\infty$.

From equations (3) and (4),

$$z = \frac{s}{\pi}\left\{\frac{\mathrm{sn}\,\alpha\,\mathrm{dn}\,\alpha}{\mathrm{cn}\,\alpha}p - \Pi(p,\alpha,k)\right\}. \quad . \quad . \quad (19)$$

Along the smooth pole-face,

$$\left.\begin{aligned} p &= \mathrm{F}(j\eta, k), \\ &= j\mathrm{F}\left(\frac{\eta}{(1+\eta^2)^{\frac{1}{2}}}, k'\right), \\ &= j\beta \text{ say, where } \beta \text{ is a quantity lying between 0 and K'} \end{aligned}\right\}; \quad . \quad . \quad (20)$$

therefore

$$z = \frac{s}{\pi}\left\{ j\beta \frac{\operatorname{sn}\alpha \operatorname{dn}\alpha}{\operatorname{cn}\alpha} - \Pi(j\beta, \alpha, k) \right\} = \frac{s}{\pi}\left\{ j\beta \left(\frac{\operatorname{sn}\alpha \operatorname{dn}\alpha}{\operatorname{cn}\alpha} - \mathrm{Z}(\alpha) \right) + \tfrac{1}{2} \log \frac{\Theta(\alpha + j\beta)}{\Theta(\alpha - j\beta)} \right\} \quad (21)$$

[Fig. 6.]

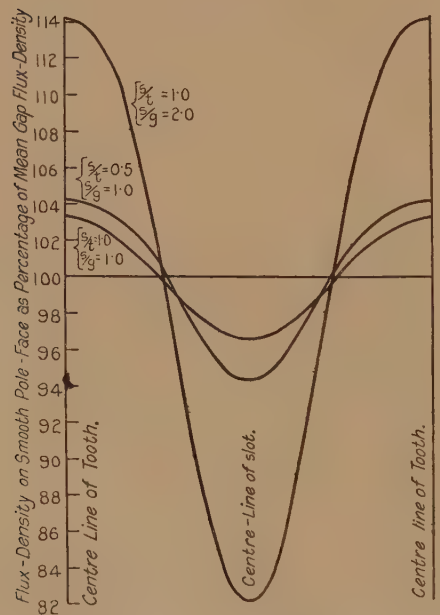

Curves showing variation of flux-density on smooth pole-face opposite uniformly slotted pole-face.

Jacobi's Θ function, which occurs in the above expression, is defined for modulus k by the series

$$\Theta(t) = 1 - 2q\cos\frac{\pi t}{\mathrm{K}} + 2q^4\cos\frac{2\pi t}{\mathrm{K}} - 2q^9\cos\frac{3\pi t}{\mathrm{K}} + \ldots. \quad (22)$$

in which $q = e^{-\frac{\mathrm{K}'}{\mathrm{K}}\pi}$.

Expanding the Θ functions of equation (21) in series form, and separating their real and imaginary parts, and also using the relation from equation (6) that

$$\frac{\operatorname{sn}\alpha \operatorname{dn}\alpha}{\operatorname{cn}\alpha} - \mathrm{Z}(\alpha) = \frac{\pi}{2\mathrm{K}'}\left(\frac{t}{s} + \frac{\alpha}{\mathrm{K}}\right),$$

the expression for z in a form convenient for calculation reduces to

$$z=j\frac{s}{2}\left\{\left(\frac{t}{s}+\frac{r^\circ}{90}\right)\frac{\beta}{K'}+\frac{\mu^\circ}{90}\right\}, \quad . \quad . \quad . \quad (23)$$

where

$$\frac{r^\circ}{90}=\frac{\alpha}{K},$$

and

$$\mu^\circ=\arctan\frac{2q\sinh\frac{\pi\beta}{K}\sin 2r^\circ-2q^4\sinh\frac{2\pi\beta}{K}\sin 4r^\circ+\ldots}{1-2q\cosh\frac{\pi\beta}{K}\cos 2r^\circ+2q^4\cosh\frac{2\pi\beta}{K}\cos 4r^\circ+\ldots}$$

expressed in degrees.

In the above expression for μ° the quantities q, K, and r° depend on the dimensions of the problem and so are fixed for any particular case. Thus β is the only quantity in the expression for z which varies as one moves along the smooth pole-face, and so it is best to make the numerical calculations by taking a number of values of $\frac{\beta}{K'}$ between 0 and 1.

The flux-density is obtained by putting $\zeta=j\eta$ in equation (13), giving

$$\frac{d\chi}{dz}=\frac{\phi_0}{g}\times\frac{K}{K'}\left(1-\frac{Z(\alpha)}{\tan\phi\cos\theta_1}\right)\frac{(1+\sin^2\theta_1.\eta^2)^{\frac{1}{2}}}{(1+\sin^2\theta.\eta^2)^{\frac{1}{2}}}, \quad (24)$$

where as before

$$\sin\theta=k,$$

$$\sin\phi=\mathrm{sn}\,\alpha,$$

and

$$\sin\theta_1=\sin\theta.\sin\phi.$$

For given dimensions of the slot, tooth, and gap, the only quantity that varies in the above expression for the flux-density on the pole-face is η, and this is related to β by the equation

$$\beta=F\left(\frac{\eta}{(1+\eta^2)^{\frac{1}{2}}},k'\right),$$

so that the value of η corresponding to any chosen value of $\frac{\beta}{K'}$ can be found by the use of tables of the first elliptic integral.

The variation of flux-density along the smooth pole-face has been calculated for three typical cases, as below.

Case 1. $\frac{s}{t}=1{\cdot}0$, $\frac{s}{g}=1{\cdot}0$.

Corresponding to $\theta=54{\cdot}9°$ and $\phi=69{\cdot}3°$ as given by Table I., the value of $r°$ is $63{\cdot}31°$, so that equation (23) reduces to

$$z=j\frac{s}{2}\left(1{\cdot}7035\frac{\beta}{K'}+\frac{\mu°}{90}\right),$$

where

$$\mu°=\arctan\frac{0{\cdot}11042\sinh 2{\cdot}676\frac{\beta}{K'}+0{\cdot}000429\sinh 5{\cdot}352\frac{\beta}{K'}}{1{\cdot}0+0{\cdot}08204\cosh 2{\cdot}676\frac{\beta}{K'}-0{\cdot}0000129\cosh 5{\cdot}352\frac{\beta}{K'}}.$$

Equation (24) giving the flux-density reduces to

$$\frac{d\chi}{dz}=\frac{\phi_0}{g}\times 0{\cdot}9533\frac{(1+0{\cdot}58572\eta^2)^{\frac{1}{2}}}{(1+0{\cdot}66936\eta^2)^{\frac{1}{2}}}.$$

The wave-form of the flux-density variation over one slot pitch as calculated from the above expressions is shown in fig. 6. On analysis its equation as represented by the first five harmonics is given by

$$B=B_m+\frac{B_1-B_2}{2}(1{\cdot}012\cos\theta-0{\cdot}012\cos 2\theta-0{\cdot}002\cos 3\theta+0{\cdot}004\cos 4\theta-0{\cdot}002\cos 5\theta),$$

the amplitudes of the harmonics being expressed as fractions of half the total variation between the maximum and minimum flux-densities. From the smoothness of the wave-form it is expected that all higher harmonics will be negligible.

Assuming the effective permeability of the surface skin of the pole-face to be the same for all the harmonics, the loss per unit area due to each harmonic is proportional to $\frac{A^2}{n^{\frac{1}{2}}}$ *, where A = amplitude and n = order of harmonic.

On this basis, the loss factor which gives the ratio of the actual loss to the loss calculated for a single sine wave of amplitude $\frac{B_1-B_2}{2}$ is found to be 1·024.

* See F. W. Carter, "Pole-face Eddy-current Loss," Journal I. E. E. liv. p. 170. (1916).

Case 2. $\frac{s}{t}=1{\cdot}0$, $\frac{s}{g}=2{\cdot}0$.

From Table I., $\theta=21{\cdot}4°$ and $\phi=46{\cdot}0°$, giving $r°=44{\cdot}98°$,

$$z=j\frac{s}{2}\left(1{\cdot}4998\frac{\beta}{K'}+\frac{\mu°}{90}\right),$$

where

$$\mu°=\arctan\frac{0{\cdot}01786\sinh 4{\cdot}719\frac{\beta}{K'}}{1{\cdot}0-0{\cdot}0000104\cosh 4{\cdot}719\frac{\beta}{K'}},$$

and

$$\frac{d\chi}{dz}=\frac{\phi_0}{g}\times 0{\cdot}9827\frac{(1+0{\cdot}06889\eta^2)^{\frac{1}{2}}}{(1+0{\cdot}13314\eta^2)^{\frac{1}{2}}}.$$

The flux-density is represented by the equation

$$B=B_m+\frac{B_1-B_2}{2}(1{\cdot}019\cos\theta-0{\cdot}117\cos 2\theta-0{\cdot}017\cos 3\theta+0{\cdot}005\cos 4\theta+0{\cdot}005\cos 5\theta),$$

giving a loss factor of 1·049.

Case 3. $\frac{s}{t}=0{\cdot}5$, $\frac{s}{g}=1{\cdot}0$.

From Table I., $\theta=26{\cdot}9°$ and $\phi=64{\cdot}7°$, giving $r°=63{\cdot}38°$,

$$z=j\frac{s}{2}\left(2{\cdot}7043\frac{\beta}{K'}+\frac{\mu°}{90}\right),$$

where

$$\mu°=\arctan\frac{0{\cdot}02294\sinh 4{\cdot}247\frac{\beta}{K'}}{1{\cdot}0+0{\cdot}01714\cosh 4{\cdot}247\frac{\beta}{K'}},$$

and

$$\frac{d\chi}{dz}=\frac{\phi_0}{g}\times 0{\cdot}9889\frac{(1+0{\cdot}16732\eta^2)^{\frac{1}{2}}}{(1+0{\cdot}20470\eta^2)^{\frac{1}{2}}}.$$

The flux-density is represented by the equation

$$B=B_m+\frac{B_1-B_2}{2}(0{\cdot}990\cos\theta-0{\cdot}143\cos 2\theta+0{\cdot}002\cos 3\theta+0{\cdot}013\cos 4\theta+0{\cdot}007\cos 5\theta),$$

giving a loss factor of 0·995.

It will be apparent that the calculation of the exact wave-form of the flux-density variation on the smooth pole-face is too tedious to be performed except in special cases. The results obtained for the three cases worked out above

indicate that, as regards the eddy-current loss in the pole-face, sufficiently close approximation can be obtained by treating the variation of flux-density as sinusoidal between the limits indicated by the curves of fig. 3.

III. The Flux-Distribution associated with a Slot of Finite Depth.

(a) *Analysis of Problem.*

In cases where slots of comparatively small depth form part of the air-gap boundary, it is sometimes desirable to

Fig. 7.

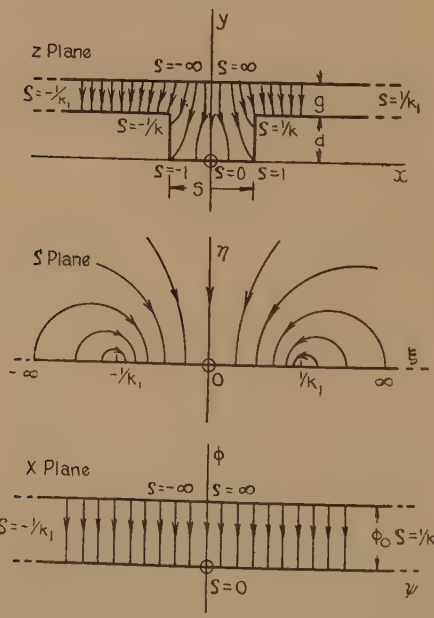

The flux-distribution due to a slot of finite depth.

have means of estimating the effective slot width as affected by the finite depth.

Considering a single slot with the air-gap extending to infinity on either side as shown in fig. 7, the same transformation as in the previous problem can be employed between the z and ζ planes, so that it is fairly simple to

calculate results over a range of values of $\frac{d}{s}$ and $\frac{s}{g}$, where

d = depth of slot,

s = width of slot,

and g = length of gap.

Taking $\frac{d}{s}$ and $\frac{s}{g}$ as variables and identifying d, s, and g with $\frac{t}{2}$, $2g$, and $\frac{s}{2}$ in the results for the previous problem as given by equations (1), (4), (5), and (6) the transformation from the z plane to the ζ plane is seen to be given by

$$\frac{dz}{d\zeta} = \frac{2g}{\pi} \frac{\operatorname{sn}\alpha \operatorname{dn}\alpha}{\operatorname{cn}\alpha} \frac{(1-k^2\zeta^2)^{\frac{1}{2}}}{(1-k^2 \operatorname{sn}^2\alpha \,.\, \zeta^2)(1-\zeta^2)^{\frac{1}{2}}}, \quad . \quad (25)$$

or

$$z = \frac{2g}{\pi} \left\{ \frac{\operatorname{sn}\alpha \operatorname{dn}\alpha}{\operatorname{cn}\alpha} p - \Pi(p, \alpha) \right\}, \quad . \quad . \quad . \quad (26)$$

where $p = \mathrm{F}(\zeta \,.\, k)$.

The parameters α and k are determined by the equations

$$\frac{s}{g} = \frac{4\mathrm{K}}{\pi} \left(\frac{\operatorname{sn}\alpha \operatorname{dn}\alpha}{\operatorname{cn}\alpha} - \mathrm{Z}(\alpha) \right), \quad . \quad . \quad . \quad . \quad (27)$$

and

$$\frac{d}{g} = \frac{2\mathrm{K}'}{\pi} \left(\frac{\operatorname{sn}\alpha \operatorname{dn}\alpha}{\operatorname{cn}\alpha} - \mathrm{Z}(\alpha) \right) - \frac{\alpha}{\mathrm{K}}, \quad . \quad . \quad . \quad (28)$$

or in form best suited for calculation, the equivalent parameters θ and ϕ are determined by

$$\frac{s}{g} = \frac{4\mathrm{K}}{\pi} (\tan\phi \cos\theta_1 - \mathrm{Z}(\alpha)) \quad . \quad . \quad . \quad (29)$$

and

$$\frac{d}{g} = \frac{2\mathrm{K}'}{\pi} (\tan\phi \cos\theta_1 - \mathrm{Z}(\alpha)) - \frac{r^\circ}{90}, \quad . \quad . \quad (30)$$

where

$$\sin\theta = k, \quad \sin\phi = \operatorname{sn}\alpha, \quad \sin\theta_1 = k \operatorname{sn}\alpha,$$

and

$$\frac{r^\circ}{90} = \frac{\alpha}{\mathrm{K}} = \frac{\mathrm{F}(\phi, \theta)}{\mathrm{K}}.$$

In Table III. are given the associated values of θ and ϕ required for a number of particular cases for $\frac{d}{s}$ between 0 and 2·0 and $\frac{s}{g}$ between 0 and 5.

The Schwarz transformation between the ζ and χ planes is given by

$$\frac{d\chi}{d\zeta} = \frac{B}{1-k^2 \operatorname{sn}^2 \alpha \,.\, \zeta^2}, \quad . \quad . \quad . \quad . \quad (31)$$

TABLE III.

Values of θ and ϕ in Degrees for Problem of Single Slot of Finite Depth.

	$\frac{s}{g}$	0·25	0·5	1·0	2·0	3·0	5·0
$\frac{d}{s} = 0{\cdot}1$	θ	58·4	59·1	61·5	67·4	72·9	80·5
	ϕ	9·2	18·0	33·9	56·7	69·8	81·4
$\frac{d}{s} = 0{\cdot}2$	θ	43·6	44·1	46·1	51·7	57·7	65·8
	ϕ	8·2	16·1	30·5	51·4	63·8	75·9
$\frac{d}{s} = 0{\cdot}3$	θ	32·2	32·7	34·4	39·2	44·1	51·3
	ϕ	7·8	15·2	28·7	48·5	60·3	72·5
$\frac{d}{s} = 0{\cdot}4$	θ	23·8	24·1	25·5	29·3	32·7	38·1
	ϕ	7·5	14·7	27·7	47·0	58·7	70·5
$\frac{d}{s} = 0{\cdot}5$	θ	17·5	17·7	18·7	21·5	24·4	28·9
	ϕ	7·25	14·4	27·2	46·0	57·2	69·5
$\frac{d}{s} = 0{\cdot}75$	θ	8·01	8·13	8·58	9·88	11·23	13·87
	ϕ	7·15	14·13	26·70	45·22	56·58	68·48
$\frac{d}{s} = 1{\cdot}0$	θ	3·67	3·70	3·92	4·52	5·13	6·13
	ϕ	7·12	14·07	26·60	45·07	56·37	68·20
$\frac{d}{s} = 2{\cdot}0$	θ	0·16	0·16	0·17	0·20	0·22	0·27
	ϕ	7·12	14·05	26·57	45·0	56·32	68·20

whence, on making the origins of the two planes correspond

$$\chi = B\int_0^{\zeta} \frac{d\zeta}{1-k^2 \operatorname{sn}^2 \alpha.\, \zeta^2}$$

$$= \frac{B}{k \operatorname{sn} \alpha} \operatorname{arc\,tanh} (k \operatorname{sn} \alpha.\, \zeta) \quad . \quad . \quad . \quad (32)$$

By considering the point $\zeta = \frac{1}{k \operatorname{sn} \alpha}$ where χ takes on a sudden increment $j\phi_0$ where ϕ_0 is the potential difference between the two sides of the gap, we obtain

$$B = \frac{2\phi_0 k \operatorname{sn} \alpha}{\pi}, \quad . \quad . \quad . \quad . \quad . \quad (33)$$

so that in calculation form

$$\chi = \frac{2\phi_0}{\pi} \text{arc tanh } (\sin\theta_1 . \zeta). \quad . \quad . \quad . \quad (34)$$

The flux-density at any point is given by

$$\frac{d\chi}{dz} = \frac{d\chi}{d\zeta} \cdot \frac{d\zeta}{dz} = \frac{\phi_0}{g} \times \frac{\sin\theta\cos\phi}{\cos\theta_1} \frac{(1-\zeta^2)^{\frac{1}{2}}}{(1-\sin^2\theta . \zeta^2)^{\frac{1}{2}}}, \quad (35)$$

$\frac{\phi_0}{g}$ being the flux-density in the given gap where it has become uniform.

Fig. 8.

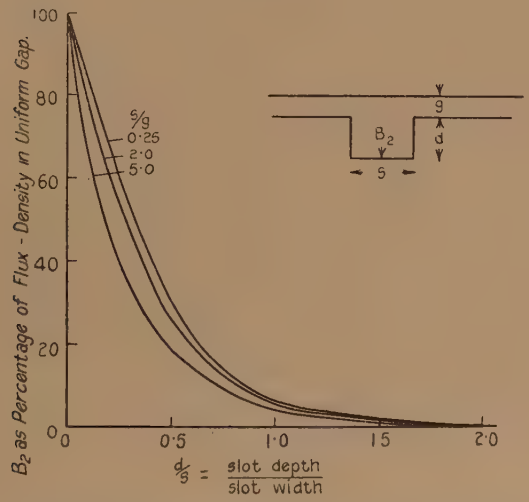

Curves giving flux-density of centre of slot bottom.

(b) *Practical Deductions.*

(i.) *Flux-Density at Centre of Slot Bottom.*

This is obtained by putting $\zeta = 0$ in equation (35) giving

$$B_2 = \frac{\phi_0}{g} \times \frac{\sin\theta\cos\phi}{\cos\theta_1} . \quad . \quad . \quad . \quad . \quad (36)$$

The variation of the flux-density at the middle of the slot bottom with the ratio $\frac{d}{s}$ is shown in fig. 8 for a number of values of $\frac{s}{g}$.

From the curves it is seen that the flux-density at the bottom of the slot depends chiefly on the ratio $\frac{d}{s}$ and becomes almost negligible (less than 1 per cent.) when the depth of the slot exceeds 1·6 times its width. Slots deeper than this can obviously be considered as of infinite depth as far as concerns their effect on the magnetic field of the air-gap.

(ii.) *Effective Width of Slot.*

By the effective width of the slot is meant a width that can be used for calculation purposes on the basis that the flux in the air-gap is uniform on either side of the effective slot but is zero across it. The effective width slot is obviously less than the actual width slot by an amount which allows for the reduced density across the actual slot and the fringing at the corners.

Considering any point on the slotted side of the air-gap but outside the slot, the "lost flux" on the side due to the presence of the slot is given by the real part of $\left(\frac{\phi_0}{g}z-\chi\right)$ where z and χ correspond to the point considered. Although the value of this expression becomes constant as the flux-density in the gap becomes uniform, it is best calculated as the mathematical limit corresponding to the point of the gap which is at an infinite distance from the slot. Thus the lost flux for the whole slot is given by the real part of

$$2\lim_{\zeta\to\frac{1}{k\,\mathrm{sn}\,\alpha}}\left(\frac{\phi_0}{g}z-\chi\right).$$

Let

$$\zeta=\frac{1}{k\,\mathrm{sn}\,(\alpha+t)},$$

so that

$$t\to 0 \quad \text{as} \quad \zeta\to\frac{1}{k\,\mathrm{sn}\,\alpha}.$$

Then

$$p=\mathrm{F}(\zeta,\,k)=\alpha+t+j\mathrm{K}',$$

and substituting this value in equation (26)

$$z=\frac{2g}{\pi}\left\{\frac{\mathrm{sn}\,\alpha\,\mathrm{dn}\,\alpha}{\mathrm{cn}\,\alpha}(\alpha+t+j\mathrm{K}')-\Pi(\alpha+t+j\mathrm{K}',\alpha)\right\}$$

$$=\frac{g}{\pi}\left\{\frac{s\pi}{2g\mathrm{K}}(\alpha+t+j\mathrm{K}')+\log\frac{\Theta(2\alpha+t+j\mathrm{K}')}{\Theta(t+j\mathrm{K}')}\right\}.$$

$$= \frac{g}{\pi}\left\{\frac{s\pi}{2g\mathrm{K}}(\alpha+t+j\,\mathrm{K}')-j\frac{\alpha\pi}{\mathrm{K}}\right.$$

$$\left.+\log\frac{\sin\dfrac{\pi(2\alpha+t)}{2\mathrm{K}}-q^2\sin\dfrac{3\pi(2\alpha+t)}{2\mathrm{K}}+q^6\sin\dfrac{5\pi(2\alpha+t)}{2\mathrm{K}}\cdots}{\sin\dfrac{\pi t}{2\mathrm{K}}-q^2\sin\dfrac{3\pi t}{2\mathrm{K}}+q^6\sin\dfrac{5\pi t}{2\mathrm{K}}\cdots}\right\}, \quad \ldots\ldots (37)$$

where $q = e^{-\frac{\kappa}{\mathrm{K}}\frac{\mathrm{K}'}{\mathrm{K}}\pi}$.

Also from equations (32) and (33)

$$\chi = \frac{2\phi_0}{\pi}\operatorname{arc\,tanh}\frac{\operatorname{sn}\alpha}{\operatorname{sn}(\alpha+t)}$$

$$= \frac{\phi_0}{\pi}\log\frac{\operatorname{sn}(\alpha+t)+\operatorname{sn}\alpha}{\operatorname{sn}(\alpha+t)-\operatorname{sn}\alpha}. \quad \ldots\ldots (38)$$

Using equations (37) and (38) the "lost flux" for the whole slot is given by the real part of

$$2\lim_{t\to 0}\left(\frac{\phi_0}{g}z-\chi\right) = \frac{\phi_0}{\pi}\left[\frac{s\pi\alpha}{g\mathrm{K}}\right.$$

$$\left.+2\log\left\{\frac{\mathrm{K}}{\pi}\frac{\operatorname{cn}\alpha\operatorname{dn}\alpha}{\operatorname{sn}\alpha}\frac{\left(\sin\dfrac{\pi\alpha}{\mathrm{K}}-q^2\sin\dfrac{3\pi\alpha}{\mathrm{K}}+q^6\sin\dfrac{5\pi\alpha}{\mathrm{K}}\cdots\right)}{(1-3q^2+5q^6\ldots)}\right\}\right]. \quad \ldots\ldots (39)$$

The effective width of the slot s_e is the width which would be occupied by the above quantity of flux in a uniform gap of length g and with a potential difference ϕ_0 and is therefore obtained by dividing the above expression by $\frac{\phi_0}{g}$;

$$\therefore \quad s_e = \frac{s\alpha}{\mathrm{K}}$$

$$+\frac{2g}{\pi}\log\left\{\frac{\mathrm{K}}{\pi}\frac{\operatorname{cn}\alpha\operatorname{dn}\alpha}{\operatorname{sn}\alpha}\frac{\left(\sin\dfrac{\pi\alpha}{\mathrm{K}}-q^2\sin\dfrac{3\pi\alpha}{\mathrm{K}}+q^6\sin\dfrac{5\pi\alpha}{\mathrm{K}}\cdots\right)}{(1-3q^2+5q^6\ldots)}\right\}. \quad \ldots\ldots (40)$$

In a form better suited for calculation purposes

$$\frac{s_e}{s} = \frac{r^\circ}{90} + \frac{2g}{\pi s}\log_e\left\{\frac{K}{\pi}\frac{\cos\theta_1}{\tan\phi}\frac{(\sin 2r^\circ - q^2\sin 6r^\circ + q^6\sin 10r^\circ \ldots)}{(1-3q^2+5q^6\ldots)}\right\}. \quad \ldots \quad (41)$$

The values of K, q, θ_1, and r° are derived directly from the parameters θ and ϕ by the relations

Fig. 9.

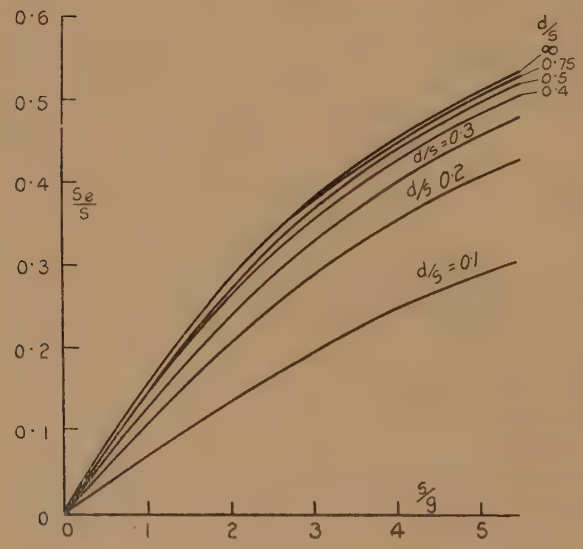

Curves giving effective width of a slot of finite depth.

K = complete first elliptic integral to modular angle θ.

$q = e^{-\frac{K'}{K}\pi}$.

$\theta_1 = \text{arc sin}\,(\sin\theta \sin\phi)$,

and

$$\frac{r^\circ}{90} = \frac{F(\phi\,.\,\theta)}{K}.$$

The numerical value of q is usually so small that only two or three terms need be taken in the series of equation (41) to give 4-figure accuracy.

The final results are given in the form of curves in fig. 9.

(iii.) *Gap Coefficient* K_g *for repeated Slots.*

For the case of repeated slots of infinite depth it was shown that the gap coefficient could be obtained with sufficient accuracy for practical purposes by taking the effective width of the slot the same as for a single slot with the gap extending to infinity on either side.

In the same way it is expected that a similar approximation can be made in the case of slots of finite depth, so that the gap coefficient is given approximately by

$$K_g = \frac{s+t}{s+t-s_e} = 1 + \frac{\frac{s_e}{s}}{1+\frac{t}{s}-\frac{s_e}{s}} \quad . \quad . \quad . \quad (42)$$

IV. The Temperature indicated by an Embedded Temperature-Detector placed between the two Layers of Conductors in a large Stator Winding.

Since the heat generated in the conductors of a machine by the load current has to pass through the surrounding layer of insulation before it is finally conducted away to the ventilating channels by the iron of the core, a considerable temperature difference exists across this insulation in virtue of its bad thermal conductivity.

In representative present-day designs the temperature drop in the insulation round the conductor is of the order of 40° C. for a total temperature rise of 80° C. above the ambient air, as indicated by an embedded temperature detector generally placed at a point on the centre line of the slot and midway between the two conductors or groups of conductors.

The highest temperature in the insulation occurs at the surface of the conductor, so that an embedded temperature detector located midway between two adjacent layers of conductors will indicate a temperature somewhat lower than this maximum value.

The present investigation was made to determine the extent to which the actual conductor temperature exceeds the indicated temperature over a wide range of practical cases.

For the problem considered it assumed that there is a constant temperature difference between the conductors and the iron of the core and also that the material of the

insulation is isotropic, that is, has the same conductivity in all directions.

The former assumption is justified since, owing to the much greater conductivity of the copper and iron compared with the insulation, any temperature variations existing in the conductor itself or in the iron adjacent to the slot must be very small compared with the total temperature drop across the insulation. The latter assumption must also be reasonably true, since all processes of insulating the conductors of large stator windings aim at excluding air films or pockets from the body of the insulation.

With the above assumptions the flow of heat through the insulation is subject to the same laws as magnetic flux in air, and so the isothermals or lines of constant temperature, and the lines of heat flow, can be obtained by methods similar to those already employed in the magnetic problems.

In general, the height of the conductor or layer of conductors will be several times the thickness of the insulation between the conductors, so that a close approximation to the actual problem can be preserved by considering only the region between two conductors of infinite depth. This enables use to be made of the same primary transformation between the z and ζ planes as employed in the two previous problems.

The result obtained by considering two conductors will also apply with a reasonable degree of approximation to the case of laminated conductors, as the thickness of insulation between individual laminations is small compared with the thickness of their common wrapping.

The problem under consideration is represented by the top diagram of fig. 10. The portion of the figure indicated by $OABCDC_1B_1A_1O$ is of the same shape as that considered in the previous magnetic problems and therefore leads to the same transformation from the z plane to the ζ plane.

In the present problem the most convenient variables to employ are the two ratios $\frac{d_1}{W}$ and $\frac{d_2}{d_1}$, where

d_1 = thickness of side insulation,

d_2 = half thickness of insulation between conductors,

and

W = width of conductors.

By identifying d_1, d_2, and W with $\frac{s}{2}$, g, and t respectively in equations (1), (4), (5), and (6) of the first magnetic

problem, the transformation from the z plane to the ζ plane is seen to be given by

$$\frac{dz}{d\zeta} = \frac{2d_1}{\pi}\frac{\mathrm{sn}\,\alpha\,\mathrm{dn}\,\alpha}{\mathrm{cn}\,\alpha}\frac{(1-k^2\zeta^2)^{\frac{1}{2}}}{(1-\zeta^2)^{\frac{1}{2}}(1-k^2\,\mathrm{sn}^2\,\alpha\,.\,\zeta^2)}, \quad . \quad (43)$$

Fig. 10.

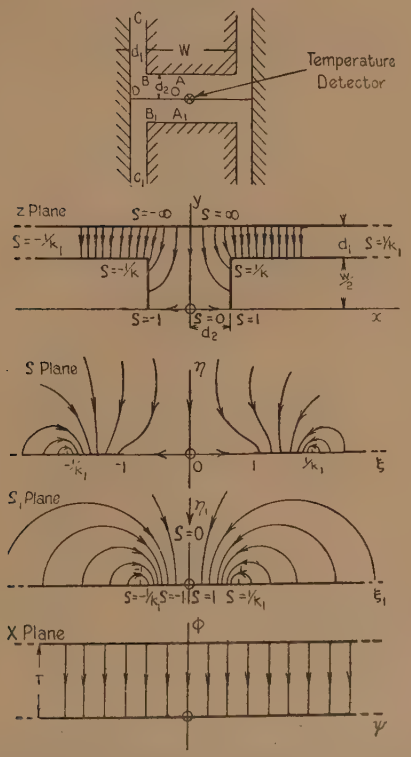

Flow of heat through insulation between conductors and iron.

where $$\frac{d_2}{d_1} = \frac{2\mathrm{K}}{\pi}\left\{\frac{\mathrm{sn}\,\alpha\,\mathrm{dn}\,\alpha}{\mathrm{cn}\,\alpha} - \mathrm{Z}(\alpha)\right\}, \quad . \quad . \quad . \quad (44)$$

and $$\frac{\mathrm{W}}{d_1} = \frac{4\mathrm{K}'}{\pi}\left\{\frac{\mathrm{sn}\,\alpha\,\mathrm{dn}\,\alpha}{\mathrm{cn}\,\alpha} - \mathrm{Z}(\alpha)\right\} - \frac{2\alpha}{\mathrm{K}} \quad . \quad . \quad . \quad (45)$$

The ranges of values of the two variables likely to be met with in practice are

$$\frac{d_1}{\mathrm{W}} \text{ from 0 to 0·5} \quad \text{and} \quad \frac{d_2}{d_1} \text{ from 1·0 to 2·0.}$$

Table IV. has been drawn up showing the associated values of θ and ϕ required to give various values of $\frac{d_1}{W}$ and $\frac{d_2}{d_1}$ in this range. ($k = \sin\theta$ and $\mathrm{sn}\,\alpha = \sin\phi$.)

For the mathematical treatment it is immaterial whether the heat flows upwards or downwards in the z plane figure and so to preserve similarity with the other problems it is taken as flowing downwards. The portions of the lower

TABLE IV.

Values of θ and ϕ in Degrees for Temperature-Detector Problem.

	$\frac{d_2}{d_1}$	1·0	1·2	1·4	1·6	1·8	2·0
$\frac{d_1}{W}=0$	θ	0	0	0	0	0	0
	ϕ	45·0	50·2	54·4	58·0	60·9	63·4
$\frac{d_1}{W}=0{\cdot}1$	θ	0·03	0·14	0·43	0·89	1·60	2·60
	ϕ	45·0	50·2	54·4	58·0	60·9	63·4
$\frac{d_1}{W}=0{\cdot}2$	θ	2·06	4·18	7·06	10·4	14·2	18·4
	ϕ	45·0	50·2	54·4	58·2	61·3	63·4
$\frac{d_1}{W}=0{\cdot}3$	θ	7·55	12·25	17·75	23·35	28·75	34·25
	ϕ	45·1	50·5	55·1	59·1	62·5	65·6
$\frac{d_1}{W}=0{\cdot}4$	θ	14·55	21·4	28·2	34·5	40·8	46·7
	ϕ	45·5	50·7	56·0	60·4	64·2	67·6
$\frac{d_1}{W}=0{\cdot}5$	θ	21·4	29·1	36·6	43·4	49·5	54·9
	ϕ	46·0	52·0	57·3	62·0	65·9	69·3

boundary between $\zeta = 1$ and $\frac{1}{k}$ and between $\zeta = -1$ and $-\frac{1}{k}$ are assumed to be at zero temperature and the whole upper boundary from $\zeta = \frac{1}{k}$ to ∞ and from $\zeta = -\frac{1}{k}$ to $-\infty$ at a temperature T.

Owing to the fact that there are two disconnected portions of the ζ plane real axis which are at zero temperature, the transformation from the ζ plane to a portion of the uniform χ plane cannot be completed in one operation. We therefore use an additional plane which will be called the ζ_1 plane and

in which these two disconnected portions of isothermal are brought together. In doing this, the intermediate part of the ζ real axis, representing the two halves of a portion of the middle stream line of the figure, becomes transformed into the two sides of a finite portion of the imaginary axis of the ζ_1 plane.

By the Schwarz transformation theorem

$$\frac{d\zeta_1}{d\zeta} = \frac{B\zeta}{(\zeta^2-1)^{\frac{1}{2}}}, \quad \ldots\ldots \quad (46)$$

whence, making the origins of the two planes correspond,

$$\zeta_1 = B\int_0^{\zeta} \frac{\zeta d\zeta}{(\zeta^2-1)^{\frac{1}{2}}} = B(\zeta^2-1)^{\frac{1}{2}}. \quad \ldots \quad (47)$$

Since the constant B only occurs in an intermediate transformation, its value may be chosen in any convenient way.

The final transformation from the ζ_1 plane to the χ plane can be simplified somewhat by choosing B so that

$$\zeta_1 = 1 \text{ when } \zeta = \frac{1}{k_1}.$$

Then from equation (47)

$$B = \frac{k_1}{k_1'}, \quad \ldots\ldots\ldots \quad (48)$$

so that

$$\zeta_1 = \frac{k_1}{k_1'}(\zeta^2-1)^{\frac{1}{2}}. \quad \ldots\ldots \quad (49)$$

The transformation from the ζ_1 plane to the uniform χ plane is given by

$$\frac{d\chi}{d\zeta_1} = \frac{C}{1-\zeta_1^2}, \quad \ldots\ldots \quad (50)$$

and on making the origins of the two planes correspond

$$\chi = \psi + j\phi = C\int_0^{\zeta_1} \frac{d\zeta_1}{1-\zeta_1^2}$$

$$= C \operatorname{arc\,tanh} \zeta_1. \quad \ldots \quad (51)$$

To evaluate the constant C we use the fact that when ζ_1 increases through the value unity, χ increases by jT. Therefore from the above equation

$$j\mathrm{T} = \frac{C}{2} \times j\pi,$$

giving

$$C = \frac{2}{\pi}\mathrm{T},$$

so that

$$\chi = \frac{2}{\pi} \mathrm{T\,arc\,tanh}\,\zeta_1$$

$$= \frac{2}{\pi} \mathrm{T\,arc\,tanh}\left\{\frac{k_1}{k_1'}(\zeta^2-1)^{\frac{1}{2}}\right\}. \quad (52)$$

At the point where the detector is placed, $\zeta = 0$, so that

$$\chi_d = \frac{2}{\pi} \mathrm{T\,arc\,tanh}\, j\frac{k_1}{k_1'}$$

$$= j\frac{2}{\pi} \mathrm{T\,arc\,tan}\,\frac{k_1}{k_1'}$$

$$= j\frac{2}{\pi} \mathrm{T\,arc\,sin}\,k_1. \quad . \quad . \quad . \quad . \quad . \quad (53)$$

The temperature difference between the detector and conductors as a fraction of the total temperature difference between the iron core and the conductors is therefore given by

$$\frac{2}{\pi}\mathrm{arc\,sin}\,k_1.$$

In calculation form, $\mathrm{arc\,sin}\,k_1 = \theta_1$ and is found in degrees, so that the fraction of the total temperature is given by the simple expression

$$\frac{\theta_1^\circ}{90}.$$

The curves of fig. 11 show the temperature difference between the detector and core as a percentage of the total temperature drop across the insulation. These curves were calculated from Table IV. using the relation that

$$\theta_1 = \mathrm{arc\,sin}\,(\sin\theta\,\sin\phi).$$

If the two layers of insulated conductors were assembled together in the slot so as to touch one another the value of $\frac{d_2}{d_1}$ would be unity. Actually, however, it is necessary to separate them by say a wooden strip, and in this case if we assume the detector to be embedded in the middle of the strip, the value of $\frac{d_2}{d_1}$ will be greater than unity, depending on the relative thicknesses of the coil insulation and separator.

The following figures are typical of an 11,000 volt turbo-alternator winding :—

Width of slot ... ... = 1·0 inch.
Depth of conductors ... = 2·5 inches.
Width of conductors... = 0·6 inch.
Thickness of insulation = 0·2 inch.
Thickness of separator . = 0·2 inch.

From the above values $\frac{d_1}{W} = 0{\cdot}333$.

Fig. 11.

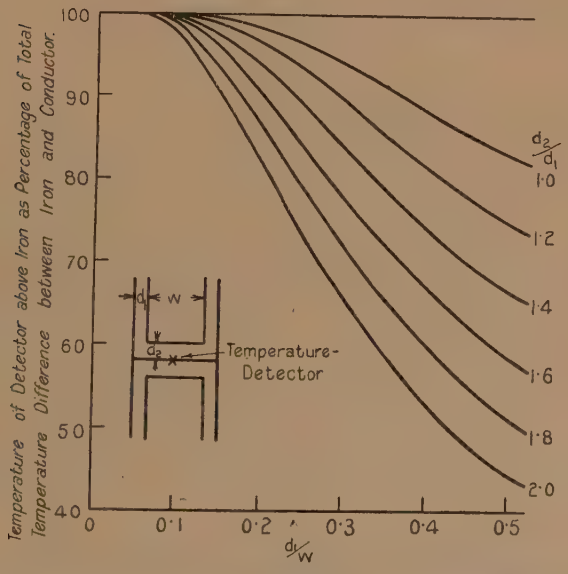

Curves giving the temperature indicated by an embedded temperature-detector between the two layers of a stator winding.

If the separator were absent the detector would indicate 92·5 per cent. of the total temperature difference between the conductors and the core. If the detector were inserted in the middle of the separator we should have a value of 1·5 for $\frac{d_2}{d_1}$ giving an observed temperature difference of 77 per cent. of the actual value. The detector, however, would probably be placed on one side of the separator, and

in this case would indicate about 83 per cent. of the total temperature drop in the insulation.

If this machine were designed to give an indicated temperature rise of 80° C. above ambient by the embedded temperature detector and if the temperature rise of the core iron were 40° C. then the temperature of the conductor would exceed the recorded temperature by

$$40 \times \frac{17}{83} = 8° \text{ C. approx.}$$

The insulation in contact with the copper is therefore subjected to a temperature 88° C. above the ambient air.

V. The Flux-Distribution associated with a Grooved Pole-face.

(a) *Analysis of Problem.*

For some time past it has been a common practice to turn circumferential grooves in pole-faces, particularly of turbo-alternator rotors in cases where these seemed liable to overheat due to the effect of eddy-current losses caused by flux-tufting from opposing teeth. The cooler running which is known to result from this procedure seems to be due partly to the better cooling caused by the increased turbulence of the stream of ventilating air, and partly to an actual reduction in the pole-face losses caused by the change in the configuration of the pole-face and the flux-distribution along it.

In this latter connexion a knowledge of the flux-distribution round these grooves along a longitudinal section of the rotor is of interest as providing a step towards a complete understanding of the nature of the pole-face losses in this case.

If the length of the air-gap were small compared with the width of the projection between adjacent grooves the flux-distribution could be obtained from that due to a single slot of finite depth as considered in section III. of this paper.

However, with the turbo-alternator the air-gap will usually be several times the width of either the grooves or projections, and in this case a better approximation can be obtained by taking the flux-distribution round the grooves as due to flux streaming to the rotor surface from infinity. The flux-distribution is expected to have become sensibly uniform at a distance from the rotor surface equal to the length of the actual air-gap.

The variation of flux-density round the rotor due to the

main poles, together with superimposed ripples due to the stator slots, will be comparatively gradual, so that as a first approximation the flux-distribution at any section may be treated as two-dimensional.

A symmetrical z plane figure is obtained by taking a parallel strip of the field corresponding to half a groove

Fig. 12.

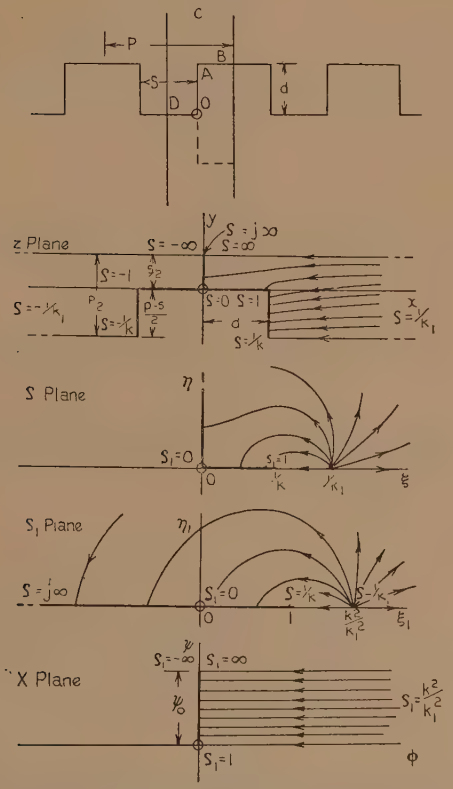

The flux-distribution round the circumferential grooves of a turbo-alternator rotor.

pitch as shown by OABCD in fig. 12, together with its image relative to the line OD. It is interesting to compare this figure with the z plane figure of the previous problems (see fig. 1).

Making the points O, A, B, C, D correspond to values for of 0, 1, $\frac{1}{k}$, $\frac{1}{k_1}$, and ∞ respectively with negative values for

the image points, the transformation from the z plane to the upper half of the ζ plane is given by the Schwarz theorem as

$$\frac{dz}{d\zeta} = A\frac{(1-\zeta^2)}{(1-k_1^2\zeta^2)(1-k^2\zeta^2)^{\frac{1}{2}}}, \quad . \quad . \quad . \quad (54)$$

whence, on making the origins of the two planes correspond,

$$z = A\int_0^{\zeta} \frac{(1-\zeta^2)^{\frac{1}{2}}d\zeta}{(1-k_1^2\zeta^2)(1-k^2\zeta^2)^{\frac{1}{2}}}. \quad . \quad . \quad . \quad (55)$$

This integral is best calculated in terms of elliptic functions by making the same change of variable as in the first problem.

Thus let $\zeta = \mathrm{sn}\, q$ to modulus k,

also let $k_1 = k\,\mathrm{sn}\,\alpha$ to modulus k.

With these substitutions the above integral reduces to

$$z = A\left\{ q - \frac{\mathrm{dn}\,\alpha}{k^2\,\mathrm{sn}\,\alpha\,\mathrm{cn}\,\alpha}\Pi(q, \alpha)\right\}. \quad . \quad . \quad (56)$$

The constant A can be determined by using the fact that as ζ increases through the value $\frac{1}{k_1} = \frac{1}{k\,\mathrm{sn}\,\alpha}$, z takes on a sudden increment $j\frac{p}{2}$ where p = pitch of groove.

Thus from equation (55),

$$A = \frac{p}{\pi}\frac{k^2\,\mathrm{sn}\,\alpha\,\mathrm{cn}\,\alpha}{\mathrm{dn}\,\alpha}. \quad . \quad . \quad . \quad . \quad . \quad (57)$$

The constants k and α are obtained in terms of the dimensions of the problem by considering the point for which

$$z = d - j\frac{p-s}{2},$$

where d = depth of groove,

and s = width of groove.

At this point

$$\zeta = \frac{1}{k},$$

therefore $$q = \mathrm{F}\left(\frac{1}{k}, k\right) = \mathrm{K} + j\mathrm{K}'.$$

Since $$\Pi(\mathrm{K}+j\mathrm{K}', \alpha) = (\mathrm{K}+j\mathrm{K}')\mathrm{Z}(\alpha) + j\frac{\pi\alpha}{2\mathrm{K}},$$

we have from equations (56) and (57),

$$d-j\frac{p-s}{2}=\frac{p}{\pi}\left\{(\mathrm{K}+j\mathrm{K}')\left(\frac{k^2\,\mathrm{sn}\,\alpha\,\mathrm{cn}\,\alpha}{\mathrm{dn}\,\alpha}-\mathrm{Z}(\alpha)\right)-j\frac{\pi\alpha}{2\mathrm{K}}\right\},$$

from which, on equating real and imaginary parts,

$$\frac{d}{p}=\frac{\mathrm{K}}{\pi}\left(\frac{k^2\,\mathrm{sn}\,\alpha\,\mathrm{cn}\,\alpha}{\mathrm{dn}\,\alpha}-\mathrm{Z}(\alpha)\right), \quad . \quad . \quad . \quad (58)$$

and

$$\frac{s}{p}=\frac{2\mathrm{K}'}{\pi}\left(\frac{k^2\,\mathrm{sn}\,\alpha\,\mathrm{cn}\,\alpha}{\mathrm{dn}\,\alpha}-\mathrm{Z}(\alpha)\right)+1-\frac{\alpha}{\mathrm{K}}. \quad (59)$$

In forms more suited for calculation purposes, the above equations become

$$\frac{d}{p}=\frac{\mathrm{K}}{\pi}\left(\frac{\sin^2\theta\sin\phi\cos\phi}{\cos\theta_1}-\mathrm{Z}(\alpha)\right), \quad . \quad . \quad (60)$$

and

$$\frac{s}{p}=\frac{2\mathrm{K}'}{\pi}\left(\frac{\sin^2\theta\sin\phi\cos\phi}{\cos\theta_1}-\mathrm{Z}(\alpha)\right)+1-\frac{r^\circ}{90}, \quad (61)$$

where

$$\sin\theta=k, \quad \sin\phi=\mathrm{sn}\,\alpha, \quad \sin\theta_1=k\,\mathrm{sn}\,\alpha,$$

and

$$\frac{r^\circ}{90}=\frac{\mathrm{F}(\phi,\theta)}{\mathrm{K}}.$$

The most convenient variables in this problem are $\frac{d}{s}$ and $\frac{s}{p}$. As in the previous problems, it is desirable to know the associated values of the parameters θ and ϕ that correspond to particular values of $\frac{d}{s}$ and $\frac{s}{p}$, and so Table V. has been prepared as a result of calculations and cross-plotting from equations (60) and (61) and covers a range of values of $\frac{d}{s}$ up to unity and $\frac{s}{p}$ between 0·1 and 0·9.

In considering the further transformation from the ζ plane to the uniform χ plane we note that, in addition to fixing the nature of the boundaries of the complete symmetrical figure that have been transformed into the real axis of the ζ plane, we have to arrange that the line OD which has been transformed into the imaginary axis of the ζ plane shall be at the same potential as the portion OAB of the original figure.

The first step is to simplify the problem so that all the boundaries we wish to fix are represented by the real axis of a plane, and we do this by transforming the first quadrant of the ζ plane into the top half of an auxiliary plane which will be called the ζ_1 plane.

By the Schwarz theorem the necessary transformation is

$$\frac{d\zeta}{d\zeta_1} = \frac{B}{\zeta_1^{\frac{1}{s}}}, \quad \ldots\ldots\ldots \quad (62)$$

and on making the origins of the two planes correspond

$$\zeta = B\int_0^{\zeta_1} \frac{d\zeta_1}{\zeta_1^{\frac{1}{s}}} = 2B\zeta_1^{\frac{1}{2}}. \quad \ldots\ldots \quad (63)$$

Table V.

Values of θ and ϕ in Degrees for Grooved Rotor Problem.

	$\frac{s}{p}$	0·1	0·3	0·5	0·7	0·9
$\frac{d}{s}=0{\cdot}1$	θ	32·0	33·1	36·0	41·5	55·0
	ϕ	83·8	71·1	58·3	44·5	28·7
$\frac{d}{s}=0{\cdot}25$	θ	52·5	54·0	56·1	60·1	70·0
	ϕ	86·1	78·4	70·0	60·9	50·1
$\frac{d}{s}=0{\cdot}5$	θ	72·6	73·2	74·3	76·3	81·1
	ϕ	88·7	84·6	80·9	76·7	71·1
$\frac{d}{s}=0{\cdot}75$	θ	81·9	82·4	82·95	83·7	85·85
	ϕ	89·2	87·55	85·9	83·9	81·3
$\frac{d}{s}=1{\cdot}0$	θ	86·3	86·5	86·75	87·15	88·2
	ϕ	89·65	88·85	88·0	87·2	86·0

Since this is only an intermediate transformation it is convenient to choose the constant B so that $\zeta_1 = 1$, when $\zeta = \frac{1}{k}$. Thus from equation (63),

$$B = \frac{1}{2k}, \quad \ldots\ldots\ldots \quad (64)$$

and

$$\zeta_1 = k^2\zeta^2. \quad \ldots\ldots\ldots \quad (65)$$

Noting that the flux concerned is finite, we now transform the top half of the ζ_1 plane into a strip of the uniform χ plane. To preserve the similarity between the figures in

the various planes the strip in the χ plane is taken parallel to the real axis, and as the flux lines go in this direction we take $\chi = \phi + j\psi$ where ϕ represents potential.

The point for which $\zeta = \frac{1}{k_1}$ and therefore $\zeta_1 = \frac{k^2}{k_1^2} = \frac{1}{\mathrm{sn}^2\alpha}$ has now been taken back to infinity as in the original z plane figure.

By the Schwarz theorem the necessary transformation is

$$\frac{d\chi}{d\zeta_1} = \frac{C}{(1-\zeta_1)^{\frac{1}{2}}(1-\mathrm{sn}^2\alpha\,.\,\zeta_1)}. \quad . \quad . \quad . \quad (66)$$

Making the origin in the χ plane correspond to the point $\zeta_1 = 1$, we have

$$\chi = C\int_1^{\zeta_1} \frac{d\zeta_1}{(1-\zeta_1)^{\frac{1}{2}}(1-\mathrm{sn}^2\alpha\,.\,\zeta_1)} \quad . \quad . \quad . \quad . \quad . \quad . \quad (67)$$

$$= -\frac{2C}{\mathrm{sn}\,\alpha\,\mathrm{cn}\,\alpha}\arcsin\left\{\mathrm{sn}\,\alpha\,\frac{(1-k^2\zeta^2)^{\frac{1}{2}}}{(1-k^2\,\mathrm{sn}^2\alpha\,.\,\zeta^2)^{\frac{1}{2}}}\right\}. \quad (68)$$

To evaluate the constant C we use the fact that as ζ increases through the value $\frac{1}{k_1}$, that is, as ζ_1 increases through the value $\frac{1}{\mathrm{sn}^2\alpha}$, there is a sudden increase in χ of amount $j\psi_0$ where ψ_0 is the amount of flux entering the rotor surface per half groove pitch.

Using equation (67) this gives

$$C = -j\frac{\mathrm{sn}\,\alpha\,\mathrm{cn}\,\alpha}{\pi}\psi_0, \quad . \quad . \quad . \quad . \quad . \quad (69)$$

and substituting this value in equation (68),

$$\chi = j\psi_0\frac{2}{\pi}\arcsin\left\{\mathrm{sn}\,\alpha\,\frac{(1-k^2\zeta^2)^{\frac{1}{2}}}{(1-k^2\,\mathrm{sn}^2\alpha\,.\,\zeta^2)^{\frac{1}{2}}}\right\}. \quad . \quad (70)$$

The flux-density at any point is given by

$$\frac{d\chi}{dz} = \frac{d\chi}{d\zeta_1}\cdot\frac{d\zeta_1}{d\zeta}\cdot\frac{d\zeta}{dz}.$$

On using equations (66), (62), and (54) after inserting the values of the constants given by equations (69), (64), and (57), the final expression for the flux-density becomes

$$\frac{d\chi}{dz} = \frac{2\psi_0}{p}\,\mathrm{dn}\,\alpha\,\frac{\zeta}{(\zeta^2-1)^{\frac{1}{2}}}. \quad . \quad . \quad . \quad . \quad (71)$$

The mean flux-density in the air-gap is given by

$$B_m = \frac{2\psi_0}{\pi},$$

and so

$$\frac{d\chi}{dz} = B_m \times \mathrm{dn}\,\alpha \frac{\zeta}{(\zeta^2-1)^{\frac{1}{2}}}. \quad . \quad . \quad . \quad (72)$$

(b) *Practical Deductions.*

(i.) *Flux-Density on Grooved Surface.*

Along the top of the projection between two grooves the minimum flux-density B_1 occurs at the middle point where $\zeta = \frac{1}{k}$; therefore

$$B_1 = B_m \times \mathrm{dn}\,\alpha \frac{1}{(1-k^2)^{\frac{1}{2}}}$$

$$= B_m \times \frac{\cos\theta_1}{\cos\theta}, \quad . \quad . \quad . \quad . \quad . \quad . \quad (73)$$

where $\theta_1 = \arcsin(\sin\theta \sin\phi)$.

Along the bottom of the rotor groove the maximum flux-density B_2 occurs at the mid-point where $\zeta = \infty$; therefore

$$B_2 = B_m \times \mathrm{dn}\,\alpha$$

$$= B_m \times \cos\theta_1 \quad . \quad . \quad . \quad . \quad . \quad (74)$$

Fig. 13 shows B_1 and B_2 plotted against $\frac{d}{s}$ for a number of values of $\frac{s}{p}$ and obtained from the values of θ and ϕ given in Table V.

Should it be desired to obtain the variation of flux-density round the complete groove, this can be done by a method similar to that employed in the problem of flux distribution due to consecutive slots.

Along the bottom of the groove in going from the corner O to the centre point D, ζ varies from 0 to $j\infty$ and the value of z in terms of ζ is obtained by using the Θ function series when evaluating the third elliptic integral in equation (56). Along the side of the groove where ζ varies from 0 to 1 the third elliptic integral may be evaluated either from its Θ function series or directly from suitable tables. Along the top of the projection between the grooves ζ is greater than unity, and here, again, the third elliptic integral can only be evaluated from its series.

In each of these three regions, the flux-density in terms of ζ can be calculated directly from the simple expression of equation (72).

(ii.) *The Additional Gap-Length Equivalent to the Grooves.*

An expression for this additional gap-length is obtained by considering the extra potential required to send the flux across the infinite gap due to the grooving. This extra potential is given by the real part of

$$\lim_{\zeta \to \frac{1}{k \operatorname{sn} \alpha}} \{\chi - B_m(z-d)\}.$$

Fig. 13.

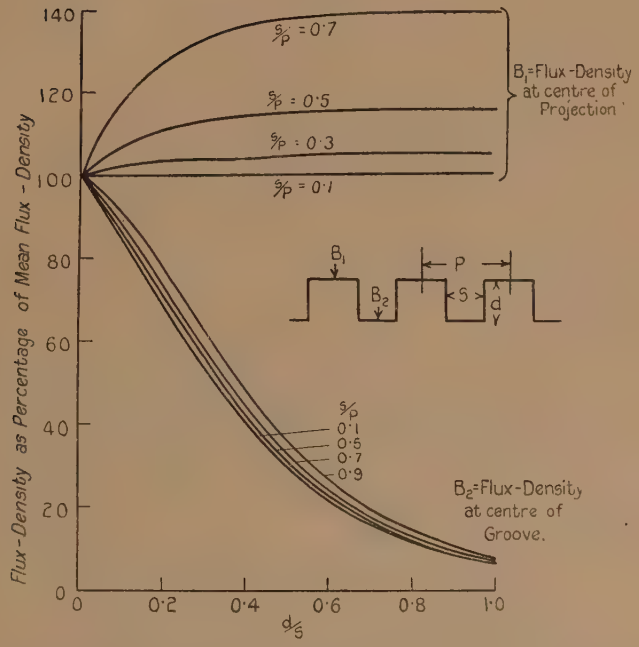

Curves giving flux-densities at middles of projection and groove on grooved rotor.

From equations (56) and (57),

$$z = \frac{p}{\pi}\left\{\frac{k^2 \operatorname{sn}\alpha \operatorname{cn}\alpha}{\operatorname{dn}\alpha} q - \Pi(q, \alpha)\right\}$$

$$= \frac{p}{\pi}\left\{\left(\frac{k^2 \operatorname{sn}\alpha \operatorname{cn}\alpha}{\operatorname{dn}\alpha} - Z(\alpha) + \tfrac{1}{2}\log\frac{\Theta(q+\alpha)}{\Theta(q-\alpha)}\right\}.$$

Using equation (58) this simplifies to

$$z = \frac{p}{\pi}\left\{\frac{d\pi}{p\mathrm{K}}q + \tfrac{1}{2}\log\frac{\Theta(q+\alpha)}{\Theta(q-\alpha)}\right\} \quad . \quad . \quad . \quad . \quad (75)$$

To evaluate the limit which gives the extra amount of potential required, let

$$\zeta = \frac{1}{k\,\mathrm{sn}\,(\alpha+t)}$$

so that $$t \to 0 \text{ as } \zeta \to \frac{1}{k\,\mathrm{sn}\,\alpha}.$$

Now

$$q = \mathrm{F}(\zeta . k) = \alpha + t + j\mathrm{K}',$$

so that substituting in equation (75),

$$z = \frac{p}{\pi}\left\{\frac{d\pi}{p\mathrm{K}}(\alpha+t+j\mathrm{K}') + \tfrac{1}{2}\log\frac{\Theta(2\alpha+t+j\mathrm{K}')}{\Theta(t+j\mathrm{K}')}\right\}$$

$$= \frac{p}{\pi}\left\{\frac{d\pi}{p\mathrm{K}}(\alpha+t+j\mathrm{K}') + j\frac{\alpha\pi}{2\mathrm{K}}\right.$$

$$\left. + \tfrac{1}{2}\log\frac{\sin\frac{\pi(2\alpha+t)}{2\mathrm{K}} - q^2\sin\frac{3\pi(2\alpha+t)}{2\mathrm{K}} + \ldots}{\sin\frac{\pi t}{2\mathrm{K}} - q^2\sin\frac{3\pi t}{2\mathrm{K}} + q^6\sin\frac{5\pi t}{2\mathrm{K}} - \ldots}\right\} .$$

$$. \quad . \quad . \quad (76)$$

From equation (70)

$$\chi = j\psi_0\frac{2}{\pi}\arcsin\left\{\mathrm{sn}\,\alpha\frac{(1-k^2\zeta^2)^{\frac{1}{2}}}{(1-k^2\,\mathrm{sn}^2\,\alpha\,.\,\zeta^2)^{\frac{1}{2}}}\right\},$$

whence on substituting

$$\zeta = \frac{1}{k\,\mathrm{sn}\,(\alpha+t)}$$

and noting that

$$2\psi_0 = \mathrm{B}_m p,$$

we have

$$\chi = j\frac{p\mathrm{B}_m}{\pi}\arcsin\left\{-j\frac{\mathrm{sn}\,\alpha\,\mathrm{cn}\,(\alpha+t)}{(\mathrm{sn}^2\,(\alpha+t)-\mathrm{sn}^2\,\alpha)^{\frac{1}{2}}}\right\}.$$

Turning this into the logarithmic form by the relation

$$\text{arc sin}\, ju = j \log \{u + (u^2+1)^{\frac{1}{2}}\},$$

$$\chi = \frac{p\mathrm{B}_m}{\pi} \log \frac{\text{sn}\,\alpha\,\text{cn}\,(\alpha+t) + \text{cn}\,\alpha\,\text{sn}\,(\alpha+t)}{(\text{sn}^2\,(\alpha+t) - \text{sn}^2\,\alpha)^{\frac{1}{2}}} \quad . \quad . \quad (77)$$

Using equations (76) and (77), the extra potential required, due to the grooves, is given by :—

$$\text{Real part of } \lim_{t\to 0} \{\chi - \mathrm{B}_m(z-d)\}$$

$$= \frac{p\mathrm{B}_m}{\pi} \left\{ \frac{1}{2} \log \frac{2\,\text{sn}\,\alpha\,\text{cn}^2\,\alpha}{\sin\frac{\pi\alpha}{\mathrm{K}} - q^2 \sin\frac{3\pi\alpha}{\mathrm{K}} + \ldots} + \frac{d\pi}{p}\left(1 - \frac{\alpha}{\mathrm{K}}\right) \right.$$

$$\left. + \lim_{t\to 0} \tfrac{1}{2} \log \frac{\sin\frac{\pi t}{2\mathrm{K}} - q^2 \sin\frac{3\pi t}{2\mathrm{K}} + q^6 \sin\frac{5\pi t}{2\mathrm{K}} - \ldots}{\text{sn}\,(\alpha+t) - \text{sn}\,\alpha} \right\}$$

$$= \frac{p\mathrm{B}_m}{\pi} \left\{ \frac{1}{2} \log \frac{\pi}{\mathrm{K}} \frac{\text{sn}\,\alpha\,\text{cn}\,\alpha}{\text{dn}\,\alpha} \frac{(1 - 3q^2 + 5q^6 - \ldots)}{\left(\sin\frac{\pi\alpha}{\mathrm{K}} - q^2 \sin\frac{3\pi\alpha}{\mathrm{K}} + \ldots\right)} \right.$$

$$\left. + \frac{d\pi}{p}\left(1 - \frac{\alpha}{\mathrm{K}}\right) \right\}.$$

The increase in the effective gap-length corresponding to the above amount of extra potential is obtained by dividing the latter by the potential gradient or flux-density in the uniform field at a great distance from the grooved surface. This potential gradient is given by B_m, so that the additional gap-length is

$$\delta g = \frac{p}{2\pi} \log \left\{ \frac{\pi}{\mathrm{K}} \frac{\text{sn}\,\alpha\,\text{cn}\,\alpha}{\text{dn}\,\alpha} \frac{(1 - 3q^2 + 5q^6 - \ldots)}{\left(\sin\frac{\pi\alpha}{\mathrm{K}} - q^2 \sin\frac{3\pi\alpha}{\mathrm{K}} + \ldots\right)} \right\}$$

$$+ d\left(1 - \frac{\alpha}{\mathrm{K}}\right). \quad . \quad . \quad . \quad . \quad . \quad . \quad (78)$$

Putting this in a form more suitable for calculation purposes, we have

$$\frac{\delta g}{s} = \frac{1}{2\pi} \frac{p}{s} \log_e \left\{ \frac{\pi}{\mathrm{K}} \frac{\sin\phi\cos\phi}{\cos\theta_1} \frac{(1 - 3q^2 + 5q^6 - \ldots)}{(\sin 2r^\circ - q^2 \sin 6r^\circ + \ldots)} \right\}$$

$$+ \frac{d}{s}\left(1 - \frac{r^\circ}{90}\right). \quad . \quad . \quad . \quad . \quad . \quad (79)$$

The notation employed is the same as in the previous problems, so that the various quantities involved in the above formula are obtained directly from the two parameters θ and ϕ by the following relations :—

$$q = e^{-\frac{K'}{K}\pi},$$

K and K′ = complete first elliptic integrals to modular angle θ,

$$\theta_1 = \text{arc sin}\,(\sin\theta \sin\phi),$$

$$\frac{r^\circ}{90} = \frac{F(\phi, \theta)}{K}$$

Fig. 14.

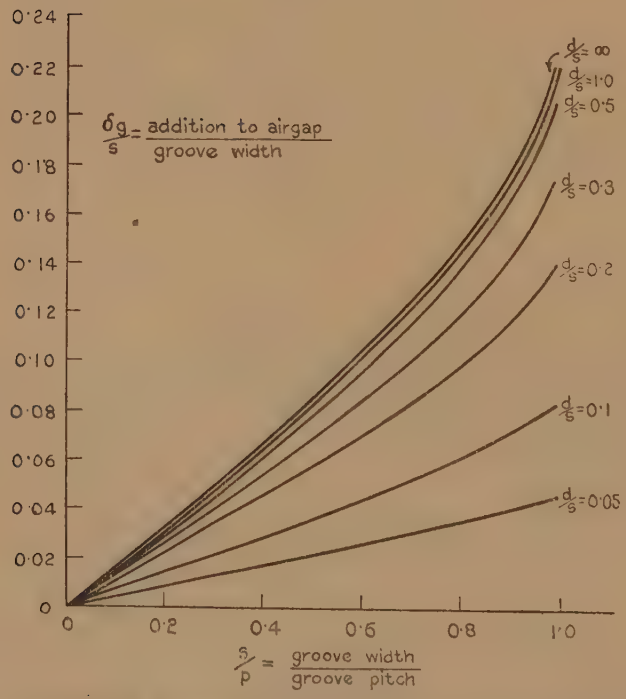

Curves giving increase in effective gap-length due to presence of grooves.

Using the values of θ and ϕ given in Table V., the curves of fig. 14 have been calculated from equation (79). These curves show the value of $\frac{\delta q}{s}$ plotted against $\frac{s}{p}$ for a

number of values of $\frac{d}{s}$. Over the whole range of cases covered the numerical value of q is so small that only the first two or three terms are required in evaluating the two series involved.

The values of $\frac{\delta g}{s}$ for the limiting case where $\frac{s}{p}=1$ and the projections between adjacent grooves have zero width, were calculated by considering the simplified transformations holding in this case. The required limit reduces to

$$\lim_{\frac{s}{p}\to 1}\left(\frac{\delta g}{s}\right)=\frac{1}{\pi}\left\{\log_e 2-\log_e\left(1+e^{-\frac{2\pi p}{d}}\right)\right\}. \quad . \quad (80)$$

The limiting case where the grooves are of infinite depth was dealt with in a similar manner, the additional gap-length in this case being given by

$$\lim_{\frac{d}{s}\to\infty}\left(\frac{\delta g}{s}\right)=\frac{1}{2\pi}\frac{p}{s}\left\{\left(1+\frac{s}{p}\right)\log_e\left(1+\frac{s}{p}\right)+\left(1-\frac{s}{p}\right)\log_e\left(1-\frac{s}{p}\right)\right\}. \quad (81)$$

From fig. 14, it will be seen that when the depth of the groove is greater than its width it has no appreciable effect on the additional gap-length.

(iii.) *Gap Coefficient* K_g *for Air-gap of Finite Length.*

Owing to the fact that the flux distribution in the case of an infinite gap rapidly becomes uniform away from the grooved surface, a reasonable approximation to the value of the gap coefficient for cases where the gap-length is not less than several times the groove width can be obtained by taking

$$\text{Gap coefficient } K_g=\frac{g+\delta g}{g}=1+\frac{s}{g}\left(\frac{\delta g}{s}\right), \quad . \quad (82)$$

where $\frac{\delta g}{s}$ is obtained from the curves of fig. 14.

Engineering Department,
British Thomson-Houston Co. Ltd., Rugby.
March 1928.

IX. *The Theory of Wave Filters containing a finite number of Sections.* *By* HAROLD A. WHEELER, *B.S. in Phys., and* FRANCIS D. MURNAGHAN, *M.A., Ph.D., Associate Professor of Applied Mathematics, Johns Hopkins University* *.

I. INTRODUCTION.

THE simple electric wave filter is built up of a number of recurrent sections connected in succession as shown in fig. 1. When a steady alternating voltage E_0 is impressed at one end of the filter, the resulting voltage E_n at the other end bears a ratio to the impressed voltage which is a function of the frequency of alternation. In the present uses to which filters are put, it is desirable that this response ratio be constant in certain predetermined frequency bands—the transmission (pass) bands—and as small as possible in the remaining suppression (stop) bands. The degree to which this condition can be realized determines the merit of any given filter. The location of the frequency bands depends on the structure of the recurrent sections.

The response-ratio functions of the frequency can be expressed in terms of determinants. The simplest determinant of this type—D_n in Part V. of this paper—was evaluated fifty years ago by Rayleigh † in connexion with the problem of determining natural frequencies of vibration of a loaded string. The complete determinant, $D_n(a, b)$, was given by Pupin ‡, and was evaluated by a different method. The most extensive study of the wave filter has been made in connexion with loaded telephone lines, and is based on Campbell's solution of the infinite line §, *i.e.*, the filter with an infinite number of sections. The real distinction between the infinite line and the finite line is the presence of reflexions at the terminations of the latter. The behaviour of a finite line is similar to that of the same number of sections in an infinite line, when the terminating impedances are so chosen as nearly to avoid reflexions, so that the infinite line solution has been found very useful.

In the present paper response formulæ are developed for finite Campbell filters, so that reflexions are taken account of without having to make special adjustment of the end conditions, automatically taking account of reflexions.

* Communicated by the Authors.
† 'Theory of Sound,' vol. i. p. 120 (1877).
‡ Proc. A. I. E. E. xvi. p. 93 (1899).
§ Bell System Tech. Jour. p. 1 (Nov. 1922).

Particular attention is given to the non-dissipative constant-K type filter, terminated by any values of resistance. The M-derived type, due to Zobel *, is also treated, and its advantages over the former type are shown. These response formulæ are useful in that they show the deviations from the ideal performance and from the approximate solution based on the infinite line. The solution for the latter ideal case is then obtained as a limiting case of the solution for the actual finite line, and the expressions for the iterative impedance and propagation exponent are derived.

The natural frequencies of finite, conservative lines of recurrent structure are of theoretical interest, and bear a close relationship to the filter properties of the same lines. On applying our method to this problem, a convenient graphical solution, which is applicable to lines of any recurrent structure, however complex, is obtained. In this

Fig. 1.

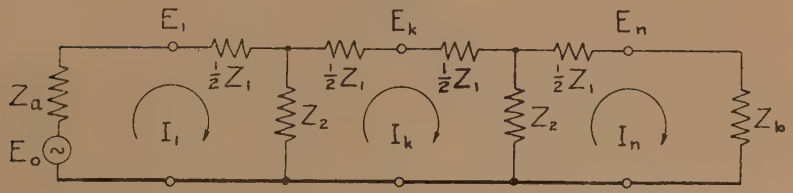

Wave filter with mid-series terminations, $(n-1)$ sections.

connexion two variations from the recurrent line will be described. The first may be called an exponential line, and is built up of sections whose impedances change in geometric progression from section to section. The second is an alternating line with two recurrent sections in alternating succession.

Throughout our paper the terminology and notation generally used in papers dealing with the electric wave filter are adhered to. The term "frequency" denotes the number f of cycles per second; the "angular frequency" is the number ω of radians per second, so that $\omega = 2\pi f$.

II. Wave-Filter Circuits, Mid-Series Termination.

1. *The Solution for a Finite Line.*—Fig. 1 shows a Campbell (*loc. cit.*) filter circuit built up of recurrent

* Bell System Tech. Jour. ii. p. 16 (1923).

sections (Z_1, Z_2) and terminated by input and output circuits (Z_a, Z_b) connected at mid-series terminations. This network of $(n-1)$ sections gives rise to a system of n linear equations in I_1, I_2, ... I_n, the currents in the successive meshes of the network. E_0 denotes the applied alternating voltage, and E_1, E_2 ... E_n denote the resulting voltages at successive pairs of terminals along the filter. Z denotes an electric impedance of any character, in general a complex function of the frequency. The equations for the currents in the successive meshes are

$$E_0 = I_1(\tfrac{1}{2}Z_1 + Z_a) + (I_1 - I_2)Z_2$$

. . . . . .

$$0 = (I_k - I_{k-1})Z_2 + I_k Z_1 + (I_k - I_{k+1})Z_2$$

. . . . . .

$$0 = (I_n - I_{n-1})Z_2 + I_n(\tfrac{1}{2}Z_1 + Z_b).$$

It is convenient to introduce the following notation

$$\cosh \Gamma = w = 1 + \frac{Z_1}{2Z_2}, \quad w_a = \frac{Z_a}{Z_2}, \quad w_b = \frac{Z_b}{Z_2},$$

so that Γ, w, w_a, and w_b are functions of the frequency

Our equations take, then, the form

$$\frac{E_0}{Z_2} = (w + w_a)I_1 - I_2$$

. . . . . .

$$0 = -I_{k-1} + 2wI_k - I_{k+1}$$

. . . . . .

$$0 = -I_{n-1} + (w + w_b)I_n.$$

The determinant of the coefficients is $D_n(a, b)$, Part V., in which the cofactor of the element in the first row and last column is unity, so that

$$I_n = \frac{E_0}{Z_2} \cdot \frac{1}{D_n(a, b)}.$$

We may define a response function G_n as the ratio of output voltage E_n to applied voltage E_0. Noting that $E_n = Z_b I_n$, we have

$$G_n = \frac{E_n}{E_0} = \frac{w_b}{D_n(a, b)}$$

for a filter of $(n-1)$ sections. The corresponding ratio with no filter sections interposed $(n-1=0)$ is

$$G_1=\frac{E_{n=1}}{E_0}=\frac{Z_b}{Z_a+Z_b}=\frac{w_b}{w_a+w_b}.$$

In the response solutions to be developed, it is most convenient to solve for the relative response ratio

$$\frac{G_n}{G_1}=\frac{w_a+w_b}{D_n(a,\,b)},$$

which shows immediately the result of interposing the $(n-1)$ filter sections between the terminating impedances. The reciprocal of this ratio is given by Eqs. (14) and (15) for the general case.

2. *Iterative Impedance of Infinite Line.*—Fig. 2 shows a segment of $(n-1)$ sections removed from an infinite line.

Fig. 2.

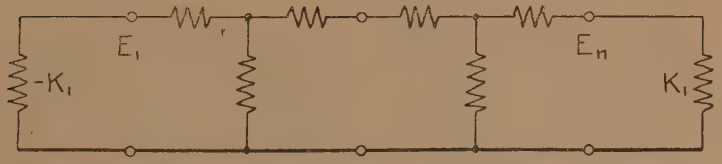

Wave filter with mid-series terminations, arranged to assimilate a segment of an infinite line.

The remainder of the line on the left (input) side has been replaced by its equivalent impedance $-K_1$ *, and the remainder of the line on the right (output) side is replaced by its impedance K_1. This equivalent impedance is known as the iterative impedance of the infinite line. In applying the analysis of the preceding paragraph to the present case, we note that $E_0=0$ (absent), so that $D_n(a,\,b)$ must vanish if the other voltages are to exist in the line. Since we desire a solution independent of n, we note in Eq. (13) for $D_n(a,\,b)$ that the even powers of $(n-1)\Gamma$ are concentrated in $\cosh(n-1)\Gamma$ and the odd powers in $\sinh(n-1)\Gamma$. The

* Any generator circuit connected to an impedance, $Z=E/I$, may be represented as the negative impedance, $-Z=-E/I$, since the terminal voltage E of the generator circuit is equal to that of the impedance, and the current *into* the former is $-I$, the reverse of the current into the latter.

expression vanishes for all values of n when the two respective coefficients are equated to zero :

$$w_a + w_b = 0, \quad w_a w_b + \sinh^2 \Gamma = 0.$$

It is convenient to substitute for this case

$$w_k = \frac{K_1}{Z_2}, \quad w_a = -w_k, \quad w_b = w_k.$$

Then the two coefficients vanish when $w_k = \sinh \Gamma$. Since

$$\cosh \Gamma = 1 + \frac{Z_1}{2Z_2} : \quad \sinh \Gamma = \sqrt{\frac{Z_1}{Z_2}} \sqrt{1 + \frac{Z_1}{4Z_2}},$$

$$\cosh \tfrac{1}{2}\Gamma = \sqrt{1 + \frac{Z_1}{4Z_2}},$$

and therefore

$$K_1 = \sqrt{Z_1 Z_2} \sqrt{1 + \frac{Z_1}{4Z_2}} = \sqrt{Z_1 Z_2} \,.\, \cosh \tfrac{1}{2}\Gamma$$

is the required impedance.

3. *Propagation Exponent* of Infinite Line.*—The finite line behaves as the same number of sections in an infinite line when either or both of the terminating impedances are made equal to the iterative impedance, thereby avoiding repeated terminal reflexions. We have

$Z_a = K_1$, $w_a = w_k = \sinh \Gamma$; and (or) $Z_b = K_1$, $w_b = w_k = \sinh \Gamma$,

so that Eq. (15) reduces to the simple form

$$\frac{G_n}{G_1} = \frac{w_a + w_b}{D_n(a, b)} = \exp - (n-1)\Gamma, \quad \frac{G_2}{G_1} = \exp - \Gamma. \quad (1)$$

The latter equation defines the propagation exponent Γ in terms of the voltage ratio across a single section, while the former equation gives the voltage ratio across $(n-1)$ sections, in an infinite line.

The propagation exponent is complex in general, and we write $\Gamma = A + iB$, where the attenuation exponent A accounts for changes in magnitude of the voltage from section to section, and the phase angle B accounts for the corresponding phase displacements.

* The usual term "propagation constant" is misleading, since the quantity is not constant but a function of the frequency. In such cases the terms "coefficient," "factor," etc., are to be preferred, since they are descriptive, and do not imply constancy.

The "velocity of propagation" may be defined as

$$V = \frac{\omega}{B} \text{ (sections per second).}$$

If an irregular wave is to be transmitted without distortion, the velocity must be independent of the frequency, which requires that the phase angle vary in proportion to the frequency.

The ideal wave-filter is non-dissipative. By this we mean that there is no power dissipation in the filter sections, but only the unavoidable or required dissipation in the terminating circuits. In this case Z_1 and Z_2 are imaginary, as explained in Part VI., making w real. The field of w is then logically divided into three parts, in which Γ is real, imaginary, and complex respectively. The frequency bands of the filter may be classified in this way, since each value of w corresponds to one or more frequencies. Such a classification follows.

Direct-suppression (stop) bands:

$$+\infty \geqq w \geqq +1, \quad +\infty \geqq A \geqq 0, \quad B = 0,$$

$$w = \cosh \Gamma = \cosh A, \quad \sinh \Gamma = \sinh A,$$

$$\cosh \tfrac{1}{2}\Gamma = \cosh \tfrac{1}{2}A, \quad \sinh \tfrac{1}{2}\Gamma = \sinh \tfrac{1}{2}A.$$

Transmission (pass) bands:

$$+1 \geqq w \geqq -1, \quad A = 0, \quad 0 \leqq B \leqq \pi,$$

$$w = \cosh \Gamma = \cos B, \quad \sinh \Gamma = i \,.\, \sin B,$$

$$\cosh \tfrac{1}{2}\Gamma = \cos \tfrac{1}{2}B, \quad \sin \tfrac{1}{2}\Gamma = i \,.\, \sin \tfrac{1}{2}B.$$

Reverse-suppression (stop) bands:

$$-1 \geqq w \geqq -\infty, \quad 0 \leqq A \leqq +\infty, \quad B = \pi,$$

$$w = \cosh \Gamma = -\cosh A, \quad \sinh \Gamma = -\sinh A,$$

$$\cosh \tfrac{1}{2}\Gamma = i \,.\, \sinh \tfrac{1}{2}A, \quad \sinh \tfrac{1}{2}\Gamma = i \,.\, \cosh \tfrac{1}{2}A.$$

In the transmission bands the attenuation is zero; in the direct- and reverse-suppression bands, respectively, there is attenuation without or with reversal of polarity across each section. The boundary between a transmission and an adjacent suppression band, $w = \pm 1$, corresponds to a cut-off frequency f_c. The boundary between adjacent direct- and reverse-suppression bands, $w = \pm \infty$, corresponds to a frequency f_∞ of infinite attenuation.

4. *Response of Non-Dissipative Finite Lines with Resistance Terminations.*—In the absence of the theory of the present paper, Eq. (1) has been used as an approximate solution for the finite line, nearly correct when the terminating impedances are approximately equal to the iterative impedance. The errors in the approximate solution will appear in the following discussion.

We will proceed to derive the response formulæ for non-dissipative filters with a finite number of sections and with resistance terminations. The non-dissipative condition can be nearly realized in practice, so these formulæ will represent very nearly the actual performance of such filters. In these cases Z_1 and Z_2 are imaginary, while $Z_a=R_a$ and $Z_b=R_b$ are real, so that we have w real, w_a and w_b imaginary. The response formula is then given by Eq. (16), since

$$\left|\frac{G_1}{G_n}\right|^2 = \left|\frac{D_n(a,\,b)}{w_a+w_b}\right|^2.$$

On substituting

$$w_a=\frac{R_a}{Z_2}, \quad w_b=\frac{R_b}{Z_2}, \quad \text{and} \quad \sinh\Gamma=w_k=\frac{K_1}{Z_2},$$

we have

$$\left|\frac{G_1}{G_n}\right|^2 = 1-\frac{(R_a^2-K_1^2)(R_b^2-K_1^2)}{(R_a+R_b)^2K_1^2}\sinh^2(n-1)\Gamma. \quad (2)$$

In transmission bands this becomes

$$\left|\frac{G_1}{G_n}\right|^2 = 1+\frac{(R_a^2-K_1^2)(R_b^2-K_1^2)}{(R_a+R_b)^2.K_1^2}.\sin^2(n-1)B. \quad (3)$$

When $R_a=R_{ab}=R_b$, these formulæ simplify to

$$\left|\frac{G_1}{G_n}\right|^2 = 1-\tfrac{1}{4}\left(\frac{R_{ab}}{K_1}-\frac{K_1}{R_{ab}}\right)^2\sinh^2(n-1)\Gamma, \quad (4)$$

and, in transmission bands,

$$\left|\frac{G_1}{G_n}\right|^2 = 1+\tfrac{1}{4}\left(\frac{R_{ab}}{K_1}-\frac{K_1}{R_{ab}}\right)^2\sin^2(n-1)B. \quad (5)$$

These formulæ will be applied to examples of two classes of filter designs, the constant-K class and the M-derived class.

The constant-K class of filter structures, due to Campbell, is characterized by the condition

$$\sqrt{Z_1Z_2}=K_c \text{ (constant, real)}.$$

Fig. 3 shows a filter of this class:

$$Z_1 = i\omega L_2, \quad Z_2 = \frac{1}{i\omega C_2}, \quad K_c = \frac{L_1}{C_2}.$$

The cut-off frequencies are determined by

$$w = 1 - \tfrac{1}{2}\omega^2 L_1 C_2 = \pm 1 : \omega_c = 0, \quad \frac{2}{\sqrt{L_1 C_2}}.$$

Since one cut-off frequency is zero, this design is called a low-pass filter. Because of its simplicity, it will be used as an example in the succeeding developments. Formulæ derived in terms of Γ are readily translated to ω by noting that

$$\frac{\omega^2}{\omega_c^2} = \frac{1 - \cosh\Gamma}{2}, \quad \frac{\omega}{\omega_c} = \pm i \cdot \sinh \tfrac{1}{2}\Gamma.$$

Fig. 3.

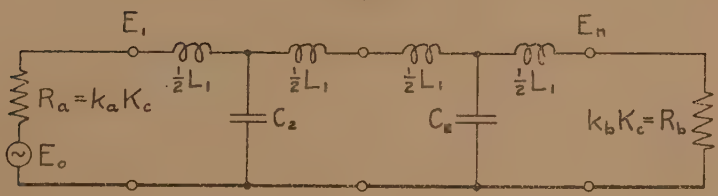

Low-pass filter, constant-K class, mid-series terminations.

In transmission band, $\frac{\omega}{\omega_c} = \sin \frac{1}{2}B$; in reverse-suppression band $\frac{\omega}{\omega_c} = \cosh \frac{1}{2}A$.

Having defined the constant-K class, and given a low-pass filter as an example, we proceed to develop response formulæ applying to all filters in this class. Since K_c is constant and real, the iterative impedance and the terminating impedances are conveniently expressed in terms of K_c:

$$K_1 = K_c \cosh \tfrac{1}{2}\Gamma, \quad Z_a = R_a = k_a K_c, \quad Z_b = R_b = k_b K_c.$$

Substituting in Eq. (2), we find

$$\left|\frac{G_1}{G_n}\right|^2 = 1 - \frac{(k_a^2 - \cosh^2 \frac{1}{2}\Gamma)(k_b^2 - \cosh^2 \frac{1}{2}\Gamma)}{(k_a + k_b)^2 \cosh^2 \frac{1}{2}\Gamma} \sinh^2 (n-1)\Gamma. \quad (6)$$

This simplifies for $k_a = k_b = 1$ to

$$\left|\frac{G_1}{G_n}\right|^2 = 1 - \frac{\sinh^4 \frac{1}{2}\Gamma}{4 \cdot \cosh^2 \frac{1}{2}\Gamma} \cdot \sinh^2 (n-1)\Gamma. \quad . \quad . \quad (7)$$

While the above expressions are real, they involve imaginary quantities, so that for computations it is desirable to write an individual formula in terms of the variable component of Γ in each class of frequency bands. Making the necessary substitutions in Eq. (7), for example, we have the following expressions for the several frequency bands.

Direct-suppression bands: This case is impossible in the constant-K class of filters because Z_1 and Z_2 are imaginary and Z_1Z_2 is real, making Z_1/Z_2 negative and $w \leqq 1$.

Transmission bands: $(K_1 = K_c \cos \frac{1}{2}B)$.

$$\left|\frac{G_1}{G_n}\right|^2 = 1 + \frac{\sin^4 \frac{1}{2}B}{4 \cdot \cos^2 \frac{1}{2}B} \cdot \sin^2 (n-1)B. \quad . \quad . \quad (8)$$

Fig. 4.

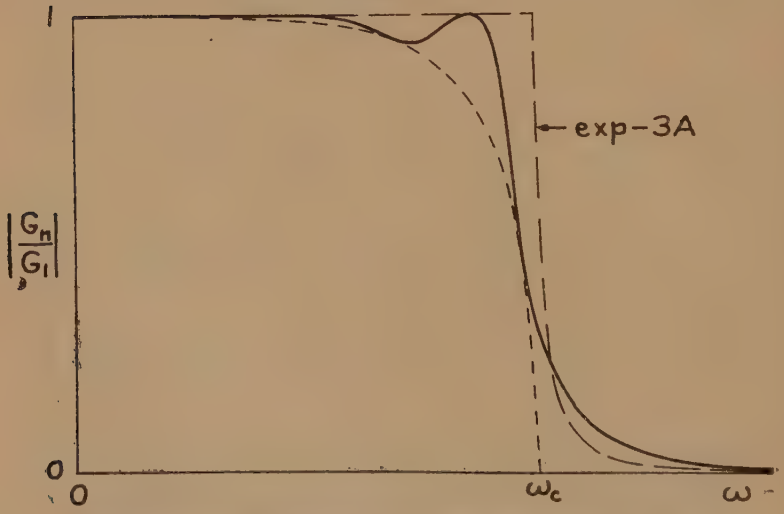

Response curve of three-section low-pass filter, constant-K class, $R_a = R_b = K_c$.

Reverse-suppression bands: $(K_1 = iK_c \sinh \frac{1}{2}A)$.

$$\left|\frac{G_1}{G_n}\right|^2 = 1 + \frac{\cosh^4 \frac{1}{2}A}{4 \cdot \sinh^2 \frac{1}{2}A} \cdot \sinh^2 (n-1)A. \quad . \quad (9)$$

Indeterminate value:

$$A = 0 : \frac{\sinh^2 (n-1)A}{4 \cdot \sinh^2 \frac{1}{2}A} = (n-1)^2 ; \quad \left|\frac{G_1}{G_n}\right|^2 = 1 + (n-1)^2. \quad (10)$$

Fig. 4 is the response curve of a three-section, low-pass filter with $R_a = R_b = K_c$, computed by formulæ (8), (9),

and (10). The dashed line (exp $-3A$) is the approximate curve based on the voltage ratio across the same number of sections in an infinite line, Eq. (1). The dotted line shows the maximum deviation from unity of the response curve for any number of sections. The computed response curve, within the transmission band, oscillates $(n-1)$ times between the dotted curve and unity.

From Eq. (6) it is apparent that the coefficient of $\sin^2(n-1)B$ can be made to vanish at two values of B, within the transmission bands, by making

$$k_a = \cos \tfrac{1}{2}B_a, \quad k^b = \cos \tfrac{1}{2}B_b.$$

Fig. 5.

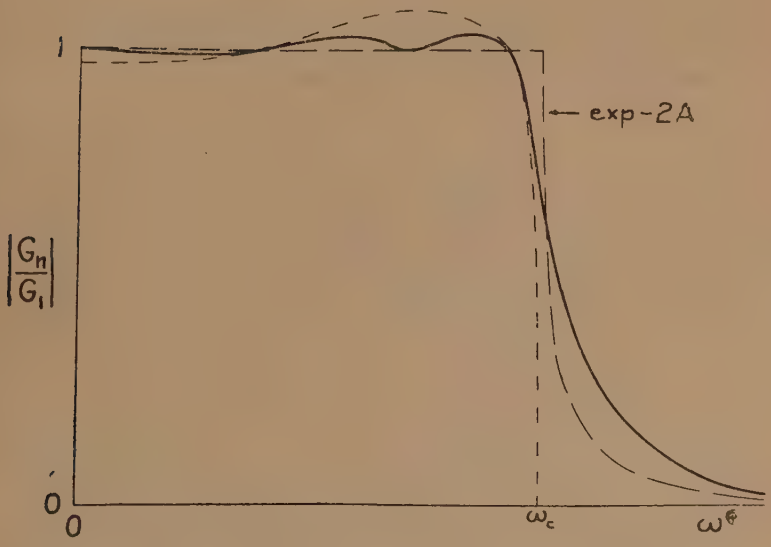

Response curve of two-section low-pass filter, constant-K class, $k_a = \cos \frac{3}{8}\pi$, $k_b = \cos \frac{1}{8}\pi$.

The departure from unity of the response curve can be reduced to a minimum by making this coefficient vanish at two values of B for which $\sin^2(n-1)B$ has its maximum value unity. Fig. 5 is a response curve of a two-section, low-pass filter following this plan, computed by Eq. (6). The value of $\sin^2 2B$ is unity when $2B = \frac{1}{2}\pi$ or $\frac{3}{2}\pi$; we take $B_a = \frac{3}{4}\pi$ and $B_b = \frac{1}{4}\pi$, so that $\cos \frac{1}{2}B_a = k_a = 0{\cdot}38$, $\cos \frac{1}{2}B_b = k_b = 0{\cdot}92$.

The second term in the response formulæ is the result of repeated terminal reflexions when neither terminating impedance is equal to the iterative impedance. In the foregoing example such reflexions were reduced to a minimum by the choice of terminating resistance values.

The M-derived class of filter structure, due to Zobel (*loc. cit.*), more closely approximates a constant iterative impedance. Any structure (Z_1, Z_2) in this class is derived from the corresponding constant-K structure (Z_{10}, Z_{20}) by the following substitutions :

$$\frac{1}{Z_1}=\frac{1}{mZ_{10}}+\frac{1-m^2}{4mZ_{20}},\quad Z_2=\frac{Z_{20}}{m},\quad 0\leqq m\leqq 1.$$

The derived Z_1 comprises the two impedances, mZ_{10} and $\frac{4mZ_{20}}{1-m^2}$, connected in parallel. Fig. 6 shows the low-pass filter derived from the constant-K structure of fig. 3.

Fig. 6.

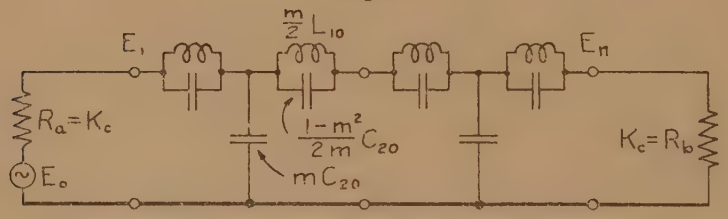

Low-pass filter, M-derived class, mid-series terminations.

We will proceed to derive the response formulæ for the M-derived class of filters having

$$R_a=R_b=R_{ab}=K_c=\sqrt{Z_{10}Z_{20}}\ \text{(constant, real)}.$$

It is required to know the iterative impedance K_1, expressed in terms of K_c and Γ, for substitution in Eq. (4). Since

$$K_1=\sqrt{Z_1Z_2}\,.\cosh\tfrac{1}{2}\Gamma,$$

$$\frac{K_1}{R_{ab}}=\cosh\tfrac{1}{2}\Gamma\sqrt{\frac{Z_1}{Z_{10}}\cdot\frac{Z_2}{Z_{20}}}=\frac{\cosh\tfrac{1}{2}\Gamma}{\sqrt{1+(1-m^2)\dfrac{Z_{10}}{4Z_{20}}}}.$$

Recalling that

$$\cosh\Gamma=1+\frac{Z_1}{2Z_2},$$

we have

$$\sinh^2 \tfrac{1}{2}\Gamma = \frac{\cosh \Gamma - 1}{2} = \frac{Z_1}{4Z_2} = \frac{Z_{10}}{4Z_{20}} \cdot \frac{m^2}{1+(1-m^2)\dfrac{Z_{10}}{4Z_{20}}},$$

from which

$$1+(1-m^2)\frac{Z_{10}}{4Z_{20}} = \frac{1}{1-\dfrac{1-m^2}{m^2}\sinh^2 \tfrac{1}{2}\Gamma}.$$

This gives

$$\frac{K_1}{R_{ab}} = \cosh \tfrac{1}{2}\Gamma \sqrt{1-c \cdot \sinh^2 \tfrac{1}{2}\Gamma},$$

where $$c = \frac{1-m^2}{m^2}.$$

Then

$$\frac{R_{ab}}{K_1} - \frac{K_1}{R_{ab}} = \frac{1-\left(\dfrac{K_1}{R_{ab}}\right)^2}{\dfrac{K_1}{R_{ab}}} = -\frac{\sinh^2 \tfrac{1}{2}\Gamma(1-c \cdot \cosh^2 \tfrac{1}{2}\Gamma)}{\cosh \tfrac{1}{2}\Gamma \sqrt{1-c \cdot \sinh^2 \tfrac{1}{2}\Gamma)}}.$$

Substituting in Eq. (4),

$$\left|\frac{G_1}{G_n}\right|^2 = 1 - \frac{\sinh^2 \tfrac{1}{2}\Gamma(1-c\cosh^2 \tfrac{1}{2}\Gamma)^2}{4 \cdot \cosh^2 \tfrac{1}{2}\Gamma(1-c\sinh^2 \tfrac{1}{2}\Gamma)} \cdot \sinh^2 (n-1)\Gamma. \quad (11)$$

The M-derived and constant-K classes merge when $k_a = k_b = 1$ and $m = 1$, $c = 0$, making Eqs. (7) and (11) identical.

This last formula simplifies somewhat when

$$m = \frac{1}{\sqrt{3}} = 0{\cdot}58, \quad c = \frac{1-m^2}{m^2} = 2,$$

and this value is in accord with design practice. Making this substitution in Eq. (11),

$$\left|\frac{G_1}{G_n}\right|^2 = 1 - \frac{\sinh^4 \tfrac{1}{2}\Gamma \cdot \cosh^2 \Gamma}{4 \cdot \cosh^2 \tfrac{1}{2}\Gamma(1-2 \cdot \sinh^2 \tfrac{1}{2}\Gamma)} \cdot \sinh^2 (n-1)\Gamma. \quad (12)$$

Fig. 7 is a response curve of a three-section, low-pass filter of this design, showing a close approximation between the actual curve given by Eq. (12) and the dashed curve (exp $-$3A). This reponse curve very closely approaches the ideal condition of uniform response within the transmission band and immediate cut-off at the edge of the band.

With Γ as the independent variable, it is necessary, before plotting the curve, to express the abscissas in terms of frequency. The cut-off frequencies of the M-derived

structures are equal to those of the corresponding constant-K structures. For the filter (L_{10}, C_{20}) of figs. 6 and 7,

$$w=1+\frac{Z_1}{2Z_2}=1+\frac{Z_{10}}{2Z_{20}}\cdot\frac{m^2}{1+(1-m^2)\dfrac{Z_{10}}{4Z_{20}}}=\pm 1$$

gives

$$-\frac{Z_{10}}{4Z_{20}}=\frac{\omega^2 L_{10}C_{20}}{4}=0,\ 1 \quad \text{and} \quad \omega_c=0,\ \frac{2}{\sqrt{L_{10}C_{20}}}.$$

Then, from the preceding results,

$$\frac{\omega^2}{\omega_c^{\,2}}=-\frac{Z_{10}}{4Z_{20}}=\frac{-\sinh^2\tfrac{1}{2}\Gamma}{m^2-(1-m^2)\sinh^2\tfrac{1}{2}\Gamma}$$

Fig. 7.

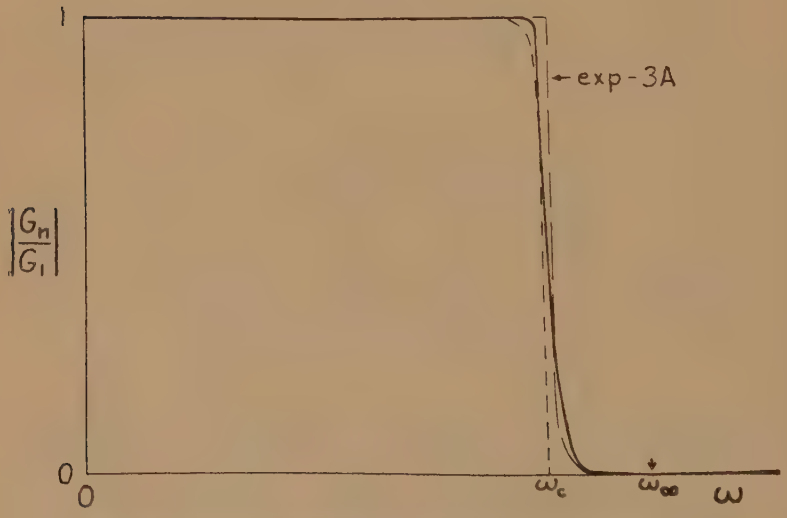

Response curve of three-section low-pass filter, M-derived class, $m=1/\sqrt{3}$.

gives the variation of frequency with Γ. In the transmission band,

$$\frac{\omega^2}{\omega_c^{\,2}}=\frac{\sin^2\tfrac{1}{2}\mathrm{B}}{m^2+(1-m^2)\sin^2\tfrac{1}{2}\mathrm{B}};$$

in the reverse-suppression band,

$$\frac{\omega^2}{\omega_c^{\,2}}=\frac{\cosh^2\tfrac{1}{2}\mathrm{A}}{m^2+(1-m^2)\cosh^2\tfrac{1}{2}\mathrm{A}};$$

and in the direct-suppression band,

$$\frac{\omega^2}{\omega_c^2} = \frac{\sinh^2 \frac{1}{2}A}{-m^2 + (1-m^2)\sinh^2 \frac{1}{2}A}.$$

The junction of the two suppression bands marks the frequency of infinite attenuation:

$$A = \infty, \quad \omega_\infty = \frac{\omega_c}{\sqrt{1-m^2}}.$$

III. Wave-Filter Circuits, Mid-shunt Termination.

1. *Determinant Solution.*—Fig. 8 shows a Campbell filter circuit similar to fig. 1, but with the sections (Z_1, Z_2) rearranged for mid-shunt termination. This network of $(n-1)$ sections gives rise to the following system of n linear

Fig. 8.

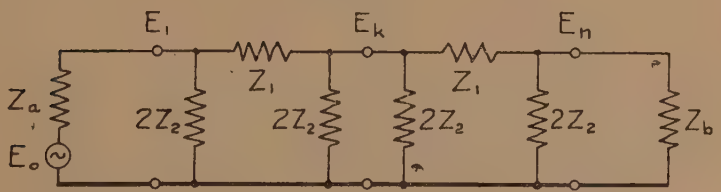

Wave filter with mid-shunt terminations, $(n-1)$ sections.

equations in E_1, E_2, ... E_n, the voltages at the successive junction-points between sections:

$$\frac{E_1 - E_0}{Z_a} + \frac{E_1}{2Z_2} + \frac{E_1 - E_2}{Z_1} = 0$$

. . . . . .

$$\frac{E_k - E_{k-1}}{Z_1} + \frac{E_k}{Z_2} + \frac{E_k - E_{k+1}}{Z_1} = 0$$

. . . . . .

$$\frac{E_n - E_{n-1}}{Z_1} + \frac{E_n}{2Z_2} + \frac{E_n}{Z_b} = 0.$$

Upon introducing the notation,

$$\cosh \Gamma = w = 1 + \frac{Z_1}{2Z_2}, \quad w_a = \frac{Z_1}{Z_a}, \quad w_b = \frac{Z_1}{Z_b}:$$

these equations take the form

$$(w+w_a)\mathrm{E}_1-\mathrm{E}_2=w_a\mathrm{E}_0$$

. . . . . .

$$-\mathrm{E}_{k-1}+2w\mathrm{E}_k-\mathrm{E}_{k-1}=0$$

. . . . . .

$$-\mathrm{E}_{n-1}+(w+w_b)\mathrm{E}_n=0.$$

The determinant of the coefficients is $\mathrm{D}_n(a, b)$, as before, and the cofactor of the element in the first row and last column being unity, we have

$$\mathrm{E}_n=\frac{w_a\mathrm{E}_0}{\mathrm{D}_n(a, b)}.$$

The response ratio is found as before; thus

$$\mathrm{G}_n=\frac{\mathrm{E}_n}{\mathrm{E}_0}=\frac{w_a}{\mathrm{D}_n(a, b)}, \quad \mathrm{G}_1=\frac{\mathrm{E}_{n=1}}{\mathrm{E}_0}=\frac{\mathrm{Z}_b}{\mathrm{Z}_a+\mathrm{Z}_b}=\frac{w_a}{w_a+w_b},$$

$$\frac{\mathrm{G}_n}{\mathrm{G}_1}=\frac{w_a+w_b}{\mathrm{D}_n(a, b)}.$$

This relative response ratio is equal to that of Part II., and its reciprocal is given by Eqs. (14) and (15).

The only real difference between the analysis of the mid-shunt structure and that of the mid-series structure is the difference in the substitutions w_a and w_b; the necessary modifications of the solutions in Part II. will be described briefly.

2. *Iterative Impedance.*—The mid-shunt iterative impedance is denoted by K_2. Corresponding to the mid-series solution,

$$\frac{\mathrm{Z}_1}{\mathrm{K}_2}=w_k=\sinh\Gamma, \quad \mathrm{K}_2=\frac{\sqrt{\mathrm{Z}_1\mathrm{Z}_2}}{\sqrt{1+\frac{\mathrm{Z}_1}{4\mathrm{Z}_2}}}=\frac{\sqrt{\mathrm{Z}_1\mathrm{Z}_2}}{\cosh\tfrac{1}{2}\Gamma}.$$

3. *Propagation Exponent.*—Since w is the same for both structures, there is no change in the propagation exponent Γ, determined by

$$\cosh\Gamma=w=1+\frac{\mathrm{Z}_1}{2\mathrm{Z}_2}.$$

4. *Response of Finite Lines.*—The general response formulæ given by Eqs. (2) to (5), in terms of K_1, are also

correct for the mid-shunt case, substituting K_2 for K_1. The formulæ given for the constant-K class of filters are correct for the latter case, after substituting the following definitions of k_a and k_b :

$$Z_a = R_a = \frac{K_c}{k_a}, \quad Z_b = R_b = \frac{K_c}{k_b}.$$

Therefore figs. 4 and 5 apply interchangeably to both structures.

The M-derived class of filters requires a different recurrent structure for mid-shunt termination, which will not be described here ; but, with this modification, the same formulæ and the curve of fig. 7 are applicable.

IV. Free Oscillations in Conservative Lines.

1. *The Solution for a Recurrent Line.*—The problem of free oscillations in conservative lines is generally familiar,

Fig. 9.

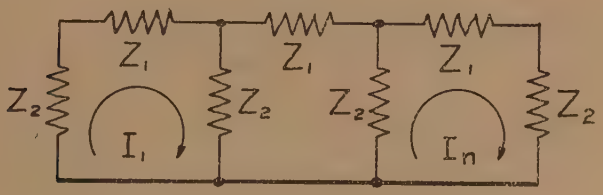

Simple recurrent line with open ends, $(2n+1)$ elements.

and it was in the solution of this problem that the elementary wave-filter determinant had its origin. After describing the simple case, two further cases will be treated, each of which has an element of novelty. The determinants referred to are treated in Part V.

The classical example of the recurrent line is the periodically loaded string ; in solving this problem, Lord Rayleigh evaluated the determinant D_n. The electric line shown in fig. 9 presents the same problem ; we shall solve for its natural frequencies of oscillation. Proceeding as in Part II., we have a system of n linear equations in terms of the currents, I_1, $I_2 \ldots I_n$, in the successive meshes of the line. On substituting

$$\cosh \Gamma = w = 1 + \frac{Z_1}{2Z_2},$$

as before, the equations take the form

$$0 = 2wI_1 - I_2$$

. . . . .

$$0 = -I_{k-1} + 2wI_k - I_{k+1}$$

. . . . . .

$$0 = -I_{n-1} + 2wI_n.$$

The determinant of the coefficients is D_n, and the condition for solutions other than zero is that

$$0 = D_n = \frac{\sinh (n+1)\Gamma}{\sinh \Gamma},$$

which is satisfied only when $\Gamma = iB$, $A = 0$; hence

$$\frac{\sin (n+1)B}{\sin B} = 0,$$

Fig. 10.

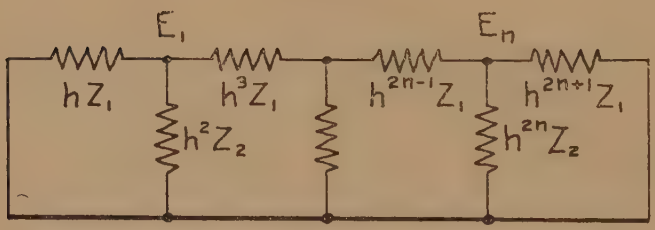

Exponential line with closed ends, $(2n+1)$ elements.

so that

$$B = \frac{k\pi}{n+1}, \quad k = 1, 2, \ldots n.$$

For any given structure (Z_1, Z_2) there are one or more natural frequencies corresponding to each of the n solutions for B.

Graphical solutions for the natural frequencies will be given for the two succeeding cases, which are more novel and interesting. It is important to note that the natural frequencies depend on the number of elements in the line, but lie within bands bounded by the cut-off frequencies ω_c, which are independent of the number of sections, depending only on the properties of the recurrent structure.

2. *Exponential Line with Closed Ends.*—Fig. 10 shows an exponential line similar to the simple recurrent line, but

built up of impedances increasing in geometric progression along the line. Proceeding as in Part III., we have a system of n linear equations in terms of voltages $E_1, E_2, \ldots E_n$ along the line

$$0 = E_1\left(\frac{1}{hZ_1} + \frac{1}{h^3Z_1} + \frac{1}{h^2Z_2}\right) - \frac{E_2}{h^3Z_1}$$

. . . . . .

$$0 = -\frac{E_{n-1}}{h^{2n-1}Z_1} + E_n\left(\frac{1}{h^{2n-1}Z_1} + \frac{1}{h^{2n+1}Z_1} + \frac{1}{h^{2n}Z_2}\right).$$

On substituting

$$\cosh\Gamma = w = \tfrac{1}{2}\left(h + \frac{1}{h} + \frac{Z_1}{Z_2}\right) = 1 + \frac{(h-1)^2}{2h} + \frac{Z_1}{2Z_2},$$

the equations take the form

$$0 = 2wE_1 - \frac{1}{h}.E_2$$

. . . . . .

$$0 = -hE_{k-1} + 2wE_k - \frac{1}{h}.E_{k+1}$$

. . . . . .

$$0 = -hE_{n-1} + 2wE_n.$$

The determinant of the coefficients is $D_n(\exp)$, so that the natural frequencies are determined by

$$0 = D_n(\exp) = \frac{\sinh(n+1)\Gamma}{\sinh\Gamma}.$$

This condition is satisfied only when $\Gamma = iB$, $A = 0$, as before:

$$\text{hence} \qquad B = \frac{k\pi}{n+1}, \quad k = 1, 2, \ldots n.$$

The natural frequencies are then determined by the solutions for B.

The natural frequencies of any recurrent structure, however complex, are readily determined graphically by the use of the chart of Part V., fig. 14. As an example, fig. 11 shows such a solution for an exponential line in which $Z_1 = i\omega L_1$, $Z_2 = \frac{1}{i\omega C_2}$. The semicircle B is divided in $(n+1)$ equal parts, and each ordinate, corresponding to $w = \cos B$, is projected on to the curve $w(\omega)$. The corresponding abscissæ are the natural frequencies. For any number of elements

in the line, the solutions all lie between the cut-off frequencies ω_c corresponding to $w = \pm 1$.

These free oscillations may be regarded as standing waves resulting from terminal reflexions, which are avoided, as far possible, in the design of wave filters. From this explanation

Fig. 11.

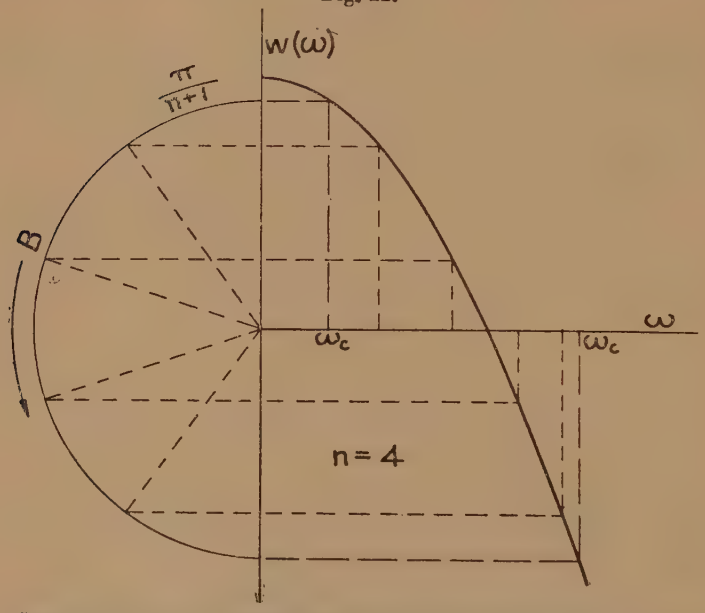

Graphical solution for natural frequencies of exponential line (L_1, C_2).

Fig. 12.

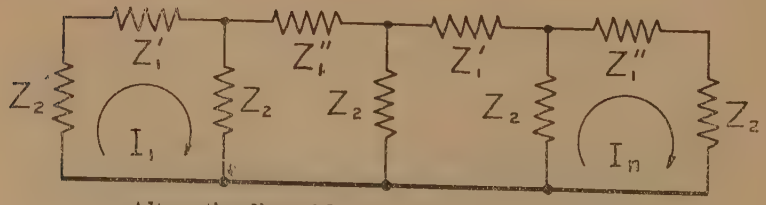

Alternating line with open ends, $(2n+1)$ elements.

it is an immediate consequence that the natural frequencies lie within the transmission bands of the line.

3. *Alternating Line with Open Ends.*—Fig. 12 shows an alternating line, similar to the simple recurrent line, but built up of two different sections recurring in alternating

succession along the line. This type of line is suggested by a doubly loaded string described by Born and von Kármán *. The procedure in this case is the same as before. Upon introduction of the notation

$$w'=1+\frac{Z_1'}{2Z_2}, \quad w''=1+\frac{Z_1''}{2Z_2},$$

the n linear equations for the currents in the various meshes of the network take the form

$$\begin{aligned}
0&=2w'I_1-I_2\\
0&=-I_1+2w''I_2-I_3\\
0&=-I_2+2w'I_3-I_4\\
&\cdots\cdots\cdots\\
0&=-I_{n-1}+2w''I_n.
\end{aligned}$$

The determinant of the coefficients is $'D_n''$, so that the natural frequencies are determined by

$$0='D_n''=\frac{\sinh(n+1)\Gamma}{\sinh\Gamma}, \quad \cosh\Gamma=\sqrt{w'w''}.$$

This condition is satisfied when $\Gamma=iB$, $A=0$:

$$0=\frac{\sin(n+1)B}{\sin B}, \quad B=\frac{k\pi}{n+1}, \quad k=1, 2, \ldots n.$$

The graphical solution, based on these values of B, is shown in fig. 13 for the structure $Z_1=i\omega L_1$, $Z_2=\frac{1}{i\omega C_2}$. The natural frequencies lie in two bands bounded by the cut-off frequencies ω_c.

V. Wave-Filter Determinants.

1. *Elementary Form.*—The simplest form of wave-filter determinant arises from the analysis of the type of line shown in fig. 9, described in Part IV. Denoting it by D_n, we have

$$D_n=\begin{vmatrix} 2w & -1 & 0 & \ldots & 0\\ -1 & 2w & -1 & \ldots & 0\\ 0 & -1 & 2w & \ldots & 0\\ \cdots & \cdots & \cdots & \cdots & \cdots\\ 0 & 0 & 0 & \ldots & 2w \end{vmatrix}_{n\text{th order}} \quad (n\geqq 1).$$

* *Phys. Zeit.* xiii. p. 303 (1912).

Expanding in terms of the first row, we have

$$D_n = 2wD_{n-1} - D_{n-2},$$

a simple linear difference equation with constant coefficients. Taking the trial solution $D_n = cx^n$ (c any constant), we have for x the quadratic equation $x^2 - 2wx + 1 = 0$, giving $x = w \pm \sqrt{w^2-1}$. This suggests the substitution $w = \cosh\Gamma$, from which

$$x = \cosh\Gamma \pm \sinh\Gamma = \exp \pm\Gamma.$$

Then D_n is a linear combination of $\exp n\Gamma$ and $\exp -n\Gamma$, or

Fig. 13.

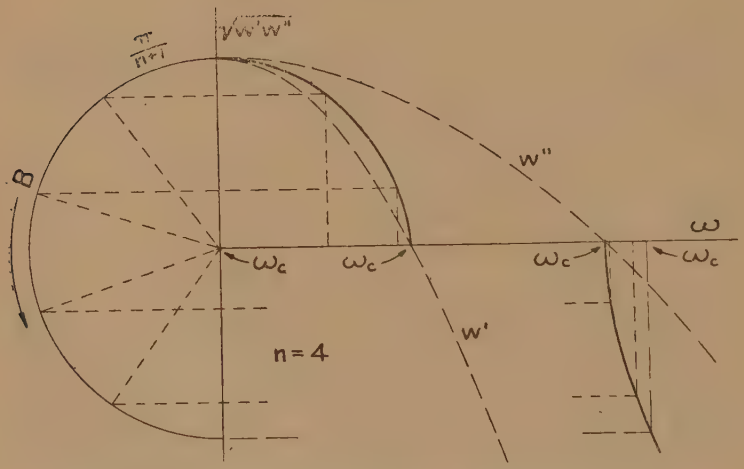

Graphical solution for natural frequencies of alternating line (L_1, C_2).

of $\cosh n\Gamma$ and $\sinh n\Gamma$: $D_n = c_1 \cosh n\Gamma + c_2 \sinh n\Gamma$. c_1 and c_2 are determined by the "initial conditions,"

$$D_1 = 2w = 2 . \cosh\Gamma = c_1 \cosh\Gamma + c_2 \sinh\Gamma$$

and

$$D_2 = 4w^2 - 1 = 4 . \cosh^2\Gamma - 1 = c_1 \cosh 2\Gamma + c_2 \sinh 2\Gamma,$$

from which $c_1 = 1$ and $c_2 = \coth\Gamma$.

Then $$D_n = \cosh n\Gamma + \coth\Gamma . \sinh n\Gamma,$$

or $$D_n = \frac{\sinh (n+1)\Gamma}{\sinh\Gamma}.$$

It is important to note that the cofactor of the element in the first row and last column of D_n is unity:

$$(-1)^{n-1}\begin{vmatrix} -1 & 2w & -1 & \dots & 0 \\ 0 & -1 & 2w & \dots & 0 \\ 0 & 0 & -1 & \dots & 0 \\ \cdot & \cdot & \cdot & \cdot & \cdot \\ 0 & 0 & 0 & \dots & -1 \end{vmatrix} = (-1)^{2n-2} = 1.$$

($(n-1)$th order)

2. *Mid-Termination Form.*—The most useful wave-filter determinant is that which arises from the filters shown in figs. 1 and 8, Parts II. and III. This determinant is

$$D_n(a, b) = \begin{vmatrix} w+w_a & -1 & 0 & \dots & 0 \\ -1 & 2w & -1 & \dots & 0 \\ 0 & -1 & 2w & \dots & 0 \\ \cdot & \cdot & \cdot & \cdot & \cdot \\ 0 & 0 & 0 & \dots & w+w_b \end{vmatrix} \quad (n \geq 2),$$

(nth order)

which is similar to one evaluated by Pupin (*loc. cit.*) by a method of infinite series. $D_n(a, b)$ is readily expressed in terms of D_n. Writing the terminal elements of the principal diagonal in the forms $2w+(w_a-w)$ and $2w+(w_b-w)$, it appears that $D_n(a, b)$ is the sum of four determinants:

$$D_n(a, b) = D_n + (w_a-w)D_{n-1} + (w_b-w)D_{n-1} + (w_a-w)(w_b-w)D_{n-2}.$$

But

$$D_n - 2wD_{n-1} = -D_{n-2}, \quad w = \cosh\Gamma, \quad D_n = \frac{\sinh(n+1)\Gamma}{\sinh\Gamma}, \text{ etc.}$$

Hence

$$D_n(a, b) = (w_a+w_b)(D_{n-1}-wD_{n-2}) + (w_aw_b+w^2-1)D_{n-2}$$

$$= (w_a+w_b)\frac{\sinh n\Gamma - \cosh\Gamma\sinh(n-1)\Gamma}{\sinh\Gamma} + (w_aw_b+\sinh^2\Gamma)\frac{\sinh(n-1)\Gamma}{\sinh\Gamma}.$$

Also

$$\sinh n\Gamma - \cosh\Gamma.\sinh(n-1)\Gamma = \tfrac{1}{2}.\sinh n\Gamma - \tfrac{1}{2}.\sinh(n-2)\Gamma = \sinh\Gamma.\cosh(n-1)\Gamma,$$

so that

$$D_n(a, b) = (w_a+w_b)\cosh(n-1)\Gamma + \frac{w_aw_b+\sinh^2\Gamma}{\sinh\Gamma}\sinh(n-1)\Gamma. \quad . \quad (13)$$

The most convenient and useful expressions of this result are

$$\frac{D_n(a,b)}{w_a+w_b}$$

$$= \cosh(n-1)\Gamma + \frac{w_a w_b + \sinh^2\Gamma}{(w_a+w_b)\sinh\Gamma}\sinh(n-1)\Gamma \qquad (14)$$

$$= \exp(n-1)\Gamma + \frac{(w_a-\sinh\Gamma)(w_b-\sinh\Gamma)}{(w_a+w_b)\sinh\Gamma}\sinh(n-1)\Gamma, \qquad (15)$$

since $\cosh(n-1)\Gamma + \sinh(n-1)\Gamma = \exp(n-1)\Gamma$.

For use in the analysis of non-dissipative filters, Parts II. and III., the modulus of this complex expression is required in the case of

w real, w_a and w_b imaginary.

This makes $\cosh(n-1)\Gamma$, $w_a w_b$, $\sinh^2\Gamma$, and $\dfrac{\sinh(n-1)\Gamma}{\sinh\Gamma}$ all real, so that in (14) the first term is real and the second term is imaginary. Multiplying (14) by its conjugate imaginary, the square of the modulus is

$$\left|\frac{D_n(a,b)}{w_a+w_b}\right|^2$$

$$= \cosh^2(n-1)\Gamma - \left[\frac{w_a w_b + \sinh^2\Gamma}{(w_a+w_b)\sinh\Gamma}\right]^2 \sinh^2(n-1)\Gamma$$

$$= \cosh^2(n-1)\Gamma - \left[\frac{(w_a-\sinh\Gamma)(w_b-\sinh\Gamma)}{(w_a+w_b)\sinh\Gamma}+1\right]^2 \sinh^2(n-1)\Gamma$$

$$= 1 - \frac{(w_a-\sinh\Gamma)(w_b-\sinh\Gamma)}{(w_a+w_b)\sinh\Gamma} \times \left[\frac{w_a-\sinh\Gamma)(w_b-\sinh\Gamma)}{(w_a+w_b)\sinh\Gamma}+2\right]\sinh^2(n-1)\Gamma$$

$$= 1 - \frac{(w_a^2-\sinh^2\Gamma)(w_b^2-\sinh^2\Gamma)}{(w_a+w)^2\sinh^2\Gamma}\sinh^2(n-1)\Gamma. \qquad (16)$$

When $\sinh\Gamma = 0$, the indeterminate forms are evaluated by making

$$\frac{\sinh^2(n-1)\Gamma}{\sinh^2\Gamma} = (n-1)^2.$$

3. *Exponential Line Form.*—This determinant arises from the exponential type of line shown in fig. 10, Part IV.:

$$D_n(\text{exp}) = \begin{vmatrix} 2w & -1/h & 0 & \dots & 0 \\ -h & 2w & -1/h & \dots & 0 \\ 0 & -h & 2w & \dots & 0 \\ \cdot & \cdot & \cdot & \cdot & \cdot \\ 0 & 0 & 0 & \dots & 2w \end{vmatrix} \quad (n \geqq 1).$$

(nth order)

Expanding in terms of the first row, we have

$$D_n(\text{exp}) = 2w D_{n-1}(\text{exp}) - D_{n-2}(\text{exp}).$$

Also we note that $D_1(\text{exp}) = D_1$, $D_2(\text{exp}) = D_2$, etc., so we conclude that

$$D_n(\text{exp}) = D_n.$$

The cofactors in $D_n(\text{exp})$, however, are different in general from those in D_n.

4. *Alternating Line Forms.*—The alternating line of the type shown in fig. 12, Part IV., gives rise to determinants similar to D_n, but with two elements in alternating succession along the principal diagonal. These forms are indispensable to some problems, and are capable of manipulation similar to the foregoing treatment of the elementary form. There are four distinct forms under this heading, differentiated by the different pairs of elements in the terminal positions of the principal diagonals:

$$'D_n'' = \begin{vmatrix} 2w' & -1 & 0 & \dots & 0 \\ -1 & 2w'' & -1 & \dots & 0 \\ 0 & -1 & 2w' & \dots & 0 \\ \cdot & \cdot & \cdot & \cdot & \cdot \\ 0 & 0 & 0 & \dots & 2w'' \end{vmatrix} \quad (n \text{ even}, \geqq 2),$$

(nth order)

$$'D_n' = \begin{vmatrix} 2w' & -1 & 0 & \dots & 0 \\ -1 & 2w'' & -1 & \dots & 0 \\ 0 & -1 & 2w' & \dots & 0 \\ \cdot & \cdot & \cdot & \cdot & \cdot \\ 0 & 0 & 0 & \dots & 2w' \end{vmatrix} \quad (n \text{ odd}, \geqq 1).$$

(nth order)

Then $''D_n'$ and $''D_n''$ are the same as $'D_n''$ and $'D_n'$ respectively, except that w' and w'' are interchanged.

Expanding as in the case of D_n, we have the equations

$$'D_n'' = 2w'.''D_{n-1}'' - 'D_{n-2}'',$$
$$''D_{n-1}'' = 2w''.'D_{n-2}'' - ''D_{n-3}'',$$
$$'D_{n-2}'' = 2w'.''D_{n-3}'' - 'D_{n-4}''.$$

Multiplying the second equation by $2w'$, and adding all three, we have $'D_n'' = 2(2w'w'' - 1)\,'D_{n-2}'' - 'D_{n-4}''$, a difference equation in $'D_n''$. Proceeding as before, taking the trial solution $'D_n'' = cx^n$ (c any constant), we have for x the biquadratic equation $x^4 - 2(2w'w'' - 1)x^2 + 1 = 0$, giving

$$x^2 = (2w'w'' - 1) \pm \sqrt{(2w'w'' - 1)^2 - 1}.$$

Making the substitution

$$2w'w'' - 1 = \cosh 2\Gamma, \quad \sqrt{w'w''} = \cosh \Gamma,$$

we have

$$x^2 = \cosh 2\Gamma \pm \sinh 2\Gamma = \exp \pm 2\Gamma, \quad x = \exp \pm \Gamma.$$

Then $'D_n''$ is a linear combination of $\exp n\Gamma$ and $\exp -n\Gamma$, or of $\cosh n\Gamma$ and $\sinh n\Gamma$: $'D_n'' = c_1 \cosh n\Gamma + c_2 \sinh n\Gamma$. c_1 and c_2 are determined by the "initial conditions," as before, $c_1 = 1$ and $c_2 = \coth \Gamma$, so that

$$'D_n'' = \frac{\sinh (n+1)\Gamma}{\sinh \Gamma}.$$

Interchanging w' and w'' makes no difference, so that also

$$''D_n' = \frac{\sinh (n+1)\Gamma}{\sinh \Gamma}.$$

Following a similar procedure, we have

$$'D_n' = c_1 \cosh n\Gamma + c_2 \sinh n\Gamma,$$

$$c_1 = \sqrt{w'/w''}, \quad c_2 = \sqrt{w'/w''}.\coth \Gamma:$$

$$'D_n' = \sqrt{w'/w''}\,\frac{\sinh (n+1)\Gamma}{\sinh \Gamma}.$$

Interchanging w' and w'',

$$''D_n'' = \sqrt{w''/w'}\,\frac{\sinh (n+1)\Gamma}{\sinh \Gamma}.$$

5. *Graphical Charts.*—In the application of the above determinants to wave-filter problems, we note that w and Γ are functions of the frequency of alternation, $w(\omega) = \cosh \Gamma(\omega)$,

the functions depending on the structure (Z_1, Z_2). The solutions in terms of F are, however, independent of the nature of the function $\Gamma(\omega)$ as long as it complies with the conditions imposed, and this fact makes these solutions particularly valuable. Several charts will be described, which can be used to show in a convenient manner the relationships between the various quantities involved.

The solutions in Parts II. and III., for non-dissipative filters, require that w be real, and the field of w is logically divided into three parts, as described. With this restriction, fig. 14 gives a convenient arrangement for showing the

Fig. 14.

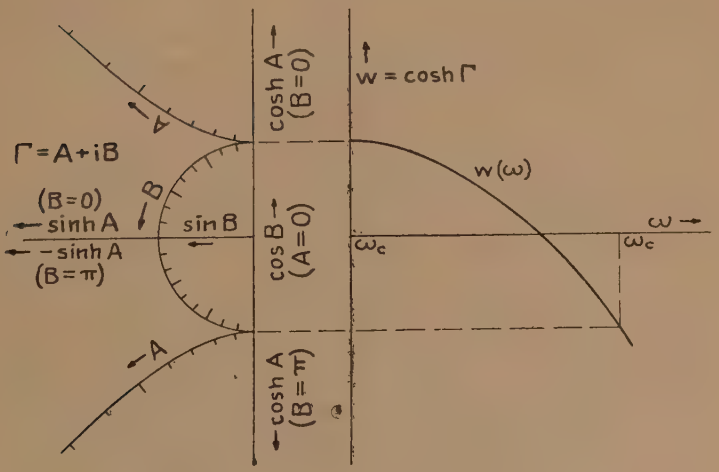

Functions of $\Gamma(\omega)$ for any function $w(\omega)$.

relationship between Γ and ω with the aid of a curve of $w(\omega)$. Corresponding to any abscissa ω, the ordinate of the curve determines the value of Γ. The partitioning of the w axis corresponds to the three kinds of frequency bands.

In fig. 14 the Γ functions shown on the left may be replaced by a curve of any solution in terms of F, plotted in the left-horizontal direction. This solution is then easily applied to any desired filter structures by drawing in the curves of $w(\omega)$.

If desired, the infinite plane (ω, w) may be represented in a square chart, as shown in fig. 15. The part of the curve which lies outside of $w = \pm 1$ in fig. 14 is folded over by

substitution in terms of the Gudermannian angle, gd Γ, as follows:—

Transmission band:

$$+1 \geqq w \geqq -1, \quad A = 0, \quad 0 \leqq B \leqq \pi,$$

$$w = \cosh \Gamma = \cos B = \cos \theta \text{ (solid curve).}$$

Fig. 15.

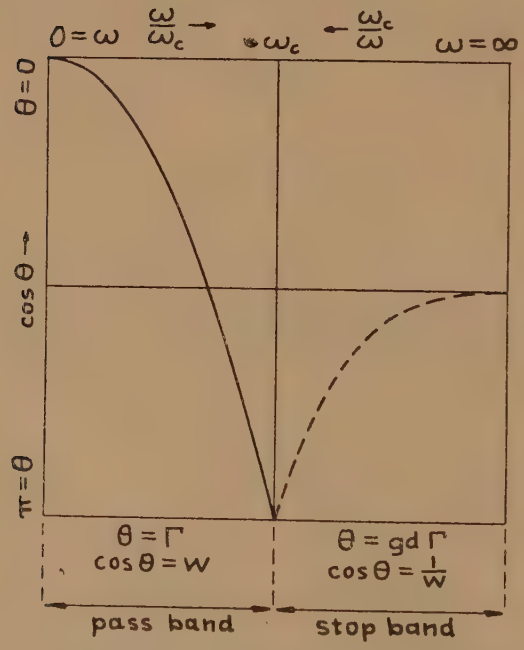

Square chart of functions shown in fig. 14.

Suppression bands:

$$+1 \geqq \frac{1}{w} \geqq -1, \quad +\infty \geqq A \geqq 0, \quad B = 0 \text{ or } \pi,$$

$$\theta = \text{gd}\,\Gamma : w = \cosh \Gamma = \pm \cosh A = \sec \theta$$

$$\sinh \Gamma = \pm \sinh A = \tan \theta,$$

$$\frac{1}{w} = \cos \theta \text{ (dotted curve).}$$

In general, both w and Γ are complex numbers, though this paper is largely restricted to w real. When w is complex, we denote its real and imaginary parts by u and v respectively :

$$w = u + iv = \cosh(A + iB) = \cosh A \cos B + i \sinh A \sin B.$$

Equating real and imaginary terms respectively,

$$u = \cosh A \,.\, \cos B, \quad v = \sinh A \,.\, \sin B.$$

Charts for reading A and B in terms of u and v can readily be prepared by drawing the level curves for A and B on the (u, v) plane, which are orthogonal families of ellipses and hyperbolas, repectively, determined by the following equations :—

A constant : $$\frac{u^2}{\cosh^2 A} + \frac{v^2}{\sinh^2 A} = \cos^2 B + \sin^2 B = 1.$$

B constant : $$\frac{u^2}{\cos^2 B} - \frac{v^2}{\sin^2 B} = \cosh^2 A - \sinh^2 A = 1.$$

VI. Differential Equations underlying Electric Impedance.

The problems treated in this paper are in reality solutions of second-order differential equations involved in the definition of the complex electric impedance. Appreciation of this situation makes it possible to apply the same solutions to other systems, such as mechanical or molecular structures, which may lead to the same differential equations.

In a simple series circuit including resistance R, inductance L, and capacitance C, the instantaneous values of current I_i and applied voltage E_i are related by the equation

$$RI_i + L\frac{dI_i}{dt} + \frac{1}{C}\int I_i\, dt = E_i.$$

In the case of steady, sinusoidal, alternating current, and applied voltage,

$$E_i = E_m \cos \omega t, \quad I_i = I_m \cos(\omega t - \phi),$$

we may choose to express these quantities in terms of the unit rotating vector, $\exp i\theta$, with the understanding that we refer to the real projection, $\cos\theta$. Then we write

$$E_i = E_m \exp i\omega t, \quad I_i = I_m \exp i\omega t,$$

in which I_m is complex, including the phase rotation, $\exp -i\phi$, as a factor. We substitute

$$\frac{dI_i}{dt} = i\omega I_i, \quad \int I_i\, dt = \frac{I_i}{i\omega}$$

in the first equation:

$$I_i\left(R + i\omega L + \frac{1}{i\omega C}\right) = E_i.$$

It is customary to use, instead of the peak values (E_m, I_m), the effective (root-mean-square) values of voltage and current:

$$E = \frac{E_m}{\sqrt{2}}, \quad I = \frac{I_m}{\sqrt{2}}.$$

We define the impedance Z as the ratio of voltage to current, which is, in this case,

$$Z = \frac{E_i}{I_i} = \frac{E_m}{I_m} = \frac{E}{I} = R + i\omega L + \frac{1}{i\omega C}.$$

An impedance is, in general, a complex function of ω, of which the real and imaginary parts are, respectively, the resistance R and the reactance X:

$$Z(\omega) = R(\omega) + iX(\omega) = |Z| \exp i\phi(\omega),$$

$$|Z| = \sqrt{R^2 + X^2} = \left|\frac{E}{I}\right|, \quad \tan\phi = \frac{X}{R}.$$

he phase angle ϕ defined by the above equations is the angle by which the current alternations lag behind the voltage alternations. This phase displacement is implicitly included in the complex impedance, in the complex factor $\exp i\phi$.

The power in any impedance is

$$(E_i I_i)_{\text{mean}} = |I|^2 . Z = R\,|I|^2 + iX\,|I|^2,$$

of which the actual power dissipation in heat (or work) is represented by the real part:

$$P = R\,|I|^2 = |E| \,.\, |I| \,.\, \cos\phi.$$

When this term is zero, the impedance is non-dissipative.

Johns Hopkins University,
Baltimore, Md.
May 31, 1927.

X. *Analogy between the Crystal Detector and a Vacuum Tube.*

By Wakasabro Ogawa *.

MANY theories of the crystal detector have been published, but none of them has been accepted as satisfactory. According to the writer's theory, the rectification by a crystal detector is brought about by the difference of electrons emitted from each electrode.

An investigation of the electron emission from crystals in the cold state was carried out to prove the theory positively. A crystal detector couple, consisting of a copper rod and a galena crystal, was sealed in a glass tube, a small space being left free without contact between the metal and the crystal. The tube was evacuated from a side tube. An electrolytic bath of Na_2SO_4 solution containing phenolphthalein was connected in series with the tube to show the polarity of the current if rectified. When A.C. potential was applied to the tube a glow discharge started between copper and galena when the voltage attained a certain value, and the colour of the phenolphthalein solution near an electrode corresponding to copper turned red. By this experiment it was known that the current is rectified by a cold vacuum tube with two electrodes of copper and galena and the rectified current flows in the same direction as the contact rectifier consisting of the same materials. In this case the only cause to which the rectifying action can be ascribed is the difference of electron emissions from the electrodes, such others as thermoelectrical or electrolytic effect having nothing to do with it. Then two electrodes of different metals or crystals of which the electron emissions were to be compared were sealed in a glass tube. As the emission is influenced by the physical state and dimension of the surface, care was taken to make the conditions of these two electrodes as equal as possible. As in the former case, the electrode which has stronger electron emission than the other was ascertained from the direction of the rectified current. Many couples of different metals and crystals were tested by this method, and as the result the following order of electron emission was obtained, magnesium having the strongest electron emission in the series : natural galena with the best sensitivity ; synthetic galena with 5 per cent. Ag ; silicon ; Pt ; Ag ; Cu ; german silver ; brass ; Pb ; Fe ; iron pyrites; simple synthetic galena ; carborundum :

* Communicated by the Author.

zincite; Al; Mg. These results all well correspond with those obtained by the writer's experiments with crystal detectors and also with the order arranged after the electron affinities of metals determined by many previous investigators. By these experiments the following facts are now established; (1) rectification is possible by two separate electrodes of different electron emissions in the cold state; (2) the direction of rectified current in this case is quite the same with that rectified by the contact rectifier composed of the same electrode materials. The essential differences between these two rectifiers are the distance between the electrodes and the surface area from which electron emissions occur. In the vacuum tube there is always a layer of air between the two electrodes and ionization of gas molecules necessarily occurs. In the crystal rectifier, it will be natural to think of the distance between the electrodes as varying from the real contact to the wide space involving the ordinary atmosphere. As the latice constant for metals and crystals has a value of $3{\cdot}2$–$5{\cdot}8 \times 10^{-8}$ cm. and the mean distance between gas molecules under normal pressure is $3{\cdot}33 \times 10^{-7}$ cm., the free space of nearly from 6×10^{-8} to 60×10^{-8} cm. will not allow the existence of gas molecules, and at least free electronic emissions may be possible in the space of this dimension. But as the free mean path of electrons in the atmosphere at normal pressure is nearly 9×10^{-5} cm., the electrons are able to reach the opposite electrode without collision with gas molecules in the wider space far beyond 60×10^{-8}. It may be, therefore, possible to say that the emission at the free space of a contact rectifier occurs in the highest vacuum, and no ionization of gas molecules is involved in an ordinary case of the wireless detector.

But in the case of the battery charger, which is another type of contact rectifiers consisting of two plate electrodes of metal and metallic oxide or sulphide and which is thought by the present writer to act on the same principle as ordinary crystal detectors, the electron emissions seem to occur even in a wider space involving an ordinary atmosphere in virtue of a higher potential.

Another difference between the crystal detector and the vacuum tube used in the preceding experiments is the surface from which electrons are emitted. In the vacuum tube the electrode surface works as a whole including any heterogeneous parts if present, while in a crystal detector only a special portion is brought to work and heterogeneous parts will work as such. For example, in an argentiferous synthetic galena, silver grains between PbS crystals will always

exert their influence upon the electron emissions in a vacuum tube, but in a crystal detector their effects will be quite different according to the position of the needle point. But there will be no difference in a homogeneous substance. At the first sight the surface area emitting electrons appears to be very different in a needle point and in a crystal. But this is not true, because the emissions only occur in the limited portion of the electrodes which come face to face within a certain limited distance and other parts will remain idle. In short, there is no substantial difference between a crystal detector and the vacuum tube except the metallic conduction at the real contact points in the former. This analogy is illustrated by figs. 1 and 2. Suppose A and B

Fig. 1.

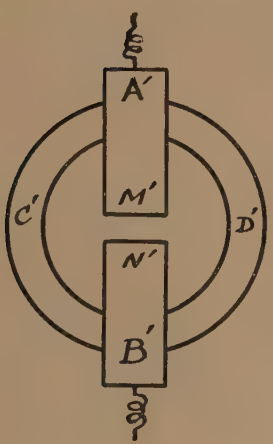

Fig. 2.

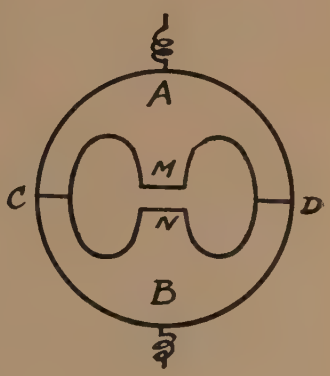

in fig. 1 to be two components of a crystal detector which are in contact really at C and D. The distance between M and N is thought to be so small that any molecules of gases are not admitted to enter between this space, that is to say, the space is vacuum. In fig. 2, A′ and B′ are the the electrodes and C′–D′ denotes a glass bulb of a vacuum tube. The real contact portions denoted by C and D will serve as the supports of the electrodes and correspond to the glass bulb C′–D′ of the vacuum tube. C–D and C′–D′ will equally make a route of leakage current if they are not good insulators and if this leakage attains to a certain value the potential difference between M and N as well as M′ and N′ will drop to such a value that electron emissions between

the electrodes will become impossible. As C and D in the crystal detector are composed of the same materials as the electrodes, it is impossible to ensure an insulation of high degree, more or less leakage as metallic conduction being inevitable. Thus it will be clear that the proper electrical resistance is of the prime importance in a crystal to be used as a detector.

In conclusion, a crystal detector is nothing else than a cold vacuum tube which works as a rectifier by the difference of electron emissions from two electrodes badly insulated.

Electrotechnical Laboratory,
Tokyo, Japan.

XI. *The Determination of the Atomic Scattering Power for X-Rays from Powders of Gold, Silver, and Aluminium for Cu Kα Radiation.* *By* J. Brentano, *D.Sc., Lecturer in Physics, Manchester University* *.

[Plate I.]

Summary.

In the present paper experiments are described intended to obtain comparative values for the scattering power of gold, silver, and aluminium.

The measurements are made with small powder particles, and a method is employed in which the intensities are measured from composite layers. Some points concerning this method, which makes it possible to overcome certain difficulties encountered in measuring the intensities of X-ray reflexions from powers, are discussed, and the procedure is indicated for evaluating the photographic records.

The results of the experiments indicate that, for the elements of high atomic weight examined in the state of very fine powders, the scattered intensities increase considerably less rapidly than F^2 and that better agreement is obtained by assuming the scattered intensity proportional to F. These results are discussed.

---

1. In a previous paper † a discussion was given of some intensity measurements of X-ray reflexions obtained from extremely fine powders of rock-salt.

* Communicated by the Author.

† J. Brentano, Phil. Mag. iv. p. 620 (1927).

The object of these measurements, which were recorded with a photographic method, was not to obtain data of a higher degree of accuracy than had been obtained from measurements on large crystal faces, but to verify whether the measurements made on large crystals were not affected to any considerable extent by extinction.

It resulted that in the particular case of rock-salt extinction effects played a very small part, but it was found that in other cases where these effects were large, the breaking up of a crystal into a powder could, in general, not be considered a reliable means for eliminating extinction, unless the particles are of the order of 10^{-6} or 10^{-5} cm. in diameter, so that only a limited advantage is obtained by using coarser powders in preference to large crystals.

2. In the present paper some measurements are described, directed to verify the general assumptions on the scattering of X-rays from atoms in crystal lattices. A problem which presents itself in this connexion is in a certain way similar to the problem discussed in the case of rock-salt.

A number of factors which determine the intensity of X-ray reflexions and which involve a certain amount of uncertainty in their numerical evaluation, assume definite values or become negligible for small angles of deflexion or, more exactly, for small values of $\sin\theta/\lambda$, where θ is the glancing angle of the reflexion and λ the wave-length. One of these factors is the quantity F, which we can define as the effective negative charge of the atom, which situated at its centre would be equivalent to the actual charge distributed in space for scattering radiation of the particular wave-length at the particular glancing angle θ *. F becomes equal to the actual charge for small values of $\sin\theta/\lambda$. Other factors are terms accounting for heat motion and for the Compton effect, which become negligible for small angles of deflexion.

On the other hand, extinction effects are greatest for the strong reflexions at small angles. They depend on the dimensions of the regular crystal units and on their distribution in the crystal and cannot be determined in a direct way.

* A more general definition of F can be given in which F is associated with the amplitude scattered from a plane of atoms, but for the purpose of the interpretation of the present experiments it is of greater interest to give to F the more special significance, rather than to introduce it in a phenomenological way.

It seemed, therefore, that a considerable simplification in the interpretation of the results could be obtained by measuring the reflexions at small glancing angles from a powder consisting of particles so small as to satisfy the conditions of negligible extinction. In this way we can avoid the superposition of too many factors, which render the interpretation of X-ray intensity measurements so difficult, and attempt to verify the fundamental assumptions before introducing them in more complex cases. The general evidence derived from the analysis of structures supports the classical relation making the contribution of each atom to the scattered intensity proportional to F^2, but most of this evidence refers to light atoms, and not so much information is available with respect to the scattering from atoms of higher atomic number. Measurements for the intensity of scattering were therefore made for gold, silver, and aluminium, which all belong to the cubic face-centered type of crystals.

In pursuing these determinations a method for measuring the intensities had to be evolved so as to be adapted to the particular conditions of a powder. We have to refer to a few points in this connexion to account for the particular way in which the determinations were carried out.

Similar conditions present themselves when quantitative intensity measurements are required in connexion with the determination of structures ; we discuss them, therefore, in a more general way than would be strictly necessary for the purpose of our experiments.

3. The effect of extinction * on the intensity of X-ray reflexions from the individual particles of a crystal powder depends mainly on the extinction in the particular crystal unit which is contributing to the reflexion, which Darwin calls primary extinction.

Darwin has given an approximate expression indicating the relative reduction of the intensity of the reflected radiation owing to the extinction in the reflecting unit. If m is the number of the reflecting planes and

$$q = \mathrm{N}(e^2/mc^2)\mathrm{F}\,\lambda^2/\sin^2\theta$$

measures the amplitude reflected from one plane, N being

* A general exposition of the phenomena of extinction in a single perfect crystal and in a crystal of "mosaic" structure has recently been given by Bragg, Darwin, & James, Phil. Mag. i. p. 897 (1926), and by P. Ewald, *Handbuch der Physik*, xxiv. (1926).

the number of atoms per unit volume, e and m being the charge and mass of the electron, c the velocity of light. Darwin's expression becomes

$$\frac{\tanh mq}{mq} \quad . \quad . \quad . \quad . \quad . \quad . \quad . \quad (1)$$

We give in Table I. the data calculated for the (111) reflexion for gold, silver, and aluminium, for which the expression (1) becomes equal to 99/100 or the extinction equal to 1 per cent., the last column gives the thicknesses corresponding to the numbers m. The F values used have been calculated according to Hartree *.

TABLE I.

Plane of reflexion.	$N.10^{-22}$	F.	q.	m.	Thickness $d.10^6$ cm.
Au (111)	5·94	72·7	12·8	135	3·2
Ag (111)	5·90	41·3	7·55	250	5·9
Al (111)	6·02	9·3	2·0	880	20·5

We can make sure of reducing this extinction effect below a given value by limiting the size of the crystal particles to the dimensions imposed for the individual crystal unit according to (1).

It will be noted that expression (1) increases very rapidly with mq, *i. e.*, with the thickness of the reflecting crystal unit ; on the other hand, this expression refers to the unit, not to the particle, and it might appear unlikely that the whole of one powder particle is perfect, *i. e.*, acts as one single unit.

In discussing extinction effects in the case of a powder, it has been pointed out by the writer † that when the conditions for negligible extinction in the individual particle are satisfied, there still exists a particular extinction effect, which could better be described as the additive absorption effect of the various crystal forms. All possible crystal faces contribute to it according to the number of times p they are represented on the crystal form, and according to their scattering power. The additive effect is thus a discontinuous function of the wave-length, as this limits the total number of faces which can reflect, but it is the same

* D. R. Hartree, Phil. Mag. l. p. 289 (1925).
† *Loc. cit.*

for all reflexions and appears as an additive term in the absorption coefficient.

When making absolute determinations from a powder layer of finite thickness, the proper coefficient of absorption could be determined for the actual powder, in such cases where the effect is appreciable. But the measurement of absorption coefficients from powders is exposed to a serious source of error, owing to the varying density of a powder mass, and this raises a difficulty in all absolute intensity measurements from powders in which the coefficient of absorption has to be introduced in an explicit or implicit form.

Another reason which makes powders less suitable for absolute measurements is the weakness of the reflected beams; this involves that for absolute determinations two intensities in the ratio 1 : 10,000 or 1 : 100,000 have to be compared, so that absolute measurements seem to require very great precautions.

It was therefore decided not to undertake absolute determinations, but to limit ourselves to relative measurements. It will be seen that the conditions of reflexion from a powder lend themselves particularly well to such determinations.

4. If dV is a volume element of powder, so small that absorption can be neglected, θ the glancing angle with respect to a set of lattice planes corresponding to a certain reflexion, so that 2θ is the angle between the incident and the reflected radiation, and I the intensity of a parallel beam of X-rays falling upon the volume element, the radiation scattered for this reflexion in unit time is given by

$$dP = \tfrac{1}{2} I p \cos\theta Q \, dV. \quad . \quad . \quad . \quad . \quad . \quad (2)$$

where $$Q = \frac{e^4}{m^2 c^4} \cdot F^2 N^2 \frac{\lambda^3}{\sin^2\theta} \frac{1+\cos^2 2\theta}{2} e^{-b\frac{\sin^2\theta}{\lambda^2}}. \quad . \quad (3)$$

The expression Q is the generally accepted value derived from classical theory, assuming that each electron scatters independently *. The exponential factor accounts for the heat motion of the atoms. A further factor should be added for the Compton effect, which limits the part of the incident radiation available for scattering †.

* C. G. Darwin, Phil. Mag. xliii. p. 800 (1922).

† Williams, Phil. Mag. ii. p. 657 (1926); Jauncey, Phys. Rev. xxix. p. 757 (1927).

This expression has to be integrated according to the conditions imposed by the particular method.

In the method used a beam of X-rays diverging from the focal spot of the anticathode, or from a slit near to it, falls on a flat layer of powder situated at a distance a from the point from which the X-rays diverge. The scattered radiation is observed at a distance b from the powder layer. Details of the arrangement have been described in another paper *, and certain focussing properties of it have been discussed. The glancing angle of incidence of the central beam being α and the glancing angle of emergence being β, we measure more conveniently not the quantity P, which is the radiation scattered according to the surface of a cone of semi-apex 2θ, but the part P_b of it, which falls at the distance b on a strip of unit height placed normally to the plane of deflexion in which the angles α and β are measured, and $\alpha+\beta=2\theta$.

We have thus for the central beam

$$dP_b = \frac{I p Q \, dV}{8\pi b \sin\theta} \quad . \quad . \quad . \quad . \quad . \quad . \quad (4)$$

Integrating for finite thickness z of the layer we have ,

$$P_b = \frac{I p Q f}{8\pi b \sin\theta \mu (1+\sin\alpha/\sin\beta)} \cdot \left(1 - \frac{1}{e^{-\mu z\left(\frac{1}{\sin\alpha}+\frac{1}{\sin\beta}\right)}}\right),$$

where f is the cross-section of the beam.

If the layer is sufficiently thick to absorb the incident radiation completely, and introducing X as the intensity of the divergent incident beam measured by the energy incident in unit time in the solid angle one and χ as the actual solid angle of a narrow incident pencil defined by the diaphragms of the instrument

$$P_b = X \frac{p Q \chi}{8\pi b \sin\theta} \cdot \frac{1}{\mu\left(1+\frac{\sin\alpha}{\sin\beta}\right)} \quad . \quad . \quad . \quad (5)$$

The focussing condition requires for the central beam

$$\frac{\sin\alpha_0}{\sin\beta_0} = \frac{a}{b} = \text{const.} \quad . \quad . \quad . \quad . \quad . \quad (6)$$

to be satisfied for all angles of reflexion. We see, therefore,

* J. Brentano, Proc. Phys. Soc. Lond. xxxvii. p. 184 (1925). There the arrangement is described in view of making exact angular measurements; its advantages for quantitative intensity measurements are indicated, but not fully discussed.

that for a narrow pencil which satisfies the focussing condition the particular intensity factor of the instrument is the same for all angles of deflexion.

In the actual experiment the finite width of the incident beam introduces a certain range in the angles of incidence α. Further, while measuring a given reflexion the powder layer is rotated through a certain range. The result of both these facts is that the focussing condition is satisfied only in approximation.

In order to consider the effect of the rotation of the layer on the radiation scattered from its centre, we have to integrate over the range $2\alpha'$, where α' is the greatest deviation of the powder layer from the correct setting.
Then

$$P_b = X \frac{pQ}{\mu \sin\theta} \cdot \text{const.} \int_{\alpha_0-\alpha}^{\alpha_0+\alpha'} \frac{1}{\omega_\alpha} \frac{d\alpha}{1+\frac{\sin\alpha}{\sin\beta}}.$$

In this expression the constant in front of the integral contains factors which depend on the particular arrangement. The term ω_α accounts for the angular velocity of the powder layer, which in general varies with θ *.

If for the small range $2\alpha'$, ω_α can be considered constant the expression becomes

$$P_b = X \frac{pQ}{\mu \sin\theta} \frac{\text{const.}}{\omega_\alpha} \left(\alpha' + \tfrac{1}{2}\cot\theta \log \frac{\cos(\alpha_0-\theta+\alpha')}{\cos(\alpha_0-\theta-\alpha')}\right),$$

and when in this case it is arranged to measure various reflexions during equal times, α' becomes proportional to ω_α, and the effect of the rotation of the layer on the reflexion from a point near to its centre is expressed by the additive term. We can thus estimate its value for any given conditions.

* In measuring with a photographic method a rotating slit is employed which moves with uniform velocity in front of the photographic film and uncovers an angular extension η of it at one time. The integration of (4) gives

$$P_b = X \frac{pQ\chi}{8\pi\mu b \sin\theta} \frac{t}{T} \frac{1}{\eta} \int_0^\eta \frac{d\eta}{1+\frac{\sin\alpha}{\sin\beta}},$$

where t is the time during which any particular point of the film is exposed, and T is the total time for one swing of the layer. For each reflexion α and β extend over a certain range determined by η always satisfying $\alpha+\beta=2\theta$. P_b is in this case an average effect over the time T.

By a similar reasoning we can estimate the effect of the finite angular extension ϵ of the incident beam in the plane of deflexion. It results that the effect of the larger and smaller values of α largely compensate one another except for small glancing angles. When making measurements at small glancing angles, ϵ must necessarily be small, in order that the whole incident beam may fall on the powder layer. So it is found that, in general, the experimental conditions are such as to allow to refer to expression (5). For relative measurements of different reflexions from a sufficiently thick layer keeping χ constant, we have then,

$$P_b = X \frac{pQ}{\sin\theta} \cdot \text{const.} \quad . \quad . \quad . \quad . \quad . \quad (7)$$

The quantity P_b in (5) is the energy entering into an ionization chamber in unit time, when the entrance slit at the distance b has the height one and is sufficiently wide to embrace the whole radiation scattered for the particular reflexion.

In the photographic record the quantity P_b is represented by the total blackening of the film taken for the whole width of the line. For the quantitative evaluation of photographic blackenings it is, of course, essential that the X-rays fall vertically on the film, which condition is satisfied with the apparatus. Different reflexions have also to be recorded for equal times.

It is desirable to make the incident beam diverging from the anticathode or from a point close to it, so that its intensity is uniform for the whole of its extension ϵ. In this case inequalities of the layer have less effect. This requires that a should be made somewhat larger than b.

5. In order to compare intensities of reflexion from different crystals, simple conditions are obtained by making measurements on composite layers containing both substances. We have then to consider that the expressions for P_b are obtained by an integration over a volume. In the case in which the experimental conditions allow us to use expression (7), and when X is the same for different reflexions, the ratio of two reflexions from a layer containing two substances in the proportion M_1/M_2 becomes

$$\frac{P_{b1}}{P_{b2}} = \frac{M_1 \rho_2 p_1 Q_1 \sin\theta_2}{M_2 \rho_1 p_2 Q_2 \sin\theta_1}, \quad . \quad . \quad . \quad . \quad . \quad (8)$$

where the quantities which refer to the one and to the other

crystalline substance are distinguished by the indices 1 and 2 and ρ are the densities.

As will be seen, the absorption coefficient and other constants which depend on the particular conditions of the measurement do not enter in this expression.

When only two lines or two groups of lines of similar intensity have to be compared the proportion of the two masses M_1/M_2 can be so adjusted as to make intensities of corresponding reflexions approximately equal. The shortcomings of the photographic method in comparing widely different intensities can thus be overcome to a considerable extent.

In the particular case of gold, silver, and aluminium, the lattice constants are 4·08 Å., 4·07 Å., and 4·06 Å. respectively. The reflexions fall, therefore, so near together that a comparison substance had to be used and measurements made from layers containing one of the metals and the comparison substance.

Nickel oxide, which had been employed as admixture in other measurements *, is in general a very suitable comparison substance in combination with Cu radiation, owing to its density and to the fact that the characteristic radiation of nickel is not excited by the radiation of copper. Its lattice constant is 4·1705 Å., and the metal and nickel oxide lines are thus so near that a proper determination of the background is rendered difficult. Therefore cadmium oxide was used, the lattice constant of which is 4·72 Å. Its (200) reflexion falls very near to the (111) reflexion of the metals, so that the (220) reflexion of cadmium oxide was compared with the (200) reflexion of gold, silver, and aluminium.

6. It seemed to be of some interest to ascertain whether it would actually be necessary to have recourse to so small particles as indicated by Table I.

For gold and silver it is known that the reflexions obtained from sheets of these metals are broadened, and this has recently been made the subject of an investigation by Dehlinger †. It could be expected that in such cases the mechanical treatment of preparing a coarse powder would produce a powder with sufficiently small crystal units.

Fig. 1 (Pl. I.) shows comparative photographs taken from two composite layers consisting of equal parts by weight of

* Brentano & Dawson, Phil. Mag. iii. p. 411 (1927).

† U. Dehlinger, *Zeitschrift f. Kristallographie*, lxv. (5) p. 615 (1927).

gold and nickel oxide *. The gold contained as impurities about 2·2 per cent. of silver and 1 per cent. of copper in each case. In the first photograph (*a*) extremely fine fragments of gold were used, obtained from gold leaves of $5 \cdot 10^{-6}$ cm. thickness. In the second photograph (*b*) the gold consisted of fine filings obtained from a thin sheet. Since the spacing for gold is slightly less than the spacing for nickel oxide, the reflexions from the latter occur at smaller angles than those of the former; on the photographs the lines corresponding to smaller angles are on the left.

It will be seen that in the case of the coarse gold particles the gold reflexions are by far the weaker, indicating considerable extinction in particular for small angles. At larger angles the difference between corresponding reflexions from the two films is less pronounced, which is what should be expected for an extinction effect †.

It is possible that the extinction effect observed with the coarser gold particles is not entirely due to primary extinction, but in part produced by secondary extinction. It indicates, in any case, that small particles had to be adopted for the measurements.

To obtain these particles, foils of gold, silver, and aluminium were powdered with the addition of a volatile substance. Taking the thickness of the foils as indicating the maximum dimension of the crystal units to be expected in these particles, for gold, the less favourable case, the corresponding extinction for the (200) reflexion amounted to 3 per cent.

7. In applying expression (8) to the particular conditions of our experiments, a simplification can be introduced, as the same reflexions are compared in each case and the value of $\sin\theta$ is nearly the same for the three metals. Therefore, we can write

$$\frac{P_{b1}}{P_{b2}} = \frac{M_1 \rho_2 Q_1}{M_2 \rho_1 Q_2} \cdot \text{const.} \quad . \quad . \quad . \quad . \quad (9)$$

The P_b values were measured from photographic records, and the photometry was carried out in the same way as for the measurements from rock-salt, but a more accurate

* This comparison of coarse and fine gold forms part of the early stages of this research undertaken in collaboration with Mr. W. E. Dawson, M.Sc., and I wish to express my indebtedness to him for his assistance.

† The exposure (*b*) (with coarse gold) was considerably longer than exposure (*a*) and the lines are darker. This does not show so much on the reproduction, but it accounts for certain nickel oxide lines appearing in (*b*) which are only faintly indicated in (*a*).

evaluation has been adopted in view of the different width of the lines obtained from different metals. The galvanometer deflexions taken for the various points of the lines were plotted in a logarithmic scale. By means of a suitable blackening curve it was then easy to express them in terms of X-ray intensities.

Fig. 2 shows examples of the curves so obtained. The ordinates in the upper curves represent the logarithms of the galvanometer deflexions, the ordinates in the lower curves represent the corresponding X-ray intensities, and their areas are proportional to the quantities P_b. The scale of the abscissæ is chosen so as to obtain areas convenient for measurement. The agreement between different measurements taken with the same substances is 5 per cent.

Table II. represents the results obtained from a greater number of measurements using Cu Kα radiation. The quantities referring to the metals gold, silver, and aluminium are marked by the index 200 of the corresponding reflexion; the quantities referring to the comparison substance are indicated by the index 220. The last column gives comparative values of Q for the three metals by introducing the ratio of the masses and the densities in (9).

Table II.

	ρ.	$\frac{P_{b200}}{P_{b220}}$.	M_{200}/M_{220}.	Q, const.
Au	19·3	0·310	1·00	585
Ag	10·5	0·270	0·67	405
Al	2·58	0·409	1·00	196

8. When discussing these Q values we can neglect the small differences in the numbers N, owing to the close agreement between the lattice constants for the three metals, so that referring to equation (3) for the comparison of the reflexions from gold, silver, and aluminium, F^2 becomes proportional to Q.

We have calculated the F values for the (200) reflexions from the three metals according to Hartree *, assuming Stoner's distribution of electrons. The values so found are $F_{200}=69{\cdot}55$ for gold, $F_{200}=38{\cdot}65$ for silver, $F_{200}=9{\cdot}23$ for aluminium. From calculation we obtain thus for the ratio,

* *Loc. cit.*

Fig. 2.

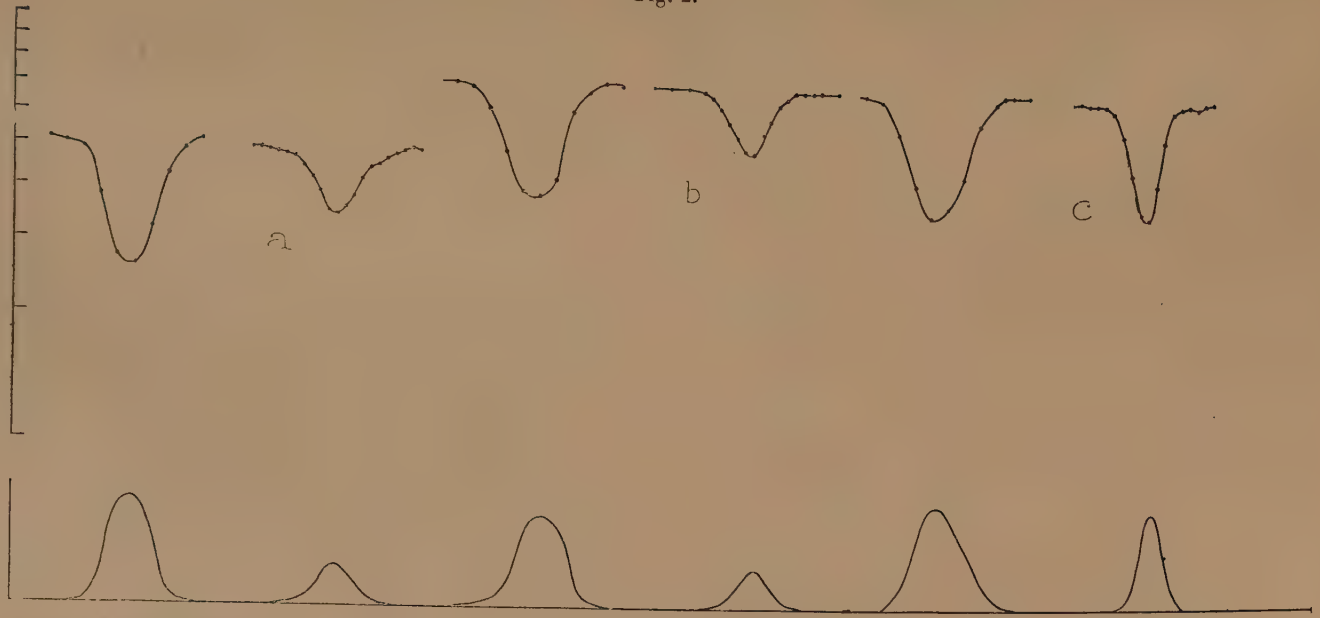

Photometry of (200) reflexions from gold (*a*), silver (*b*), and aluminium (*c*). The corresponding comparison reflexions are on the left.

gold and silver, $\frac{F^2_{Au}}{F^2_{Ag}} = 3{\cdot}23$, while the ratio of the experimental Q values gives 1·44.

The discrepancy is too great to be easily attributable to extinction effects or to the approximative character of the calculation.

A particular anomaly in the scattering power has been brought into evidence by an experiment by Mark and Szillard *, and is discussed in a more general treatment of scattering phenomena by Kallmann and Mark †. This anomaly is associated with the excitation of characteristic radiation of the scattering atom by the incident radiation and is effective only when the wave-length of the scattered radiation is near to one of the absorption edges of the scattering atom. This phenomenon cannot account for the present discrepancy.

The possibilities present themselves that either a general falling off of scattering power takes place as compared with the value given by Thomson's expression, for those electrons which are in the vicinity of a heavy nucleus, or that for the elements of higher atomic weight definite orbits do not contribute to the scattering. Comparing the gold and silver values with those from aluminium we find from calculation $\frac{F^2_{Au}}{F^2_{Al}} = 56{\cdot}8$ and $\frac{F^2_{Ag}}{F^2_{Al}} = 17{\cdot}6$, while the ratio of the experimental Q values gives 5·70 and 3·95 respectively. This indicates that on the latter hypothesis groups of electrons from gold and from silver should be excluded. It does not seem permissible to introduce the present experimental values in a treatment in which some factors, notably the factor for heat-motion, have been neglected for justifying any particular assumption as to the omission of the scattering from certain orbits. Determinations at low temperature and for different wave-lengths are in progress.

If we consider the experimental Q values without referring to equation (3), which is based on the assumption of independently scattering electrons and not on the continuous distribution of quantum-mechanics, and simply introduce the Q's to measure the scattering power per unit volume under the condition for (2) and (4), it appears that much closer agreement exists by comparing them with the calculated F values and not with their squares.

* Mark and Szillard, *Zeitschr. f. Phys.* xxxiii. p. 688 (1925).
† Kallmann and Mark, *Ann. der Phys.* lxxxii. p. 585 (1927).

We find from calculation, $\frac{F_{Au}}{F_{Al}} = 7{\cdot}54$ and $\frac{F_{Ag}}{F_{Al}} = 4{\cdot}2$, the corresponding experimental ratios, 5·70 and 3·95, give thus a relative value for gold which is somewhat too small, but show very good agreement for the relative values of silver and aluminium.

Retaining for F its significance as "effective" negative charge, so as to account for the spacial distribution of the electrons, this would indicate a contribution from each atom proportional to its charge.

Here two remarks present themselves: one that when applying an expression for Q to the scattering from a volume, in which extinction and absorption are nil, it would be very satisfactory to find the contribution of the individual atom to the total intensity of one reflexion proportional to F and not to F^2. In fact, F in such a case only determines the scattering from the individual unit of the pattern, so that a variation of F does not affect the range through which reflexion occurs, different from N in expression (3); the other that it is questionable whether an equation of this type can actually be applied to express the scattering when extinction is absent.

The two points are not so widely different as they appear, since, in considering the scattering from crystals, the scattering from one atom by itself has no physical meaning.

On the other hand, in making these remarks we must bear in mind that the general evidence from structure analysis and from absolute determinations on lighter elements is in agreement with (3) also in cases where this expression has been applied to measurements from microcrystalline mosaics and fine powders. It seems, therefore, of interest to discuss the present measurements in terms of this expression, when they indicate that the relations verified for lighter elements seem not to be satisfied in a general way.

The writer is indebted to Prof. W. L. Bragg, F.R.S., for various facilities, among which is the use of a transformer obtained by means of a grant of the Royal Society, and to the Leembruggen Trust for a special grant. He wishes in particular to express his thanks to Mr. W. E. Dawson, M.Sc., for his help in the earlier stages of this work, and to Mr. J. Adamson, M.Sc., for assistance received in the more recent experiments.

Manchester,
April 5th, 1928.

XII. *The Magnetic Energy of Permanent Magnets and of Linear Currents.* *By* H. V. Lowry *.

SUPPOSE the field has an applied electric force E′ and permanent magnetism I_0, then using Maxwell's equations

$$\int(E'j)dv-\int(Ej)dv=-\int\left(E-E',\ \text{curl}\ H-\frac{\partial D}{\partial t}\right)dv$$

$$=-\int(\text{curl}\,E-E',H)dv+\int\left(E-E',\frac{\partial D}{\partial t}\right)dv+\int[EH]_n dS$$

$$=\int\left(\frac{\partial}{\partial t}(B-I_0),H\right)dv+\int\left(E-E',\frac{\partial E}{\partial t}\right)dv, \quad . \ . \ . \quad (1)$$

the integrals being taken over all space, so that

$$\int[EH]_n dS=0.$$

In an isotropic medium of constant permeability and capacity the right-hand side of 1 becomes

$$\frac{\partial}{\partial t}\left\{\frac{1}{2}\int\mu H^2+K(E-E')^2\,dv\right\}.$$

$\int(E'j)dv$ is the rate at which work is done on the field by the applied forces; $\int(Ej)\,dv$ is the rate of dissipation of energy; and hence the right-hand side of (1) represents the rate of increase of the electrical energy of the field. This energy is in two parts, the first of which definitely depends on the magnetic properties of the field. If the field contains permanent magnets and no currents, this part becomes

$$W=-\tfrac{1}{2}\int(I_0H)\,dv$$

because $\int(BH)\,dv$ becomes zero in a magnetostatic field.

If the field contains no permanent magnets and the currents are steady and flow in circuits,

$$\tfrac{1}{2}\int\mu H^2\,dv \quad \text{transforms to} \quad \tfrac{1}{2}\Sigma\,iN=(T),$$

N being the total induction through a circuit carrying a current i.

If we regard the permanent magnets as made up of

* Communicated by the Author.

molecular currents, we can look on W and T as two different ways of uniting $\frac{1}{2}\int \mu H^2 dv$, just as

$$W_e = \tfrac{1}{2}\Sigma p_{rs} e_r e_s \quad \text{and} \quad W_v = \tfrac{1}{2}\Sigma q_{rs} V_r V_s$$

are different ways of writing the electrostatic energy $\frac{1}{2}\Sigma eV$.

From the magnetostatic point of view the force corresponding to the coordinate x is $\left(-\frac{\partial W}{\partial x}\right)$, and, as this is obtained by keeping I_0 constant, it is better to write it

$$\left(-\frac{\partial W}{\partial x}\right)_{I_0=\text{const.}}$$

But when the magnets are replaced by currents, the currents must be kept constant during the displacement δx in order that the equivalent magnetization shall remain constant. For two circuits

$$T = \tfrac{1}{2}\{L_1 i_1^2 + 2M i_1 i_2 + N i_2^2\},$$

so that keeping L_1 and L_2 and the shapes of the two circuits constant

$$\delta T = \delta M i_1 i_2.$$

The equations that give the currents are

$$\frac{\partial}{\partial t}(L i_1 + M i_2) + R_1 i_1 = E_1$$

and

$$\frac{\partial}{\partial t}(M i_1 + N i_2) + R_2 i_2 = E_2.$$

In the displacement

$$i_2 \delta M = (E_1 - R_1 i_1)\,\delta t$$

and

$$i_1 \delta M = (E_2 - R_2 i_2)\,\delta t.$$

Hence the increase of energy of the circuit

$$E_1 i_1 + E_2 i_2 - R_1 i_1^2 - R_2 i_2^2 - X\,\delta x = 2 i_1 i_2 \delta M - X\,\delta x$$
$$= 2\delta T - X\,\delta x.$$

Therefore

$$2\delta T - X\,\delta x = \delta T.$$

We have therefore two expressions for the force X

$$X = \left(-\frac{\partial W}{\partial x}\right)_{I_0-\text{const.}} = \left(+\frac{\partial T}{\partial x}\right)_{i=\text{const.}}.$$

These different expressions arise solely from the two

different ways of writing $\frac{1}{2}\int \mu H^2 dv$, and are analogous to the electrostatic equations

$$X = \left(-\frac{\partial W_e}{\partial x}\right)_{V=\text{const.}} = \left(+\frac{\partial W_V}{\partial x}\right)_{e=\text{const.}}.$$

If absolutely permanent magnets were possible the energy $2\delta T$ would have to be supplied from molecular sources.

We obtain the same result if we assume that the magnets have induced magnetization only, and that during a displacement this is kept constant by the application of an external magnetic force.

For such magnets the energy is $W' = -\frac{1}{2}\int (IH) dv$. In a displacement in which I is kept constant,

$$\delta W' = -\tfrac{1}{2}\int (I\delta H) dv.$$

To keep I constant in such a displacement an external magnetic force δH must be applied, and this will do work

$$-\int (I\delta H)\, dv = 2\delta W'.$$

Hence, as above, we have

$$2\delta W' - X\delta x = \delta W';$$

therefore

$$X = \frac{\delta W'}{\partial x}.$$

This expression for X is equivalent to the value

$$\left(\frac{\partial T}{\partial x}\right)_{i=\text{const.}}.$$

It is only the gradients of the energy that occur in the equations of motion and in the expressions for the generalized forces. The potential energy of a system of magnets is not necessarily $-\frac{1}{2}\int \mu H^2 dv$, because its kinetic energy is $+\frac{1}{2}\int \mu H^2 dv$; both T and W are equal to $\frac{1}{2}\int \mu H^2$, and the equations

$$X = -\frac{\partial W}{\partial x} = +\frac{\partial T}{\partial x}$$

are consistent with this, because

$$\left(\frac{\partial W}{\partial x}\right)_{I_0=\text{const.}} + \left(\frac{\partial T}{\partial x}\right)_{i=\text{const.}} = 0.$$

The confusion arises because the quantities kept constant in the partial differentiation are often omitted.

XIII. *Chemical Interactions corresponding to the Constant of Mass Action, being a Function of the Volume and Masses of the Constituents, as well as of the Temperature and Catalytic Action.*—I. *By* R. D. Kleeman, *B.A., D.Sc.* *

§ 1. *Introductory Remarks.*

THE writer has shown † that, in general, the constant of mass action of a gaseous interacting mixture is a function of its volume and masses of the constituents as well as of the temperature. In a subsequent paper ‡ the differential equations were developed which determine the functional nature of the constant of mass action in any given case. They were applied to investigate some well-known reactions by the help of the gas equation

$$pv = \mathrm{MRT}, \quad . \quad . \quad . \quad . \quad . \quad . \quad (1)$$

where p denotes the pressure of M mols of a pure gas at the volume v and absolute temperature T. In the particular cases considered, it was found that the constants of mass action are independent of the volumes of the reacting mixtures, as shown by experiment. The effect of the masses of the constituents on the constant of mass action was not investigated.

It was shown in a subsequent paper § that, strictly according to thermodynamics, the equation of a perfect gas is

$$pv = \mathrm{MRT}\xi, \quad . \quad . \quad . \quad . \quad . \quad . \quad (2)$$

where ξ is a function of T, v, and M, which is practically equal to unity except for temperatures close to the absolute zero, and for very large volumes. It would follow, then, that strictly in all cases the constant of mass action of a mixture in the perfectly gaseous state is a function of the volume, notably when it is very large, and the masses of the constituents, as well as of the temperature, though it may be practically independent of these quantities except of the temperature over a large range of values. In this paper it will be shown that the constant of mass action may be appreciably a function of the foregoing three quantities for reactions

* Communicated by the Author.
† Phil. Mag. v. p. 263 (1928).
‡ Phil. Mag. v. p. 620 (1928).
§ Phil. Mag. v. p. 1191 (1928).

taking place under certain conditions, even when equation (1) is supposed to hold strictly.

§ 2. *The Functional Nature of the Constants of Mass Action of Gaseous Mixtures reacting under Certain Conditions, and Catalytic Action.*

If the reacting mixture involves the constituents $a, b, \ldots$. whose masses in gram atoms are $M_a, M_b, \ldots$. the differential equation of the reaction in respect to volume as independent variable is

$$v\frac{\partial p}{\partial v} - M_a v_a \frac{\partial p_a}{\partial v} - M_b v_b \frac{\partial p_b}{\partial v} - \ldots = 0, \quad (3)$$

where p denotes the total pressure of the mixture, $p_a, p_b, \ldots$, the partial pressures of the constituents not in combination with each other, or the pressures they exert through membranes each of which is permeable to one of them, and $v_a, v_b, \ldots$, the corresponding volumes per gram atom. If the constituents when isolated form certain molecules the form of the equation may be altered accordingly, examples of which have already been given. The application of the gas equation (1) gives besides

$$p = RT\Sigma C, \quad (4)$$

where ΣC denotes the sum of the concentrations of the various molecules. Similarly, for the partial pressures $p_1, p_2, \ldots$, of the various molecules, we have

$$\left.\begin{aligned} p_1 &= RTC_1 \\ p_2 &= RTC_2 \\ &\ldots \end{aligned}\right\}, \quad (5)$$

where $C_1, C_2, \ldots$, denote their concentrations. The masses in gram atoms of the constituents are given by

$$\left.\begin{aligned} v\Sigma n_a C_{a_n} &= M_a \\ v\Sigma n_b C_{b_n} &= M_b \\ &\ldots \end{aligned}\right\}, \quad (6)$$

where C_{a_n} denotes the concentration in mols of the molecules which contain n_a gram atoms of atoms a, etc. Besides there are a number of mass action equations, each of which may be written in the generalized form

$$KC_1C_2 \ldots = C_4C_5 \ldots \quad (7)$$

The differential equation with respect to the mass M_a as independent variable is

$$v\frac{\partial p}{\partial M_a} - M_a v_a \frac{\partial p_a}{\partial M_a} - M_b v_b \frac{\partial p_b}{\partial M_a} - \ldots = 0, \quad . \quad (8)$$

and so on.

Now, the differential equations of the type (3) and (8) are derived by passing a mixture through a certain isothermal cycle. If the mixture consists of two constituents it is initially contained in the chamber C_{ae} of an apparatus shown diagrammatically in fig. 1, this chamber being separated from the chambers C_a and C_e by membranes, each of which is permeable to one of the constituents. An essential condition of the process is that in passing the mixture from the chamber C_{ae} into the chambers C_a and C_e, or *vice versa*, the pressures in the chambers are kept constant. We will

Fig. 1.

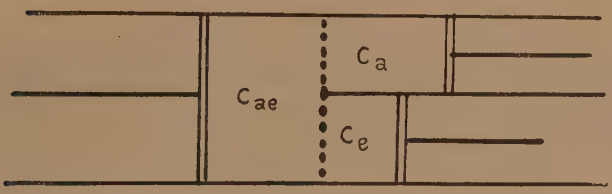

now vary this process by supposing that the walls of one of the chambers C_a and C_e—say C_a, is permeable to a gas contained in an adjacent infinitely large reservoir. Whatever the nature of the reaction now going on in this chamber, it is evident that the foregoing condition will still be satisfied, since the pressure in the chamber does not depend on its volume for constant pressures in the chambers C_{ae} and C_e. The general forms of the differential equations obtained will therefore be the same as before, but the forms of equations (4) and (5) may now be different. Now, if it can be shown by means of these equations that, corresponding to the first arrangement, the constant of mass action of the reacting mixture in the chamber C_{ae} is a function of the temperature only, it will be evident that with the second arrangement this may no longer be true. It follows, therefore, that a reaction taking place in one of the chambers C_a and C_e may affect catalytically the reaction in the chamber C_{ae}, causing the constant of mass action to become a function of the volume and masses of the constituents as well as of the

temperature. Examples of this will be considered in Sections 3, 4, and 6.

Instead of supposing that the chamber walls of the chamber C_a are permeable to molecules c, we may suppose that this is not the case, but that the chamber contains permanently a mass M_c of molecules c. In order to derive the differential equations in this case, we must now suppose that when the mixture is initially contained in the chamber C_{ae} the chamber C_a is at a volume V_{a1}, and contains molecules of the constituent a as well as molecules c. On transferring the mixture in the chamber C_{ae} into the chambers C_a and C_e we must further suppose that the pressures in the chambers C_{ae} and C_e only are kept constant.

Let us now pass the mixture through a cycle similar to the one used * to derive equation (3), to which the reader is referred for information. The external work done by the chamber C_a during the process (a) is now not $p_a v_a M_a$, but

$$\int_{V_{a1}}^{V_{a2}} p_a \cdot \partial V_a,$$

where V_{a1} and V_{a2} denote the volumes of the chamber at the beginning and end of the process. The work done by the chamber during the process (b) is not $p_a M_a \cdot \partial v_a$, but

$$p_{a2} \cdot \partial V_{a2},$$

where p_{a2} denotes the pressure when the volume is V_{a2}. The work done during the process (c) is

$$-\int_{V_{a1}}^{V_{a2}} p_a \cdot \partial V_a - \partial \int_{V_{a1}}^{V_{a2}} p_a \cdot \partial V_a,$$

instead of $-M_a v_a p_a - \partial(M_a v_a p_a)$. Finally, on equating the external work done, we obtain

$$v\frac{\partial p}{\partial v} - M_e v_e \frac{\partial p_e}{\partial v} - \frac{\partial}{\partial v}\int_{V_{a1}}^{V_{a2}} p_a \cdot \partial V_a + p_{a2} \cdot \frac{\partial V_{a2}}{\partial v} = 0. \quad (9)$$

If the last two terms in this equation, on substituting from equations (4), (5), and (6), assume a different functional form than the term $M_a v_a \frac{\partial p_a}{\partial v}$, which corresponds to no molecules c being present in the chamber C_a (compare with equation (3)), the molecules c in the chamber influence catalytically the reaction going on in the chamber C_{ae}. The constant of mass

* Phil. Mag. v. p. 621 (1928).

action of the reaction is then necessarily a function of the volume and masses of the constituents, if it is a function of the temperature only when the molecules c are absent *.

§ 3. *The Catalytic Effect of the Molecular Volume of a Gas on the Constant of Mass Action of a Reaction.*

Suppose that the walls of the chamber C_a are permeable to molecules c in the gaseous state contained in an adjacent infinitely large reservoir. Let us further suppose that these molecules have a volume associated with them which is equal to b per c.c. If we suppose that we are dealing with a reaction between molecules a and e in the chamber C_{ae}, the chamber C_a will contain also molecules a, and the chamber C_e molecules e. The differential equation of the reaction in the chamber C_{ae} with respect to its volume v as independent variable is

$$v\frac{\partial p}{\partial v} - M_e v_e \frac{\partial p_e}{\partial v} - M_a v_a \frac{\partial p_a}{\partial v} = 0, \quad . \quad . \quad . \quad (10)$$

where M_a and M_e denote the masses in mols of the substances a and e, and v_a and v_e the volumes of mols in the chambers C_a and C_e at the pressures p_a and p_e respectively, and p denotes the total pressure of the mixture in the chamber C_{ae}. Let us next suppose that the molecules a and c in the chamber C_a do not interact chemically, in which case the pressure p_a of the molecules a is given by

$$p_a = \frac{RT}{v_a}\frac{1}{1-b} = RTC_a'\frac{1}{1-b}, \quad . \quad . \quad . \quad (11)$$

* It will be helpful to point out that the equation of state of the matter in the chamber C_a may be written $p_a = \phi_1(T, V_a, C_a)$, where C_a denotes the concentration of the uncombined molecules a in the chamber C_{ae}. Its form may be determined directly by experiment with the chamber C_{ae} containing only molecules a. The mass M_{a1} of molecules a in the chamber C_a is given by the equation $M_{a1} = \phi_2(T, V_a, C_a)$, whose form may also be determined by experiment. It should also be observed that M_a, the total mass of the substance a in the chamber C_{ae} at the volume v, is now a function of v, and that

$$\frac{\partial M_a}{\partial v} = -\frac{\partial M_{a_1}}{\partial v} = -\frac{\partial M_{a1}}{\partial C_a}\frac{\partial C_a}{\partial v}.$$

The volume V_{a2} corresponds to the total and constant mass $M_a + M_{a'}$ of the substance a in the chamber C_a, and is given by the equation $V_{a2} = \phi_3(T, C_a)$, whose form is determined by experiment. Hence

$$\frac{\partial V_{a2}}{\partial v} = \frac{\partial V_{a2}}{\partial C_a}\frac{\partial C_a}{\partial v}.$$

where C_a' denotes the concentration of the molecules a in the chamber, $v_a = 1/C_a'$, and the factor $1/1-b$ expresses the effect of the volume of the molecules c on the pressure. If C_a denotes the concentration of the free molecules a in the chamber C_{ae}, the partial pressure they exert is equal to RTC_a. This pressure must be equal to the pressure in the chamber C_a, otherwise diffusion from one chamber to the other will take place, and hence

$$C_a = C_a' \frac{1}{1-b}, \quad \ldots \quad (12)$$

which gives the relation between C_a and C_a'. The term $M_a v_a \frac{\partial p_a}{\partial v}$ in equation (3) may now be written

$$M_a v_a \frac{\partial p_a}{\partial v} = \frac{M_a RT}{C_a'(1-b)} \frac{\partial C_a'}{\partial v} = \frac{M_a RT}{C_a(1-b)} \frac{\partial C_a}{\partial v}$$

by means of equations (11) and (12) and since $v_a = 1/C_a'$. If the chamber C_a did not contain molecules c, the foregoing term expressed in terms of C_a would have the form $\frac{M_a RT}{C_a} \frac{\partial C_a}{\partial v}$. Hence, if in the latter case the constant of mass action of the reaction in the chamber C_{ae} is a function of the temperature only, this will not be the case when the chamber C_a contains molecules possessing molecular volume, the constant now being a function of the volume as well *.

Similarly, it can be shown, by means of the differential equations involving the masses of the constituents as independent variables, that the constant of mass action is now a function of the masses of the constituents. The molecular volume of the molecules c thus has a catalytic action on the reaction in the chamber C_{ae} through contact by means of the molecules a, which is exhibited by a change in the constant of mass action.

This effect should also occur if the reacting molecules themselves possess molecular volume, as is the case in practice. If this volume be known, its effect on the constant of mass action may easily be calculated by means of the differential equations given in Section 2. The same effect would be produced by the addition of an inert gas possessing molecular volume to the reacting mixture. The effect might be large enough to measure in practice.

* This will be immediately evident from the investigations in the second paper quoted. The conditions that K is independent of v for the cases considered are now obviously not satisfied.

§ 4. *The Effect of the Functional Form of the Constant of Mass Action of a Reaction on the Form of the Constant of another Reaction.*

Let us suppose that the molecules c in the chamber C_a in the arrangement of the preceding Section interact with the molecules a, and that the corresponding constant of mass action K_{ac} is a function of the volume of the chamber C_a, or what amounts to the same thing, a function of the volume v of the chamber C_{ae}. The term $M_a v_a \frac{\partial p_a}{\partial v}$ in equation (3) may then be written in the form

$$M_a v_a \left\{ \left(\frac{\partial p_a}{\partial v} \right)_{K_{ac}} + \left(\frac{\partial p_a}{\partial K_{ac}} \right)_v \frac{\partial K_{ac}}{\partial v} \right\}.$$

Since $\frac{\partial K_{ae}}{\partial v}$ occurs only once and represents an independent function it will not disappear from the equation. Hence, if the equation is solved, we finally obtain the constant of mass action of the reaction in the chamber C_{ae} expressed in terms of $\frac{\partial K_{ac}}{\partial v}$, which is a function of v. This shows that the reaction in the chamber C_a affects that in the chamber C_{ae}, and *vice versa*, and therefore the reactions will also affect each other if they take place in the same mixture.

§ 5. *The Effect of a Maynetic and Electric Field on the Constant of Mass Action of a Reaction.*

Let us suppose that a gaseous reaction between molecules a and e takes place in the chamber C_{ae}, and that the molecules a in the chamber C_a are subjected to a magnetic field. If the molecules a are paramagnetic, energy must be expended to take a molecule out of the field. The concentration of the molecules inside the field will therefore be greater than outside of it, since the velocities of the molecules are distributed according to Maxwell's law, and only those are able to escape whose velocities lie above a certain value. An analogous case is a liquid in contact with its vapour, the attraction of the liquid taking the place of the magnetic field. The pressure in the chamber C_a will therefore be given by

$$p_a = RTC_a'\alpha, \quad . \quad . \quad . \quad . \quad . \quad . \quad (13)$$

where C_a' denotes the concentration of the molecules a and α a quantity less than unity depending on the strength of the field. The pressure of the free molecules in the chamber C_{ae} is RTC_a, which must be equal to the pressure in the chamber C_a, otherwise diffusion from one chamber to the other will take place, and hence

$$C_a = C_a'\alpha. \quad . \quad . \quad . \quad . \quad . \quad . \quad (14)$$

The term $M_a v_a \frac{\partial p_a}{\partial v}$ in equation (3) may now be written

$$M_a v_a \frac{\partial p_a}{\partial v} = \frac{\alpha M_a RT}{C_a'} \frac{\partial C_a'}{\partial v} = \frac{\alpha M_a RT}{C_a} \frac{\partial C_a}{\partial v}$$

by means of equations (13) and (14) and since $v_a = 1/C$. If no magnetic field were present the value of α would be equal to unity. Thus, if the differential equation (3) is solved corresponding to a magnetic field existing in the chamber C_a, the constant of mass action of the reaction in the chamber C_{ae} appears a function of the volume. Similarly, it can be shown by using equations of the type (8) that the constant of mass action is a function of the masses of the constituents.

The same result is obtained on applying the field to the chamber C_{ae}. The value of α, it will be observed, will have different values for the different molecules. It will not be difficult to see from an inspection of equations (3), (4), (5), and (6), that the effect of the field on the constant of mass action is in this case different from that obtained by applying the field to both the chambers C_a and C_e.

If we suppose that the magnetic field is applied to the three chambers C_a, C_e, and C_{ae} at the same time, it will not be difficult to see that the effect on the constant of mass action is different from the previous cases considered. This indicates that the magnetic field produces a change in a molecule which gradually disappears when it wanders out of the field, as may happen in the first two arrangements.

If an electric field is applied instead of a magnetic field similar results are obtained.

§ 6. *The Effect of a Dense Substance on the Constant of Mass Action and Catalytic Action.*

If in the process to which equation (9) refers, the substance c in the chamber C_a does not obey the gas laws, the expression, taking into account that M_a is now a function of v,

$$\left\{v\left(\frac{\partial p}{\partial \mathrm{M}_a}\right)_v - \mathrm{M}_e v_e \left(\frac{\partial p_e}{\partial \mathrm{M}_a}\right)_v\right\}\frac{\partial \mathrm{M}_a}{\partial v} - \frac{\partial}{\partial v}\int_{\mathrm{V}_{a1}}^{\mathrm{V}_{a2}} p_a . \partial \mathrm{V}_a + p_{a2}\frac{\partial \mathrm{V}_{a2}}{\partial v}$$

will involve quantities depending on the nature of the substance c. That this is so will be evident from supposing that the substance c in the chamber C_a is in the gaseous state, but possesses a considerable molecular co-volume, in which case it can easily be shown, similarly as in Section 3, that the above expression involves this co-volume. The constants depending on the substance c do not occur elsewhere in the equation than in the above expression, and also do not occur in the equations (4), (5), and (6) used to effect the solution of equation (3). They will be associated with factors which may be expressed as functions of the variables v, M_a, M_e, M_a', M_c, where M_a' and M_c denote the masses of the constituents a and c in the chamber C_a when its volume is V_{a1}, and v denotes the volume of the reacting mixture in the chamber C_{ae} and M_a and M_e the masses of the constituents a and e it contains. Hence the solution of equation (3), from which the concentrations of the various molecules in the chamber C_{ae} may be determined *, when substituted in equation (7), gives the constant of mass action a function of the above variables. If the equation of state of the mixture in the chamber C_a under the changing conditions during the cycle be known, the calculations can actually be carried out. The differential equations involving the masses of the constituents as independent variables may similarly be used.

Thus, we have the very important result that *a dense substance in contact with a gaseous reaction of which it occludes to a certain extent one or more of the constituents, renders the constant of mass action a function of the volume and masses of the constituents.* A catalytic agent thus is not only likely to change the velocities of the various changes continually going on in the reacting mixture, but the value of the constant of mass action as well, and to an extent depending on the volume and masses of the constituents of the reacting mixture. The far-reaching nature of these results will be further discussed in a separate paper.

Shenectady, N.Y., U.S.A.

* *Loc. cit.*

XIV. *On the Theory of Light-scattering in Liquids.*

To the Editors of the Philosophical Magazine.

GENTLEMEN,—

IN a paper published in the Phil. Mag. v. pp. 498–512 (1928), under the title of "A Theory of Light-scattering in Liquids," Prof. C. V. Raman and K. S. Krishnan refer to a new theory of light-scattering which they attribute to Dr. K. R. Ramanathan ('Indian Journal of Physics,' i. p. 413, 1927), and which, in their notations, leads to the formulæ :—

$$i = i_0 \frac{\pi^2}{2d^2} \cdot \frac{RT\beta}{N\lambda^4} (\mu^2-1)^2 \cdot \frac{6+6r}{6-7r},$$

$$r = \frac{2n_0F}{\frac{RT\beta}{N}\left(\frac{\mu^2-1}{4\pi}\right)^2 + \frac{7}{3}n_0F}.$$

Now these formulæ have already been given by myself with equivalent notations (*C. R.* p. 212, Aug. 1925). In my work I named these "Formulæ type Vessot-King," in order to remind us that Prof. Vessot-King ('Nature,' cxi. p. 667, 1923), was the first to give a molecular theory of light-scattering. This author implicitly supposed that the polarization-field had no fluctuation. In my paper mentioned above, I brought this hypothesis into full evidence, showing that it was sustainable, and that the disagreement between Vessot-King's theory and those of Gans and Ramanathan was due to the fact that the latter replaced that hypothesis by others.

Krishnan's experiments, instigated by my work mentioned above, having shown the superiority of the theory "type Vessot-King," Dr. K. R. Ramanathan, wishing to correct his formulæ, simply adopted the hypothesis in question, only justifying it by qualitative reasons. He therefore fell again into the "Formulæ type Vessot-King" which I gave in my paper, without apparently adding anything. The same conclusions hold for the theory proposed by Prof. C. V. Raman and K. S. Krishnan, which has also, however, the special interest of giving a very suggestive explanation for the apparent difference of anistropy which the molecules in a liquid or a gaseous state seem to offer.

To say the truth, the question of the fluctuations of the polarization field is still an open one ; I will show, in a paper

to be published soon in the *Annales de Physique*, that these fluctuations exist, but that one can bring them in the calculations of the intermolecular field, which must be considered contrary to the opinion expressed some time ago by Dr. K. R. Ramanathan.

Collège de France, Paris.
March 29th, 1928.

Yours faithfully,
Dr. Y. Rocard.

XV. *A Note on the Magnetic Field of a Rectilinear Circuit and the Attraction of a Straight Wire.* *By* J. A. Tomkins, *A.R.C.Sc., F.Inst.P.* (*Technical College, Bradford*) *.

HAVING had occasion recently to consider at about the same time with different students, the apparently diverse problems of the magnetic field of a rectangular coil and the gravitational attraction of a straight wire, I was led to note that the relation between them was such that a simple geometrical construction for the one was, with a slight extension, applicable to the other. As the latter has not, so far as I am aware, been previously described, and the former, judging from its absence from most of the text-books, does not appear to be generally known, a brief account of it may be of interest. The geometrical construction referred to is that for the magnetic field of a long straight conductor which was described by Dr. G. F. C. Searle in 1891 *.

Taking Ampère's formula $i \,.\, ds \,.\, \sin\theta/r^2$ for the magnetic force due to a current element ds, let NAB (fig. 1) be the conductor, ab the current element, and P the given point. From P drop the perpendicular PN, and with P as centre and radius PN draw a circle touching the wire at N. Join Pa, Pb, meeting the circle in d and e. Through d and e draw df, eg perpendicular to the diameter parallel to the wire and dh, ek perpendicular to PN. Through a draw ac perpendicular to Pb.

Then if PN$=a$, P$b=r$, and the angle PbN$=\theta$, the magnetic force at P, perpendicular to the plane of the paper due to the current element ab, is

$$\frac{i \,.\, \overline{ab} \,.\, \sin\theta}{r^2} = \frac{i \,.\, \overline{ac}}{r^2} = \frac{i \,.\, \overline{de}}{ra} = \frac{i}{a} \cdot \frac{\overline{fg}}{a} = \frac{i}{a^2} \cdot \overline{fg}.$$

* Communicated by the Author.
† 'Electrician,' Dec. 4, 1891.

Hence, for the whole conductor, the magnetic force at P is

$$\frac{i}{a^2}\Sigma\overline{fg}=\frac{2i}{a}.$$

Fig. 1.

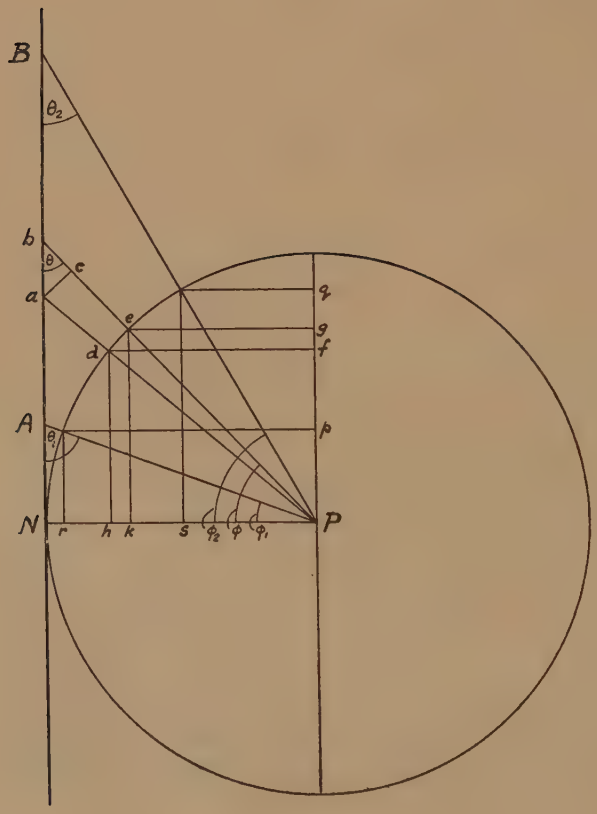

For a finite portion AB of the conductor, the contribution to the magnetic force at P will be

$$\frac{i}{a^2}\overline{pq}=\frac{i}{a}(\sin\phi_2-\sin\phi_1).$$

In the case of a thin straight wire of attracting matter, if ρ be the linear density, the attraction on unit mass at P,

due to an element of the wire, will be $\frac{G\rho \,.\, ds}{r^2}$ along r, where G is the constant of gravitation. Hence the component perpendicular to the wire is $G\rho \,.\, ds \,.\, \sin\theta/r^2$ and that parallel to it $G\rho \,.\, ds \,.\, \cos\theta/r^2$.

Comparing these expressions with that for the magnetic field due to a current element, it will be seen that a similar method can be employed for their summation. Thus for an infinite wire the resultant force perpendicular to it is $2G\rho/a$, For a wire AB of finite length, the component perpendicular to it is obviously

$$\frac{G\rho}{a^2} \,.\, \overline{pq} = \frac{G\rho}{a}(\sin\phi_2 - \sin\phi_1),$$

Fig. 2.

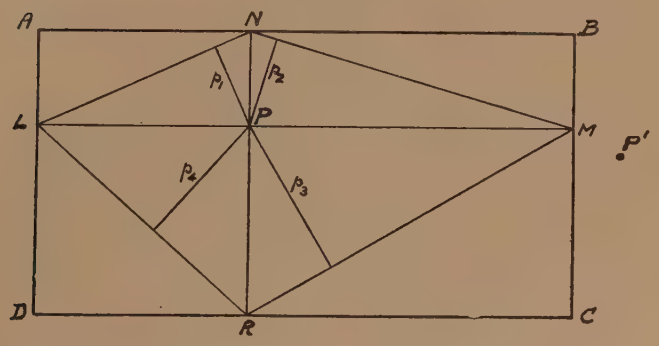

and that parallel to it is

$$\frac{G\rho}{a^2} \,.\, \overline{rs} = \frac{G\rho}{a}(\cos\phi_1 - \cos\phi_2).$$

Returning now to the magnetic field of a circuit, the magnetic force at any point due to a rectilinear circuit can be calculated by the method given, whereas, with the usual circular coil, the calculation for points not on the axis involves the use of spherical harmonics or elliptic integrals. In the case of a rectangular circuit, the expression for the magnetic force at any point in its plane was, I believe, first derived by the late Prof. G. M. Minchin *, in a form which does not appear to be usually given.

Let ABCD (fig. 2) be the rectangular circuit and P the given point. Through P draw the straight lines LM, NR,

* *Ibid.* Sept. 6, 1895.

parallel to the sides. Then denoting LA and AN by a_1 and a_2 and the angles they subtend at P by ϕ_1 and ϕ_2, the contribution of these adjacent portions to the magnetic force at P will be

$$i\left(\frac{\sin\phi_1}{a_2}+\frac{\sin\phi_2}{a_1}\right)=i\left(\frac{a_1}{a_2\sqrt{a_1^2+a_2^2}}+\frac{a_2}{a_1\sqrt{a_1^2+a_2^2}}\right)$$

$$=\frac{i}{a_1a_2/\sqrt{a_1^2+a_2^2}}=\frac{i}{p_1},$$

where p_1 is the perpendicular from P on LN.

Hence for the whole circuit the magnetic force at P is

$$i\left(\frac{1}{p_1}+\frac{1}{p_2}+\frac{1}{p_3}+\frac{1}{p_4}\right)$$

Fig. 3.

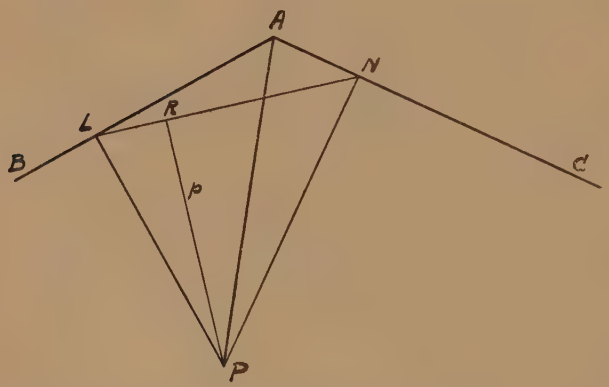

If the point is outside the circuit as at P′, it will be seen that two of the perpendiculars, p_2 and p_3, will be negative.

This result was obtained by Prof. Minchin from the consideration of the potential due to the equivalent magnetic shell, a more fundamental but less simple method than that given here, as it involves the rather troublesome calculation of the solid angle and the derivation of the magnetic force from the potential. Prof. Minchin also gave*, though without proof, a corresponding expression for the magnetic force at any point in the plane of a triangular coil, viz.,

$$i\left(\frac{\sin A}{p_1}+\frac{\sin B}{p_2}+\frac{\sin C}{p_3}\right),$$

* *Ibid.* Sept. 27, 1895.

where A, B, and C are the angles of the triangle, and p_1, p_2, and p_3 the perpendiculars from the given point on the lines joining the feet of the perpendiculars from the point on the sides.

But it can be easily shown that a similar expression holds for the magnetic force at a point in the plane of any rectilinear circuit.

For let BAC (fig. 3) be two adjacent sides of the circuit, PL and PN the perpendiculars on these two sides from the given point P, and PR the perpendicular on LN, the line joining the feet of these perpendiculars. Then the magnetic force at P due to the adjacent portions LA, AN of the circuit is

$$i\left(\frac{\sin \mathrm{APL}}{\mathrm{PL}}+\frac{\sin \mathrm{APN}}{\mathrm{PN}}\right).$$

But, since the points PLAN are concyclic, we have

$$\mathrm{PAL}=\mathrm{PNL} \quad \text{and} \quad \mathrm{PAN}=\mathrm{PLN}.$$

Hence

$$\sin \mathrm{APL}=\cos \mathrm{PAL}=\cos \mathrm{PNL},$$

and $$\sin \mathrm{APN}=\cos \mathrm{PAN}=\cos \mathrm{PLN}.$$

Thus the expression becomes

$$i\left(\frac{\cos \mathrm{PNL}}{\mathrm{PR}/\sin \mathrm{PLN}}+\frac{\cos \mathrm{PLN}}{\mathrm{PR}/\sin \mathrm{PNL}}\right)$$

$$=i\left(\frac{\sin \mathrm{PLN}\,.\cos \mathrm{PNL}+\sin \mathrm{PNL}\,.\cos \mathrm{PLN}}{\mathrm{PR}}\right)$$

$$=i\left(\frac{\sin \mathrm{PAN}\,.\cos \mathrm{PAL}+\sin \mathrm{PAL}\,.\cos \mathrm{PAN}}{\mathrm{PR}}\right)$$

$$=i\,\frac{\sin \mathrm{LAN}}{\mathrm{PR}}.$$

Hence, for the whole circuit, the magnetic force at P may be written

$$i\Sigma\frac{\sin \mathrm{A}}{p}.$$

The expressions for the rectangle and triangle are thus but particular cases of this more general theorem.

XVI. *A new Method of determining the Mobility of Ions or Electrons in Gases.* *By* R. J. Van de Graaff, B.Sc., *Queen's College, Oxford* *.

1. In many of the experiments that have been made to determine the velocity of ions or electrons in the direction of an electric force, the velocity that is measured is in some cases an upper limit of the mean velocity and in others a lower limit. This may be due to the fact that the velocities of all the ions are not the same, and also to the fact that a group of ions tends to diffuse in all directions. In order to avoid these and certain other difficulties I have devised a method for measuring the mean velocity of a group of ions moving in a gas under a steady and uniform electric force.

The principle of the method is the same as that used for the determination of the velocity of light by Fizeau, who employed a rotating toothed wheel as a periodic shutter to break up a beam of light into sections which travel a known distance and then again encounter the periodic shutter, which, depending on the time of arrival of the sections of the beam, either stops them or allows them to pass on. Thus the transmitted light may be observed as a function of the speed of rotation of the disk, and from this, taking into account the geometry of the apparatus, the velocity of light may be easily computed.

2. The apparatus used for the determination of the velocity of ions works in an analogous way. An oscillating potential in combination with grids gives the shutter effect corresponding with that of the rotating toothed wheel of Fizeau. The arrangement is shown diagrammatically in fig. 1. The plate A is maintained by the battery M at such a potential that a small glow-discharge is formed at the needle-point P, thus supplying to plate B ions of the sign whose velocity is to be measured. These, for the sake of clearness in description, may be assumed to be positive ions. Plates B, C, and D are provided, as shown, with central grids. The connexions to the batteries M and N maintain a steady potential of a few volts, opposing the passage of positive ions from plate B to plate C, and likewise from plate D to plate E. The plate E is connected to an electrometer for the measurement of the ionic current received through the

* Communicated by Prof. J. S. Townsend, F.R.S.

gas. As may also be seen from the diagram, the connexions through the batteries M and N furnish an electric field favouring the passage of positive ions from plate C to plate D, and between these plates are four equally-spaced rings connected to the resistance R, which is composed of a series of five equal high resistances. This arrangement provides, between plates C and D, a uniform field in which the velocity of positive ions is determined by measuring the time required for the ions to pass from plate C to plate D, a distance of 5 cm. It is evident then that, with no oscillating potential, positive ions cannot reach the plate E

Fig. 1.

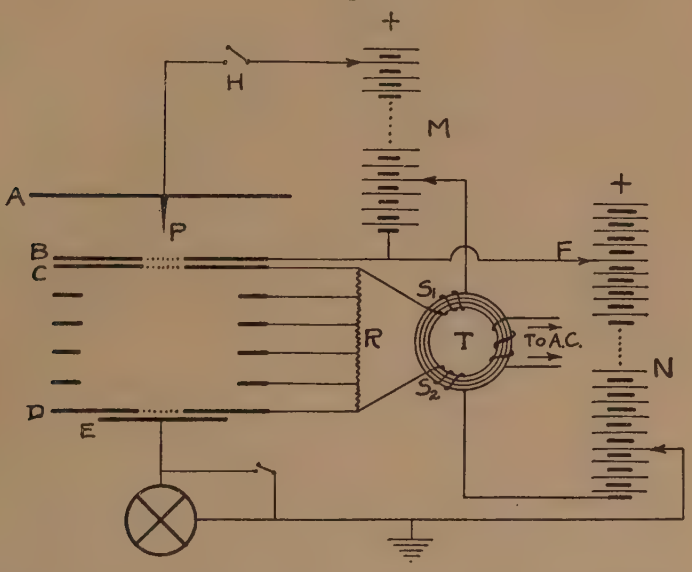

connected to the electrometer, as the forces in the space between plates B and C, and in the space between plates D and E, are in the contrary direction.

In order to reverse these forces momentarily and at regular intervals, an oscillating current is supplied to the primary of a transformer T with two secondaries, S_1 and S_2, which have the same number of turns and are wound in the same direction. A consideration of the connexions shown in fig. 1 shows that an oscillating potential is superposed over the steady potentials of the system of plates and rings connected to the resistance R. The connexions are arranged so that the potential of this system of plates and rings varies

as a whole, while the electric force between the plates C and D, where the velocity of the ions is determined, remains steady and is entirely unaffected by the oscillation. The oscillating potential is so adjusted that its maximum instantaneous value slightly exceeds the small, steady, opposing potentials between plates B and C and between plates D and E. Thus, when the oscillating potential is maximum negative, a group of positive ions will pass through the grid in plate B and on through the grid in plate C. After traversing the grid in plate C, the group moves under the action of the steady electric field with a uniform velocity toward plate D. If the group arrives at the grid of plate D when the oscillating potential is at its maximum positive value, some of the ions will pass through to the plate E and produce an electrometer deflexion. If, on the other hand, the group arrives at plate D when the oscillating potential is not near its maximum positive value, the ions will not pass through to plate E, but will be discharged on the grid of plate D. Thus it is seen that the current to the electrometer will be at a maximum when the velocity of the ions is such that the time required by a group of ions to pass from plate C to plate D is just equal to the time required for an odd number of half-cycles of the oscillating potential. Therefore the condition for a maximum current to the electrometer is that

$$W = \frac{d}{t} = \frac{2fd}{n} \quad . \quad . \quad . \quad . \quad . \quad . \quad (1)$$

where W is the velocity of the ions in the direction of the electric force ; d is the distance apart of the plates C and D ; t is the time of flight of the ions between the plates C and D ; f is the frequency of the oscillating potential ; and n is an odd integer representing the number of half-cycles elapsed during the time of flight of the ions from plate C to plate D. Thus the velocity of the ions in the electric field between the plates C and D may be found.

Laporte in some recent investigations * has used a method based on this principle, where a rotating wheel with a slit is used as a periodic shutter at each end of the space over which the ions are timed.

3. In order to simplify fig. 1 as much as possible, certain details of the apparatus are not shown. The connexions to the plates B, C, and D were provided with potentiometers for fine potential adjustment. Also a double switch was so

* M. Laporte, *Annales de Physique*, viii. p. 466 (Nov. 1927).

connected that in one of its positions the ends of the resistance R were connected as shown in fig. 1, while in the other position of the switch the ends of the resistance R were connected directly to the batteries M and N, and not through the secondaries of the transformer.

In taking the electrometer readings, the glow-discharge was first turned on by closing the switch H, then the oscillating potential was connected to the instrument for a definite period, say thirty seconds, by means of the double switch just described, after which the glow-discharge was turned off and the current to the electrometer measured by means of the induction-balance method due to Townsend, in which the insulated system connected to the electrometer is maintained at zero potential during the course of the experiment.

As a source of oscillating current for the primary of the transformer T, a small alternating generator of variable speed was used, the frequency being determined by means of a revolution counter.

The sides of the instrument, which was constructed principally of brass, were enclosed by a glass cylinder, the ends of which fitted into grooves in the end-plate A and in the base-plate. Both of these joints were coated on the outside by an elastic cement, which effectively rendered them air-tight, as was shown by the fact that the instrument gave no indication of a leak when pumped out to a pressure of 0·001 mm. of mercury and left for a period of several days.

The point P, at which the glow-discharge was obtained, was constructed by sharpening a nickel wire to a needle-point.

The principle of split insulation was used in insulating the plate E, which was connected to the electrometer. Glass insulation was used throughout in order to prevent the introduction of impurity by the evolution of occluded gases from the insulating material. The electrical leads from the various plates and rings were taken out through the base of the instrument by means of copper-glass joints, from one of which a glass side-tube led to the apparatus from which the supply of gas was obtained.

The principal dimensions of the instrument were as follows :—The diameter of the inner plates and rings was 7·5 cm. ; the distance from point P to plate B, 1·3 cm. ; from plate B to C, 0·36 cm. ; from plate C to D, 5·00 cm. ; and from plate D to E, 0·45 cm. For the construction of the grids, plates B and C were thinned at the centre to a thickness of 0·45 mm., and plate D to a thickness of

0·26 mm. In the middle of the plates a series of parallel cuts were sawed through the metal. These cuts were 0·60 mm. wide and were separated by strips of metal 0·36 mm. wide, and covered on each plate an area approximately circular and 2·1 cm. in diameter.

The gas used in the experiments was hydrogen, generated by the electrolysis of barium hydrate, and passed into the apparatus by diffusion through a heated palladium tube fused into the glass-work of the apparatus. Before each series of experiments was begun, the whole apparatus was washed out many times with hydrogen. A Toepler pump and a McLeod gauge were connected to the apparatus and were separated from the instrument by taps and a liquid-air trap to prevent the diffusion of mercury vapour into the instrument. A large glass tube was connected to the instrument in order to provide a space in which an electrodeless discharge could be formed. The spectrum of this discharge was observed at intervals with a small direct-vision spectroscope, and no lines due to impurities were seen.

4. The electrometer readings may be taken according to either of two plans. In the first method the readings corresponding to various values of the potential between plates C and D were taken, while the frequency of the oscillating potential was kept constant. In the second method the electrometer readings may be taken with different frequencies of the oscillating potential, while the field of force between plates C and D is kept constant. The second of these plans is not so convenient experimentally as the first, where, between the various readings, only the connexion F on the battery N is changed.

The experimental results obtained by the first method may be shown by a curve, where the electrometer current is plotted as a function of the voltage V between the plates C and D. Two examples of these curves for positive ions are given in figs. 2 and 3. The curve, fig. 2, represents the results obtained with hydrogen at 94 mm. pressure, and the curve, fig. 3, with hydrogen at 181 mm. Assuming for the moment that the velocity is proportional to the electric force, the time of flight t of the ions is inversely proportional at any point on the curve to the voltage V, the abscissa of the point. Thus, in passing along the curve from right to left, the increasing time of flight becomes successively equal, first to one-half cycle of the oscillating potential, then to three half cycles, then to five, etc., and in each case the current passes through a maximum value, in agreement with

equation (1) above. If V_1 is the value of the voltage at the first maximum, corresponding to $n=1$, then the successive maximums should occur at $1/3V_1$, $1/5V_1$, etc. Inspection of

Fig. 2.

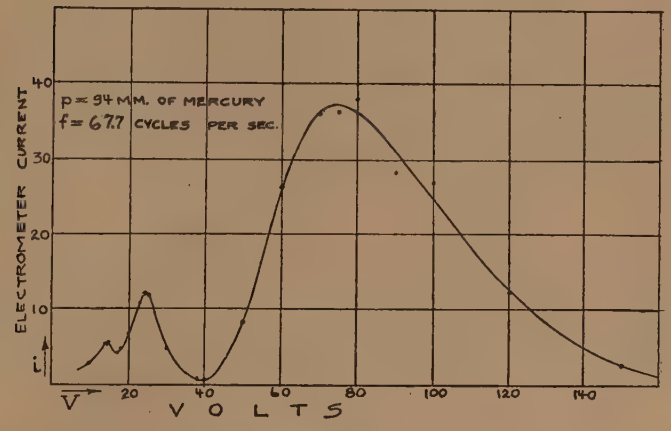

Fig. 3.

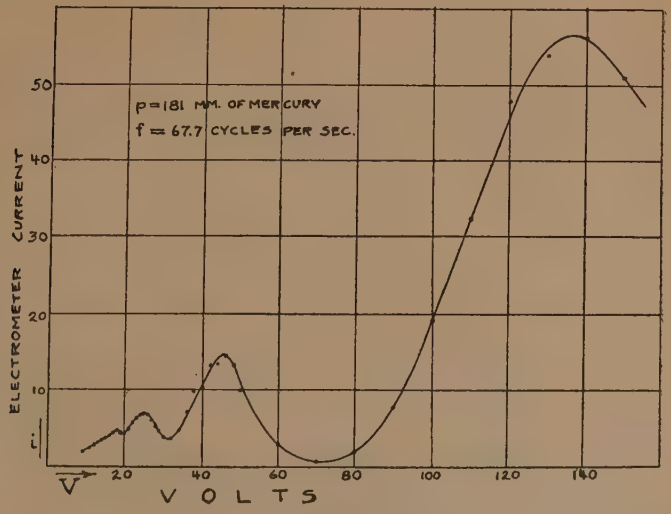

figs. 2 and 3 shows that this is the case within a few per cent., and the result confirms the assumption made above that the velocity of the positive ions is proportional to the electric force, within the range of the experiment.

As the origin is approached, it is seen that the maxima fall nearer and nearer together, until finally they become indistinguishable, due to diffusion and other causes. In fig. 3, for example, this occurs after the maximum corresponding to seven half cycles.

5. The velocities W of the ions may be found from the points of maximum current on the curves, the electric force being V/d. With hydrogen at 94 mm. pressure, the velocities W and the corresponding electric forces X obtained from the curve, fig. 2, are :—

W.	X.
677	14·8
226	4·84
135	2·96

With hydrogen at 181 mm. pressure, the values of W and X obtained from the curve fig. 3 are :—

W.	X.
677	27·2
226	9·04
135	5·00
96·7	3·60

If the mobility W_0 be defined as the velocity of the ions under an electric force of one volt per cm. in the gas at 760 mm. pressure, the velocity at the pressure p is

$$W = 760 \cdot W_0 \cdot \frac{X}{p}.$$

Using this relation, the values found for the mobility from the values of W_0 obtained with the two largest forces are 5·66 and 5·78 where the pressure was 94 mm., and 5·93 and 5·95 where the pressure was 181 mm. The mean of the above values gives $W_0 = 5·8$ cm. per second for positive ions in hydrogen.

The values obtained by different observers for the mobility of the positive ion in hydrogen vary, but most of these values lie between that of 5·34, obtained by Lattey and Tizard *, and that of 6·70 obtained by Zeleny †.

* R. T. Lattey & H. T. Tizard, Proc. Roy. Soc. A, lxxxvi. p. 349 (1912).

† J. Zeleny, Phil. Trans. A, cxcv. p. 193 (1900).

6. The method of determining mobilities described in this paper shows the presence of ions of a given velocity by a curve characterized by a series of maxima, whose sharpness and relative positions give a measure of the accuracy and reliability of the results. The accuracy of the experiments is not appreciably affected by diffusion and space-charge, as these tend not to shift the positions of the maxima, but merely to make them less sharp. The method is adapted to the investigation of cases where there may be present in the gas different kinds of ions having different velocities. Each kind of ion would then be shown by a separate series of maxima whose abscissæ would show the velocity and whose ordinates would show the relative number of ions of that kind.

The alternating-current generator used in the present experiments can be replaced by a valve oscillator capable of supplying potentials of higher frequency, which could be used to extend this method of investigation to the determination of the large velocities of free electrons, or of positive ions in gases at low pressures.

7. In conclusion, I have much pleasure in expressing my gratitude to Professor Townsend for his constant advice and inspiration throughout the course of this research.

XVII. *On the Magnetic Susceptibilities of Electronic Isomers.*—Part II.

By Professor S. S. Bhatnagar, *D.Sc.(Lond.)*, *and* R. N. Mathur, *M.Sc.**

IN a previous paper in this Journal †, S. S. Bhatnagar and C. L. Dhawan gave an empirical equation which was found to give remarkably satisfactory results for the diamagnetic susceptibilities of some twenty electronic isomers. According to this equation

$$x_m = -2{\cdot}85 \times 10^{10} \times (\mathrm{KR})^2, \quad . \quad . \quad . \quad . \quad (1)$$

where

x_m = molecular diamagnetic susceptibility.

R = radius of the molecule calculated on the assumption of closest packing of the atoms constituting the molecule, by using Bragg's data for the diameter of atoms ‡. (A complete account is given in the paper referred to above.)

* Communicated by the Authors.

† Phil. Mag. [7] v. p. 536 (1928).

‡ W. L. Bragg, Phil. Mag. xl. p. 169 (1920).

And K=an arbitrary constant, but which in a series of isomers is found to exhibit variations with the number of atoms in the isomers. (Its significance was considered in the paper referred to above, and has again been considered later on in this paper.)

According to Langevin's theory of atomic diamagnetism

$$\chi_{\text{At.}} = -\frac{e^2}{4mc^2}\Sigma_n \bar{r}^2, \quad \ldots\ldots \quad (2)$$

the summation being extended over the n electrons in the atom, and $\bar{r}^2$ being the mean square of the radius of the projected orbit in a plane perpendicular to the field. Multiplying (2) by Avagadro's number, we get

$$\chi_{\text{A}} = -\frac{e^2 \text{N}}{4mc^2}\Sigma_n \bar{r}^2.$$

And on substituting the values of constants in the equation, we get

$$\chi_{\text{A}} = -2{\cdot}85 \times 10^{10}\Sigma_n \bar{r}^2. \quad \ldots\ldots \quad (3)$$

The resemblance between our empirical equation (1) and (3) is remarkable, but while (R^2) in (1) gives the square of the radius of the molecule, $(\bar{r}^2)$ in (3) is the mean square of the radius of the projected orbit in a plane perpendicular to the field. In order to make the resemblance closer, we take in (3) the mean square of the radius of the orbit itself, instead of the mean square of the radius of the projected orbit. If r_1 (components x_1, y_1, z_1) is the distance of an electron from the nucleus, then for an atom symmetrical in the sense that

$$\bar{x}_1^2 = \bar{y}_1^2 = \bar{z}_1^2,$$
$$\Sigma\bar{r}^2 = \tfrac{2}{3}\Sigma\bar{r}_1^2.$$

and equation (3) then becomes

$$\chi_{\text{A}} = -2{\cdot}85 \times 10^{10} \times \tfrac{2}{3}\Sigma\bar{r}_1^2, \quad \ldots\ldots \quad (4)$$

and equation (1) can be written as

$$\chi_m = -2{\cdot}85 \times 10^{10} \times \tfrac{2}{3} K\text{R}^2, \quad \ldots\ldots \quad (5)^*$$

where $$K = \tfrac{2}{3}(\text{K})^2.$$

The resemblance between Langevin's equation (4) and our empirical equation (5) is now closer than that between

* Equation (3) employed in the previous paper to this Journal has been modified to equation (5) in order to facilitate the theoretical interpretation of the values of K on the Langevin's concept of the theory of diamagnetism.

equations (1) and (4), and shows the significant fact that instead of extending the summation over all the electrons in the isomer, it has to be extended only over a fraction of them, given by the value of the constant K. It has been noted by several workers * that, in order to make the equation of Langevin applicable to all atoms, an effective value of n may have to be taken, and hence the constant K in our equation (whose value is different from n, and in the case of isomers of high values of n, much less than n) assumes particular significance. In this investigation the values of the diamagnetic susceptibilities of over twenty electronic isomers have been experimentally determined, and equation (5) is found to be applicable in all cases.

The apparatus used to determine the diamagnetic susceptibilities is Wilson's modification of Curie's Balance. The substance contained in a small glass tube, attached to a light aluminium system, is suspended in a non-homogeneous magnetic field by a thin silver ribbon. The force exerted by the field is balanced by the torsion of the supension, and read off from a graduated torion-head. A complete description of the experimental arrangement is given in a paper shortly to be communicated. The susceptibilities of the substances are calculated by the formula†

$$x = \frac{1}{M}\left[x_a M_a + (x_w m_w - x_a m_a)\frac{D - D_1}{D_2 - D_1}\right]$$

where x = susceptibility of the specimen.
M = mass of the specimen in grams.
x_a = specific susceptibility of air (210×10^{-7}).
M_a = the mass of air filling the same volume as the specimen.
x^w = the specific susceptibility of water ($-7{\cdot}25 \times 10^{-7}$).
m_w = mass of water filling the same volume as the specimen.
m_a = mass of air filling the same volume as water.
D = torsion due to specimen-tube + specimen.
D_1 = torsion due to specimen-tube alone.
D_2 = torsion due to specimen-tube + water.

Before determining the susceptibilities of the substances given in this investigation, substances of known susceptibility were used, and the results obtained were within the limit of the experimental error.

The radii of the isomers used in this communication, calculated according to the method given in the previous

* Stoner's 'Magnetism and Atomic Structures,' Chap. 14.
† Oxley, Proc. Roy. Soc. A, ci. pp. 264–279.

paper to this Journal, are given in Table I. and the remaining results in Tables II. and III. :—

TABLE I.

Substance.	Radius in Å.
$BaCl_2$	2·183
$CaBr_2$	1·876
*KI	3·475
*CsCl	3·425
Ethyl acetate	1·357
Butyric acid	1·357
*NaCl	2·825
*CaO	2·350
Methyl acetate	1·263
Propionic acid	1·263
*AgCl	2·825
*BaO	2·750
Anisol	1·532
Benzyl alcohol	1·532
$CaSO_4$	1·922
K_2CO_3	2·675
Cresol	1·532
Phenyl hydrazine	1·505
Toluidine	1·534
Methyl aniline	1·534
*NaF	2·450
*MgO	2·075
Isobutylaldehyde	1·305
Methyl ethyl ketone	1·305
Phenyl acetate	1·620
Methyl benzoate	1·620
Ethyl aniline	1·601
Dimethyl aniline	1·601
TeH_2O_3	1·471
$ZnSO_4$	1·051
Glycerine	1·323
Aniline	1·460

* In the case of substances marked with * the radii have been obtained by summation of the radii of the atoms. This is as it should be.

In Table II. the results obtained by calculation from equation (5) are tabulated against the experimental values, some of which are taken from the Physico-Chemical Tables of Landolt and Börnstein, and some determined experimentally.

TABLE II.

*Atomic number.	Names.	$-x_m \times 10^6$. Experimental.	$-x_m \times 10^6$. Calculated on equation (5).
28	NaCl	23·98	22·94
28	CaO	15·12	15·74
64	BaO	18·4	21·55
64	AgCl	40·13	31·99
20	NaF	11·76	10·95
20	MgO	6·73	7·83
68	K_2CO_3	76·02	81·57
68	$CaSO_4$	51·73	43·00
72	CsCl	47·12	48·94
72	KI	51·46	50·35
78	TeH_2O_3	33·72	33·68
78	$ZnSO_4$	43·58	42·44
40	Methyl acetate	39·78	41·8
40	Propionic acid	43·83	41·8
48	Ethyl acetate	59·7	60·4
48	Butyric acid	61·13	60·42
58	Anisol	72·79	72·79
58	Benzyl alcohol	67·60	72·79
58	Cresol	71·17	72·79
58	Phenyl hydrazine	67·82	70·21
58	Toluidine	88·69	73·00
58	Methyl aniline	82·74	73·00
40	Isobutylaldehyde	47·45	47·56
40	Methyl ethyl ketone	47·45	47·56
72	Methyl benzoate	83·23	82·9
72	Phenyl acetate	82·69	82·9
66	Ethyl aniline	89·3	89·4
66	Dimethyl aniline	89·66	89·4
50	Glycerine	56·12	53·3
50	Aniline	65·1	65·1

* The atomic number in the case of compounds has been taken to mean the sum of the atomic numbers of the elements in the compound.

Significance of K employed in equation (5).

K is an arbitrary constant. Its value for every two isomeric molecules is the same, as shown in Table III., where the values of K have been assembled together with the atomic numbers and the number of atoms in the isomers :—

TABLE III.

No. of atoms.	Atomic number.	Substance.	Value of K.
2	20	NaF	0·96
2	20	MgO	0·96
2	28	NaCl	1·5
2	28	CaO	1·5
2	64	AgCl	2·1
2	64	BaO	2·1
2	72	CsCl	2·2
2	72	KI	2·2
6	68	$CaSO_4$	6·0
6	68	K_2CO_3	6·0
6	78	TeH_2O_3	8·194
6	78	$ZnSO_4$	8·194
11	40	Methyl acetate	13·79
11	40	Propionic acid	13·79
13	40	Isobutylaldehyde	14·7
13	40	Methyl ethyl ketone	14·7
14	48	Ethyl acetate	15·32
14	48	Butyric acid	15·32
14	50	Glycerine	16·04
14	50	Aniline	16·04
16	58	Anisol	16·305
16	58	Benzyl alcohol	16·305
16	58	Cresol	16·305
16	58	Phenyl hydrazine	16·305
17	58	Toluidine	16·32
17	58	Methyl aniline	16·32
18	72	Methyl benzoate	16·44
18	72	Phenyl acetate	16·44
20	66	Ethyl aniline	18·34
20	66	Dimethyl aniline	18·34

A close examination of the above table shows three significant relations between the values of K:—

(*a*) The values of K increase with the number of atoms contained in the molecule. For example, in the case of molecules having three atoms the value of K is 2·5. For molecules having 13 atoms it is 14·7, and for molecules having 20 atoms it is as great as 18·34.

(*b*) The values of K for every two isomeric molecules are the same.

(*c*) In the case of groups of isomers having the same number of atoms in the molecule, the values of K increase with the atomic numbers of the groups. For example ($CaSO_4$ and K_2CO_3) and (TeH_2O_3 and $ZnSO_4$) are two groups of isomers having the same number of atoms (six) in the molecule but having different atomic numbers, 68 and 78 respectively. And the value of K in the latter group is greater than that in the former. Similar relations also exist between the groups of isomers having 2 and 14 atoms in the molecule.

Most of the experimental data have been taken from the unpublished work of Messrs. C. L. Dhawan and S. L. Luthra, to whom our thanks are due.

The values of K for the isomorphous series given in Table V. in the previous paper (Phil. Mag., March 1928, vol. 5, No. 29) have not been discussed in this paper on account of the doubtful purity of these substances.

University Chemical Laboratories,
University of the Punjab,
Lahore, India.
23rd February, 1928.

XVIII. *Frequency Variations of the Triode Oscillator. A Reply to Lieut.-Col. Edgeworth, D.S.O., M.C., A.M.I.E.E.*

By David F. Martyn, *B.Sc., A.R.C.Sc.**

IN the April number of the Philosophical Magazine there appears a note by Lieut.-Col. K. E. Edgeworth under the above title, referring to a previous paper of mine (Phil. Mag., Nov. 1927), also with the same title. Edgeworth remarks that it is obvious that I must have overlooked his

* Communicated by Prof. E. Taylor Jones, D.Sc.

previous paper on "Frequency Variations in Thermionic Generators," read before the Institute of Electrical Engineers (Wireless Section) on 6th January, 1926. He further claims that "So far as they cover the same ground, the experimental results appear to be in agreement, and the explanations offered are substantially the same. The main cause of frequency variations is associated with damping of one sort or another in the grid circuit, and, other things being equal, the magnitude of the frequency variation is proportional to the amount of damping. This type of frequency variation is referred to in my paper as a frequency variation of the first type."

At the outset I may state that I had read Edgeworth's paper before writing my own, although I did not see occasion to refer to it. Chief among my reasons for not doing so is the fact that the causes of frequency variation considered by Edgeworth in his paper are totally incapable of explaining the large frequency variations which I obtained. Indeed, investigation of Edgeworth's experimental results, and comparison with those of others, has led me to the conviction that his own results, as well as those of others, are explained completely by the grid current theory developed in my paper, and that the four causes of frequency variation considered by Edgeworth are of very minor importance.

It has been realized for a number of years that the frequency of the triode oscillator was not exactly $\frac{1}{2\pi\sqrt{L_1C_1}}$, but depended to some extent on the values of the anode and filament voltages of the triode and on the coupling between the coils. The extent of the frequency variation has been found to be, at most, 3 per cent. Several experimental investigations of these frequency variations were made, notably by Eccles and Vincent *: but, in spite of the great importance of the subject, both in wireless technology and in the laboratory, no attempted theoretical explanation was published until Edgeworth's paper appeared in March 1926. In October 1926, while using the simple "tuned-anode" oscillator, but with abnormal values for the coil inductances and the condenser capacity, I obtained extremely large variations of frequency, extending over several octaves, when the filament current or anode voltage of the valve was altered. In order to explain these effects I developed a mathematical theory of the oscillator which took account of the flow of grid current in the valve. By the aid of this

* Proc. Roy. Soc. xcvi. & xcvii. (1920).

theory, as described in my previous paper, I succeeded in explaining every type of frequency variation which I observed. It is Colonel Edgeworth's claim that the theory which he had put forward is capable of explaining these large frequency variations. We shall now proceed to analyse the four causes of frequency variation which he considered.

(1) The first cause of frequency variation is said to be due to "grid damping" *when there is a condenser across the grid coil.* Equations are developed giving the extent of the frequency variation. This is the cause of frequency variation which Edgeworth specifically claims to be capable of explaining the large frequency variations which I observed. In my experiments there was no condenser across the grid coil. On putting $C_2=0$ in Edgeworth's equation (no. 8 in the paper) we find the frequency at once reduces to $\frac{1}{2\pi\sqrt{L_1C_1}}$, so that *no frequency variations whatever occur!* Even if we allow for a considerable self-capacity in the grid coil, the frequency variation predicted by Edgeworth's theory is exceedingly small, and quite inadequate to explain the variations which I obtained experimentally.

(2) The second cause of frequency variation only applies when a "tuned-grid" oscillator is used, and hence need not be further considered.

(3) The third cause of frequency variation is due to the presence of resistance in the anode coil. This, however, has been previously worked out by Eccles *, and I have shown that it is much too small to account for the frequency variations which I observed.

(4) An effect due to harmonics, as worked out by Appleton and Greaves †. This effect also I have considered in my paper, and have shown to be exceedingly small and unimportant.

Summing up, then, we see that none of the four causes of frequency variation put forward by Edgeworth is capable even of explaining a frequency variation which in any way approaches the order of magnitude observed by Eccles and Vincent. Still less can they explain the very large frequency changes which I obtained. The correct magnitude of frequency variation is at once obtained, however, from the

* Proc. Phys. Soc. xxxi. (1919).
† Phil. Mag. xlv. (1923).

equations which I have put forward, based solely on the flow of grid current. It is a remarkable fact that, although from the text of his paper, Edgeworth appears to have realized that grid current was a factor of importance, yet in his theoretical treatment of the subject he has neglected it almost entirely, only considering it in the very minor role of introducing damping into an oscillatory grid circuit.

Edgeworth further suggests that the magnitude of the frequency variation can be increased indefinitely merely by increasing the "grid damping." Such procedure, however, merely results in the cessation of oscillations. The order of magnitude of the frequency variations which can be obtained with a given valve depends entirely upon the values of the ratios $\frac{L_1}{C_1}$, $\frac{L_2}{L_1}$, $\frac{M}{L_1}$, as worked out in my paper under the heading "Conditions for Maximum Frequency Variation."

A careful comparison of the experimental results which I have obtained working with large variations at low frequencies, with those of other investigators working with small variations at high frequencies, has revealed the fact that there are no essential differences, other than magnitude, between the results. Since the theory based on grid current has been completely successful in explaining all my experimental results, there is every reason to believe that the same theory provides the explanation of all the frequency variations to which the oscillator is subject. In other words, when the resistances present are not large, and the frequency is not too high, *by far the most important cause of frequency variation is the flow of grid current, and all the types of variation which have been observed experimentally may be traced to this effect.*

One important consequence of this fact is that if we can succeed in eliminating grid current from the oscillator, then it should be possible to attain a frequency which will possess a very high degree of constancy. Previous experiments on the attempted elimination of grid current, described in my former paper, suggested that this was a difficult if not impossible matter. These experiments sufficed to indicate that the elimination of grid current was a problem which could not be solved merely by increasing the negative bias on the grid, the method usually recommended *. To test the possibility of having zero grid current in any particular circumstances, a series of measurements were made for the purpose of plotting V^2 (the square of the peak voltage across

* Moullin, 'Radio-Frequency Measurements,' p. 7.

the anode coil L_1) against I_g (the total grid current). If it is impossible to have the grid current zero, then we should expect these curves to pass through the origin. If, on the other hand, zero grid current is a possibility, then we should expect the curves to intersect the V^2 axis.

Some of the curves obtained showed a definite tendency towards cutting the V^2 axis, thus indicating that zero grid current was possible in these particular cases, while oscillations were occurring. An extensive series of observations were then made in order to find the best conditions for the elimination of grid current. The results may be summarized as follows :—

(1) The high tension voltage should be as large as the valve can take without damage.

(2) The coupling between the coils L_1 and L_2 must not be too loose.

(3) The negative bias on the grid should be as large as possible.

(4) The filament current should be as low as possible.

(5) The inductance of the coil L_2 should be small.

In practice, the best method of procedure is first to set (1), (2), and (5) to appropriate values. Next the filament current is gradually reduced until oscillations cease. The value of (3) is then readjusted until oscillations recommence. The filament current is again reduced, and the same procedure followed repeatedly until the filament current is so low that oscillations will only occur for a very small range of grid bias variation. With the oscillator so adjusted, the filament current may be varied over an appreciable range without causing grid current to flow. This range decreases as the coupling is decreased. An improvement in the elimination of grid current is effected by inserting a small condenser in series with the grid coil L_2. This condenser was found to increase the range of variation of filament current over which no grid current flowed. It acted by automatically adjusting the grid bias. Thus if the filament current was such as to cause a small current to flow to the grid, the condenser charged up negatively and so stopped the flow of grid current.

The conditions for the elimination of grid current having been determined, an oscillator was specially designed and set up, in order to find out how constant the frequency would be in these circumstances. In order to keep the high

frequency resistance of the coils low they were wound with Litzendraht wire. This wire is made up of a large number of well insulated strands. The two coils were wound on two ebonite cylinders of different sizes, so that one could be inserted inside the other, thus ensuring a close degree of coupling. The grid coil was several times smaller than the coil in the plate circuit. A small condenser of capacity 0·001 mfd. was inserted in series with the grid bias battery. The oscillator was adjusted in the manner described above, and the grid current eliminated. A quartz oscillator was set up, producing oscillations of a frequency very near to that of the valve oscillator. The two oscillators were loosely coupled by means of a single loop of wire in series with a pair of head telephones. A note of audible frequency was heard in the telephones. The frequency of this note could be determined by means of a monochord. In this manner a very small change of frequency of the valve oscillator could be measured. It was found that the frequency remained constant to one part in 100,000 *even when the filament current was deliberately varied*, so long as no grid current flowed. When the filament current remained steady, the frequency was, of course, constant to a much higher degree. There is no doubt that an oscillator so designed provides a source of frequency which is considerably more constant than that which is obtained from any of the complicated constant frequency circuits designed by Fromy * and others.

The only disadvantage is that the power generated is very low, but this, of course, is of little moment when the oscillator is to be used for heterodyne purposes, or as a master oscillator. For the purpose of making accurate physical measurements, the triode oscillator, with grid current eliminated, should be of great value.

The experimental work described above was carried out in the Research Laboratories of the Natural Philosophy Department of the University of Glasgow, with much appreciated financial assistance from the Department of Scientific and Industrial Research. I am greatly indebted to Professor E. Taylor Jones for much helpful advice and encouragement.

April 1928.

* *L'Onde Electrique*, 4e année, p. 433 (1925).

XIX. *On Hamilton-Jacobi's Differential Equation in Dynamics.*

To the Editors of the Philosophical Magazine.

GENTLEMEN,—

I HAVE just read Prof. J. Kunz's article "A Note on Hamilton-Jacobi's Differential Equation in Dynamics" in the January issue of your Magazine. I should like to remark that it has caused me (and probably many others of your readers) mild surprise. Unless I am mistaken, Prof. Kunz regards his manner of deriving Lagrange's equations, the equation of energy, and the Hamilton-Jacobi equation, as purely original, whereas it is surely already well known—granted the condition which Prof. Kunz should have (but has not) proved, viz., that

$$\int (\mathrm{E}_k - \mathrm{E}_p)\, dt = \int f(t, q_1, \ldots q_n, \dot{q}_1, \ldots \dot{q}_n)\, dt$$

is stationary along the actual trajectory, as compared with adjacent ones. This is easily shown by using the equations

$$(\ddot{x}, \ddot{y}, \ddot{z}) = -\partial \mathrm{E}_p / \partial (x, y, z). \quad . \quad . \quad . \quad . \quad (1)$$

Now any text-book on the Calculus of Variations (*vide* Williamson's 'Integral Calculus,' pp. 430, 437, *et seq.*, or Whittaker, 'Analytical Dynamics,' pp. 266, 267) proves that the condition that

$$\int_{t_1}^{t_2} f(t, q_1, \ldots q_n, \dot{q}_1, \ldots \dot{q}_n, \ddot{q}_1, \ldots \ddot{q}_n, \ldots)\, dt,$$

is stationary are

$$0 = \frac{\partial f}{\partial q_r} - \frac{d}{dt}\left(\frac{\partial f}{\partial \dot{q}_r}\right) + \frac{d^2}{dt^2}\left(\frac{\partial f}{\partial \ddot{q}_r}\right) - \frac{d^3}{dt^3}\left(\frac{\partial f}{\partial \dddot{q}_r}\right) + \ldots \quad (r = 1, \ldots n)$$

together with certain terminal equations. In particular, if f contain derivatives of the q's of order no higher than the first

$$0 = \frac{\partial f}{\partial q_r} - \frac{d}{dt}\left(\frac{\partial f}{\partial \dot{q}_r}\right) \quad (r = 1, 2, \ldots n). \quad . \quad . \quad (2$$

Moreover, if f is quadratic in the $\dot{q}_r$, then

$$\frac{df}{dt} = \frac{\partial f}{\partial t} + \Sigma\left(\dot{q}\frac{\partial f}{\partial q} + \ddot{q}\frac{\partial f}{\partial \dot{q}}\right), \quad \ldots\ldots \quad (3)$$

$$= \frac{\partial f}{\partial t} + \Sigma\left\{\dot{q}\frac{d}{dt}\left(\frac{\partial f}{\partial \dot{q}}\right) + \frac{d\dot{q}}{dt}\cdot\frac{\partial f}{\partial \dot{q}}\right\} \quad \text{by (2)},$$

$$= \frac{\partial f}{\partial t} + \frac{d}{dt}\left(\Sigma\dot{q}\frac{\partial f}{\partial \dot{q}}\right),$$

and if $\partial f/\partial t$ vanishes we have at once that

$$f - \Sigma\dot{q}\frac{\partial f}{\partial \dot{q}} = \text{constant}$$

is an integral, the so-called integral of energy. These results and also the method of their derivation are, I expect, familiar not only to all applied mathematicians but also to those who deal in the Calculus of Variations. So also will be the fact that

$$\mathrm{S} = \int(\mathrm{E}_k - \mathrm{E}_p)\,dt$$

is a solution of the Hamilton-Jacobi equation

$$0 = \mathrm{H}(q, \partial\mathrm{S}/\partial q) + \partial\mathrm{S}/\partial t.$$

(For all these results see, for example, Whittaker, 'Analytical Dynamics,' §§ 41, 143; Plummer, 'Dynamical Astronomy,' §§ 123, 128; Birtwistle, 'Quantum Theory of the Atom," §§ 33, 34, 35, 39; Williamson, *loc. cit.* §§ 287, 292.)

Incidentally, there is an error in an important equation of Prof. Kunz. Instead of

$$\frac{d}{dx}\left(f - \Sigma y_r'\frac{\partial f}{\partial y_r'}\right) = \frac{\partial f}{\partial x} + \Sigma y_r'\frac{\partial f}{\partial y_r} - \Sigma\left\{y_r''\frac{\partial f}{\partial y_r'} + y_r'\frac{d}{dx}\left(\frac{\partial f}{\partial y_r'}\right)\right\}$$

it should obviously read on the right-hand side

$$\frac{\partial f}{\partial x} + \Sigma\left(y_r'\frac{\partial f}{\partial y_r} + y_r''\frac{\partial f}{\partial y_r'}\right) - \Sigma\left\{y_r''\frac{\partial f}{\partial y_r'} + y_r'\frac{d}{dx}\left(\frac{\partial f}{\partial y_r'}\right)\right\}$$

$$= \frac{\partial f}{\partial x} + \Sigma y_r'\left\{\frac{\partial f}{\partial y_r} - \frac{d}{dx}\left(\frac{\partial f}{\partial y_r'}\right)\right\}$$

as in (3), though this mistake is corrected in the next equation.

97 Thornbury Road,
Osterley Park, Middx.
Feb. 28, 1928.

Yours faithfully,
ARTHUR J. CARR.

XX. *Optically Excited Iodine Bands with Alternate Missing Lines.* *By* Prof. R. W. Wood, *For.Mem.R.S., The Johns Hopkins University, and* Prof. F. W. Loomis, *New York University* *.

[Plate II.]

THIS paper is a report of some direct experimental evidence that, as predicted by the wave mechanics, the rotational states of symmetrical molecules are divided into two classes between which transitions do not occur. These classes of states are those whose eigen-functions are respectively symmetrical and anti-symmetrical in the positional coordinates of the nuclei. The evidence has been obtained as the result of improvements in the technique of exciting iodine fluorescence.

It was shown by R. W. Wood in 1910 [1] that if iodine vapour *in vacuo* is excited by monochromatic radiation—for example, the green mercury line,—the vapour emits a series of close doublets, 27 or more in number, spaced at nearly equal intervals on a frequency scale, the first doublet occurring at the wave-length of the mercury line, and the last in the remote red, brought out only by photography with a dicyanine plate. In 1920, when the methods of the Bohr theory of atomic spectra were first successfully applied to band spectra, Lenz [2] showed that this series of doublets was unmistakable evidence for the selection principle for rotational quantum numbers, $j'-j''=\pm 1$, whose introduction was the essential new step in the theory.

The accepted [3] explanation of this series of fluorescent doublets is briefly as follows. All the iodine molecules which happen to absorb the narrow green mercury line are thereby lifted into one definite state, which happens to be $n'=26, j'=34$. Since the molecular vibration is anharmonic, the correspondence principle permits return transitions to any vibrational quantum number n''. Thus the doublet which coincides with the green line (the zero-order doublet) corresponds to the vibrational transition $26\rightarrow 0$, the first-order doublet to $26\rightarrow 1$, etc. The possible values of the final rotational quantum number j'' are, however, strictly limited by the selection principle, $j''=j'\mp 1$, to $j''=33$ or 35, and these correspond to the two members of each doublet. That is, the fluorescent series is picked out of the very complex emission spectrum by the limitation to a single excited state, and consists of one line from the R branch ($j''=j'-1$), one

* Communicated by the Authors.

line from the P branch ($j''=j'+1$) of each band having $n'=26$.

If a little inert gas, say helium, is added to the iodine vapour, it was found by Wood and Franck that the fluorescent spectrum was enriched. The bands to which the doublets belong are apparently completely developed, and new bands corresponding to adjacent values of n' appear on each side of them. Obviously the iodine molecules, while in the excited state, make collisions of the second kind with helium atoms and undergo changes of n' and j', the result being that there is no longer a single initial state for the emission of the fluorescent light, but a group of vibrational and rotational states clustering about the original one. The bands represent transitions from all these states.

These bands are the subject of the present study. In order to be able to photograph them with a spectrograph of much higher resolution than heretofore, the iodine fluorescence is excited with a battery of four vertical Cooper Hewitt glass mercury lamps which gives a very powerful stimulation of the vapour. The lamps are arranged close together on a single stand, with just room enough between them for the vertical glass tube containing the iodine vapour. They are started by an auxiliary, by simply closing a switch, which is far more convenient than the older arrangement in which the lamp was lighted by tipping. The iodine tubes are about 50 cm. in length by 5 cm. in diameter, blown out at the top in the form of a thin clear bulb, and drawn off obliquely at the bottom, to prevent reflexion and secure a good background. The oblique cone at the bottom is painted black on the outside. With this arrangement it is possible to secure photographs in the second-order spectrum of a 6-inch plane grating with a lens of over 3 metres focus in about 15 hours.

Pl. II., fig. *a*, shows the spectrum obtained when the iodine is in the presence of helium at $\frac{1}{2}$ mm. pressure. The vibrational transition corresponding to each band which is brought out is marked at the head of the band. It will be noted that the bands with $n'=26$, that is, those containing the doublets, are strongest; those with $n'=25$ and $n'=27$ are fainter; those with $n'=24$ and $n'=28$ are very faint, and none are apparent with other values of n'. This means that most of the excited molecules which undergo collisions of the second kind suffer no change in n'; some have n' changed by 1, a few by 2, and hardly any by more than 2.

Much larger changes take place in the rotational quantum number, as is shown by the development of the bands to some distance on each side of the doublets. But a more

interesting point, and the one with which we are here chiefly concerned, is that these bands contain fewer lines, in any given region, than the corresponding absorption bands. For instance, on Pl. II., figs. *b* and *e*, which are enlargements of the (26, 1) and (26, 3) bands in fig. *a*, and still more distinctly in figs. *c* and *f*, which were made in the third-order spectrum, it is plain that there are only two lines within the doublets; whereas Loomis's analysis [4] of the absorption spectrum shows that there are actually ten absorption lines in this region, five on the R branch and 5 on the P branch. Compare fig. 1, the upper part of which is a Fortrat diagram of the (26, 1) band, and in which the circles, both full and

Fig. 1.

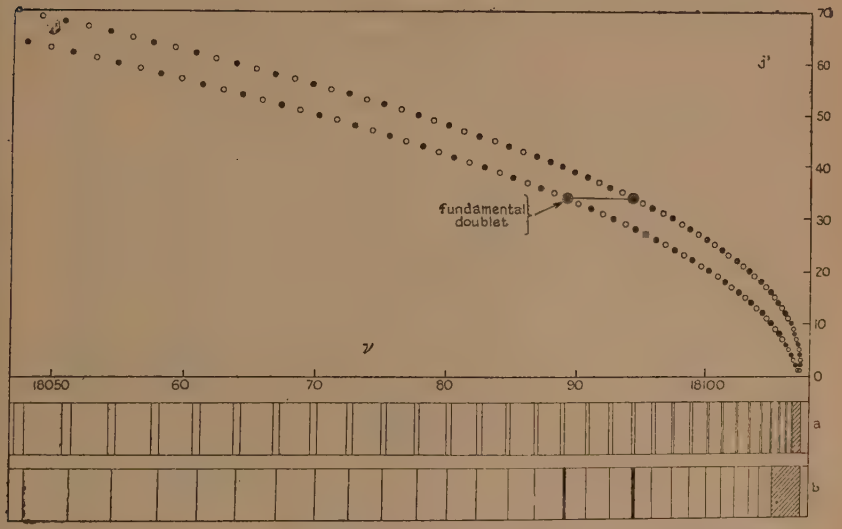

Above is a Fortrat diagram of the (26, 1) absorption band. Lines with even j' are indicated by solid circles, those with odd j' by hollow circles. (*a*) is a plot of the absorption lines having even values of j'. (*b*) is a plot of the centres of the lines of the fluorescent band as it appears when iodine is mixed with helium at 4 mm. pressure.

hollow, represent absorption lines. It happens that this band has not been measured in absorption, but its lines can be accurately calculated, by the combination principle, from those of the bands (26, 0), (29, 1), and (29, 0), which have been measured. The relation between the fluorescence and absorption bands is shown in the lower part of fig. 1. Here the upper spectrum has been obtained by pro-

j' (*i. e.*, those represented by full circles); while the lower is a plot of the centres of the lines of the same (26, 1) band as it appears in fluorescence. Clearly, the fluorescence lines correspond exactly to the absorption lines with even j', and the alternate lines are missing in the fluorescence band. It is true that each line in the R branch happens to lie so close to a line in the P branch that they are not quite resolved; but the spectra show plainly that the fluorescent lines far from the head are becoming broader. A special grating was therefore ruled for the work, exceptionally bright in the third-order spectrum. Only one or two satisfactory photographs have been made up to the present time, owing to troubles with the thermostat, for a more exact temperature control of the grating was necessary in this case. Pl. II., fig. *f*, shows the band associated with the third-order doublet (26, 3), the lines indicated by arrows being clearly resolved. The lines of the third-order doublet are 1·67 Å.U. apart, and the separation of the closest doublets marked by arrows is about 0·1 Å.U.

The lines marked by dots are "ghosts" of the strong doublet, and some of the lines correspond to weak doublets, which appear also when the iodine is *in vacuo*. They are "main" doublets due to the stimulation of fainter absorption lines, which lie within the region covered by the green mercury line. The band (25, 3) photographed in the third-order spectrum is reproduced in Pl. II., fig. *d*.

Table I. shows the correspondence between the frequencies of the lines of the (26, 1) band in absorption and fluorescence.

Table I.

Band (26, 1) in absorption.					In fluorescence.	
R branch.		P branch.		Average.		
j'.	ν.	j'.	ν.	ν.	ν.	Intensity.
head	18107·43	—	—	—	18107·4	—
16...	18105·02	10	18105·13	18105·08	05·2	2
17...	04·66	11	04·77			
18...	04·26	12	04·39	04·32	04·2	3
19...	03·80	13	03·95			
20...	03·39	14	03·50	03·44	03·4	3
21...	02·91	15	03·03			
22...	02·42	16	02·56	02·49	02·3	2
23...	01·87	17	01·95			
24...	01·32	18	01·48	01·40	01·3	4
25...	00·74	19	00·98			

TABLE I. (*continued*).

Band (26, 1) in absorption.					In fluorescence.	
R branch.		P branch.		Average.		
j'.	ν.	j'.	ν.	ν.	ν.	Intensity.
26 ...	00·14	20	00·32	00·23	00·1	4
27 ...	18099·50	21	18099·74			
28 ...	98·83	22	99·05	18098·94	18098·8	10
29 ...	98·19	23	98·39			
30 ...	97·46	24	97·63	97·54	97·5	4
31 ...	96·74	25	96·92			
32 ...	95·89	26	96·19	96·04	95·9	12 wide
33 ...	95·14	27	95·40			
34 ...	94·34	28	94·59	94·46	94·5	20 f.d.
35 ...	93·53	29	93·80			
36 ...	92·61	30	92·93	92·77	92·7	4
37 ...	91·75	31	92·04			
38 ...	90·85	32	91·11	90·98	90·9	4
39 ...	89·84	33	90·13			
40 ...	88·92	34	89·25	89·14	89·3	10 f.d.
41 ...	87·91	35	88·23			
42 ...	86·88	36	87·20	87·04	87·0	5
43 ...	85·82	37	86·18			
44 ...	84·76	38	85·10	84·93	85·0	3
45 ...	83·65	39	84·01			
46 ...	82·52	40	82·89	82·70	82·5	3
47 ...	81·36	41	81·76			
48 ...	80·17	42	80·56	80·36	80·3	4
49 ...	78·99	43	79·36			
50 ...	77·73	44	78·13	77·93	78·0	3
51 ...	76·45	45	76·88			
52 ...	75·17	46	75·60	75·38	75·3	3
53 ...	73·85	47	74·29			
54 ...	72·51	48	72·97	72·74	72·7	3 wide
55 ...	71·15	49	71·59			
56 ...	69·74	50	70·22	69·98	70·2	3 wide
57 ...	68·37	51	68·79			
58 ...	66·88	52	67·36	67·12	67·2	2 wide
59 ...	65·40	53	65·89			
60 ...	63·89	54	64·41	64·15	64·1	1 wide
61 ...	62·36	55	62·91			
62 ...	60·80	56	61·34	61·07	61·2	2 wide
63 ...	59·22	57	59·77			
64 ...	57·60	58	58·18	57·89	58·2	0 hazy
65 ...	55·98	59	56·56			

f.d.=fundamental doublet.

TABLE I. (*continued*).

Band (26, 1) in absorption.					In fluorescence.	
R branch.		P branch.		Average.		
j'.	ν.	j'.	ν.	ν.	ν.	Intensity.
66 ...	54·31	60	54·89	54·60	54·7	1 wide
67 ...	52·63	61	53·22			
68 ...	50·91	62	51·51	51·21	51·4	0 wide
69 ...	49·17	63	49·79			
70 ...	47·39	64	48·02	47·70	48·0	1 wide

The absorption line frequencies are calculated from those of other bands which have been measured, by the relation $\nu\ (26, 1) = \nu\ (26, 0) + \nu\ (29, 1) - \nu\ (29, 0)$. In some cases they have been calculated by second-difference interpolation between the lines calculated by the above equation. The fluorescent lines in Table I. are those which appear in iodine mixed with helium at 4 mm. pressure. A few extra lines which do not belong to the (26, 1) band appear on Pl. II., fig. *b*, either interspersed among the lines of the band or as irregularities in the intensity distribution. These are fluorescent doublets, like the "fundamental" doublets, but due to the stimulation of absorption lines belonging to weak overlapping bands. They disappear entirely when the helium pressure is raised to 4 mm. They do not occur in the bands with $n' \neq 26$. They are of no interest in connexion with the subject of this paper.

It is evident, then, that the fluorescent spectrum contains only lines starting from states with even values of j', the alternate lines being missing. Now, the original excited molecules, just after absorbing the light from the mercury arc, and before colliding with helium atoms, had $j' = 34$. It follows that, *during collisions in which the electronic quantum number is unchanged, the rotational quantum number of an iodine molecule can only change by an even number.*

This result, while incomprehensible on the classical Bohr-Lenz theory, is entirely in accord with the wave mechanics. According to the theory of Hund[5], successive rotational states of a symmetrical molecule, such as I_2, have alternately eigen-functions symmetric and anti-symmetric in the positional coordinates of the two nuclei. Moreover, since the symmetric and anti-symmetric eigen-functions correspond to different orientations of the spins of the two nuclei, and since these spins are very loosely coupled to the rest of the

atom, it is to be expected that transitions between symmetric and anti-symmetric states will be very infrequent. Also, it is to be expected that the eigen-functions will retain their characteristic symmetry, or anti-symmetry, even in an electric or a magnetic field or the field of a neighbouring atom, so that transitions from symmetric to anti-symmetric states will not even take place during collisions. In fact, Dennison [6] has recently solved the long outstanding problem

Fig. 2.

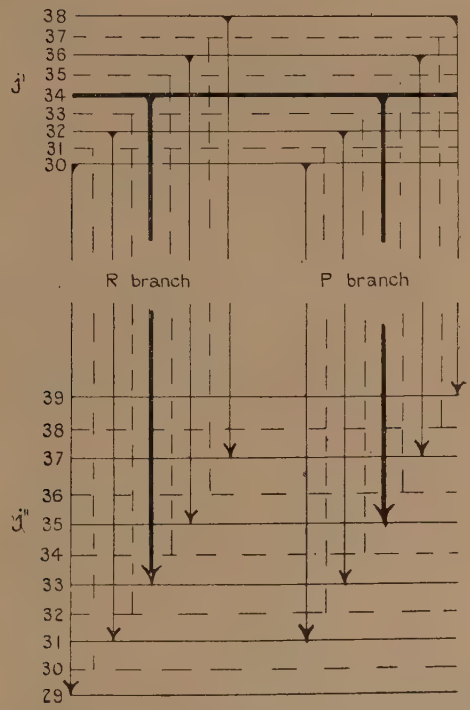

A few of the energy-levels and transitions associated with the fluorescent bands.

of the specific heat of hydrogen by assuming that such transitions do not occur in appreciable numbers, even during the time it takes to make a measurement of specific heats.

The situation is pictured in fig. 2, which shows a few of the rotational levels near those which are associated with a fundamental doublet. The level $j'=34$, which is the initial level for the emission of the fundamental doublet, is

represented by a very heavy line, as are the two transitions from this level which correspond to the fundamental doublet. The upper levels with even j', which are those having the same character, let us say, for convenience, symmetric, as the level $j'=34$, are indicated by continuous lines. The levels with odd j' will then be anti-symmetric, and are indicated by dashed lines. Now Loomis's analysis of the absorption spectrum has shown that each band consists of one P and one R branch, and that it is therefore of the ${}^1s-{}^1s$ type, with $j'-j''=\pm 1$. Since transitions only occur between levels of the same symmetry character, it follows that in the lower state the rotational levels with *odd* j'' must be symmetric, and they are so indicated in the diagram. The transitions from the upper levels with even j' to the lower levels with odd j'', *i. e.* those between symmetric states, are also represented by continuous lines. These are the transitions which result in the fluorescent spectrum. The transitions between anti-symmetric states are indicated by dashed lines. They occur, upward, in absorption, because both kinds of states are present in iodine vapour; but only those represented by continuous lines occur in the fluorescent spectrum, because the green mercury arc line happens to be absorbed by, and excite, a molecule in a symmetric state. Of course the words symmetric and anti-symmetric can equally well be interchanged in the above statements, so far as we know at present.

The writers have been unable to detect any signs of alternating intensities in the absorption bands of iodine. This doubtless means that the nuclear spin of the iodine atom is so high that the statistical weights of the symmetrical and anti-symmetrical states of the molecule are practically equal.

References.

(1) R. W. Wood, *Phys. Zeitschr.* xi. pp. 1195–1196 (1910); Phil. Mag. xxxv. pp. 236–252 (1918).
(2) Lenz, *Phys. Zeitschr.* xxi. p. 691 (1920).
(3) National Research Council Committee Report on 'Molecular Spectra in Gases,' Chapter vi. The notation of this paper is that of the Report. Primed letters refer to the upper electronic state of the molecule, double-primed letters to the lower state. j is the quantum number associated with the total angular momentum of the molecule; n is the vibrational quantum number.
(4) Loomis, Phys. Rev. xxix. pp. 112–134 (1927).
(5) Hund, *Zeitschr. f. Phys.* xlii. p. 110–111 (1927).
(6) Dennison, Proc. Roy. Soc. A, cxv. pp. 483–486 (1927).

XXI. *Notices respecting New Books.*

Introduction to Contemporary Physics. By K. K. Darrow. (Macmillan & Co., St. Martin's Street, London. Price 25*s.* net.)

THE author has given an account of the state of present day physics, theoretical and experimental, more particularly with reference to the structure of the atom, and the phenomena of spectra. He has made accessible the theories and experimental results of recent investigators and provided an interesting and readable survey of these branches of modern physics. The earlier chapters of the book are devoted to the "experimental electron," the "experimental atom," and the classification of the elements and their properties, period, non-periodic, and irregular. The deflexions of alpha particles and electrons by atoms, the photo-electric effect, stationary states, and the atomic models, with the experimental evidence provided by the study of the X-ray and other spectra, are then considered. The electric discharge in gases, which has played so important a part in atomic structure, is treated in the final chapter. A useful index of subjects is appended.

Dr. Darrow has done a real service to students by introducing them to some of the problems of modern physics; for this reason, his book can be heartily commended to their notice.

Lectures on Theoretical Physics. By H. A. Lorentz. Vol. I. *Aether Theories and Aether Models and Kinetical Problems.* (Macmillan & Co. Ltd., St. Martin's Street, London. Price 12*s.* 6*d.* net.)

Professor Lorentz's lectures on Theoretical Physics at the University of Leyden, edited by his Dutch pupils, are here translated into English and thus made available to a wider circle of readers. The subject of the first course of lectures is Aether Theories and Models, edited by Prof. H. Bremekamp; theories of Fresnel, Planck, and others are brought under review, and one chapter devoted solely to the study of Kelvin's model of the quasi-rigid aether. A brief treatment of the attraction and repulsion of pulsating spheres is given in the later sections.

The lectures on Kinetical Problems, edited by Drs. Bruins and Reudler, are largely expositions of the classical researches of M. Knudsen and O. W. Richardson, the former on surface phenomena and the flow of rarefied gases through narrow tubes and orifices, the latter on the emission of electricity from hot bodies. There are two indexes giving sources and references to original papers.

The translators have accomplished their task with success and produced a readable English version of these important topics. English readers will await with interest the translation of the remaining volumes.

The Collected Papers of Spinivasa Ramanujan. Edited by G. H. Hardy, P. V. Seshu Aiyar, and B. M. Wilson. Pp. xxxvi+355. (Cambridge: At the University Press. 1927. Price 30*s.* net.)

The publication of a collected edition of the papers of the remarkable Indian mathematician, Ramanujan, has been made possible by the aid of contributions from the University of Madras, the Royal Society, and Trinity College, Cambridge. The Editors state in their preface that there is still a large mass of unpublished material left by Ramanujan in his notebooks, much of which should certainly be edited and published. For this purpose further monetary assistance would be required, and they express the hope that the present volume will enjoy sufficient success to make further publication possible. Enough is already known of Ramanujan's work to make detailed comment here unnecessary, but collected into one volume its genius and singular quality cannot fail to impress the reader. It is pleasing to recall that, before his early death in his thirty-third year, the merit of his work had been recognised by his election to the Fellowship of the Royal Society—he was the first Indian to receive this honour—and by his election to a Fellowship at Trinity College, Cambridge.

The papers are preceded by two biographical notices. Notes on the papers are contained in an Appendix, and a second Appendix gives extracts from Ramanujan's letters to Mr. G. H. Hardy.

The Phase Rule and its Applications. By Alexander Findlay, M.A., D.Sc., F.I.C. Sixth Edition. Pp. xv+326 with 165 figures. (London: Longmans, Green & Co. 1927. Price 10*s.* 6*d.* net.)

Prof. Findlay's volume on the phase rule and its applications forms the best introduction to the study of chemical equilibria. That a sixth edition has been called for is a recognition of its value. The treatment is non-mathematical and carries the student sufficiently far to be able to read with profit the more advanced works on the subject.

For the present edition a new chapter on the practical applications of equilibrium diagrams has been added, the chapter in previous editions on the equilibria between iron, carbon monoxide, and carbon dioxide being omitted to make room for it. The chapters dealing with equilibria in one and two component systems have been recast and largely rewritten with additions which include discussions of the nature of the equilibria in intensively dried systems and of Smits's theory of allotropy. The remainder of the volume has been carefully revised and brought up to date.

[*The Editors do not hold themselves responsible for the views expressed by their correspondents.*]

Fig. 1.

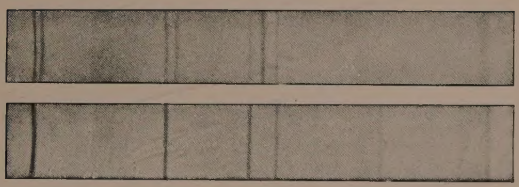

Photographs from composite layers containing equal parts of nickel-oxide and gold.

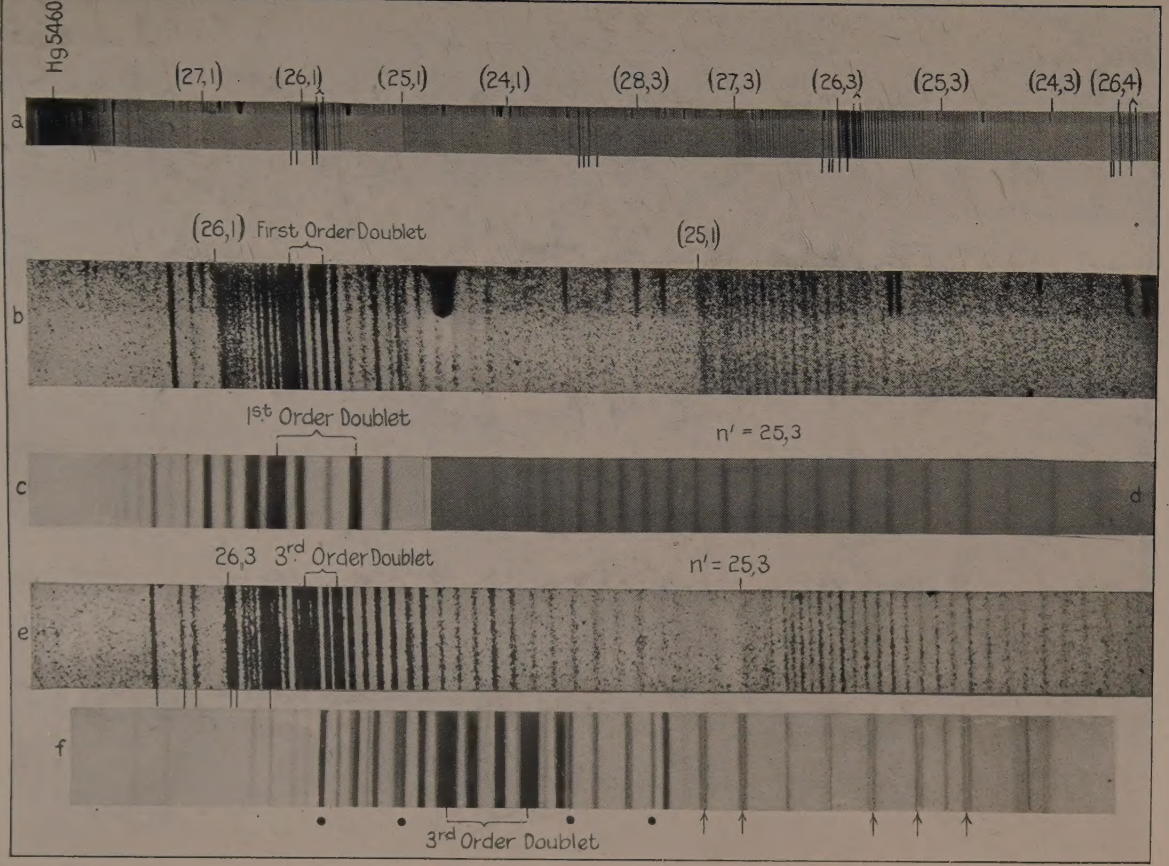

Fundamental doublets are indicated above the spectra, non-fundamental doublets below.